

**Hypercoordinated Oxazoline and Ethyl Pyridyl Organotin Compounds:
Potential Routes to Stable Polystannanes**

By

Desiree Bender

Honours Bachelor of Science in Chemistry,
Western University, London, Canada, 2012

A thesis presented to Ryerson University

in partial fulfillment of the
requirements for the degree of
Master of Science
in the program of
Molecular Science

Toronto, Ontario, Canada, 2018

© Desiree Bender 2018

Author's Declaration

I hereby declare that I am the sole author of this thesis. This is a true copy of the thesis, including any required final revisions, as accepted by my examiners.

I authorize Ryerson University to lend this thesis to other institutions or individuals for the purpose of scholarly research.

I further authorize Ryerson University to reproduce this thesis by photocopying or by other means, in total or in part, at the request of other institutions or individuals for the purpose of scholarly research.

I understand that my thesis may be made electronically available to the public.

Hypercoordinated Oxazoline and Ethyl Pyridyl Organotin Compounds: Potential Routes to Stable Polystannanes

Desiree Bender, Master of Science – Molecular Science, Ryerson University, 2018

Abstract

Tetraorganotin chelating tin (IV) compounds containing a rigid (**10**) and a semi-flexible (**18**) oxazoline ligand were synthesized by a reaction between the lithiated oxazoline and Ph₃SnCl in good yields. Conversion into their corresponding dihalide species by reaction with two equivalents of bromine was undertaken to yield the dibromide species, **13** and **20** respectively. X-ray crystallography of these compounds revealed relatively short tin-nitrogen bond distances (**10**: 2.762 **13**: 2.383, **18**: 3.234 Å). These all fall within the Van der Waal radii of a tin-nitrogen bond and all adopt a distorted trigonal bipyramidal geometry in the solid state. Compounds **13** and **20** were converted into the corresponding dihydrides by reaction with NaBH₄. Polymerization of the corresponding tin dihydrides produced low molecular weight polymers, 10,100 Da for the rigid species (**16**) and 3,200 Da for the semi-flexible tin species (**22**). A tetraorganotin compound containing a chelating ethyl pyridyl ligand (**23**) was synthesized by reacting 2-vinyl pyridine with triphenyltin hydride via a hydrostannylation reaction which was further reacted with two equivalents of bromine to yield the dibromide species (**24**). The X-ray crystallographic data of **23** and **24** showed relatively short Sn-N bond lengths of 2.888(2) Å and 2.363(5) Å respectively. Compound **24** will be investigated in the future for the stabilization of polystannanes following the synthesis of the dihydride species.

Acknowledgements

I would like to thank my supervisors Drs. Foucher and Gossage for taking me on as a Master's student. They both have been instrumental in my development as a chemist and have provided a lot of guidance and assistance over the last two years. They both always had an open door to answer any questions, provide insightful conversations and order chemicals.

I would also like to thank my committee members, Dr. George, Dr. Rousseau and Dr. Adler for providing me with feedback and pointing me in the right direction with suggestions. I would also like to thank Dr. Koivisto and Dr. Viirre's labs for allowing me to borrow chemicals.

I would like to thank my lab mates, past and present: Jeff, Joe, Jas, Julie, Gloria, Kristy, Rachel, Alex, Kathy, Jeanette, and Tristan. I would like to specifically thank Joe for always having my back and talking sports with me, Gloria, who I dedicate this thesis too, for being my best friend. Rachel, my fume hood mate, for gossiping with me, making a mess of my fume hood, clogging my needle the first week and running all my GPC samples, Kathy AKA mom for always making sure we are taken care of, and Jeff and Julie who taught me the tin ways. Thank you all for going to McDonald's and going to Blue Jay's games with me, as well as playing games and basketball! I really enjoyed my two years here, I have many fond memories and will miss all of you.

I would like to give a big thank you to my mom, all my siblings and Jack for all the love and support while being away from home.

Table of Contents

Author's Declaration	ii
Abstract.....	iii
Acknowledgements	iv
List of Figures.....	ix
List of Schemes	xi
List of Tables	xii
List of Abbreviations	xiii
1.0 Introduction.....	1
1.1 Oxazolines	1
1.2 Coordination of Oxazolines to Tin.....	2
1.3 3c-4e ⁻ Bond Concept	5
1.4 Polystannanes and Their Properties	5
1.4.1 Challenges with Polystannanes.....	7
1.5 Synthesis of Polystannanes	8
1.5.1 Electrochemical Polymerization	8
1.5.2 Wurtz Coupling.....	9
1.5.3 Dehydropolymerization	9
1.5.4 Condensation Polymerization	10
1.6 Previous Work.....	11

1.7 Thesis Objectives	12
2.0 Results and Discussion.....	13
2.1 Synthesis of 2-(2'-bromophenyl)-4,4-dimethyl-4,5-dihydrooxazole 8	13
2.2 Oxazoline Stannane Compounds	14
2.2.1 4,4-dimethyl-2-(triphenylstannyphenyl)-4,5-dihydrooxazole 10	14
2.2.2 2-(2-(chlorodiphenylstannyphenyl)-4,4-dimethyl-4,5-dihydrooxazole 11	16
2.2.3 Attempted synthesis of 2-(2-(dichloro(phenyl)stannyphenyl)-4,4-dimethyl-4,5-dihydrooxazole 12	19
2.2.4 Synthesis and characterization of compound 13	20
2.2.5 NMR Analysis of 10 , 11 and 13	22
2.3 Synthesis of 4,4-dimethyl-2-(2-(phenylstannyphenyl)-4,5-dihydrooxazole 14	24
2.3.1 Characterization of 14	25
2.4. Synthesis of homopolymer 16	29
2.4.1 Dehydropolymerization using Wilkinson's catalyst.....	29
2.4.2 Wurtz Coupling.....	33
2.5 Synthesis and characterization of 4,4-dimethyl-2-(2-((triphenylstanny)methyl)phenyl)-4,5-dihydrooxazole 18	34
2.5.1. Attempted synthesis of semi-flexible oxazoline stannane halides.....	37
2.5.2 Synthesis of 4,4-dimethyl-2-(2-((phenylstanny)methyl)phenyl)-4,5-dihydrooxazole 21 :	40

2.5.3 Synthesis of polymer 22 :.....	41
2.6 Synthesis of of 2-(triphenylstannyl)ethyl)pyridine 23 :	43
2.7 Synthesis of 2-(2-(dibromo(phenyl)stannyl)ethyl)pyridine 24 :	45
3.0 Conclusions	49
4.0 Future Work	51
5.0 Experimental	52
5.1 Synthesis of 2-(2-bromophenyl)-4,4-dimethyl-4,5-dihydrooxazole (8):	53
5.2 Synthesis of 4,4-dimethyl-2-(triphenylstannyl)phenyl)-4,5-dihydrooxazole (10):	55
5.3 Synthesis of 2-(2-(chlorodiphenylstannyl)phenyl)-4,4-dimethyl-4,5-dihydrooxazole (11):	57
5.4 Synthesis of 2-(2-(dibromo(phenyl)stannyl)phenyl)-4,4-dimethyl-4,5-dihydrooxazole (13):	58
5.5 Synthesis of 4,4-dimethyl-2-(2-(phenylstannyl)phenyl)-4,5-dihydrooxazole (14):.....	59
5.6 Synthesis of polymer (16):	60
5.7 Synthesis of 4,4-dimethyl-2-(o-tolyl)-4,5-dihydrooxazole (17):	61
5.8 Synthesis of 4,4-dimethyl-2-(2-((triphenylstannyl)methyl)phenyl)-4,5-dihydrooxazole (18) :	63
5.9 Synthesis of 2-(2-((dibromo(phenyl)stannyl)methyl)phenyl)-4,4-dimethyl-4,5- dihydrooxazole (20):	64
5.10 Synthesis of 4,4-dimethyl-2-(2-((tribromostannyl)methyl)phenyl)-4,5-dihydrooxazole (19) :	65

5.11 Synthesis of 4,4-dimethyl-2-(2-((phenylstannyl)methyl)phenyl)-4,5-dihydrooxazole (21):	66
.....
5.12 Synthesis of polymer (22):	67
5.13 Synthesis of 2-(2-(triphenylstannyl)ethyl)pyridine (23):	68
5.14 Synthesis of 2-(2-(dibromo(phenyl)stannyl)ethyl)pyridine (24):	69
References	70
Appendix	75

List of Figures

Figure 1: Structure and numbering system of 2-oxazolines.	1
Figure 2: Structures of <i>ortho</i> (A), <i>para</i> (B) substituted tin oxazoline and 2-pyridine (C), 4-pyridine (D) ethyl tin compounds.	3
Figure 3: ^{15}N NMR spectra of 5 , 1 and 3 respectively. Asterik denotes $^{117}/^{119}\text{Sn}$ Satellites. Used with permission from Elsevier.	4
Figure 4: Examples of hypercoordinate tin structures.	5
Figure 5: Schematic representation of a polystannane.	6
Figure 6: Degradation of polystannanes under light and moisture conditions.	7
Figure 7: Rigid (A) and flexible (B) hypercoordinate tin structures.	12
Figure 8: Target polymers.	12
Figure 9: ORTEP representation of 10 . Thermal ellipsoids drawn at the 30 % level.	15
Figure 10: ORTEP representation of 11 . Thermal ellipsoids drawn at the 30 % level.	17
Figure 11: ORTEP representation of a unit cell molecule of 13 . Thermal ellipsoids drawn at the 30 % level.	21
Figure 12: ORTEP representations of rigid hypercoordinate dimethylammino stannanes. Used with permission from Elsevier (a and c) and Wiley (b).	22
Figure 13: ^{119}Sn NMR spectra (CDCl_3) of compounds 10 , 11 , and 13	23
Figure 14: ^1H NMR spectra (CDCl_3) of compounds 10 , 11 , and 13	24
Figure 15: ^1H NMR (C_6D_6) spectrum of compound 14	26
Figure 16: ^{119}Sn NMR spectra (C_6D_6) over time of 14 at 27°C	27
Figure 17: ^{119}Sn NMR spectrum of a synthetic attempt to synthesize compound 14	28
Figure 18: Structure of distannane dihydride 15	29

Figure 19: GPC chromatogram of polymer 16	31
Figure 20: ^{119}Sn NMR spectrum of crude samples of 16 at RT (a), RT after cleaning four times (b), doing the polymerization at - 30 °C for 4 h (c), and doing the polymerization at -30 °C for 6 h.....	32
Figure 21: ^{119}Sn NMR spectrum of the attempted Wurtz coupling reaction of 13	34
Figure 22: ORTEP representation of two molecules of compound 18 found in the unit cell. Thermal ellipsoids shown at the 30% level.	36
Figure 23: ^{119}Sn NMR spectrum (CDCl_3) of the reaction with compound 18 and Br_2	38
Figure 24: Structure of 19	38
Figure 25: ^{119}Sn NMR spectrum (CDCl_3) of the reaction with compound 18 and $\text{HCl/Et}_2\text{O}$	39
Figure 26: ^1H NMR (C_6D_6) spectrum of 21	40
Figure 27: Crude (a) and clean (b) ^{119}Sn NMR spectrum of 22 in C_6D_6	42
Figure 28: Crude GPC (top), after cleaning GPC (bottom) chromatogram of 22	43
Figure 29: ORTEP representation of unit cell molecule of 23 . Thermal ellipsoids drawn at the 30 % level.	45
Figure 30: ^{119}Sn NMR spectra of compounds 23(a) and 24(b)	47
Figure 31: ORTEP representation of two molecules of compound 24 found in the unit cell. Thermal ellipsoids shown at the 30 % level.	48

List of Schemes

Scheme 1: Synthetic routes to 2-oxazolines.....	2
Scheme 2: Electrochemical polymerization of a dialkyltin dihalide.....	8
Scheme 3: Wurtz coupling of a tin dihalide species.....	9
Scheme 4: Dehydropolymerization of a tin dihydride species using a transition metal (TM) catalyst.	10
Scheme 5: Condensation polymerization of a tin dihydride and a tin diamide.....	11
Scheme 6: Reaction scheme for the synthesis of 8	13
Scheme 7: Reaction scheme for the synthesis of 10	14
Scheme 8: Reaction scheme of the synthesis of polymer 16	30
Scheme 9: Reaction scheme for the synthesis of 16 via Wurtz coupling.....	33
Scheme 10: Reaction scheme for the synthesis of oxazoline stannane 18	35
Scheme 11: Reaction scheme for the synthesis of 20	39
Scheme 12: Reaction scheme for the synthesis of 21	40
Scheme 13: Reaction scheme for the synthesis of polymer 22	41
Scheme 14: Reaction scheme for the synthesis of compound 23	44
Scheme 15: Reaction scheme for the synthesis of compound 24	46

List of Tables

Table 1: ^{117}Sn and ^{119}Sn NMR data of compounds A , B , C and D	3
Table 2: Relevant parameters obtained from the crystal data of compound 10	15
Table 3: Relevant parameters obtained from the crystal data of compound 11	18
Table 4: Relevant parameters obtained from the crystal data analysis of compound 13	21
Table 5: Relevant crystal structure data analysis of 18	36
Table 6: Relevant parameters obtained from the crystal data analysis of 23	45
Table 7: Relevant parameters obtained from the crystal data analysis of 24	48

List of Abbreviations

Å	Ångström
BHT	butylated hydroxytoluene
b.p.	Boiling point
CDCl ₃	hexa-deuterated chloroform
C ₆ H ₆	benzene
C ₆ D ₆	deuterated benzene
DCM	dichloromethane
Et ₂ O	diethyl ether
eV	electron volt
Da	Daltons
DMF	<i>N,N</i> - dimethylformamide
GPC	gel permeation chromatography
HCl	hydrochloric acid
Hz	hertz
K	Kelvin
kDa	kilodaltons
LiAlH ₄	lithium aluminum hydride
Me	methyl
MeOH	methanol
m.p.	melting point
NaBH ₄	sodium borohydride
NBS	<i>N</i> -bromosuccinimide

nm	nanometer
<i>n</i> -BuLi	<i>n</i> -butyl lithium
NMR	nuclear magnetic resonance
PDI	polydispersity index
Ph	phenyl
ppm	parts per million
RT	room temperature
Scm ⁻¹	Siemens per centimetre
<i>sec</i> -BuLi	<i>sec</i> -Butyllithium
SOCl ₂	thionyl chloride
THF	tetrahydrofuran
Tol.	toluene
UV-Vis	ultraviolet-visible
σ	sigma
3c-4e ⁻	3-centered-4-electron

1.0 Introduction

1.1 Oxazolines

Oxazolines, also known as 4,5-dihydro-2-oxazoles, are a subclass of azole heterocycles containing a nitrogen and an oxygen atom bonded by an sp^2 hybridized carbon in a five-membered ring (**Figure 1**).¹ Oxazolines can be derivatized via positions 2, 4 and/or 5 to add versatility and to change the properties of the heterocyclic ring. Oxazolines are generally resistant to hydrolysis, oxidation, nucleophiles, bases and radicals, however, oxazolines are generally sensitive to most acids.²

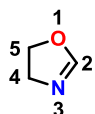
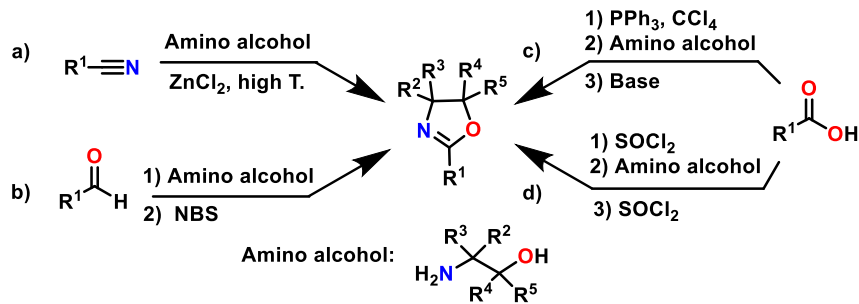


Figure 1: Structure and numbering system of 2-oxazolines.

2-Oxazolines can be synthesized by a variety of different methods including the Witte-Seeliger reaction which employs a nitrile group, an amino alcohol and a zinc catalyst at high temperatures in a one pot synthesis³ (**Scheme 1a**), or using an aldehyde and amino alcohol to form an oxazolidine which is then oxidized using *N*-bromosuccinimide to form the oxazoline⁴ (**Scheme 1b**). Other methods include utilizing a carboxylic acid in an Appel reaction followed by the addition of the amino alcohol and lastly the addition of a base to close the ring (**Scheme 1c**).⁵ Alternatively, an acid chloride can be reacted with an amino alcohol to the form the amide intermediate followed by ring closure using $SOCl_2$ (**Scheme 1d**).⁶ A microwave mediated synthesis of oxazolines has also been reported.⁷



Scheme 1: Synthetic routes to 2-oxazolines.

Oxazolines have also been used as monomers for the synthesis of poly (2-oxazolines) with biomedical applications,⁸ as protecting groups during synthesis,^{2, 6} and are able to be coordinated to a variety of metals and non-metals and can be used in symmetric and asymmetric catalysis reactions.⁵

1.2 Coordination of Oxazolines to Tin

There have been limited number of tin materials bearing oxazoline ligands reported in the literature.⁹⁻¹² Specifically, 2-phenyl-2-oxazolines are particularly interesting as they allow a five membered chelate ring when the tin center is bonded at the *ortho* position of the phenyl ring. The first reported complex of this nature was by Jastrzebski *et al.* in 1991 in which [2-(4,4-dimethyl-2-oxazoline)-5-methyl-phenyl]methylphenyltin bromide was synthesized. It was determined through X-ray crystallography of this species that the nitrogen preferentially dative bonds to the tin center over the oxygen atom.¹³ Due to the presence of dative bonding in tetraorganotin species, it essentially changes the geometry around the tin center from tetrahedral to distorted trigonal bipyramidal geometry.

The Staliński group in Poland published a series of papers detailing organotin complexes bearing a chiral 2-phenyl-2-oxazoline to present evidence of an intramolecular Sn-N interaction through the use of ¹H, ¹³C, ¹⁵N, and ¹¹⁷Sn NMR studies.¹⁴⁻¹⁷ Synthesis of these compounds was

carried out *via* a bromine-lithium exchange of the *ortho* position of the phenyl ring using *n*-BuLi and further reacting with a corresponding tin halide species. As a result of the effect of dative bonding on the electronics of the tin, the chemical shift values in the tin NMR spectra can help identify if dative bonding is present in solution. Staliński *et al.* probed this effect by synthesizing a series of *ortho*- (**Figure 2A**) and *para*- (**Figure 2B**) substituted tin complexes consisting of the same 2-phenyl oxazoline derivatives and then compared ^{117}Sn NMR chemical shifts (**Table 1**). The same trends were seen by Molloy *et al.*¹⁸ with an ethyl pyridyl chain bonded to the tin. When the nitrogen was in position -2 (**Figure 2C**), dative bonding is able to occur while when the nitrogen is in position -4 (**Figure 2D**), it was unable to bond to the tin. This was shown in **Table 1** by comparing the ^{119}Sn NMR chemical shift values of these two compounds, showing a more upfield shift of **C** in both instances.

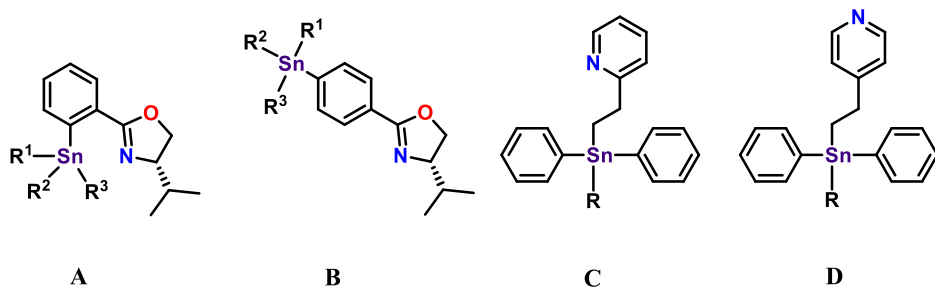


Figure 2: Structures of *ortho* (**A**), *para* (**B**) substituted tin oxazoline and 2-pyridine (**C**), 4-pyridine (**D**) ethyl tin compounds.

Table 1: ^{117}Sn and ^{119}Sn NMR data of compounds **A**, **B**, **C** and **D**.

Compound	R ¹	R ²	R ³	^{117}Sn NMR δ of A (ppm) ^{*14}	^{117}Sn NMR δ of B (ppm) ^{*14}
1	Me			-50.6	-28.6
2	Bu			-52.5	-42.0
3	Me	Br		-110.9	64.0
4	Bu	Br		-93.2	64.4
5	Me	H		-129.2	-121.4
	R			^{119}Sn NMR δ of C (ppm) ^{*18}	^{119}Sn NMR δ of D (ppm) ^{*18}
6	Ph			-110.8	-101.8
7	Br			-143.5	-85.8

*All values are relative to (Me)₄Sn in CDCl₃ at 30 °C.

As shown in **Table 1**, all ^{117}Sn NMR chemical shifts in structure **A** are shifted more upfield relative to the corresponding **B** structures. This is a result of the dative bonding from the lone pair of the ring nitrogen to the tin center, which adds electron density, leading to chemical shifts upfield in the tin NMR. Staliński *et al.* was also able to present evidence of the dative interaction in solution through ^{15}N NMR spectroscopy. Shown in **Figure 3** are compounds **1**, **3** and **5** with all three compounds containing a single nitrogen resonance accompanied by $^{117}/^{119}\text{Sn}$ satellites. This indicates the presence and the strength of the tin-nitrogen interaction. Single X-ray crystallography was performed on compounds **1** and **3** which clearly show dative interactions in the solid state.

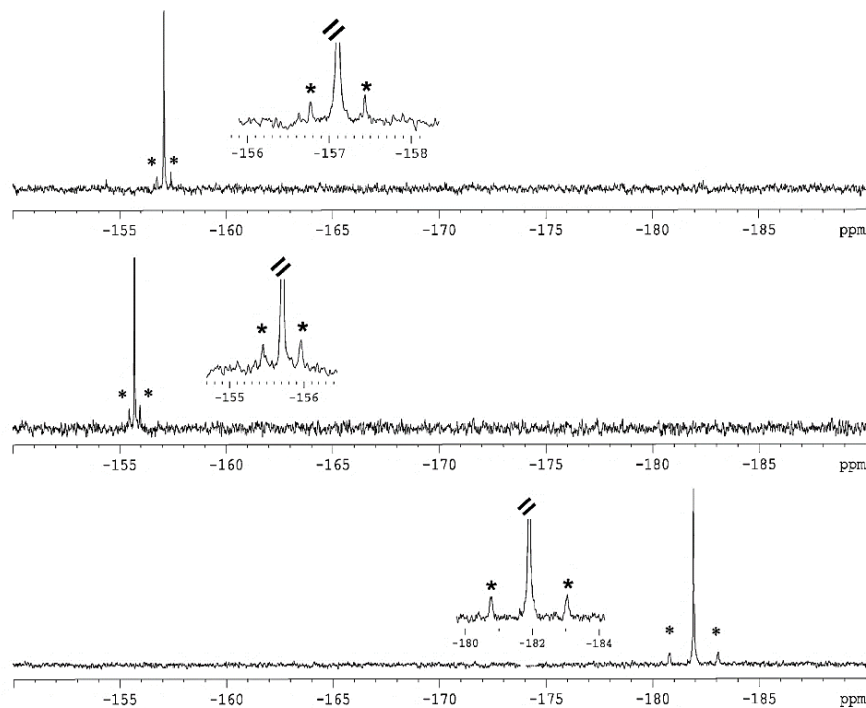


Figure 3: ^{15}N NMR spectra of **5**, **1** and **3** respectively. Asterik denotes $^{117}/^{119}\text{Sn}$ Satellites. Used with permission from Elsevier.

Compound **1** has a Sn-N bond distance of $2.89(9)$ Å, while compound **3** had a shorter Sn-N bond distance of $2.39(2)$ Å.¹⁴ These bonds lengths are within the Van der Waals radii of a tin-

nitrogen bond distance (3.72 Å). The shorter bond distance in compound **3** is likely a result of the electron withdrawing effects of the bromine which pulls electron density away from the tin and draws the nitrogen atom closer, likely due its more electropositive nature.

1.3 3c-4e⁻ Bond Concept

The 3c-4e⁻ bond is a concept used to describe hypervalent compounds which exceed the standard octet of valence electrons.¹⁹⁻²¹ In a tin (IV) compound containing a ligand capable of hypercoordination, trigonal bipyramidal geometries are preferred where the 3c-4e⁻ bonds are typically observed in the axial position (**Figure 4**).²⁰ The lone pair of electrons on Y are donated into the non-bonded molecular orbitals of the tin. This also decreases the Lewis acidic nature of the tin center. Hypercoordinate bonding is more favourable when X is an electronegative atom such as a halide.²⁰

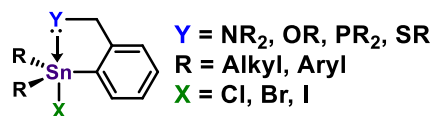


Figure 4: Examples of hypercoordinate tin structures.

The first example of a hypercoordinate tin structure was reported in the literature by van Koten *et al.* in which a crystal structure (R = Ph, Y = NMe₂, X = Br) was obtained to confirm the hypercoordinate bond.²² Other Group 14 atoms (silicon²³⁻²⁴, germanium²⁴ and lead²⁵) are capable of hypercoordination and have been reported in the literature.

1.4 Polystannanes and Their Properties

Polystannanes are polymers consisting of a backbone of covalently bonded tin atoms (**Figure 5**) and the first example was reported by Löwig in 1852.²⁶ Polystannanes possess unique

and interesting chemical, optical, thermal and electronic properties due to delocalization of electrons along the backbone. This is a result of the very diffuse tin σ orbitals.²⁶

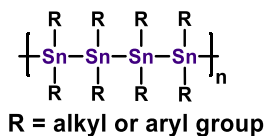


Figure 5: Schematic representation of a polystannane.

The degree of delocalization of electrons is greater than other Group 14 polymers (polysilanes and polygermanes) which leads to a smaller band gap, greater metallic character and a larger red shift in the UV-Vis spectra.²⁷ The σ -delocalization of polystannanes is seen in the UV-Vis spectra by a significant detectable absorption above 390 nm.²⁸ Polystannanes containing aromatic side chains will also exhibit σ - π conjugation, which results in a further bathochromic shift in the UV-Vis spectra.²⁹

Through computational calculations, the band gaps of polystannanes, polygermanes and polysilanes were calculated to be 2.68, 3.10 and 3.72 eV respectively.²⁹ These values agree with previously reported values.³⁰ The addition of bulky aryl side groups can further reduce this band gap.²⁹

Imori *et al.*³¹ cast films of poly(*di-n*-butylstannane) and poly(*di-n*-octylstannane) on glass films and doped with SbF₅ and found conductivities of 1×10^{-2} and 0.3 Scm⁻¹ respectively. Conductivity studies were also done by Choffat *et al.*³² on undoped poly(3-propylphenyl)stannane) and found the conductivity to be 3×10^{-8} Scm⁻¹ at 300 K, which increased with temperature.

1.4.1 Challenges with Polystannanes

Tin forms a long weak covalent metal-metal bond with a bond dissociation energy of typically between 140-183 kJmol⁻¹ relative to germanium and silicon which have bond dissociation energies between 197-261 and 239-319 kJmol⁻¹ respectively.³³ Due to the weak bond strength between tin atoms, polystannanes are extremely sensitive to ambient light and moist air and will thus degrade.³³ In the presence of light, polystannanes will readily homolytically cleave to form radicals and these typically recombine to form five or six membered cyclic rings (**Figure 6**).³⁴ In the presence of water, polystannanes will undergo a nucleophilic attack and break down into oligomeric stannoxyane structures (**Figure 6**). These undesirable cyclic and stannoxyane structures lose the interesting properties that polystannanes possess and are no longer conductive.

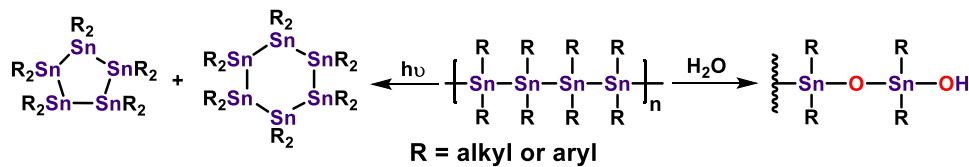


Figure 6: Degradation of polystannanes under light and moisture conditions.

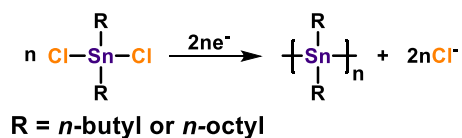
Trummer *et al.*³⁵ performed light stability studies on poly(dibutylstannane) and poly[bis(4-butylphenyl)stannane] by running UV-Vis spectra of both polymers separately in solutions of unstabilized THF and DCM. It was reported that the diaryl polymer was far more stable towards light than the dialkyl polymers in both solutions. In the presence of BHT, which is a radical scavenger found in THF, a reduced rate of degradation of both polymers was observed suggesting these degradation processes occur through a radical mechanism in the presence of light. Although polystannanes are typically light and moisture sensitive, they are known to be thermally stable typically up to 200 °C.³⁴

1.5 Synthesis of Polystannanes

Various methods have been reported in the literature for the synthesis of polystannanes. This includes electrochemical or Wurtz coupling of tin(IV) dihalides, catalytic dehydrogenation of tin(IV) dihydrides using a transition metal catalyst, or a metal-free condensation route using tin(IV) dihydrides and tin(IV) diamides which can both be used to synthesize homo- and copolymers.³⁶

1.5.1 Electrochemical Polymerization

Electrochemical polymerization of organotin dihalides to produce polystannanes was reported by Okano *et al.* in 1998.³⁷ The authors described the synthesis of poly(dibutylstannane) and poly(diethylstannane) using a one-compartment cell containing a syringe port, a Pt cathode, Ag anode, TBAP, and dry DME as the solvent with a constant voltage of 20 V (**Scheme 2**). Yields ranged from 27.9 – 56.1 % with moderate molecular weights ranging from $0.59 - 1.09 \times 10^4$ Da with a PDI value ranging from 1.3 -2.6 depending on the current applied.

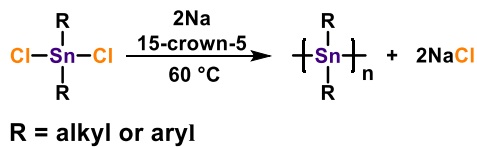


Scheme 2: Electrochemical polymerization of a dialkyltin dihalide.

Okano *et al.*³⁸ also reported the copolymerization of tin with both organo- silicon and germanium dihalides. Higher molecular weights up to 25×10^4 Da were obtained depending on the ratios compared to the homopolymers however, yields were fairly poor. There has been no reported synthesis of poly (diarylstannanes) *via* electrochemical polymerization, which is likely a result of poly (diarylsilanes) and poly (diarylgermanes) being more difficult to synthesize than the dialkyl tin dihalides.³⁹

1.5.2 Wurtz Coupling

Wurtz coupling has been a useful method to synthesize both organic and inorganic polymers.²⁶ In the case of polystannanes, it involves a tin(IV) dihalide species in the presence of a fine sodium metal dispersion and a crown ether typically at 60 °C (**Scheme 3**). Cyclic stannanes are a common by-product of Wurtz coupling, but have a higher tolerance of functional groups than the previously mentioned electrochemical polymerization of dihalide species.

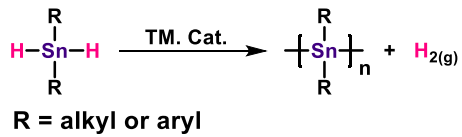


Scheme 3: Wurtz coupling of a tin dihalide species.

Molloy *et al.*⁴⁰ first reported the synthesis of high molecular weight poly (di-*n*-butylstannane) of molecular weights of 1.09×10^6 Da with PDI of 1.4 via Wurtz coupling of the corresponding tin dichloride species in 1996. Since then Molloy *et al.*²⁷ has reported the synthesis of asymmetric polystannanes with high molecular weights of $2.5\text{--}3.0 \times 10^5$ Da with PDI values of 1.30-1.96. In 2010, Foucher *et al.*⁴¹ reported the synthesis of fluorinated diaryl polymers with molecular weights of 1.73×10^4 and 1.47×10^5 Da with PDI values of 1.4 and 3.8, respectively.

1.5.3 Dehydropolymerization

Many transition metal catalysts have been utilized for the synthesis of polystannanes via dehydropolymerization (**Scheme 4**). Tin dihydrides can readily be synthesized from the corresponding dihalide species via hydrogenation using a hydride source such as NaBH₄ or LiAlH₄.^{31, 42}



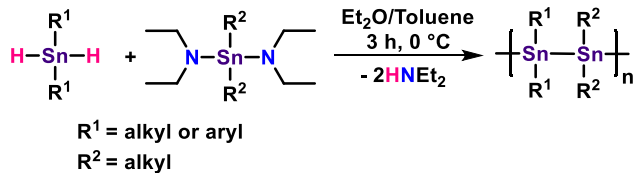
Scheme 4: Dehydropolymerization of a tin dihydride species using a transition metal (TM) catalyst.

Tilley *et al.*^{31, 42} reported the dehydrogenative coupling of a dialkyl tin dihydride using a zirconium based catalyst in 1993 obtaining molecular weights of $\sim 1.7 \times 10^4$ Da of linear polymers. However, cyclic products were always obtained as a by-product. Other catalysts incorporating Zr, Ti, Hf, Rh, or Pt have been used to produce high molecular weight polystannanes, which also include a considerable amount of cyclic impurities.⁴³⁻⁴⁶

Choffat *et al.*^{32, 47-49} tested over thirty transition metal complexes for the dehydropolymerization of dialkytin dihydride of which Wilkinson's catalyst ($\text{RhCl}(\text{PPh}_3)_3$) was found to be the most suitable. Using Wilkinson's catalyst, they were able to achieve high molecular weight dialkyl polymers ($\times 10^4$ Da) and PDI values ranging from 1.4 - 2.7. There was no detectable amount of cyclic by-products and monomer conversion was essentially 100 %. However, they reported that the catalyst was limited to alkyl substituents on the tin atom and a tertiary carbon was needed to be at least two methylene carbons away from the tin center for polymerization to occur.⁴⁹

1.5.4 Condensation Polymerization

In 2015, Foucher *et al.*⁵⁰ developed a new method which utilizes a metal-free condensation polymerization to synthesize homopolymers ($\text{R}^1 = \text{R}^2$) or unprecedented alternating ($\text{R}^1 \neq \text{R}^2$) polystannanes (**Scheme 5**). This method produces volatile diethyl amine as a by-product which can be easily removed in *vauco* after the reaction. Molecular weights upwards of 2.43×10^5 Da with a PDI of 2.03 were obtained when $\text{R}^1 = \text{Ph}$ and $\text{R}^2 = \text{Me}$.



Scheme 5: Condensation polymerization of a tin dihydride and a tin diamide.

1.6 Previous Work

As mentioned in sections 1.1 and 1.2, oxazolines are useful ligands for main group metals as they are readily synthesized from commercially available reagents and are inert to a variety of reaction conditions. Staliński *et al.* have synthesized a variety of tin complexes bearing hypercoordinate oxazoline ligands.¹⁴⁻¹⁷ They also synthesized tin dihydrides which are an important monomer in the synthesis of polystannanes via dehydropolymerization using a transition metal catalyst, however the authors did not report any attempted synthesis of polystannanes from these tin dihydrides bearing oxazoline substituents.

Molloy *et al.*¹⁸ reported the synthesis of triphenyl and a monohalide tin containing the ethyl pyridyl ligand which is an important step in the synthesis of polystannanes, however they did not synthesize any tin dihalides nor tin dihydride species containing the ethyl pyridyl grouping which have also been shown to be nitrogen donors through dative interactions.

The Foucher group has reported the synthesis of asymmetric polystannanes incorporating ligands capable of hypercoordination, specifically propyl alkoxy chains containing a hydroxy group, phenyl, biphenyl or an azo-benzene moiety.^{36, 51-52} The incorporation of these propyl alkoxy chains has shown an increase in stability to both light and moisture. Both these examples were flexible (**Figure 7B**) rather than rigid (**Figure 7A**) and both employed oxygen donor atoms. In this work, the polystannanes were reported to have two ^{119}Sn NMR chemical signals presumably

associated with the bound and unbound tin centers. This is attributed to the ability of the flexible side chain containing the oxygen atom to move freely to and away from the tin center. A polymer containing rigid ligands would not have this ability to freely move out of the way, resulting in a stronger dative interaction and steric bulk around the tin center. To date, there have been no reported hypercoordinate rigid or flexible nitrogen based polystannanes reported in the literature.

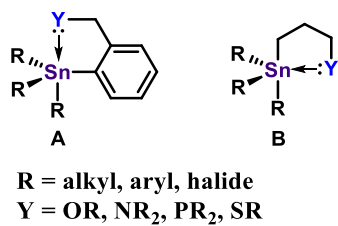


Figure 7: Rigid (**A**) and flexible (**B**) hypercoordinate tin structures.

1.7 Thesis Objectives

This thesis focuses on synthesizing a series of stabilized nitrogen based hypercoordinate polystannanes, specifically continuing the work done by Staliński *et al.* with the oxazolines and with Molloy *et al.* with the tin ethyl pyridine small molecules respectively (**Figure 8**). This will be done by synthesizing the necessary ligands, the triphenyl, dihalide, and dihydride tin species and polymerize these species primarily using Wilkinson's catalyst.

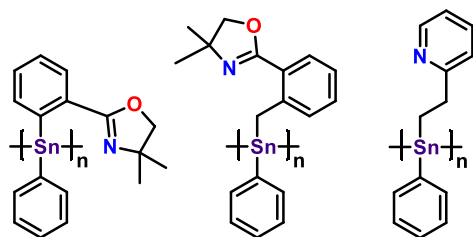
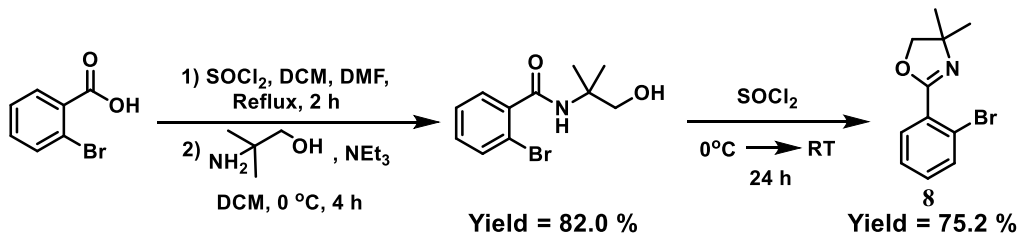


Figure 8: Target polymers.

2.0 Results and Discussion

2.1 Synthesis of 2-(2'-bromophenyl)-4,4-dimethyl-4,5-dihydrooxazole 8

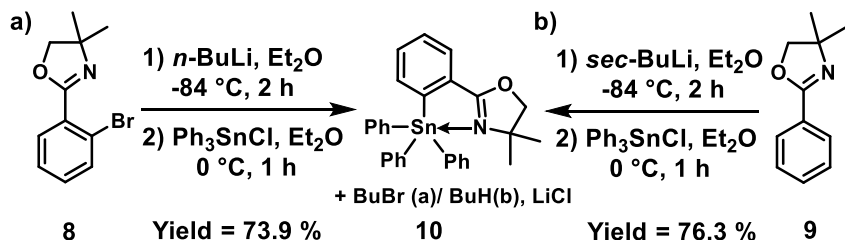


Scheme 6: Reaction scheme for the synthesis of **8**.

Oxazoline **8** was synthesized using two different methods as reported in the literature. In the first method, known as the Witte-Seeliger method,³ 2-bromobenzonitrile is used in the presence of 2-amino-2-methyl-1-propanol and a catalytic amount of anhydrous ZnCl_2 .⁵³ This reaction yielded oxazoline **8** in a 74.2 % yield. However, the 2-bromobenzonitrile starting material is fairly expensive and alternate methods were explored. This was achieved by (**Scheme 6**) converting 2-bromobenzoic acid into an acid chloride using SOCl_2 as the chloride source and DMF as a catalyst. The acid chloride was further reacted with 2-amino-2-methyl-1-propanol in a Schotten-Baumann reaction⁵⁴ to form the benzamide intermediate and finally reacted directly with excess thionyl chloride. In this step, the terminal alcohol is converted into a chloride which is followed by an intramolecular $\text{S}_{\text{N}}2$ reaction with the nucleophile being the carbonyl oxygen. After 24 h, Et_2O is added which results in the precipitation of the oxazoline salt, which is collected and re-dissolved in DCM and subsequently washed with a weak base (NaHCO_3). After separation and DCM removal, **8** was obtained as a white powder and no further purification was required. The NMR data collected correlated to data from the literature for this compound.⁵⁵ This synthetic route was the one that was primarily used in this research.

2.2 Oxazoline Stannane Compounds

2.2.1 4,4-dimethyl-2-(triphenylstannylyl)phenyl)-4,5-dihydrooxazole **10**



Scheme 7: Reaction scheme for the synthesis of **10**.

Two different methods were employed to synthesize compound **10** (**Scheme 7**). The first method (**Scheme 7a**) took **8** in Et_2O with $n\text{-BuLi}$ added at $-84\text{ }^\circ\text{C}$ ($\text{EtOAc}/\text{N}_2\text{(l)}$). This was allowed to react for 2 h, after which the EtOAc bath was switched to an ice bath and allowed to warm up to $0\text{ }^\circ\text{C}$ before the addition of Ph_3SnCl in Et_2O for 1 h. After the solvent was removed, toluene was added resulting in the precipitation of the LiCl by-product. The salt was filtered off and the solvent was removed under reduced pressure to afford a yellow coloured powder of crude **10**. Purification from trituration with MeOH resulted in the isolation of pure **10** as a white coloured powder.

The second method (**Scheme 7b**) was adapted from Gschwend *et al.*⁵⁶ in which they reported the lithiation using $sec\text{-BuLi}$ of **9** and reacted with a variety of non-tin containing electrophiles. Fortunately, when this synthesis was attempted with Ph_3SnCl , it was successful and compound **10** was obtained in a slightly higher yield than stated in **Scheme 7a**. Oxazoline **9** is commercially available and therefore synthesis of this is not required. The authors reportedly lithiated **9** using $n\text{-BuLi}$, however 15 % of the reported products involved the addition of the $n\text{-BuLi}$ to the oxazoline. They found this was mitigated by the use of $sec\text{-BuLi}$.

The ^{119}Sn NMR (CDCl_3) spectroscopic analysis of **10** showed only a single resonance ($\delta_{119\text{Sn}} = -157.13\text{ ppm}$). Although compound **10** has not been previously synthesized in the

literature, Staliński *et al.* synthesized a similar compound previously shown in **Figure 2**, (compound **A** where $R^1, R^2, R^3 = \text{Ph}$) and reported a ^{117}Sn NMR (CDCl_3) chemical shift of -155.5 ppm.¹⁶ A crystal of compound **10** suitable for single crystal X-ray diffraction was obtained (**Figure 9**). The relevant bond lengths and bond angles are shown in **Table 2**.

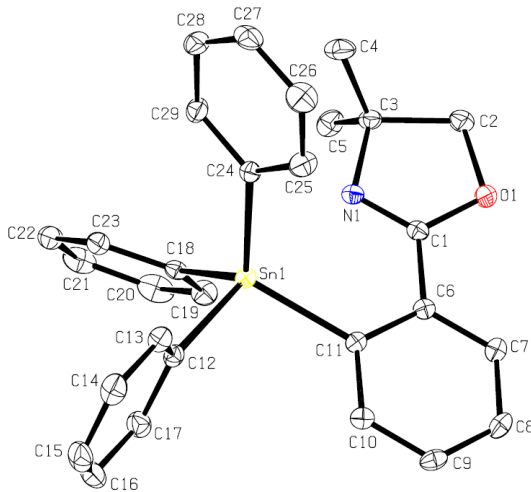


Figure 9: ORTEP representation of **10**. Thermal ellipsoids drawn at the 30 % level.

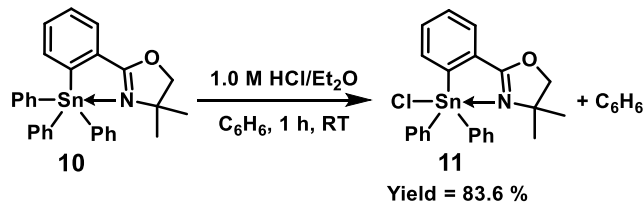
Table 2: Relevant parameters obtained from the crystal data of compound **10**.

Bond	Bond Lengths (Å)
Sn1-N1	2.762(1)
Sn1-C11	2.1602(16)
Sn1-C12	2.1752(17)
Sn1-C18	2.1378(16)
Sn1-C24	2.1425(17)
Angle	Bond Angles (°)
N1-Sn1-C12	172.20(6)

The geometry of this compound around the Sn center is distorted trigonal bipyramidal ($\tau_5 = 0.92$)⁵⁷ with the equatorial bond angles around the tin center ranging from 102° to 117° (**Table A1**) and the axial bond angle being $172.20(6)^\circ$. The structural parameter (τ_5) is a value that ranges from 0 to 1 which is calculated by using angles from the crystallographic data. This value indicates

the geometry of the metal of interest. When τ_5 = zero, the geometry of the coordination center is square pyramidal and when τ_5 = one, the geometry of the coordination center is trigonal bipyramidal ($\tau_5 = (\beta - \alpha)/60^\circ$, where β is the axial angle and α is the largest equatorial angle).⁵⁷ The Sn1-C12 bond is slightly longer than the other Sn-C bonds likely a result of it being para to the donating nitrogen as a result of 3c-4e⁻ sharing. The tin nitrogen bond distant is relatively short, it is not as short as a covalent Sn-N bond which is typically 2.15 Å⁵⁸ but it is within the sum of the van der Waals radii of tin and nitrogen (3.72 Å). This bond distance is comparable to a related rigid triphenyltin species with a benzyl amine donor (**Figure 7A**, R = Ph, Y = NMe₂) collected by a member of the Foucher group which has a Sn-N bond distance of 2.917 Å.⁵⁹ Staliński *et al.* did not report crystal structure data of their triphenyltin oxazoline containing a chiral oxazoline, however they did collect a crystal structure of the complimentary trimethyltin oxazoline in which they reported a Sn-N bond distance of 2.888(9) Å.¹⁶ Even though this compound is less sterically hindered around the tin, the Sn-N bond distance may be longer due to the isopropyl group on the oxazoline ring (**Figure 2A**) being more sterically encumbering than the two analogous methyl groups in compound **10**.

2.2.2 2-(2-(chlorodiphenylstannylyl)phenyl)-4,4-dimethyl-4,5-dihydrooxazole **11**



Scheme 8: Reaction scheme for the mono chlorination to synthesize **11**.

In a method first described by Pannell *et al.* to synthesize tin halides from the corresponding triphenyl species, compound **10** was treated with one molar equivalent of a 1.0 M solution of HCl / Et₂O for 1 h at RT. The crude ¹¹⁹Sn NMR spectrum of the reaction mixture showed a single tin

resonance ($\delta_{119\text{Sn}} = -225.99$ ppm). However, the ^1H NMR spectrum revealed some unidentified impurities which were removed by trituration with hexanes to yield pure **11** as a white coloured powder in an 83.6 % yield. Staliński *et al.* never synthesized a monochloride tin oxazoline, however they did synthesize a monobromide species which has a similar ^{117}Sn NMR chemical shift ($\delta_{117\text{Sn}} = -222.1$ ppm). In our case, the integration of the aromatic region relative to the oxazoline methylene and two methyl groups in the ^1H NMR spectrum confirmed that one phenyl group was replaced by a chloride. A crystal of compound **11** suitable for single crystal X-ray diffraction was thereafter obtained (**Figure 10**). The relevant bond lengths and bond angles are shown in **Table 3**. Two unique molecules were obtained within the unit cell of the crystal that differ in terms of some bond lengths and angles.

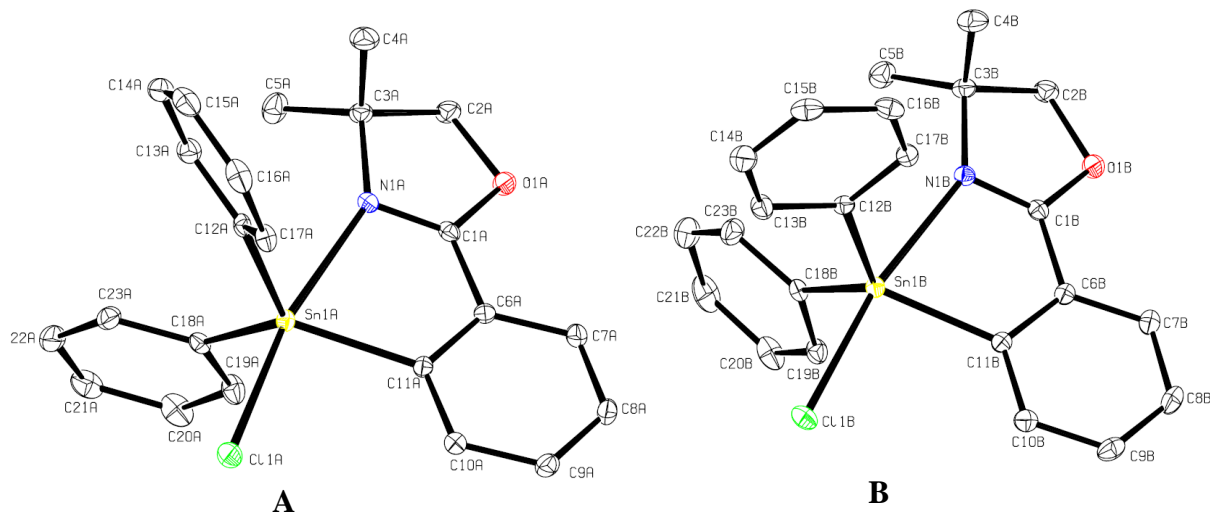


Figure 10: ORTEP representation of **11**. Thermal ellipsoids drawn at the 30 % level.

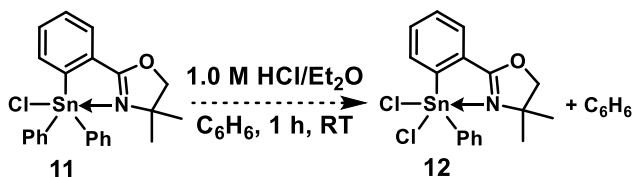
Table 3: Relevant parameters obtained from the crystal data of compound **11**.

Bond	Bond Lengths of A (Å)	Bond	Bond Lengths of B (Å)
Sn1A-N1A	2.4658(14)	Sn1B-N1B	2.4502(14)
Sn1A-C11A	2.1401(16)	Sn1B-C11B	2.1422(17)
Sn1A-C12A	2.1322(16)	Sn1B-C12B	2.1330(17)
Sn1-C18A	2.1250 (17)	Sn1B-C18B	2.1232(17)
Sn1-Cl1A	2.4832(5)	Sn1-Cl1B	2.4955(5)
Angle	Bond Angles of A (°)	Angle	Bond Angles of B (°)
N1A-Sn1A-Cl1A	169.33(3)	N1B-Sn1B-Cl1B	170.40(4)

The geometry around the tin center in both molecules is distorted trigonal bipyramidal (**A**: $\tau_5 = 0.81$, **B**: $\tau_5 = 0.82$)⁵⁷. For both structures, the angles of N1-Sn-Cl are almost 180°, while the angles between the equatorial ligands range from 117-121°. While the angles between the axial and the equatorial phenyl ligands range between 90-95°. The 3c-4e⁻ sharing between the nitrogen, tin and chlorine atoms is evident by result of the Sn-Cl bond is elongated relative to the average Sn-Cl bond length of 2.414 Å.⁵⁸ This also results in a shorter Sn-N bond length relative to the triphenyltin analogue likely due to the increased Lewis acidity at the tin center as a result of the presence of an electronegative chlorine atom. Staliński *et al.* did not report crystal structure analysis of their diphenyltin bromide species containing the chiral oxazoline, however they did collect a crystal structure of the dimethyltin bromide oxazoline complex. They reported a Sn-N bond distance of 2.39(2) Å¹⁴ which, comparing to the solid state structure of compound **11**, has an average Sn-N bond distance of 2.458 Å. This distance is obviously longer. This is likely due to the greater steric hindrance of the phenyl substituents relative to methyl substituents on tin.

Van Koten *et al.*²² also collected crystal structure data of the related compound *C,N*-(2-((dimethylamino)methyl) phenyl)diphenyltin bromide (**Figure 12a**) which is more closely related to the structure of **11**. The former material has a Sn-N bond distance of 2.511(12) Å. The Sn-C bonds in this structure are also comparable to that found in the solid state structure of **11**.

2.2.3 Attempted synthesis of 2-(2-(dichloro(phenyl)stannylyl)phenyl)-4,4-dimethyl-4,5-dihydrooxazole 12



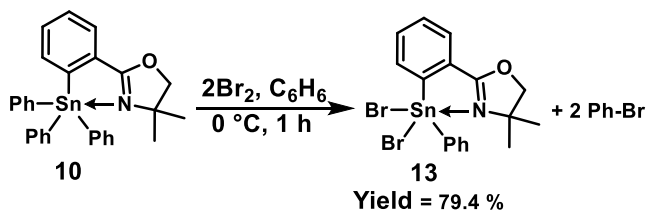
Scheme 9: Reaction scheme of the attempted synthesis of **12**.

A successive chlorination was attempted with another molar equivalent of 1.0 M of HCl/Et₂O using compound **11** (**Scheme 9**). However, ¹H and ¹¹⁹Sn NMR analysis of this mixture showed that no reaction had occurred. Additional equivalents were added but again, no reaction was observed through NMR analysis. Next, a stronger chlorinating source, SOCl₂ was utilized. The addition of SOCl₂ in C₆H₆ for 1 h to the triphenyl compound **10** did successfully synthesize compound **11**. This same procedure was then applied to **11** in hopes of synthesizing the dichloride species however, SOCl₂ was unable to substitute an additional phenyl ring for a second chlorine.

These unsuccessful attempts at synthesizing the dichloride species may be a result of the shorter, stronger Sn-C bond, therefore less reactive and less labile. It could also be a result of increased steric hindrance around the tin because of the short Sn-N and Sn-C bonds, which may cause the tin center to be inaccessible to a chloride anion.

Another possible method to synthesize the dichloride species is *via* direct route by reacting the lithiated **8** with phenyltin trichloride. After removal of the salt by-product and solvent, ^{119}Sn NMR (CDCl_3) analysis revealed three tin resonances were present: -117.1, -225.9 and -237.5 ppm. The appearance of -225.9 ppm in this spectrum was previously confirmed to be the monochloride species, **11**. This suggests the chlorine and phenyl groups underwent redistribution at the tin center and therefore this is likely not a good route to take to synthesize a dihalide species.

2.2.4 Synthesis and characterization of compound 13



Scheme 10: Reaction scheme for the synthesis of **13** via bromination.

Having failed to successfully chlorinate compound **11**, bromination was investigated as a possible alternative route to the desired dihalide species. Therefore, compound **10** was reacted with two equivalents of Br₂ to yield **13** (**Scheme 10**). As the reaction proceeded, the colour faded from a dark red solution to a yellow solution and after the solvent was removed, a yellow coloured powder remained. A crude NMR (CDCl₃) analysis showed only a single ¹¹⁹Sn resonance at -290.63 ppm, however the ¹H NMR showed some impurities, specifically quantities of bromobenzene (b.p. = 156 °C). Removal of this under reduced pressure is a slow process. However, the bromobenzene and other impurities could be easily removed by the addition of methanol to the solution. The product, **13** immediately precipitated out of solution as a white coloured powder and the methanol, which became yellow, was carefully decanted off. This process was repeated until the resulting methanol layer ran colourless. The aromatic signals in a subsequent ¹H NMR spectrum integrates for the correct number relative to the methylene and two methyl group protons on the oxazoline. The NMR chemical shift ($\delta_{^{119}\text{Sn}} = -290.6$ ppm) also corresponds closely to the shift reported by Staliński *et al.* ($\delta_{^{117}\text{Sn}} = -288.5$ ppm).¹⁷ A crystal of compound **13** suitable for single crystal X-ray diffraction was thereafter obtained (**Figure 11**).

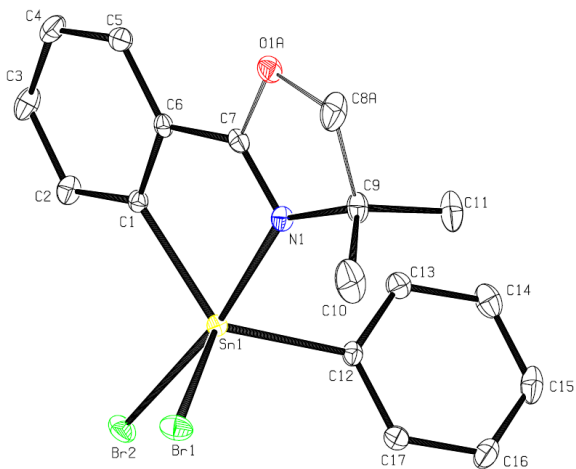


Figure 11: ORTEP representation of a unit cell molecule of **13**. Thermal ellipsoids drawn at the 30 % level.

Table 4: Relevant parameters obtained from the crystal data analysis of compound **13**.

Bond	Bond Lengths (Å)
Sn1-N1	2.383(3)
Sn1-C1	2.137(2)
Sn1-C12	2.127(2)
Sn1-Br1	2.4943(3)
Sn1-Br2	2.6180(3)
Angle	Bond Angles (°)
N1-Sn1-Br2	171.36(5)
N1-Sn1-Br1	87.98(5)
Br1-Sn1-Br2	91.994(11)

The geometry around the Sn center of **13** is distorted trigonal bipyramidal in nature ($\tau_5 = 0.74$).⁵⁷ The angle between the axial atoms (N1-Sn1-Br2) being $171.36(5)^\circ$ and the angles between the three equatorial atoms (Br1, C12 and C1) ranging from $112.14(7)$ - $126.73(9)^\circ$. The angles between the axial and the equatorial atoms range from $76.06(8)$ - $98.14(6)^\circ$. The 3c-4e⁻ sharing is evident in the solid-state structure due to the relatively short Sn1-N1 bond length and the elongated Sn1-Br2 bond length. The average covalent Sn-Br bond length is 2.562 Å.⁵⁸ In the solid state structure of **13**, Br1 is in the equatorial position and presumably not participating in the 3c-4e⁻

sharing. This is evident due to the shorter bond length of the Sn1-Br1 relative to that of Sn1-Br2 and that of the average covalent length of a Sn-Br bond. Since Sn1-Br2 in the axial position, it is presumably participating in the 3c-4e⁻ sharing and the Sn-Br bond length is significantly longer than Sn1-Br1 and that of an average Sn-Br bond length. The electron withdrawing effects of the bromine atoms are likely involved in drawing the nitrogen closer to the tin atom, with a Sn-N bond length of 2.383 Å. Novák *et al.*⁶⁰ reported a related hypercoordinate tin structure, with a chelating rigid benzyl amine substituent (**Figure 12b**) with a reported Sn-N bond length of 2.444(5) Å. Švec *et al.*⁶¹ later synthesized the diiodo analogue (**Figure 12c**) which was reported to have a Sn-N bond distance of 2.476(3) Å. The Sn-C bonds for both structures are also comparable to those obtained for the solid-state structure of **13**. In the latter two structures of **Figure 12**, the 3c-4e⁻ sharing is evident with elongated Sn-Cl1 and Sn-I1 bonds relative to the Sn-Cl2 and Sn-I2 bond lengths respectively.

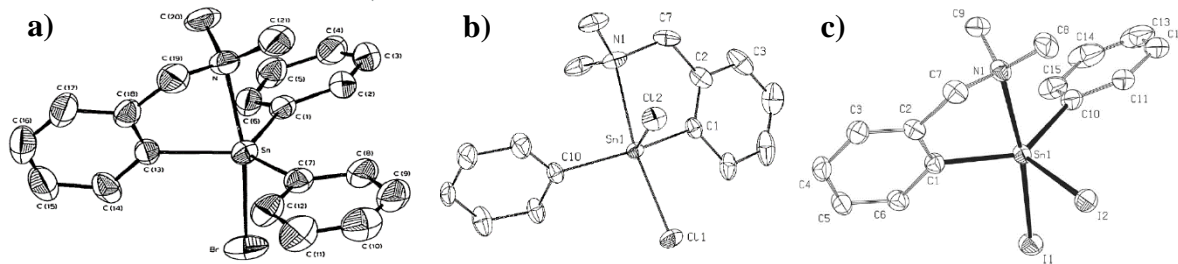


Figure 12: ORTEP representations of rigid hypercoordinate dimethylamino stannanes. Used with permission from Elsevier (a and c) and Wiley (b).

2.2.5 NMR Analysis of **10**, **11** and **13**

Upon the replacement of an alkyl or aryl group by the addition of an electronegative atom to a tin center such as a halide, it is expected to cause a downfield shift in the ¹¹⁹Sn NMR spectrum because of the deshielding effect of the halides. However, in the case of **10**, **11** and **13**, the opposite effect is in fact, observed (**Figure 13**).

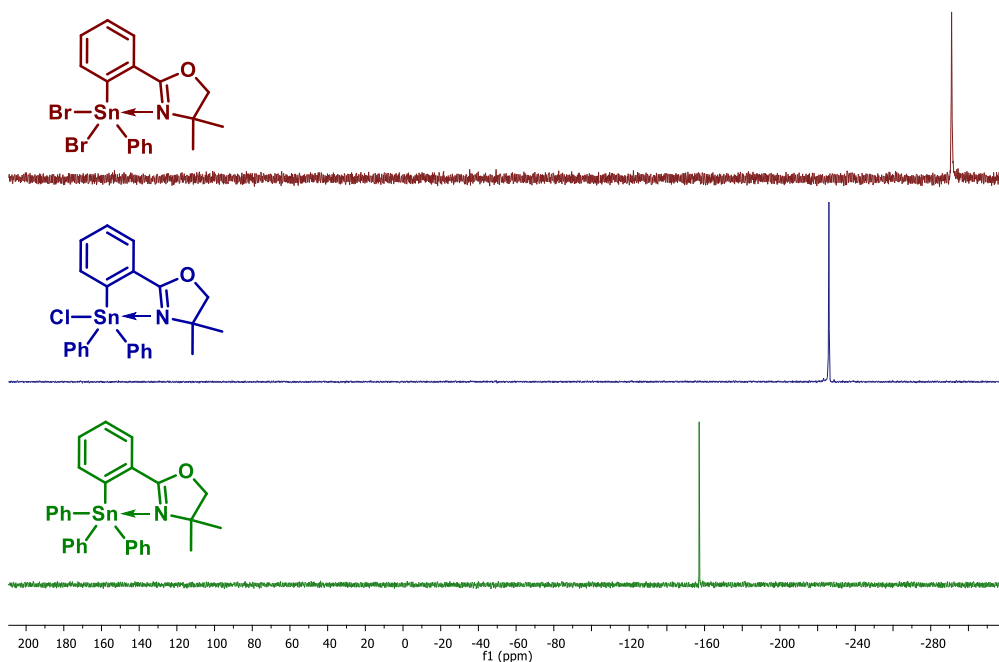


Figure 13: ^{119}Sn NMR spectra (CDCl_3) of compounds **10**, **11**, and **13**.

This observation might be a result of a change in geometry around tin from tetrahedral to trigonal bipyramidal and entails a stronger interaction between the nitrogen and the tin as it drawn closer with each addition of a halide. Similar results have been reported in literature for other hypercoordinate tin compounds.^{14, 16, 18} In the ^1H NMR spectra of compounds **10**, **11** and **13** (Figure 14), the methylene protons of the oxazoline (marked by an asterisk) are shifted downfield with each additional halide, possibly as a result of the inductive effects. This same effect can also be seen with both methyl groups of the oxazoline and all aromatic protons.

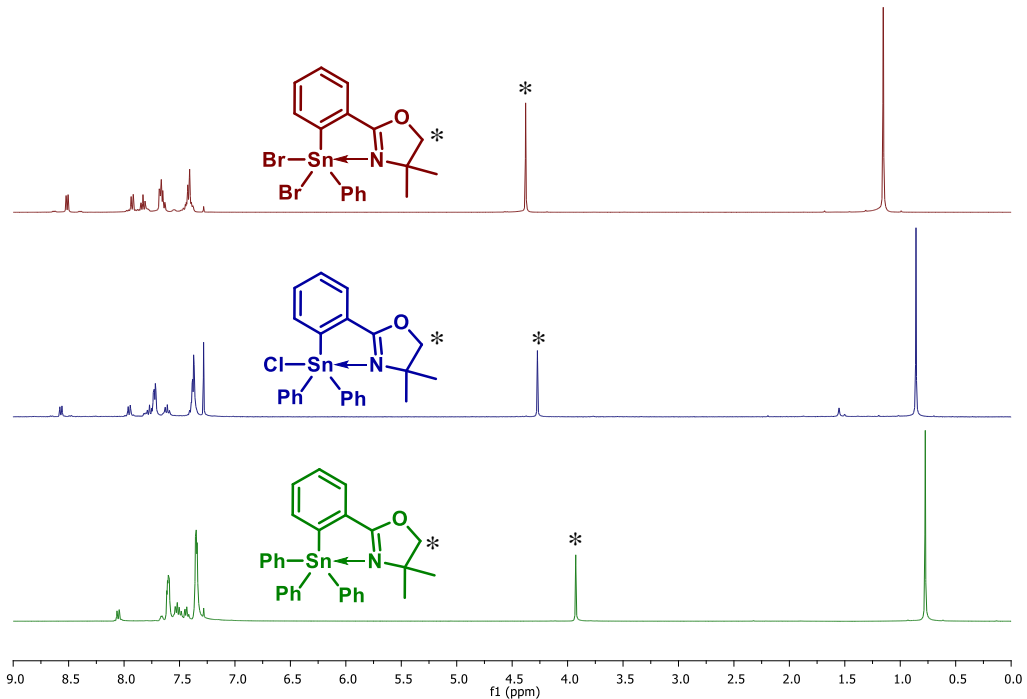
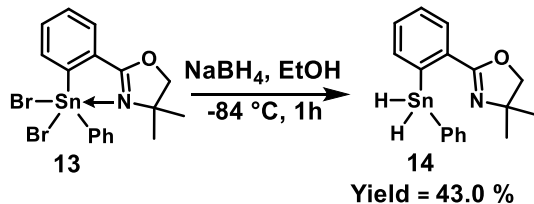


Figure 14: ^1H NMR spectra (CDCl_3) of compounds **10**, **11**, and **13**.

2.3 Synthesis of 4,4-dimethyl-2-(phenylstannylyl)phenyl)-4,5-dihydrooxazole **14**

The synthesis of dihydride **14** (**Scheme 11**) proved quite difficult. In the Foucher group, hydrides are typically synthesized from NaBH_4 in a large excess (~ 10 mol equivalents) or LiAlH_4 in slight excess (~ 1 mol equivalent) at 0 °C for 1-3 h followed by an aqueous work-up. However, neither of these conditions worked to give product **14**; ^{119}Sn NMR analysis showed many unidentifiable resonances. Staliński *et al.*¹⁶ reported the synthesis of a very similar dihydride utilizing a 10 mol equivalent of NaBH_4 in EtOH at 0 °C for 5 min with an aqueous work-up. These synthetic conditions did not work in this case and immediately after the removal of solvent, the product was isolated as a viscous bright yellow coloured oil, indicative of oligomerization. ^{119}Sn NMR analysis showed many unidentifiable resonances. After many trials, it was established that using 1.5 mol equivalent of NaBH_4 , at -84 °C for 1 h with an aqueous work up was the best, reproducible procedure.



Scheme 11: Reaction scheme for the synthesis of **14**.

During the work-up, the product is kept at -84 °C as much as possible to slow decomposition as **14** appears to be very temperature sensitive. Stalisnki *et al.* reported the analogous compound to be sensitive above -20 °C. Compound **14** was isolated as a colourless viscous oil and when in the NMR tube dissolved in C₆D₆, the mixture quickly (~1 min.) turned from a colourless solution to a bright yellow solution with precipitate forming after a few hours.

2.3.1 Characterization of **14**

In the ¹H NMR spectrum of **14** (**Figure 15**), the appearance of a singlet at 6.79 ppm has ^{117/119}Sn satellites equidistant from this singlet, which is indicative of a hydride bound to a tin atom. These coupling constants shown in **Figure 15** are comparable to other tin hydrides, specifically the ones reported by Staliński *et al.*¹⁶ It is also seen relative to **Figure 14**, the chemical shifts of the methylene and methyl protons of the oxazoline are shifted back upfield likely because the hydrides are electron donating.

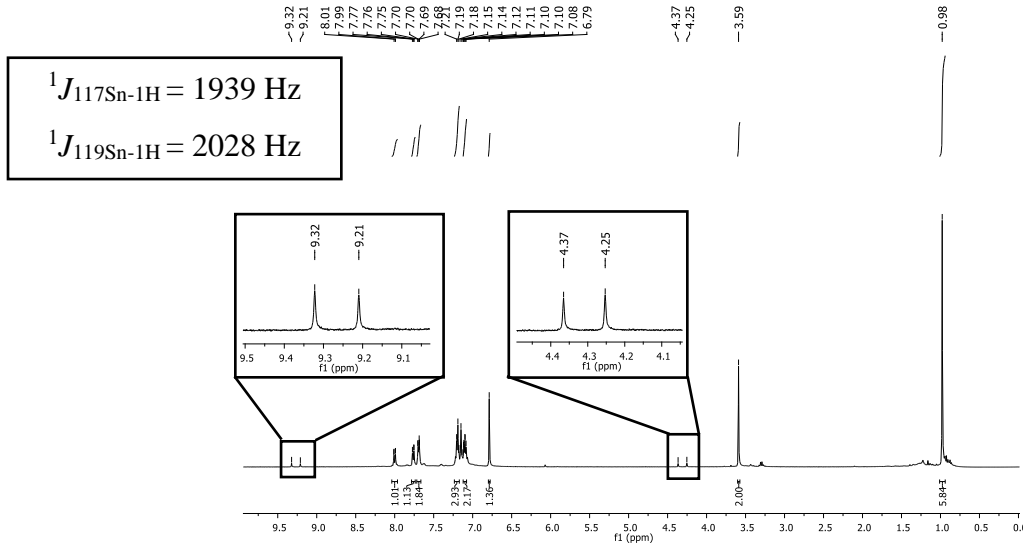


Figure 15: ^1H NMR (C_6D_6) spectrum of compound **14**.

The ^{119}Sn NMR shows a single resonance at -249.5 (Figure 16, $t = 0$) ppm which is relatively close to that reported by Staliński *et al.* of their related phenyltin dihydride (IV) species containing an oxazoline substituent ($\delta_{117\text{Sn}} = -244.5$ ppm in toluene-d₈). Chemical shifts in the ^{119}Sn NMR spectrum of reported flexible hypercoordinate tin dihydrides typically appear from approximately -200 to -220 ppm.^{51-52, 62} The upfield shift of compound **14** relative to these others may be a result of the close proximity of the nitrogen to the tin center. ^{119}Sn NMR spectrum were collected consecutively for 13 h. After 2 h, the appearance of two other signals, -42 and -173 ppm is detected in the ^{119}Sn NMR spectrum. These two resonances frequently appear through all the trials of the attempted syntheses of compound **14**. After 8 h (not shown below), there is no evidence of starting material **14** ($\delta = -249.5$ ppm). The NMR tube was left untouched and was hidden from light using aluminum foil for a week and another ^{119}Sn NMR spectrum was collected of the sample. After a week, the disappearance of the resonance at -42 and -173 ppm had occurred with the appearance of several new unidentified resonances ($\delta_{119\text{Sn}} = -192, -210, -211, -215, -223, -228, -231$ and -233 ppm) as shown in Figure 16.

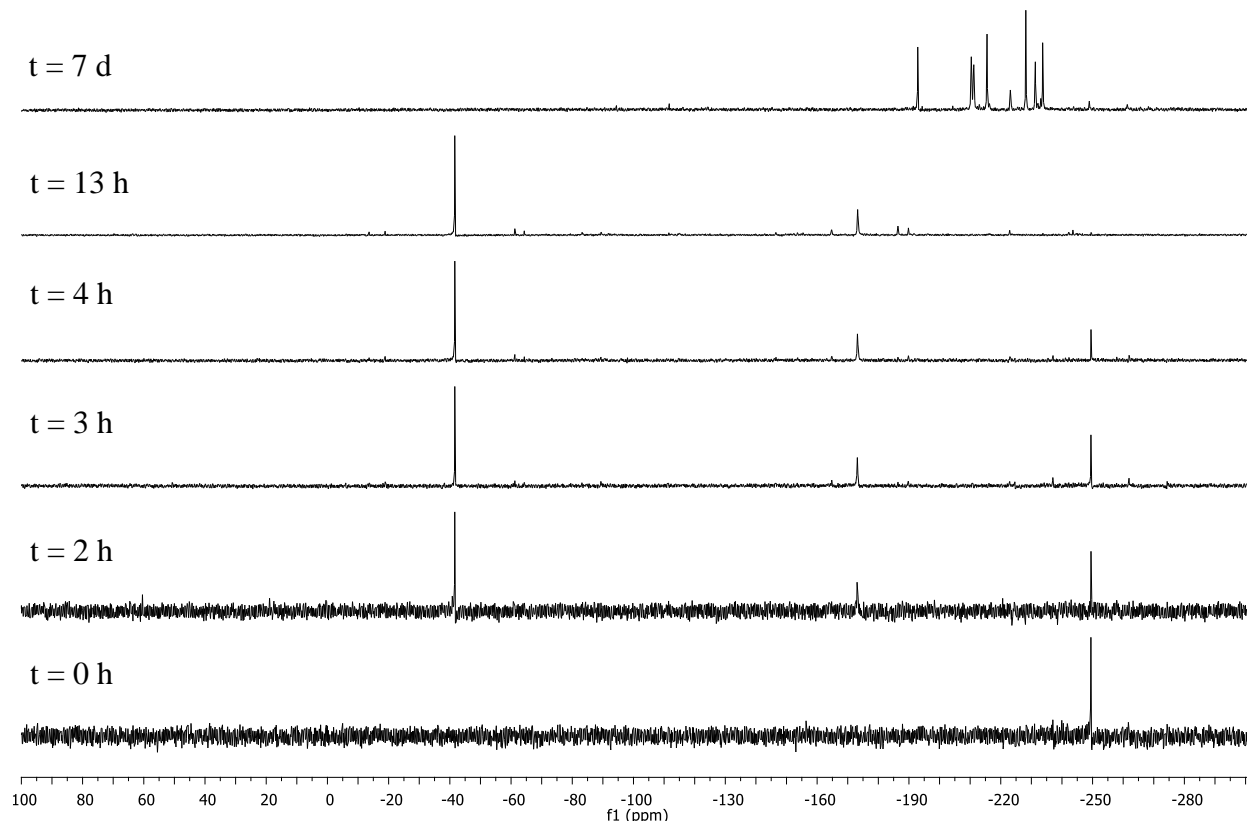


Figure 16: ^{119}Sn NMR spectra (C_6D_6) over time of **14** at 27°C .

In **Figure 16**, specifically at $t = 3 \text{ h}$, the appearance of satellite resonances are noted equidistant from the resonance at -249.5 ppm (these signals are not likely seen in $t = 0 \text{ h}$ and 2 h : likely due to less scans being run on these spectra resulting in decreased spectral resolution). These satellites are indicative of tin satellites, suggesting that there are two tin atoms directly attached to each other; the coupling constant of these satellites is large (3713 Hz). This result has been previously seen in two of the attempts to synthesize compound **14**. During these attempts, the reaction was carried out at -84°C , with two molar equivalents of NaBH_4 for 1 h in EtOH . The workup was done in the absence of water and instead, after 1 h, a large excess of hexane was added. This causes the excess of NaBH_4 to be precipitated out of solution. This could be filtered off leaving a solution containing ethanol, hexane and compound **14**. The majority of the solvent

was then removed under reduced pressure. As a result, the ^1H NMR spectrum largely consisted of signals corresponding to EtOH and hexanes, while the signals for **14** were unable to be clearly identified. The ^{119}Sn NMR spectrum of this clearly showed the satellites equidistant of the resonance at -249 ppm with a small impurity at -42 ppm evident immediately upon running the ^{119}Sn NMR (**Figure 17**).

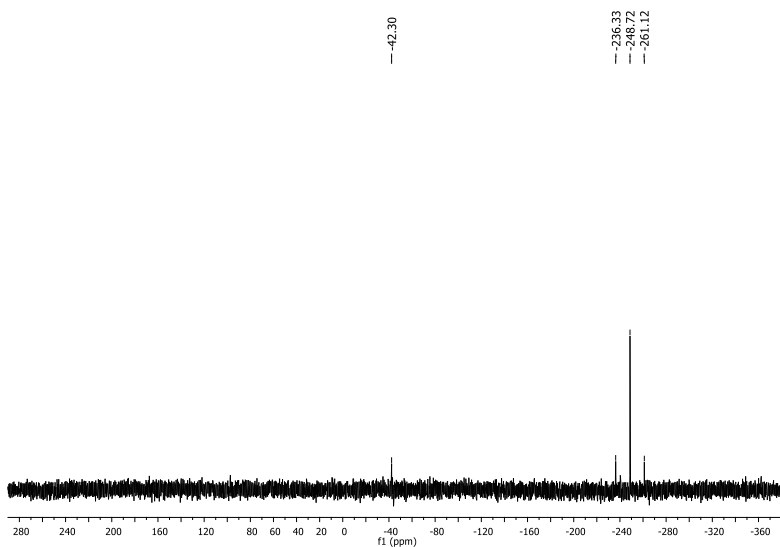


Figure 17: ^{119}Sn NMR spectrum of a synthetic attempt to synthesize compound **14**.

In the ^1H NMR spectrum, a presumed hydride resonance with the corresponding to $^{117/119}\text{Sn}$ Satellites are present. Typical tin dihydrides are reported to resonate at $\delta_{1\text{H}} = 5.5$ ppm. Staliński *et al.* reported their very similar tin dihydride at approximately 6.7 ppm, with confirmation of the compound by HRMS, however they did not report any tin satellite signals. Tin monohydrides typically show up more upfield, such as Ph_3SnH ($\delta_{1\text{H}} = 6.93$ ppm). There is a possibility in combination with the tin satellites and the chemical shift of the SnH_2 , that the compound might be compound **15** (**Figure 18**) rather than compound **14** that is being isolated and analyzed.

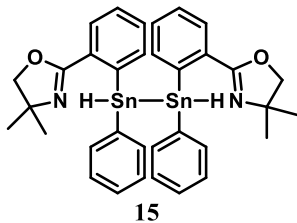


Figure 18: Structure of distannane dihydride **15**.

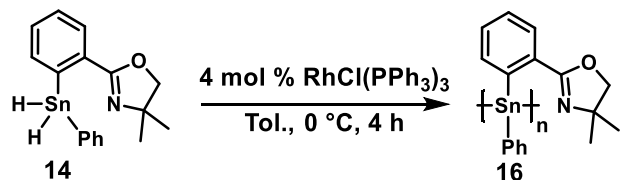
There is little to no studies or prevalence of distannane dihydrides in the literature, probably due to their presumed instability and the likely difficult synthesis of these compounds. HRMS of this product was collected and a $[M-H]^-$ was observed which could be a result of either compound **14** or **15** ionizing. There was evidence in the HRMS spectrum of compound **15**, however resolution was inadequate, so an accurate mass could not be determined. However, due to the integration of the hydride signal (int. = 2H) plus the corresponding $^{117/119}\text{Sn}$ satellites in the ^1H NMR spectrum, it is believed that compound **14** is being isolated. If **15** was being isolated this hydride signal at 6.79 ppm should integrate to one relative to the methylene protons on the oxazoline, however the integration of the ^1H NMR shows the expected 2:2 ratio, giving evidence for **14**. The assignment of these apparent tin satellites is currently undetermined and conclusive evidence for **15** was therefore not revealed.

2.4. Synthesis of homopolymer **16**

2.4.1 Dehydropolymerization using Wilkinson's catalyst

Since dihydride **14** is temperature sensitive and starts reacting readily in an NMR tube, the tin dihydride is carried through to the polymerization without spectroscopic confirmation. Typically, dehydropolymerization of this type are performed at room temperature, however in this case a temperature of 0 °C was used (**Scheme 8**). This was done to try and slow down the

decomposition reaction of **14**, seemingly with itself before it would interact with Wilkinson's catalyst and initiate polymerization.



Scheme 8: Reaction scheme of the synthesis of polymer **16**.

The crude ^{119}Sn NMR spectrum of product **16** showed a few unidentified resonances so the crude polymer was cleaned by dissolving it in a minimal amount of THF and dropping the solution into cold stirring hexanes (3×75 mL) and heptane (1×75) which results in the polymer being isolated as a pale-yellow powder. A single broad tin resonance at -268.09 ppm in the ^{119}Sn NMR spectrum is obtained of this material. This is about a 20 ppm upfield shift relative to that of the dihydride. Polymer **16** is only partially soluble in C_6D_6 and therefore is difficult to get a concentrated sample. The ^1H NMR spectrum showed the disappearance of the Sn-H signal ($\delta_{\text{IH}} = 6.79$ ppm) and a broadening of the other resonances, a characteristic of polymers. The integration of the methylene protons of the oxazoline correspond relative to the aromatic signals however, the methyl groups overlap with residual hexane/ heptane and therefore accurate integration value for that signal is likewise problematic.

Triple detection gel permeation chromatography (GPC) was performed to determine the absolute molecular weight of **16**. Polymer **16** has low solubility in THF in which the GPC is performed but a chromatogram was still able to be collected at this low concentration (< 10 mg/mL). The chromatogram (**Figure 19**) shows a bimodal distribution. From the 18-19 mL retention volume is indicative of the higher molecular weight chains than those represented by the peak between 20-20.50 mL. Low molecular weight chains are likely represented in the signal at

approximately 20.00 mL. The molecular weight determined from this distribution will not be precise as a result of the bimodal distribution, but preliminary results show a molecular weight of ~ 10,100 Da, which corresponds to approximately 27 repeat units. A PDI value of 1.73 is likewise obtained.

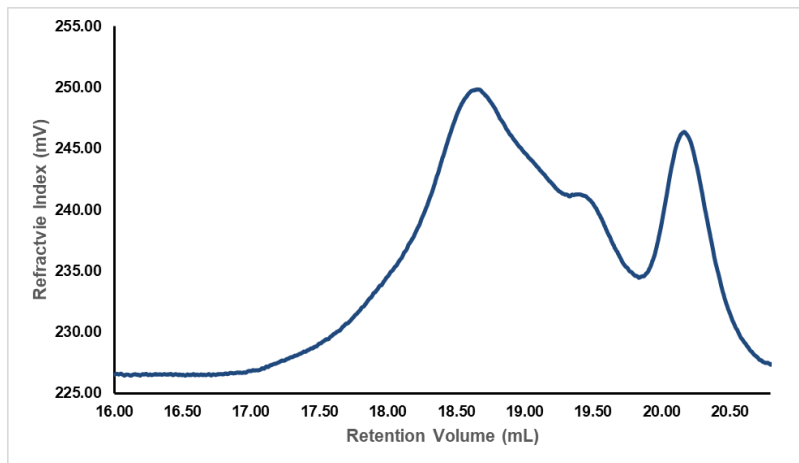


Figure 19: GPC chromatogram of polymer **16**.

A second attempt at the polymerization was done, however this time it was performed at RT in hopes of increasing the molecular weight by increasing the rate of reaction of Wilkinson's catalyst. However, upon ^{119}Sn NMR analysis showed complete consumption of **14** and the appearance of several sharp resonances and a small broad signal at -268 ppm resembling polymer **16** (**Figure 20a**). After cleaning several times, solubility further decreased, and several sharp signals are still present (**Figure 20b**). No detectable amount of polymer was present when GPC analysis was performed. Due to the reactive nature of **14**, proceeding at RT may cause **14** to react irreversibly with itself forming cyclic and other unreactive oligomers before interacting with Wilkinson's catalyst.

An attempt at the polymerization of **14** at -30 °C for 4 h was undertaken to try and limit undesired side reactions. No evidence of the previously obtained polymer ($\delta_{^{119}\text{Sn}} = -268$ ppm) was

observed, however a broad signal was noted ($\delta_{^{119}\text{Sn}} = -280$ ppm) (**Figure 20c**). Unfortunately, GPC analysis showed no evidence of polymer under these conditions.

Another attempt at the polymerization of **14** was conducted at -30 °C for 6 h. A longer reaction time was attempted due to the decreased reactivity of Wilkinson's catalyst at a lower temperature. However, upon cleaning of the resulting products, no polymer was detected via ^{119}Sn NMR spectroscopy (**Figure 20d**). After these attempts, it was assumed that the polymerization of **14** likely yielded only short oligomeric chains.

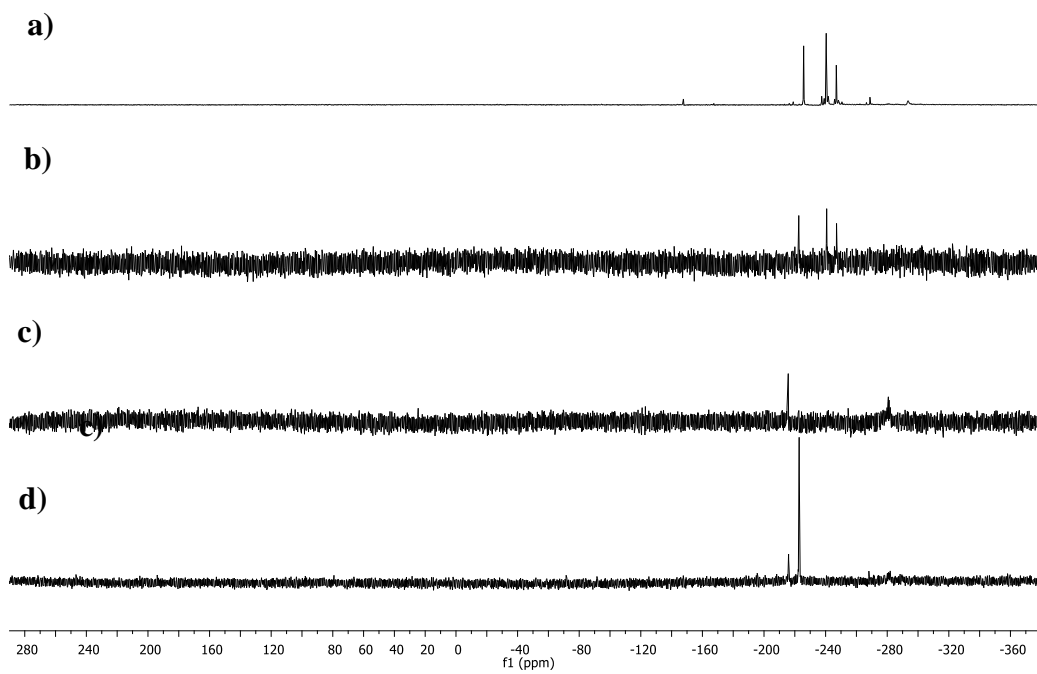
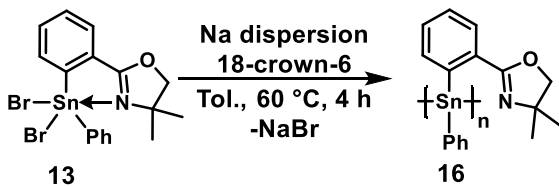


Figure 20: ^{119}Sn NMR spectrum of crude samples of **16** at RT (a), RT after cleaning four times (b), doing the polymerization at -30 °C for 4 h (c), and doing the polymerization at -30 °C for 6 h.

2.4.2 Wurtz Coupling



Scheme 9: Reaction scheme for the synthesis of **16** via Wurtz coupling.

A Wurtz coupling reaction using dibromide **13** to yield polymer **16** was attempted. In the Wurtz coupling, clean, shaven Na metal was dispersed into toluene and refluxed at 110 °C for 1 h. After which, the Na dispersion was cooled down to RT, followed by the addition of a mixture of **13** and 18-crown-6. This was further allowed to react for 4 h at 60 °C. After 4 h, the reaction mixture was filtered in an inert atmosphere to dispose of the Na metal. After removal of the solvent, of a bright yellow coloured gel was obtained. ^{119}Sn NMR analysis showed a small broad resonance at -268 ppm similar to that previously obtained by dehydropolymerization, however the major resonance was starting material ($\delta_{119\text{Sn}} = -268$ ppm -286.7 (C₆D₆)) (**Figure 21a**). No further analysis was done of this material. A second attempt was likewise performed, however after NMR analysis, it was determined that only compound **13** was present and hence no reaction had occurred (**Figure 21b**).

A third attempt was performed, however in this attempt 15-crown-5 was used rather than 18-crown-6. This reaction yielded a white coloured powder; the yellow colour indicative of polystannanes were not visible. In this attempt, a small broad resonance at -268 ppm similar to what was previously obtained with both the Wurtz coupling and dehydropolymerization was noted (**Figure 21c**). Upon cleaning with the same method previously described, all species present seemingly precipitated out of solution after NMR analysis. GPC analysis was performed on this mixture; however no evidence of polymer was detected. The lack of significant polymer formation

via these three attempts might be a result of the difficulty in obtaining finely dispersed good sodium metal before **13** is added into the solution.

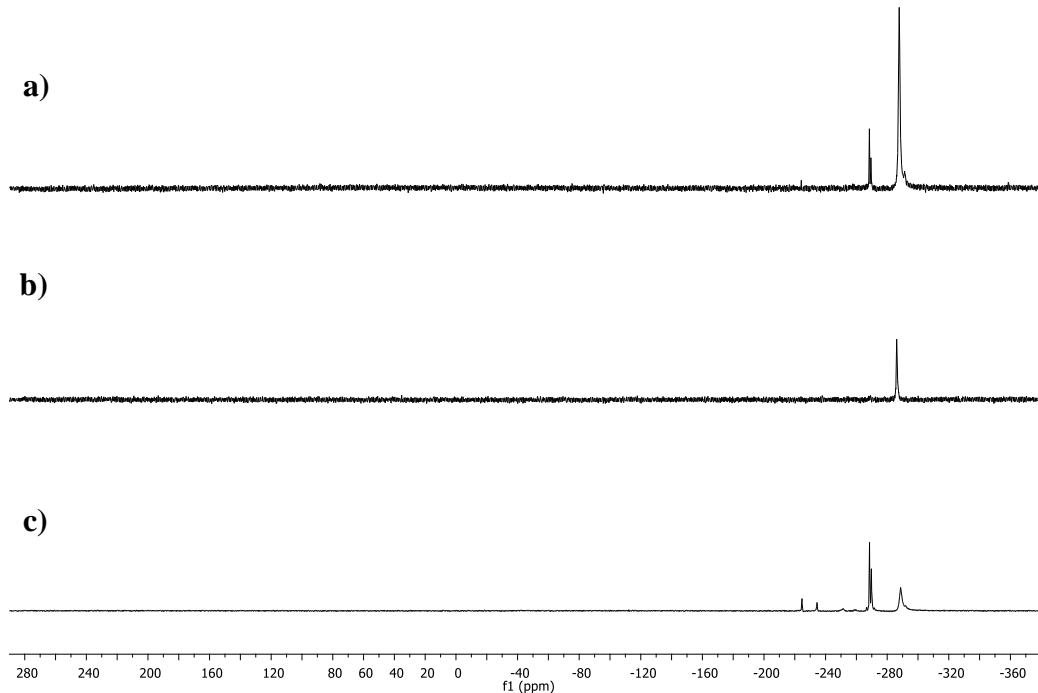


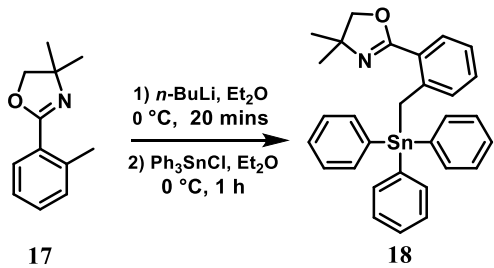
Figure 21: ^{119}Sn NMR spectrum of the attempted Wurtz coupling reaction of **13**.

2.5 Synthesis and characterization of 4,4-dimethyl-2-(2-((triphenylstannylyl)methyl)phenyl)-4,5-dihydrooxazole **18**

As mentioned previously by Choffat *et al.*⁴⁹, diaryl tin hydrides were determined to be incompatible with Wilkinson's catalyst. However, it has been recently shown that diaryl species can be dehydrogenative coupled using Wilkinson's catalyst.⁶³ Unfortunately, only low molecular weight polymer is obtained. A more flexible version of the previously mentioned oxazolines was sought in the dehydropolymerization to hopefully yield high molecular weight polystannanes.

Gschwend *et al.*⁵⁶ demonstrated that the methyl group of the phenyl ring in 4,4-dimethyl-2-(o-tolyl)-4,5-dihydrooxazole (**17**) can be lithiated at 0 °C and then reacted with various

electrophiles, however no examples with tin as the electrophile are present in literature. This oxazoline **17** (**Scheme 10**) was synthesized using the same method mentioned earlier (section 2.1) for the synthesis of **8**, however *o*-toluic acid was used instead of 2-bromobenzoic acid. Lithiation of this oxazoline was performed as reported⁵⁶ and after the addition of *n*-BuLi, the clear colourless solution turned a cloudy deep red colour. After the addition of Ph₃SnCl, the solution turned an opaque yellow. Following removal of the reaction solvent (Et₂O), precipitation of the salt (LiCl) was carried out with the use of toluene. Gravity filtration was carried out, and removal of the toluene, a yellow coloured powder was obtained. The ¹¹⁹Sn and ¹H NMR spectra showed impurities, but these could be easily removed through trituration using methanol to afford compound **18** as white crystals.



Scheme 10: Reaction scheme for the synthesis of oxazoline stannane **18**.

The ^1H NMR spectrum of **18** showed similar chemical shifts to that of compound **8** with the addition of the signal corresponding to the methylene protons between the tin and oxazoline. This signal displays ^{119}Sn satellites ($^2J_{1\text{H}-119\text{Sn}} = 75.5$ Hz). A crystal of compound **18** suitable for single crystal X-ray diffraction was obtained (**Figure 22**).

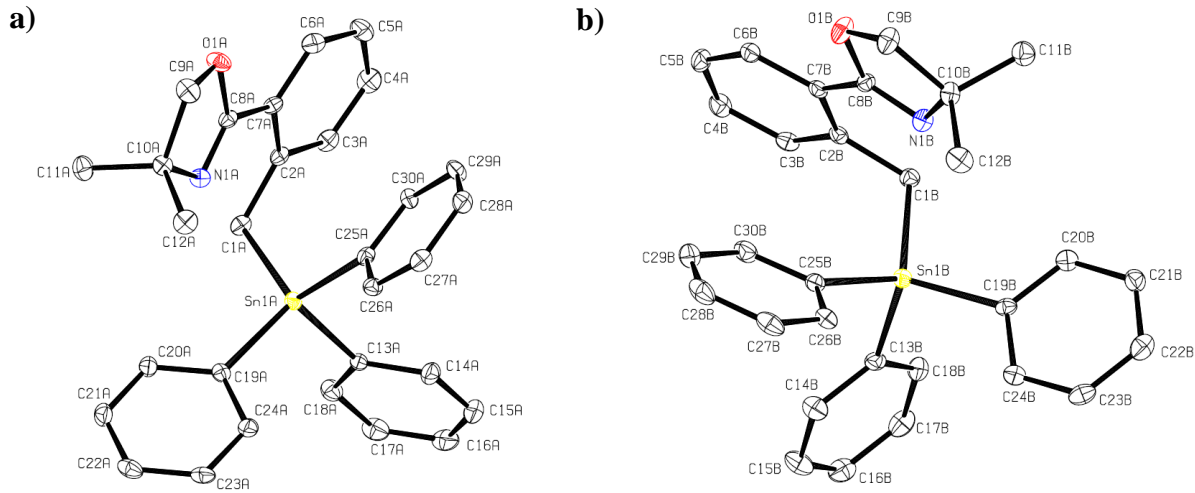


Figure 22: ORTEP representation of two molecules of compound **18** found in the unit cell. Thermal ellipsoids shown at the 30% level.

Table 5: Relevant crystal structure data analysis of **18**.

Bond	Bond Lengths of A (Å)	Bond	Bond Lengths of B (Å)
Sn1A-N1A	3.176(4)	Sn1B-N1B	3.234(4)
Sn1A-C1A	2.162(4)	Sn1B-C1B	2.153(4)
Sn1A-C13A	2.158(4)	Sn1B-C13B	2.155(4)
Sn1-C19A	2.150(4)	Sn1B-C19B	2.139(4)
Sn1-C25A	2.143(4)	Sn1-C25B	2.144(4)

Two unique molecules of **18** are found within the unit cell, each with slightly different bond lengths and angles. The geometry around the tin center of these molecules is a distorted trigonal bipyramidal ($\tau_5 = 0.80, 0.76$ respectively). The equatorial angles around the tin center for both structures are between 103.6° and 116.1° . With the axial angles around the tin centers being $163.2(1)$ and $162.0(1)^\circ$ respectively. The Sn-N bond distance is significantly longer than in compound **10** which is expected due to the CH_2 group present between the tin and the oxazoline. However, it is still within the sum of the van Der Waals radii of tin and nitrogen bond (3.72 Å). Comparing the solid state structures of **10** and **18**, the Sn-C bond lengths are similar however the

elongation of the Sn-C13 in compound **18** bond isn't as prevalent as it was in compound **10** for the related Sn-C12 bond. This is likely a result of the 3c-4e⁻ sharing being less prominent in these molecules due to the longer distance between the tin and the nitrogen leading to a weaker dative interaction.

2.5.1. Attempted synthesis of semi-flexible oxazoline stannane halides

The addition of bromine was added stoichiometrically and done under the same reaction conditions as reported for **10**. Upon addition of the one equivalent of Br₂ (to try and synthesize the monobromide species), three tin resonances were present in the ¹¹⁹Sn NMR spectrum (**Figure 23a**) of the resulting mixture. Compound **18** is assigned to the major resonance at ($\delta_{119\text{Sn}} = -125$ ppm) with two others at -215 and -248 ppm. Assuming the resonance at -215 ppm is the monobromide and the resonance at -248 represents the dibromide, another equivalent of Br₂ was added to this mixture. A ¹¹⁹Sn NMR spectrum of this mixture is shown in **Figure 23b**. Although it appears in the ¹¹⁹Sn NMR spectrum that there is only one tin species, the ¹H NMR shows two sets of resonances corresponding to the oxazoline signals and for this reason another equivalent of Br₂ was added. This then resulted in the appearance of only a single set of oxazoline signals in the ¹H NMR being present and a single resonance in the ¹¹⁹Sn NMR spectrum ($\delta_{119\text{Sn}} = -449$ ppm: **Figure 23c**). This presumably corresponds to the tribromide species, **19** (**Figure 24**). The ¹H NMR spectrum integration values also show this as being the likely product due to the integration of the aromatic protons equalling four, and no evidence of the other phenyl substituents is observed. Attempts to separate the mixture represented in **Figure 22a** was deemed unsuccessful as these compounds would not elute on a TLC plate using polar or non-polar solvents.

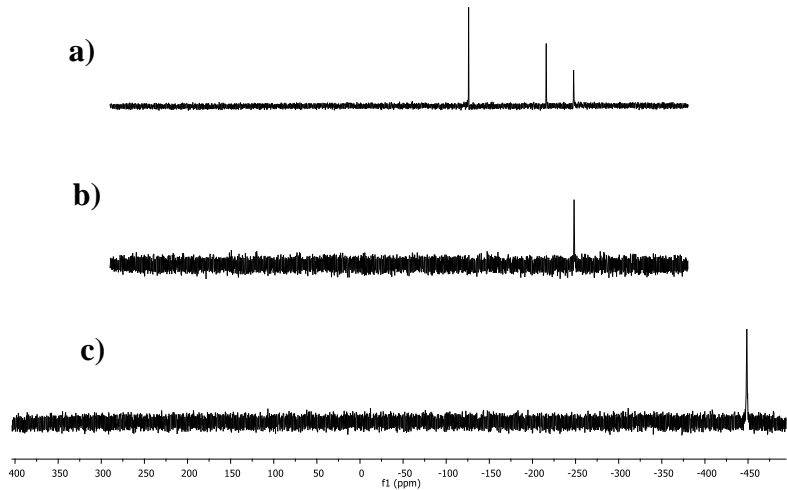


Figure 23: ^{119}Sn NMR spectrum (CDCl_3) of the reaction with compound **18** and Br_2 .



Figure 24: Structure of **19**.

Attempts were also undertaken to perform a step-wise chlorination of compound **18**. However, the results weren't comparable to that of the attempted bromination. A broad ^{119}Sn resonance appears at -60 ppm with a smaller resonance at -206 ppm (**Figure 25a**) in this experiment. A second equivalent of $\text{HCl}/\text{Et}_2\text{O}$ was added to this same reaction mixture which resulted in two different tin resonances, -90 and -233 ppm (**Figure 25b**). The resonance at -233 ppm might correspond to the dichloride however no separation was attempted. The order of

addition, temperatures and the speed of addition of the HCl/Et₂O were all varied, however similar results were observed *via* ¹¹⁹Sn NMR spectroscopy.

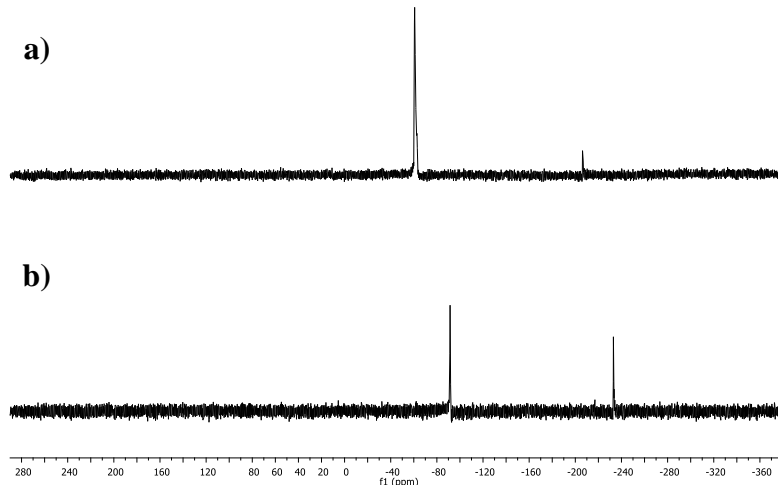
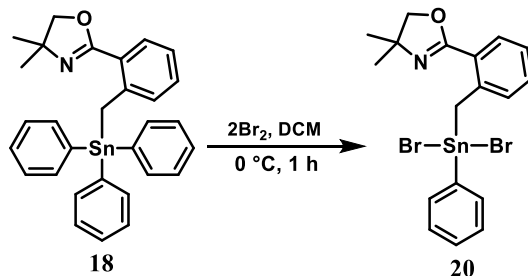


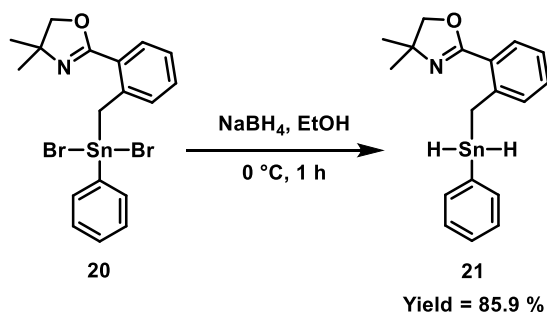
Figure 25: ¹¹⁹Sn NMR spectrum (CDCl₃) of the reaction with compound **18** and HCl/Et₂O.

Bromination of organotin (IV) compounds have been reported in literature in solvents such as CCl₄, CHCl₃ and CH₂Cl₂ so the attempted synthesis of **20** was performed in dry DCM (**Scheme 11**). This resulted in the observation of a single tin resonance was seen in the ¹¹⁹Sn NMR spectrum at -248.2 ppm in CDCl₃ and no additional bromine was needed for this reaction. The upfield shift of about 120 ppm may be due to the increased interaction between the nitrogen and the tin atoms. The ¹H NMR showed some impurities, but these could be removed through trituration with MeOH to yield **20** as a white coloured powder.



Scheme 11: Reaction scheme for the synthesis of **20**.

2.5.2 Synthesis of 4,4-dimethyl-2-(2-((phenylstannyl)methyl)phenyl)-4,5-dihydrooxazole 21:



Scheme 12: Reaction scheme for the synthesis of **21**.

The synthesis of **21** was carried out through a more traditional route that is often used to synthesize tin dihydrides from tin dihalides. A large excess of NaBH_4 in EtOH for 1 h at 0°C was used in this case (**Scheme 12**) to yield hydride **21** after work-up as a colourless viscous oil in good yield. This compound also quickly started turning yellow in colour, however, NMR analysis was still able to be carried out.

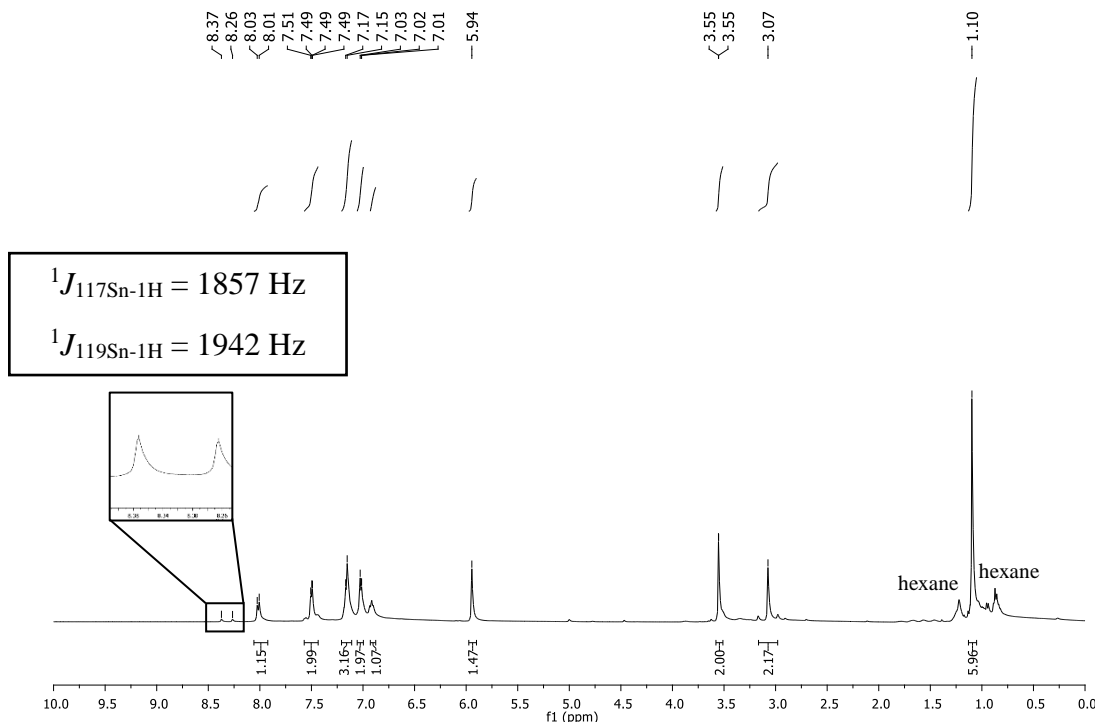
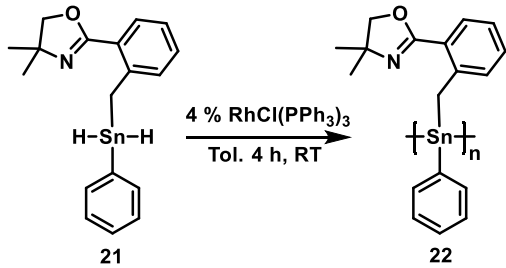


Figure 26: ^1H NMR (C_6D_6) spectrum of **21**.

In the ^1H NMR spectrum (**Figure 26**), the hydride signal appears at $\delta_{\text{IH}} = 5.94$ ppm which has $^{117}/^{119}\text{Sn}$ satellites equidistant from this singlet, however only one set is visible with the other set being overlaid by the signal at $\delta_{\text{IH}} = 3.55$ ppm. A single resonance was seen in the ^{119}Sn NMR spectrum ($\delta_{119\text{Sn}} = -221.02$). This is about a thirty ppm downfield shift relative to dihydride **14**. This difference in shift is likely a result of **21** being more flexible than **14** allowing the nitrogen to be at a greater distance away from the tin which is less Lewis acidic when hydrides are bonded to it relative to halides.

2.5.3 Synthesis of polymer **22**:



Scheme 13: Reaction scheme for the synthesis of polymer **22**.

Due to the better stability of **21** compared to **14**, the synthesis of polymer **22** was carried out using Wilkinson's catalyst for 4 h at RT (**Scheme 13**) to yield a yellow coloured powder after work up. Preliminary ^{119}Sn NMR analysis showed five tin resonances ($\delta_{119\text{Sn}} = -186.6, -204.8, -217.9, -220.9$, and -268.8 ppm) in the crude NMR spectrum (**Figure 27a**). It is unclear what signal corresponds to **22** until cleaning is done. The crude polymer was cleaned by dissolving it in a minimal amount of THF and dropping the solution into cold stirring hexanes (2×75 mL) and heptane (2×75) which results in the polymer being isolated as a pale-yellow powder. After cleaning, a single resonance is present ($\delta_{119\text{Sn}} = -183.8$ ppm: **Figure 27b**). This chemical shift

indicates that the oxazoline substituent is likely not coordinating to the tin center. Polystannanes containing a hypercoordinating ligand typically show a resonance of > 200 ppm.^{51-52, 62}

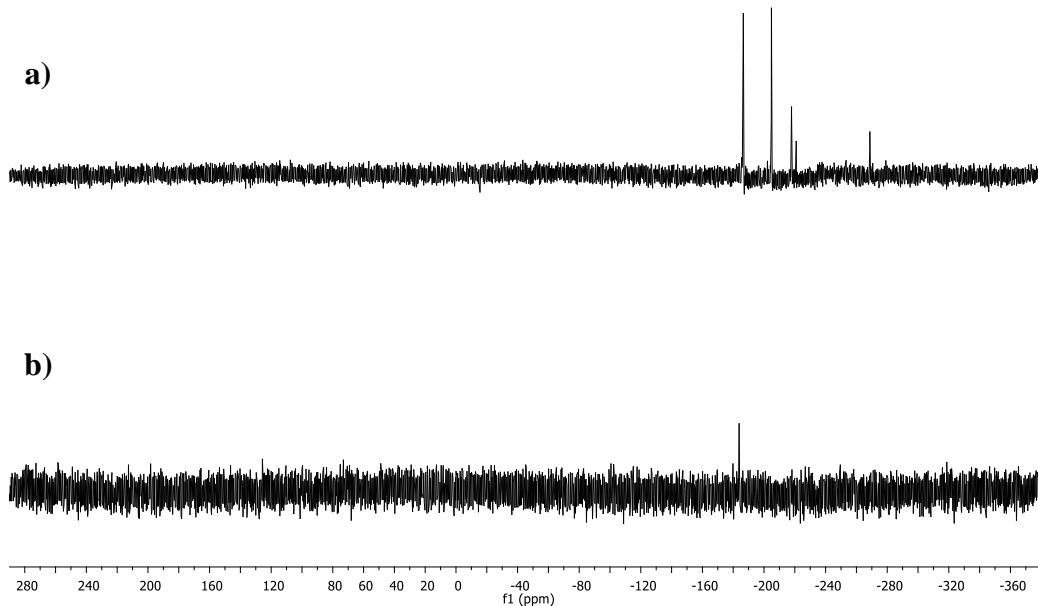


Figure 27: Crude (a) and clean (b) ^{119}Sn NMR spectrum of **22** in C_6D_6 .

Preliminary GPC analysis of this crude mixture showed three different signals (**Figure 28:** top). One at approximately 18.00 mL and a second at 20.00 mL. The peak at 18.00 mL is indicative of a higher molecular weight polymer which has a molecular weight of approximately 15,400 Da with a PDI value of 1.03. Together both signals within the GPC showed a molecular weight of 24,400 Da and a PDI value 1.82. These values are rough estimates and will change after cleaning of the polymer. After cleaning, the GPC chromatograph (**Figure 28:** bottom) showed the disappearance of the signal at 20.00 retention volume, and a bimodal distribution at about 18.00 mL. However, GPC analysis showed a molecular weight of 3,200 Da, which corresponds to

approximately seven repeat units, with a PDI value of 1.56. This molecular weight is lower than that obtained with polymer **16**.

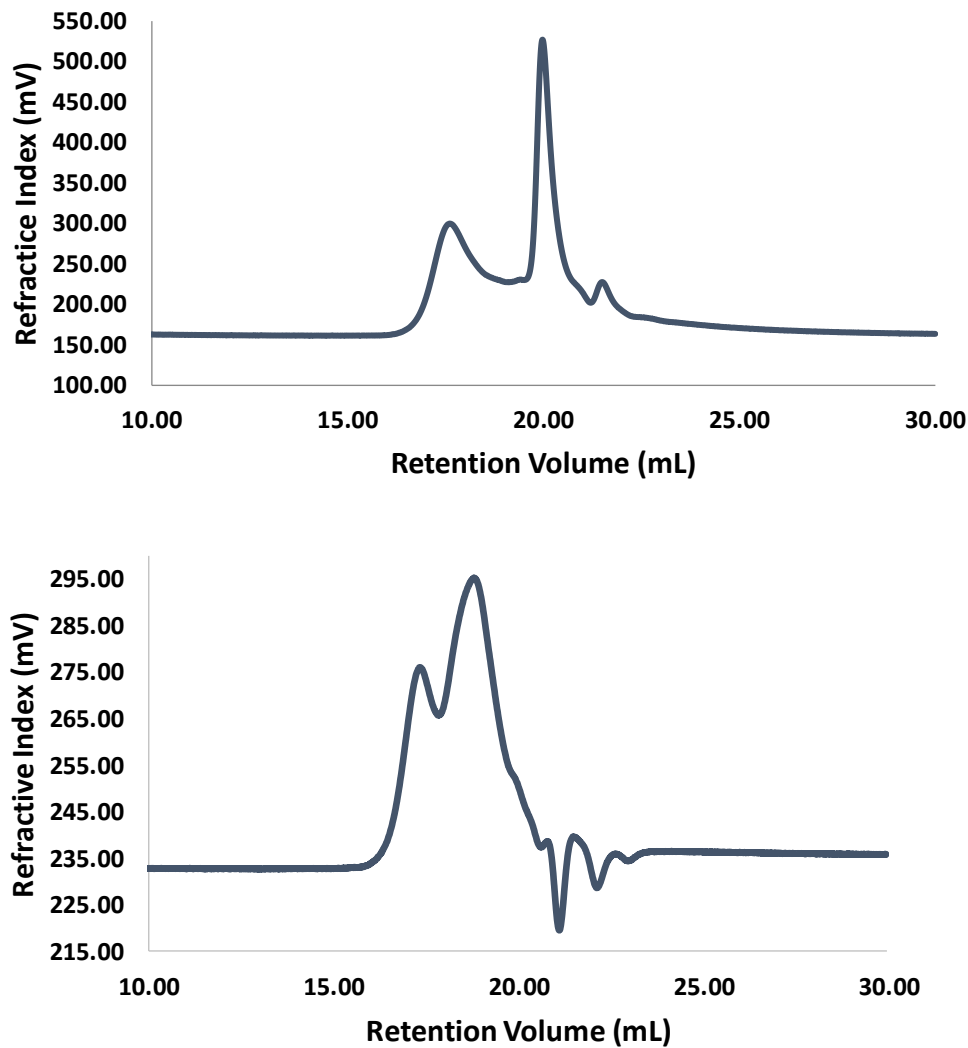
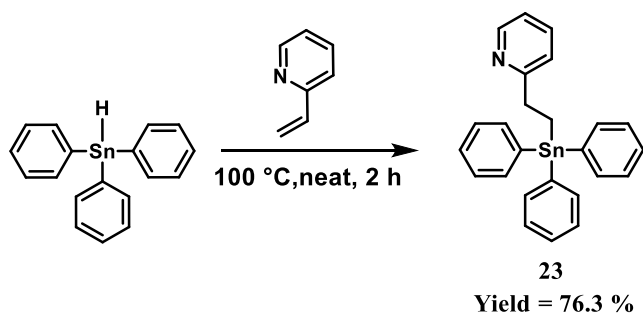


Figure 28: Crude GPC (top), after cleaning GPC (bottom) chromatogram of **22**.

2.6 Synthesis of of 2-(2-(triphenylstannylyl)ethyl)pyridine **23**:

Mollov *et al.*¹⁸ previously reported the synthesis of 2-(2-(triphenylstannylyl)ethyl)pyridine through the addition of 2-vinylpyridine in a slight excess to triphenyltin hydride, neat and heated to 100 °C for 2 h (**Scheme 12**). This results in a couple of by-products as seen in the ¹¹⁹Sn NMR

spectrum, one being hexaphenyl distannane. This can be removed through recrystallization to yield **23** as a white coloured powder. Alternate routes including the addition of AIBN, a radical initiator was used in different ratios to try to prevent the unwanted by-products. However, this proved ineffective therefore the reaction was performed without AIBN. After purification, the ^1H , ^{13}C and ^{119}Sn NMR (**Figure 30a**) spectra of **23** agreed with that reported by Molloy *et al.*¹⁸



Scheme 14: Reaction scheme for the synthesis of compound **23**.

A crystal of compound **23** suitable for single crystal X-ray diffraction was obtained (**Figure 29**). The geometry of this molecule around tin is distorted trigonal bipyramidal ($\tau_5 = 0.74$) with equatorial bond angles around the tin center between 102.4° and 120.8° and an axial bond angle of $165.14(7)^\circ$. The bond length between Sn1 and C20 is longer than the other tin carbon bonds (**Table 6**) due to these atoms being in the axial position along with the nitrogen atom, presumably resulting in 3c-4e⁻ sharing. The tin nitrogen bond distance is 2.888 \AA which is slightly longer than what is present in the solid state structure of **10** (Sn-N: 2.762 \AA) but shorter than the bond distances found in the solid state structures of **18** (Sn-N: 3.176 \AA , 3.234 \AA). The shorter Sn-N bond distance seen in **23** relative to **18**, despite there being a flexible ethyl chain which allows the pyridine ring to extend away from the tin center, is likely a result of the pyridine ring being less sterically encumbering than the oxazoline ring in **18**. This allows the ring nitrogen of the pyridine ring to be drawn closer to the Lewis acidic tin.

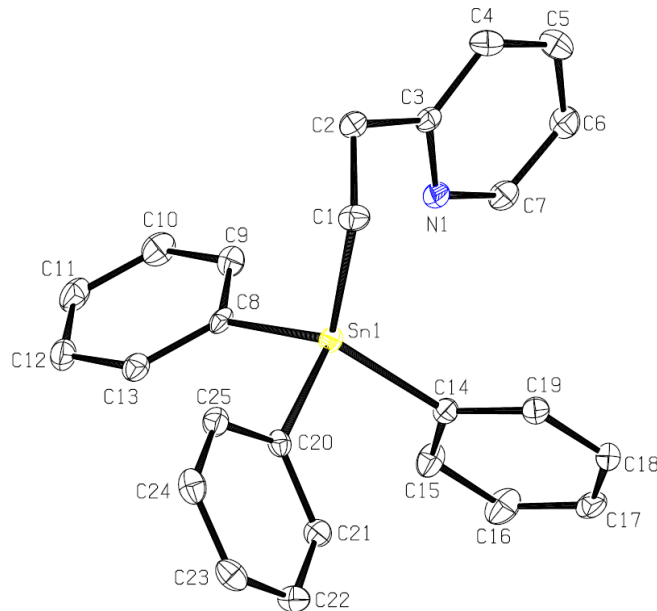


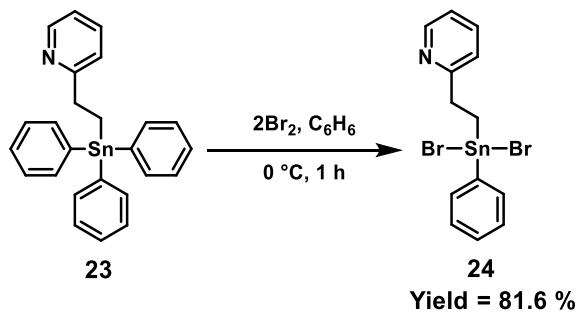
Figure 29: ORTEP representation of unit cell molecule of **23**. Thermal ellipsoids drawn at the 30 % level.

Table 6: Relevant parameters obtained from the crystal data analysis of **23**.

Bond	Bond Lengths (Å)
Sn1-N1	2.888
Sn1-C8	2.154(2)
Sn1-C14	2.144(2)
Sn1-C20	2.162(2)
Angle	Bond Angle (°)
N1-Sn1-C20	165.14

2.7 Synthesis of 2-(2-(dibromo(phenyl)stannyl)ethyl)pyridine **24**:

Molloy *et al.*¹⁸ reported the reaction between compound **23** (¹¹⁹Sn δ = -108.5 ppm: **Figure 30a**) and one equivalent of Br₂ to yield the monobromide species after recrystallization; a compound yielding a single ¹¹⁹Sn tin resonance at -143.5 ppm. However, no dihalides of these compounds have been reported in the literature.



Scheme 15: Reaction scheme for the synthesis of compound **24**.

The synthesis of the monobromide was not attempted and two equivalents of Br_2 were added directly to compound **23**. This resulted in a mixture of four tin resonances in the ^{119}Sn NMR spectrum: -60, -75, -143, and -184 ppm (major). Due to the presence of a signal at -143 ppm, reported as the chemical shift of the monobromide species, another equivalent of Br_2 was added which resulted in two tin resonances ($\delta_{^{119}\text{Sn}} = -73$ and -184 ppm) being observed by NMR. This mixture was isolated as a viscous dark orange gel and was recrystallized with the method as reported by Molloy of the monobromide using a mixture of petroleum ether and ethyl acetate. This resulted in compound **24** being isolated as a white coloured powder. The integration of the ^1H NMR matches to what is expected of the dibromide species; a single tin resonance is also present in the ^{119}Sn NMR spectra ($\delta_{^{119}\text{Sn}} = -184$ ppm: **Figure 30b**). A crystal of **24** suitable for single crystal X-ray diffraction was obtained (**Figure 31**)

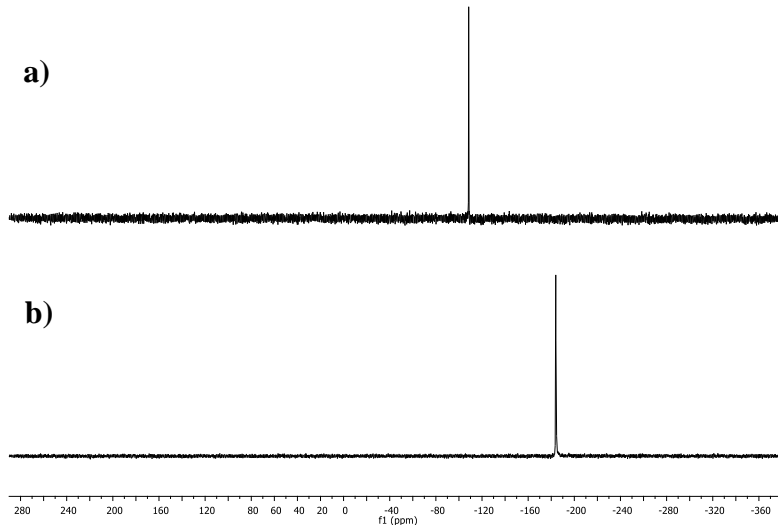


Figure 30: ^{119}Sn NMR spectra of compounds **23(a)** and **24(b)**.

Two unique molecules of **24** were formed within the unit cell, differing slightly in bond lengths and angles (**Figure 31**). The geometry around the tin center of both these molecules is distorted trigonal bipyramidal ($\tau_5 = 0.56$, $\tau_5 = 0.59$ respectively). Equatorial angles around the tin center range between $76.7(2)$ and $136.9(2)$ $^{\circ}$. The Sn-N bond lengths are considerably shorter than the triphenyl analogue **23**. This is likely a result of the withdrawing effect of the bromine atoms, causing the tin center to be more electropositive than the tin center in **23**, resulting in the nitrogen atom being drawn closer to the tin center. After the synthesis of the monobromide species, Molloy *et al.* reported substitution of the bromine atom with a *N,N*-dimethyldithiocarbamate substituent. A solid-state structure of this molecule revealed a Sn-N bond length of $2.486(7)$ \AA . The 3c-4e $^{-}$ sharing is evident between the nitrogen, tin and bromine atoms. The Sn1-Br1 atoms in both molecules are present in the axial positions, presumably participating in the 3c-4e $^{-}$ sharing. This causes the Sn1-Br1 bond length to be elongated relative to the Sn1-Br2 bonds which are in the equatorial positions and therefore, presumably not participating in the 3c-4e $^{-}$ sharing (**Table 7**).

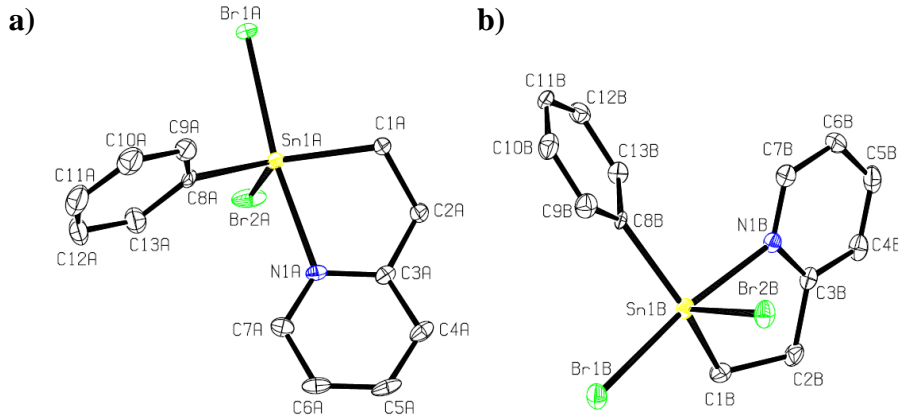


Figure 31: ORTEP representation of two molecules of compound **24** found in the unit cell.
Thermal ellipsoids shown at the 30 % level.

Table 7: Relevant parameters obtained from the crystal data analysis of **24**.

Bond	Bond Lengths of A (Å)	Bond	Bond Lengths of B (Å)
Sn1A-N1A	2.382(5)	Sn1B-N1B	2.363(5)
Sn1A-C1A	2.120(6)	Sn1B-C1B	2.115(6)
Sn1A-C8A	2.131(7)	Sn1B-C8B	2.138(6)
Sn1A-Br1A	2.6298(7)	Sn1B-Br1B	2.6176(8)
Sn1A-Br2A	2.5058(8)	Sn1B-Br2B	2.5223(8)

In the future, compound **24** will be synthesized into the corresponding dihydride and further undergo dehydropolymerization to synthesize the polymer which will be further investigated.

3.0 Conclusions

A series of novel rigid hypercoordinate organotin compounds containing a chelating oxazoline ring (**10**, **11**, **13**, **14**) were synthesized and characterized by NMR spectroscopy (^1H , ^{13}C , ^{119}Sn , HSQC, COSY and HMBC). These compounds were also characterized by HRMS and/or X-ray crystallography. X-ray crystallography of compounds **10**, **11**, and **13** showed relatively short tin-nitrogen bond distances, the distance becoming shorter with the addition of electronegative atoms (Cl, Br). The synthesis of compound **14** proved quite difficult as a result of the product being quite reactive at temperatures above -20 °C. The dehydropolymerization of this compound was attempted with a variety of conditions, however synthesis of high molecular weight polymers proved difficult. This is likely a result of the steric hindrance around the tin center and the close proximity of the chelating oxazoline ring causing interaction with Wilkinson's catalyst troublesome. The Wurtz coupling of **13** was also explored, however the synthesis of polymer from this method also proved quite difficult. The addition of a methylene group between the chelating oxazoline and tin was explored in hopes of producing higher molecular weight polymers.

The novel semi-flexible organotin compounds containing a chelating oxazoline ring (**18**, **20**, and **21**) were synthesized and characterized by NMR spectroscopy (^1H , ^{13}C , ^{119}Sn , HSQC, COSY and HMBC). These compounds were also characterized by HRMS and/or X-ray crystallography. X-ray crystallography of **18** revealed a larger tin-nitrogen bond distance from the ring nitrogen to the tin compared to that of **10** which was expected due to the methylene bridge. The synthesis of **21** was relatively easy and more stable than dihydride **14** which resulted in a low molecular weight polymer in the preliminary GPC analysis.

Organotin compounds containing a flexible ethyl pyridine chain (**23** and **24**) were also explored. These compounds were also characterized by NMR spectroscopy (^1H , ^{13}C , ^{119}Sn , HSQC,

COSY and HMBC). These compounds were also characterized by HRMS and/or X-ray crystallography. X-ray crystallography revealed a relatively short tin-nitrogen bond distance in between that of **10** and **13**. Due to time restrictions, and focus on the oxazoline projects, the tin dihydrides of the pyridine analogues was not attempted.

4.0 Future Work

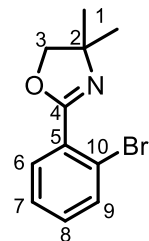
In this work, novel organotin compounds containing chelating nitrogen donors were explored. It is likely in the case of polymer **16** that the dative interaction is preserved due to the upfield chemical shift ($\delta_{^{119}\text{Sn}} = -268$ ppm) relative to known 4-coordinate polystannanes which typically resonate around -190 - -200 ppm. Other catalysts should be explored in the polymerization of **16** in hopes of producing higher molecular weight polymers. The more flexible chelating oxazoline showed greater promise in the synthesis of a polymer and should be further explored. An organotin compound containing an ethyl bridge between the tin atom and the oxazoline might offer more flexibility and even higher molecular weights with the stability of the three polymers being compared. This monomer can be synthesized by lithiating **9** and further reacting this compound with allyl bromide⁵⁶ to yield an ortho allyl group. This can further undergo a hydrostannaylation reaction. The organotin compounds containing the ethyl pyridyl compounds show promise in synthesizing stabilized polystannanes through hypercoordination and should further be explored.

5.0 Experimental

General Considerations

All reagents and solvents were obtained from Sigma-Aldrich and used as received, unless otherwise indicated. Solvents were dried either through an MBraun solvent drying system, or through vacuum distillation and stored under an inert nitrogen atmosphere. All reactions were carried out under nitrogen atmosphere using Schlenk techniques unless otherwise noted. Nuclear magnetic resonance (NMR) spectroscopic experiments were carried out on a Bruker 400 MHz Spectrometer using CDCl₃ or C₆D₆ as the solvent. ¹H NMR (400 MHz) and ¹³C NMR (100.6 MHz) spectra were referenced to the residual proton and central carbon resonance of the solvent. The ¹¹⁹Sn NMR (149 MHz) was referenced to SnMe₄, respectively as internal standards. All the chemical shifts are given in δ (ppm) relative to the solvent and assigned to atoms. All NMR spectra were analyzed on MestReNova v6.0.2 software. High-resolution mass spectrometry was performed using an accuTOF DART-MS at the University of Toronto. Molecular weights of polymers were determined by gel permeation chromatography (GPC) using a Viscotek Triple Model 302 Detector system equipped with a Refractive Index Detector (RI), a four capillary differential viscometer (VISC), a right angle (90°) laser light scattering detector. GPC columns were calibrated versus polystyrene standards (American Polymer Standards). A flow rate of 1.0 mL min⁻¹ was used with ACS grade THF as eluent. GPC sample were prepared using 10-15 mg of polymers per mL THF, and filtered using a 0.45 μm filter. All reactions were carried out under a nitrogen atmosphere using Schlenk techniques unless otherwise described. A Bruker-Nonius Kappa-CCD diffractometer at the University of Toronto was used to obtain the X-ray diffraction data for crystal structures.

5.1 Synthesis of 2-(2-bromophenyl)-4,4-dimethyl-4,5-dihydrooxazole (8):



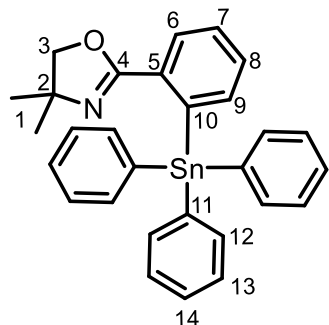
Method 1⁵⁵:

Thionyl chloride (3.60 mL, 49.8 mmol) and 3 drops of DMF were added to a 250 mL round bottom flask containing 2-bromobenzoic acid (5.00 g, 24.9 mmol) in 100 mL of dry DCM. The reaction mixture was heated to reflux temperature for 2 h. The solvent and excess thionyl chloride were then removed under reduced pressure to afford a yellow coloured liquid. The product was dissolved in 30 mL of dry DCM and then added dropwise to a 250 mL round bottom flask containing a stirring solution of distilled 2-amino-2-methyl-1-propanol (2.66 g, 29.9 mmol) and triethylamine (5.20 mL, 37.3 mmol) in 100 mL of dry DCM at 0 °C. The reaction mixture was then stirred for 4 h at RT. The crude sample was washed once with 30 mL of 1 M solution of aqueous HCl and 2 × 30 mL of a saturated aqueous brine solution. The organic layer was then dried over anhydrous MgSO₄, filtered and the solvent removed under reduced pressure to afford 2-bromo-N-(1-hydroxy-2-methylpropan-2-yl)benzamide as a white coloured powder in a 82.0 % yield. The benzamide (5.55 g, 20.4 mol) was dissolved in SOCl₂ (15.0 mL, 206 mmol) at 0 °C. The solution was stirred at room temperature for 24 h, after which 100 mL of Et₂O was added and the precipitate collected via vacuum filtration and dissolved in 50 mL of DCM. The DCM mixture was washed with a saturated aqueous solution of NaHCO₃ until the organic layer was neutral and then dried over anhydrous MgSO₄. After filtration, the solvent was removed under reduced pressure to yield 2-(2-bromophenyl)-4,4-dimethyl-2-oxazoline as a white coloured powder. Yield: 4.75 g, 75.2 %. NMR data (¹H, ¹³C) matches reported literature data within experimental error.⁵⁵

Method 2⁵³:

A solution containing 2-bromobenzonitrile (0.50 g, 2.75 mmol), 2-amino-2-methyl-1-propanol (0.37 g, 4.12 mmol) and anhydrous ZnCl₂ (0.037 g, 0.27 mmol) were heated to reflux temperature in 15 mL of chlorobenzene for 24 h. The solvent was then removed under reduced pressure. The crude product was purified via flash chromatography (EtOAc/Hex (1:1)) to yield 2-(2-bromophenyl)-4,4-dimethyl-2-oxazoline as a white coloured powder. Yield: 0.52 g, 74.2 %. m.p. 39–40 °C (Lit. 36–38 °C) NMR data (¹H, ¹³C) matches reported literature data within experimental error.² **¹H NMR** (400.13 MHz, CDCl₃, δ): 7.66 (dd, 1H, H6, ³J_{1H-1H}= 7.78 Hz, ⁴J_{1H-1H}= 1.51 Hz), 7.63 (dd, 1H, H9, ³J_{1H-1H}= 7.78 Hz, ⁴J_{1H-1H}= 1.00 Hz), 7.34 (ddd, 1H, H7, ³J_{1H-1H}= 7.53 Hz, ⁴J_{1H-1H}= 1.00 Hz), 7.28 (ddd, 1H, H8, ³J_{1H-1H}= 7.53 Hz, ⁴J_{1H-1H}= 1.76 Hz), 4.16 (s, 2H, H3), 1.43 (s, 6H, H1) ppm. **¹³C{¹H} NMR** (100.61 MHz, CDCl₃, δ): 161.79 (C4), 133.59 (C9), 131.56 (C8), 131.26 (C6), 130.27 (C10), 127.07 (C7), 121.82 (C5), 79.44 (C3), 68.05 (C2), 28.25 (C1) ppm.

5.2 Synthesis of 4,4-dimethyl-2-(2-(triphenylstannylyl)phenyl)-4,5-dihydrooxazole (10):



Method 1:

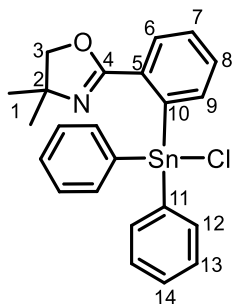
2-(2-bromophenyl)-4,4-dimethyl-4,5-dihydrooxazole (0.565 g, 2.22 mmol) and 15 mL of dry Et₂O were added to a dry 100 mL Schlenk flask. The solution was cooled to -84 °C and 1.6 M *n*-BuLi/hexane (1.52 mL, 2.45 mmol) was added dropwise. The reaction mixture stirred for 2 h at -84 °C then allowed to warm up to 0 °C before the addition of triphenyltin chloride (0.857 g, 2.22 mmol) in 20 mL of Et₂O was added dropwise. The reaction mixture was stirred for 1 h at 0 °C. The solvent was removed under reduced pressure and 20 mL of toluene was added. The mixture was filtered via gravity filtration and the solvent was removed under reduced pressure to yield a pale yellow coloured powder. The crude product was triturated with MeOH and the yellow solution was decanted off. The residual solvent was removed under reduced pressure to yield the product as a white coloured powder. Yield: 0.86 g, 73.9 %.

Method 2:

4,4-dimethyl-2-phenyl-2-oxazoline (5.00 g, 28.5 mmol) and 50 mL of dry Et₂O were added to a dry 250 mL Schlenk flask. The solution was cooled to -84 °C and 1.3 M *sec*-BuLi/cyclohexane (24.14 mL, 31.39 mmol) was added dropwise. The reaction mixture stirred for 1.5 h at -84 °C then allowed to warm up to 0 °C before the addition of triphenyltin chloride (11.0 g, 28.5 mmol) in 20

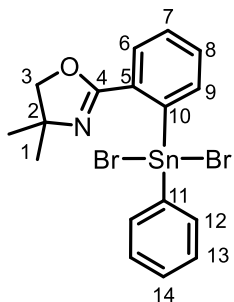
mL of Et₂O was added dropwise. The reaction mixture was stirred for 1 h at 0 °C. The solvent was then removed under reduced pressure and 40 mL of toluene was added. The mixture was filtered via gravity filtration and the solvent was removed under reduced pressure to yield a pale yellow coloured powder. The crude product was triturated with methanol and the yellow solution was decanted off. The residual solvent was removed under reduced pressure to yield the product as a white coloured powder. Yield: 11.42 g, 76.3 %. m.p. 139-141 °C. **¹H NMR** (400.13, CDCl₃, δ): 8.05 (d, 1H, H9, ³J_{1H-1H}= 7.78 Hz, ³J_{1H-119Sn}= 24.59 Hz), 7.61-7.59 (m, 6H, H12), 7.54-7.52 (m, 1H, H6), 7.50-7.48 (m, 1H, H7), 7.45- 7.42 (m, 1H, H8), 7.36-7.34 (m, 9H, H13 & H14), 3.93 (s, 2H, H3), 0.77 (s, 6H, H1) ppm. **¹³C {¹H} NMR** (100.61 MHz, CDCl₃, δ): 163.19 (C4), 143.19 (C11), 141.28 (C10), 138.71 (C6), 137.11 (C12, ²J_{13C-119Sn}= 37.42 Hz), 133.71 (C5), 131.02 (C8), 129.08 (C7), 128.10 (C14), 128.04 (C13), 127.80 (C9), 80.05 (C3), 67.49 (C2), 27.62 (C1) ppm. **¹¹⁹Sn {¹H} NMR** (149.21 MHz, CDCl₃, δ): -157.13 ppm. HRMS-DART (m/z) = 448.07234 (M-C₆H₆) calculated for ¹²C₂₃¹H₂₂¹⁴N₁¹⁶O₁¹²⁰Sn₁; found 448.07136.

5.3 Synthesis of 2-(2-(chlorodiphenylstannyl)phenyl)-4,4-dimethyl-4,5-dihydrooxazole (11):



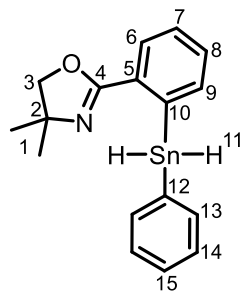
4,4-dimethyl-2-(2-(triphenylstannyl)phenyl)-4,5-dihydrooxazole (0.250 g, 0.477 mmol) and 10 mL of benzene were added to a dry 100 mL Schlenk flask. HCl/ Et₂O (0.47 mL, 0.477 mmol) was added and the solution was stirred for 1 h at RT. The solvent was removed under reduced pressure to yield 2-(2-(chlorodiphenylstannyl)phenyl)-4,4-dimethyl-4,5-dihydrooxazole. The crude product was triturated with hexanes and the cloudy solution was decanted off and residual solvent was then removed under reduced pressure to afford 2-(2-(chlorodiphenylstannyl)phenyl)-4,4-dimethyl-4,5-dihydrooxazole as a white coloured powder. Yield: 0.192 g, 83.6 %. M.p: 222-223 °C. ¹H NMR (400.13, CDCl₃, δ): 8.57 (d, 1H, H9, ³J_{1H-1H}= 7.03 Hz, ³J_{1H-117Sn}= 25.85 Hz, ³J_{1H-119Sn}= 74.54Hz), 7.95 (d, 1H, H6, ³J_{1H-1H}= 7.53 Hz), 7.79- 7.75 (m, 1H, H8), 7.74- 7.71 (m, 4H, H12), 7.63-7.61 (m, 1H, H7), 7.39- 7.37 (m, 6H, H13 & H14), 4.27 (s, 2H, H3), 0.86 (s, 6H, H1) ppm. ¹³C {¹H} NMR (100.61 MHz, CDCl₃, δ): 168.90 (C4), 143.23 (C11), 143.02 (C10), 138.42 (C9), 135.62 (C12, ²J_{13C-117/119Sn}= 47.68 Hz), 133.25 (C8), 130.76 (C5), 130.01 (C7), 129.25 (C14), 128.55 (C13, ³J_{13C-117/119Sn}= 75.56 Hz), 126.76 (C6), 82.58 (C3), 66.91 (C2), 27.73 (C1) ppm. ¹¹⁹Sn {¹H} NMR (149.21 MHz, CDCl₃, δ): -225.99 ppm.

5.4 Synthesis of 2-(2-(dibromo(phenyl)stannylyl)phenyl)-4,4-dimethyl-4,5-dihydrooxazole (13):



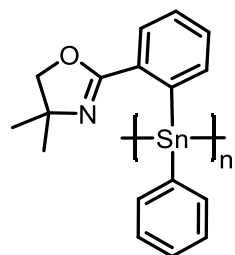
4,4-dimethyl-2-(2-(triphenylstannylyl)phenyl)-4,5-dihydrooxazole (8.224 g, 15.69 mmol) and 50 mL of C₆H₆ was added to a 250 mL Schlenk flask and cooled to 0 °C. Br₂ (1.61 mL, 31.45 mmol) was added dropwise and the reaction mixture stirred for 1 h. The solvent was removed under reduced pressure to yield a brown-yellow coloured powder. The crude product was triturated with MeOH and the yellow solution was decanted off. The residual solvent was removed under reduced pressure to afford the product as a white coloured powder. Yield = 6.60 g, 79.4 %. M.p. 197-198 °C. ¹H NMR (400.13, CDCl₃, δ): 8.51 (d, 1H, H9, ³J_{1H-1H}= 7.28 Hz, ³J_{1H-117Sn}= 86.33 Hz, ³J_{1H-119Sn}= 101.39 Hz), 7.92 (d, 1H, H6, ³J_{1H-1H}= 7.53 Hz), 7.81 (dd, 1H, H8, ³J_{1H-1H}= 7.53 Hz, ³J_{1H-1H}= 7.03 Hz), 7.68-7.63 (m, 3H, H7 & H12), 7.45-7.38 (m, 3H, H13 & H14), 4.38 (s, 2H, H3), 1.15 (s, 6H, H1) ppm. ¹³C {¹H} NMR (100.61 MHz, CDCl₃, δ): 168.52 (C4), 144.62 (C11), 140.58 (C10), 137.81 (C9), 133.88 (C7), 133.34 (C12, ²J_{13C-119Sn}= 68.22 Hz), 131.41 (C8), 130.20 (C14, ⁴J_{13C-119Sn}= 20.54 Hz), 129.16 (C5), 129.01 (C13, ³J_{13C-117Sn}= 96.83 Hz, ³J_{13C-119Sn}= 101.24 Hz), 126.95 (C6), 83.69 (C3), 67.09 (C2), 27.98 (C1) ppm. ¹¹⁹Sn {¹H} NMR (149.21 MHz, CDCl₃, δ): -290.63 ppm. HRMS-DART (m/z): [M+] calculated for ¹²C₁₇¹H₁₈⁷⁹Br₂¹⁴N₁¹⁶O₁¹²⁰Sn₁: 529.87771; found 529.87682.

5.5 Synthesis of 4,4-dimethyl-2-(2-(phenylstannyl)phenyl)-4,5-dihydrooxazole (14):



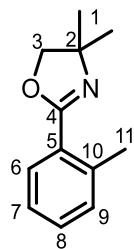
A suspension of 2-(2-(dibromo(phenyl)stannylyl)phenyl)-4,4-dimethyl-4,5-dihydrooxazole (0.50 g, 0.94 mmol) in 15 mL of dry EtOH was added dropwise to a solution of NaBH₄ (0.053 g, 1.42 mmol) in 5 mL of dry EtOH at -84 °C. The solution continued to stir at -84 °C for 1 h. Cold hexane (15 mL) was added to the solution and then quenched with 5 mL of chilled degassed distilled water. The mixture was extracted and the organic layer was dried over anhydrous MgSO₄. The solution was filtered and the solvent was removed under reduced pressure to yield the product as a colourless viscous oil. Yield = 0.151 g, 43 %. ¹H NMR (400.13, CDCl₃, δ): 8.01-7.99 (m, 1H, H6), 7.77-7.75 (m, 1H, H9), 7.70-7.68 (m, 1H, H7), 7.21-7.18 (m, 3H, H14 & H15), 7.15-7.14 (m, 1H, H8), 7.12-7.08 (m, 2H, H13), 6.79 (s, H, H11), 3.59 (s, 2H, H3), 0.98 (s, 6H, 1H) ppm. ¹³C {¹H} NMR (100.61 MHz, CDCl₃, δ): 164.22 (C4), 141.60 (C10) 141.56 (C12), 138.68 (C9), 137.28 (C13), 137.21 (C5), 133.21 (C7), 130.97 (C8), 128.88 (C14), 128.15 (C15), 128.03(C6), 79.82 (C3), 67.07 (C2) 28.28 (C1) ppm. ¹¹⁹Sn {¹H} NMR (149.21 MHz, CDCl₃, δ): -249.52 ppm. HRMS-DART (m/z): [M-H] calculated for ¹²C₁₇¹H₁₈⁷⁹¹⁴N₁¹⁶O₁¹²⁰Sn₁: 372.04451; found 372.04104.

5.6 Synthesis of polymer (16):



A solution of 4,4-dimethyl-2-(2-(phenylstannyl)phenyl)-4,5-dihydrooxazole (0.327 g, 0.879 mmol) in 3 mL of dry toluene was added dropwise to a dry Schlenk wrapped in aluminum foil containing Wilkinson's catalyst (0.033 g, 0.035 mmol) in 10 mL of dry toluene at 0 °C. The solution continued to be stirred at 0 °C for 4 h then the solvent was removed under reduced pressure. The crude product was dissolved in minimal dry THF (2 mL) and added dropwise to cold stirring hexanes (3 × 75 mL) and heptane (1 × 75 mL) and the residual solvent was then removed under reduced pressure to yield a pale-yellow powder. Yield = 0.052 g, 15.9 %. ¹H NMR (400.13, C₆D₆, δ): 7.74 – 7.69 (m, 4H), 7.09 – 7.00 (m, 5H), 3.57 (m, 2H). ¹¹⁹Sn {¹H} NMR (149.21 MHz, C₆D₆, δ): -268.09 ppm.

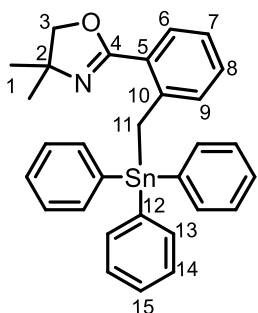
5.7 Synthesis of 4,4-dimethyl-2-(o-tolyl)-4,5-dihydrooxazole (17):



Thionyl chloride (5.35 mL, 73.4 mmol) and 3 drops of DMF were added to a 250 mL round bottom flask containing *o*-toluic acid (5.00 g, 36.7 mmol) in 100 mL of dry DCM. The reaction mixture was heated to reflux temperature for 2 h. The solvent and excess SOCl_2 were then removed under reduced pressure to afford a yellow coloured liquid. The product was dissolved in 30 mL of dry DCM and then added dropwise to a 250 mL round bottom flask containing a stirring solution of distilled 2-amino-2-methyl-1-propanol (4.26 g, 47.7 mmol) and triethylamine (7.68 mL, 55.1 mmol) in 100 mL of dry DCM at 0 °C. The reaction mixture was then stirred for 4 h at RT. The crude sample was washed once with 30 mL of 1 M solution of aqueous HCl and 2 × 30 mL of a saturated aqueous brine solution. The organic layer was then dried over anhydrous MgSO_4 , filtered and the solvent was then removed under reduced pressure to afford *N*-(1-hydroxy-2-methylpropan-2-yl)-2-methylbenzamide as a white coloured powder in an 69.9 % yield. The benzamide (5.32 g, 25.7 mmol) was dissolved in thionyl chloride (15.0 mL, 206 mmol) at 0 °C. The solution was stirred at room temperature for 24 h. 100 mL of Et_2O was added and the precipitate was collected via vacuum filtration and dissolved in 50 mL of DCM. The solution was washed with a saturated aqueous solution of NaHCO_3 until the organic layer was neutral and then dried over anhydrous MgSO_4 . After filtration, the solvent was removed under reduced pressure to yield 4,4-dimethyl-2-(*o*-tolyl)-4,5-dihydrooxazole as a yellow coloured liquid. Yield: 4.07 g, 58.6 %. NMR data (^1H , ^{13}C) matches reported literature data within experimental error.

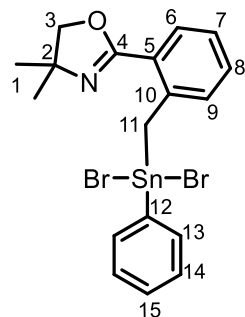
¹H NMR (400.13 MHz, CDCl₃, δ): 7.86 (d, 1H, H6, ³J_{1H-1H}=7.78), 7.33-7.29 (m, 1H, H9), 7.21-7.17 (m, 2H, H7 & H8) 4.15 (s, 2H, H3), 2.53 (s, 3H, H11) 1.42 (s, 6H, H1) ppm. **¹³C{¹H} NMR** (100.61 MHz, CDCl₃, δ): 164.45 (C4), 138.92 (C10), 131.42 (C9), 131.27 (C8), 130.36 (C6), 125.93 (C5), 125.78 (C7), 79.52 (C3), 66.85 (C2), 28.06 (C1), 21.44 (C11) ppm.

5.8 Synthesis of 4,4-dimethyl-2-(2-((triphenylstannyl)methyl)phenyl)-4,5-dihydrooxazole (18) :



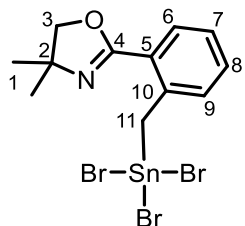
4,4-dimethyl-2-(o-tolyl)-4,5-dihydrooxazole (0.50 g, 26.4 mmol) and 10 mL of dry Et₂O were added to a dry 50 mL Schlenk flask. The solution was cooled down to 0 °C and 1.6 M n-BuLi/hexane (1.82 mL, 2.91 mmol) was added dropwise to produce a dark red opaque solution and allowed to stir for 20 mins. A solution of triphenyltin chloride (1.02 g, 26.4 mmol) in 15 mL of Et₂O was then added dropwise to produce a yellow opaque solution. The solution continued to be stirred for 1 h at 0 °C. The solvent was removed under reduced pressure and 10 mL of toluene was added. The mixture was filtered via gravity filtration and the solvent was removed under reduced pressure to yield a pale yellow coloured powder. The crude product was triturated with methanol and the yellow solution was decanted off. The residual solvent was removed under reduced pressure to yield the product as white coloured crystals. Yield: 1.10 g, 77.4 %. ¹H NMR (400.13, CDCl₃, δ): 7.77 (d, 1H, H9, ³J_{1H-1H}= 7.78 Hz), 7.46-7.44 (m, 6H, H13), 7.36-7.31 (m, 9H, H14 & H15), 7.29-7.28 (m, 2H, H6 & H7), 7.12-7.10 (m, 1H, H8), 3.74 (s, 2H, H3), 3.57 (s, 2H, H11, ²J_{1H-119Sn}= 75.54 Hz), 1.11 (s, 6H, H1) ppm. ¹³C {¹H} NMR (100.61 MHz, CDCl₃, δ): 161.69 (C4), 143.53 (C10), 140.10 (C12), 136.97 (C13), 130.62 (C6), 129.91 (C9), 129.34 (C7), 128.55 (C15), 128.12 (C14), 124.37 (C5), 123.72 (C8), 77.58 (C3), 68.20 (C2), 28.24 (C1), 23.34 (C11) ppm. ¹¹⁹Sn {¹H} NMR (149.21 MHz, CDCl₃, δ): -125.96 ppm. HRMS-DART (m/z): (M-C₆H₆) calculated for ¹²C₂₄¹H₂₄¹⁴N₁¹⁶O₁¹²⁰Sn₁: 462.08799; found 462.08871.

5.9 Synthesis of 2-((dibromo(phenyl)stannylmethyl)phenyl)-4,4-dimethyl-4,5-dihydrooxazole (20):



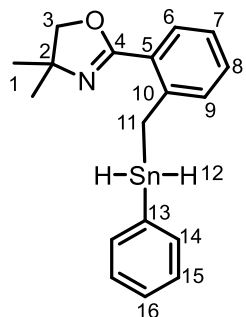
A solution of **18** (2.46 g, 4.57 mmol) and 20 mL of DCM was added to a 100 mL Schlenk flask and cooled to 0 °C. A solution of Br₂ (0.466 mL, 9.14 mmol) in 10 mL of DCM was added dropwise and the reaction mixture stirred for 1 h at 0 °C. The solvent was removed under reduced pressure to yield a brown-yellow coloured powder. The crude product was triturated with MeOH and the yellow solution was decanted off. The residual solvent was removed under reduced pressure to afford the product as a white coloured powder. Yield 2.05 g, 82.3 %. ¹H NMR (400.13, CDCl₃, δ): 7.93 (d, 1H, H6, ³J_{1H-1H}= 7.64 Hz), 7.54-7.52 (m, 2H, H8 & H9), 7.39-7.32 (m, 6H, H7, H13, H14 & H15), 4.05 (s, 2H, H3), 3.63 (s, 2H, H11, ²J_{1H-119Sn}= 112.68 Hz), 1.25 (s, 6H, H1) ppm. ¹³C {¹H} NMR (100.61 MHz, CDCl₃, δ): 166.48 (C4), 144.59(C12), 139.89 (C10), 133.91 (C13), 133.28 (C8), 130.54 (C9), 130.22 (C6), 130.18 (C7), 128.97 (C14), 126.80 (C15), 121.84(C5). 79.21 (C3). 69.27 (C2), 41.50 (C11), 27.67 (C1) ppm. ¹¹⁹Sn {¹H} NMR (149.21 MHz, CDCl₃, δ): -248.24 ppm. HRMS-DART (m/z): [M+H] calculated for ¹²C₁₈¹H₂₀⁷⁹Br₂¹⁴N₁¹⁶O₁¹²⁰Sn₁: 543.89336; found 543.89537.

5.10 Synthesis of 4,4-dimethyl-2-(2-((tribromostannylyl)methyl)phenyl)-4,5-dihydrooxazole (19):



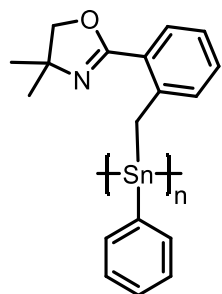
A solution of **18** (0.250 g, 0.464 mmol) and 20 mL of C₆H₆ was added to a 100 mL Schlenk flask and cooled to 0 °C. Br₂ (0.047 mL, 0.929 mmol) was added dropwise and the reaction mixture stirred for 1 h at 0 °C. The solvent was removed under reduced pressure to yield a brown-yellow coloured powder. The crude product was triturated with MeOH and the yellow solution was decanted off. The residual solvent was removed under reduced pressure to afford the product as a white coloured powder. Yield = 0.244 g, 96.2 %. **¹H NMR** (400.13, CDCl₃, δ): 7.96 (d, 1H, H6, ³J_{1H-1H}= 7.77 Hz), 7.60-7.56 (m, 1H, H8), 7.50-7.43 (m, 2H, H7 & H9), 4.20 (s, 2H, H3), 3.70 (s, 2H, H11, ²J_{1H-119Sn}= 121.53 Hz), 1.71 (s, 6H, H1) ppm. **¹³C {¹H} NMR** 167.11 (C4), 138.35 (C10), 133.73 (C8), 130.69 (C6), 130.47 (C9), 127.53 (C7), 121.05 (C5), 79.73 (C3), 69.83 (C2), 47.10 (C11), 27.93 (C1) ppm. **¹¹⁹Sn {¹H} NMR** (149.21 MHz, CDCl₃, δ): -448.6 ppm.

5.11 Synthesis of 4,4-dimethyl-2-(2-((phenylstannyl)methyl)phenyl)-4,5-dihydrooxazole (21):



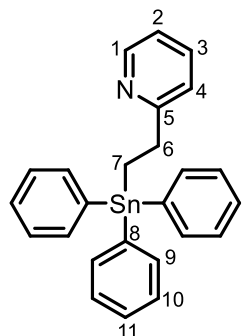
A suspension of **20** (0.50 g, 0.919 mmol) in 15 mL of dry EtOH was added dropwise to a solution of NaBH₄ (0.174 g, 4.70 mmol) in 5 mL of dry EtOH at -0 °C. The solution continued to stir at -0 °C for 1 h. Cold hexane (15 mL) was added to the solution and then quenched with 5 mL of chilled degassed distilled water. The mixture was extracted, and the organic layer was dried over anhydrous MgSO₄. The solution was filtered, and the solvent was removed under reduced pressure to yield the product as a colourless viscous oil. Yield = 0.305 g, 85.9 %. ¹H NMR (400.13, CDCl₃, δ): 8.02 (d, 1H, H6, ²J_{1H-1H} = 7.72 Hz), 7.51-7.49 (m, 2H, H14), 7.16-7.15 (m, 3H, H15 & H16), 7.03-7.01 (m, 2H, H7 & H8), 6.93-6.91 (m, 1H, H9), 5.94 (s, 2H, H12, ¹J_{117Sn-1H} = 1856.56 Hz, ¹J_{119Sn-1H} = 1942.82 Hz) 3.55 (s, 2H, H3), 3.07 (s, 2H, H11, ²J_{119Sn-1H} = 76.11 Hz) ppm. ¹³C {¹H} NMR 161.64 (C4), 145.43 (C10), 140.53 (C13), 137.03 (C14), 130.72 (C8), 129.81 (C6), 129.31 (C7), 128.22 (C16), 128.13 (C15), 77.25 (C3), 68.23 (C2), 27.88 (C1), 21.86 (C11) ppm. ¹¹⁹Sn {¹H} NMR (149.21 MHz, CDCl₃, δ): -221.02 ppm.

5.12 Synthesis of polymer (22):



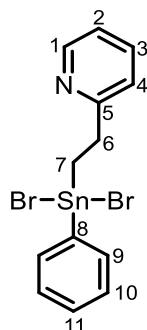
A solution of **21** (0.432 g, 1.119 mmol) in 3 mL of dry toluene was added dropwise to a dry Schlenk wrapped in aluminum foil containing Wilkinson's catalyst (0.0414 g, 0.045 mmol) in 10 mL of dry toluene at 0 °C. The solution continued to be stirred at 0 °C for 4 h then the solvent was removed under reduced pressure. The crude product was dissolved in minimal dry THF (2 mL) and added dropwise to cold stirring hexanes (3×75 mL) and heptane (1×75 mL) and the residual solvent was then removed under reduced pressure to yield a pale-yellow powder. Yield = 0.096 g, 22.2 %. ^1H NMR (400.13, C₆D₆, δ): 7.96 – 7.61 (m, 4H), 7.10 – 7.6.98 (m, 5H), 3.58-3.25 (m, 4H). $^{119}\text{Sn} \{^1\text{H}\}$ NMR (149.21 MHz, C₆D₆, δ): -183.84 ppm.

5.13 Synthesis of 2-(2-(triphenylstannylyl)ethyl)pyridine (23):



Triphenyltin hydride (0.500 g, 1.42 mmol) and 2-vinylpyridine (0.23 mL, 2.14 mmol) were added into a 50 mL dry Schlenk flask attached with a reflux condenser and heated to 100 °C for 2 h. The solution was cooled down and recrystallized from petroleum ether (b.p. 60-95 °C) and the mother liquor was removed under reduced pressure and the remaining solid was recrystallized from 1:1 MeOH: Et₂O to yield the product as a white coloured powder. Yield: 0.496 g, 76.3 %. NMR data (¹H, ¹³C) matches reported literature data within experimental error.¹⁸ ¹H NMR (400.13, CDCl₃, δ): 8.30 (d, 1H, H1, ³J_{1H-1H}= 4.02 Hz), 7.59-7.56 (m, 6H, H9), 7.52-7.49 (m, 1H, H3), 7.37-7.36 (m, 9H, H10 & H11), 7.09 (d, 1H, H4, ³J_{1H-1H}= 7.78 Hz), 7.03-7.00 (m, 1H, H2) 3.27 (t, 2H, H6, ³J_{1H-1H}= 7.80 Hz), 1.91 (t, 2H, H7, ³J_{1H-1H}= 7.80 Hz) ppm. ¹³C {¹H} NMR (100.61 MHz, CDCl₃, δ): 162.92 (C5), 148.64 (C1), 140.44 (C8), 137.08 (C9), 136.26 (C3), 128.51 (C11), 128.28 (C10), 122.46 (C4), 121.13 (C2), 34.04 (C6), 10.60 (C7) ppm. ¹¹⁹Sn {¹H} NMR (149.21 MHz, CDCl₃, δ): -108.45 ppm. HRMS-DART (m/z): [M-C₆H₆] calculated for ¹²C₁₉¹H₁₈¹⁴N₁¹²⁰Sn₁: 380.04612; found 380.04610.

5.14 Synthesis of 2-(2-(dibromo(phenyl)stannylyl)ethyl)pyridine (24):



A solution of **23** (0.500 g, 1.09 mmol) 10 mL of C₆H₆ was added to a 50 mL Schlenk flask and cooled to 0 °C. Br₂ (0.350 g, 2.19 mmol) was added dropwise and the reaction mixture stirred for 1 h. The solvent was removed under reduced pressure to yield a brown coloured gel. The crude product was recrystallized from 9:1 petroleum ether (60-95 °C): ethyl acetate to yield the pure product as white coloured needles. Yield: 0.415 g 82.0 %. ¹H NMR (400.13, CDCl₃, δ): 8.15 (d, 1H, H1, ³J_{1H-1H} = 4.91 Hz), 7.86 – 7.84 (m, 1H, H3), 7.64 – 7.62 (m, 2H, H9), 7.42-7.39 (m, 4H, H10, H11, H4), 7.31-7.28 (m, 1H, H2), 3.47 (t, 2H, H7, ³J_{1H-1H} = 7.30 Hz), 2.22 (t, 2H, H6, ³J_{1H-1H} = 7.30 Hz) ppm. ¹³C {¹H} NMR (100.61 MHz, CDCl₃, δ): 158.37 (C5), 145.90 (C1), 142.23 (C8), 139.81 (C3), 134.69 (C9), 130.26 (C11), 128.91 (C1), 124.82 (C4), 123.49 (C2), 30.69 (C6), 21.68 (C7) ppm. ¹¹⁹Sn {¹H} NMR (149.21 MHz, CDCl₃, δ): -183.92 ppm. HRMS-DART (m/z): [M-Br] calculated for ¹²C₁₃¹H₁₃⁷⁹Br₁¹⁴N₁¹¹²⁰Sn₁: 381.92534; found 381.92478.

References

1. Meyers, A. I.; Mihelich, E. D., *Angew. Chem. Int. Ed.* **1976**, *15*, 270-281.
2. Gómez, M.; Muller, G.; Rocamora, M., *Coord. Chem. Rev.* **1999**, *193-195*, 769-835.
3. Helmut, W.; Wolfgang, S., *Angew. Chem. Int. Ed.* **1972**, *11*, 287-288.
4. Schwekendiek, K.; Glorius, F., *Synthesis* **2006**, *2006*, 2996-3002.
5. Vorbrüggen, H.; Krolkiewicz, K., *Tetrahedron* **1993**, *49*, 9353-9372.
6. Gant, T. G.; Meyers, A. I., *Tetrahedron* **1994**, *50*, 2297-2360.
7. Sharma, R.; Vadivel, S. K.; Duclos, R. I.; Makriyannis, A., *Tetrahedron Lett.* **2009**, *50*, 5780-5782.
8. Adams, N.; Schubert, U. S., *Adv. Drug Deliv. Rev.* **2007**, *59*, 1504-1520.
9. Arii, H.; Matsuo, M.; Nakadate, F.; Mochida, K.; Kawashima, T., *Dalton Trans.* **2012**, *41*, 11195-11200.
10. Lee, J.-D.; Kim, H.-S.; Han, W.-S.; Kang, S. O., *J. Organomet. Chem.* **2010**, *695*, 463-468.
11. Selvaratnam, S.; Lo, K. M.; Das, V. G. K., *J. Organomet. Chem.* **1994**, *464*, 143-148.
12. Stol, M.; Snelders, D. J. M.; de Pater, J. J. M.; van Klink, G. P. M.; Kooijman, H.; Spek, A. L.; van Koten, G., *Organometallics* **2005**, *24*, 743-749.
13. Jastrzebski, J. T. B. H.; Wehman, E.; Boersma, J.; van Koten, G.; Goubitz, K.; Heijdenrijk, D., *J. Organomet. Chem.* **1991**, *409*, 157-162.
14. Cmoch, P.; Urbańczyk-Lipkowska, Z.; Petrosyan, A.; Stępień, A.; Staliński, K., *J. Mol. Struct.* **2005**, *733*, 29-39.
15. Staliński, K.; Urbańczyk-Lipkowska, Z.; Cmoch, P.; Rupnicki, L.; Grachev, A., *J. Organomet. Chem.* **2006**, *691*, 2394-2402.

16. Rupnicki, L.; Urbańczyk-Lipkowska, Z.; Stępień, A.; Cmoch, P.; Pianowski, Z.; Staliński, K., *J. Organomet. Chem.* **2005**, 690, 3690-3696.
17. Matkowska, D.; Gola, M.; Śnieżek, M.; Cmoch, P.; Staliński, K., *J. Organomet. Chem.* **2007**, 692, 2036-2045.
18. Mahon, M. F.; Molloy, K. C.; Waterfield, P. C., *Organometallics* **1993**, 12, 769-774.
19. Musher, J. I., *Angew. Chem. Int. Ed.* **1969**, 8, 54-68.
20. Khan, A.; Foucher, D., *Coord. Chem. Rev.* **2016**, 312, 41-66.
21. Minyaev, R. M.; Gribanova, T.; Minkin, V., *Hyperbonding and Hypercoordination in Main-Group Chemistry*. **2013**; Vol. 9, p 109-132.
22. van Koten, G.; Noltes, J. G.; Spek, A. L., *J. Organomet. Chem.* **1976**, 118, 183-189.
23. Boyer, J.; Breliere, C.; Corriu, R. J. P.; Kpoton, A.; Poirier, M.; Royo, G., *J. Organomet. Chem.* **1986**, 311, C39-C43.
24. Breliere, C.; Carre, F.; Corriu, R. J. P.; De Saxce, A.; Poirier, M.; Royo, G., *J. Organomet. Chem.* **1981**, 205, C1-C3.
25. De Wit, P. P.; Van Der Kooi, H. O.; Wolters, J., *J. Organomet. Chem.* **1981**, 216, C9-C11.
26. Caseri, W., *Chem. Soc. Rev.* **2016**, 45, 5187-5199.
27. Deacon, P. R.; Devylder, N.; Hill, M. S.; Mahon, M. F.; Molloy, K. C.; Price, G. J., *J. Organomet. Chem.* **2003**, 687, 46-56.
28. Lu, V. Y.; Tilley, T. D., *Macromolecules* **2000**, 33, 2403-2412.
29. Harrypersad, S.; Liao, L.; Khan, A.; Wylie, R. S.; Foucher, D. A., *J. Inorg. Organomet. Polymer. Mater.* **2015**, 25, 515-528.
30. Takeda, K.; Shiraishi, K., *Chem. Phys. Lett.* **1992**, 195, 121-126.
31. Imori, T.; Lu, V.; Cai, H.; Tilley, T. D., *J. Am. Chem. Soc.* **1995**, 117, 9931-9940.

32. Choffat, F.; Buchmüller, Y.; Mensing, C.; Smith, P.; Caseri, W., *J. Inorg. Organomet. Polymer. Mater.* **2009**, *19*, 166-175.
33. Ciccioli, A.; Gigli, G., *J. Phys. Chem. A* **2012**, *116*, 7107-7122.
34. Fabien, C.; Pascal, W.; Paul, S.; Walter, C., *Macromol. Mater. Eng.* **2010**, *295*, 210-221.
35. Trummer, M.; Nauser, T.; Lechner, M.-L.; Uhlig, F.; Caseri, W., *Poly. Degrad. Stab.* **2011**, *96*, 1841-1846.
36. Trummer, M.; Choffat, F.; Smith, P.; Caseri, W., *Macromol. Rapid Commun.* **2012**, *33*, 448-460.
37. Okano, M.; Matsumoto, N.; Arakawa, M.; Tsuruta, T.; Hamano, H., *Chem. Commun.* **1998**, 1799-1800.
38. Okano, M.; Watanabe, K., *Electrochem. Commun.* **2000**, *2*, 471-474.
39. Okano, M.; Takeda, K.-i.; Toriumi, T.; Hamano, H., *Electrochim. Acta* **1998**, *44*, 659-666.
40. Devylder, N.; Hill, M.; Molloy, K. C.; Price, G. J., *Chem. Commun.* **1996**, 711-712.
41. Miles, D.; Burrow, T.; Lough, A.; Foucher, D., *J. Inorg. Organomet. Polymer. Mater.* **2010**, *20*, 544-553.
42. Imori, T.; Tilley, T. D., *J. Chem. Soc., Chem. Commun.* **1993**, 1607-1609.
43. Babcock, J. R.; Sita, L. R., *J. Am. Chem. Soc.* **1996**, *118*, 12481-12482.
44. Woo, H. G.; Park, J. M.; Song, S. J.; Yang, S. Y.; Kim, I.-S.; Kim, W. G., *Bull. Korean Chem. Soc.* **1997**, *18*, 1291-1295.
45. Neale, N. R.; Tilley, T. D., *Tetrahedron* **2004**, *60*, 7247-7260.
46. Thompson, S. M.; Schubert, U., *Inorg. Chim. Acta* **2004**, *357*, 1959-1964.
47. Choffat, F.; Smith, P.; Caseri, W., *J. Chem. Mat.* **2005**, *15*, 1789-1792.

48. Choffat, F.; Käser, S.; Wolfer, P.; Schmid, D.; Mezzenga, R.; Smith, P.; Caseri, W., *Macromolecules* **2007**, *40*, 7878-7889.
49. Choffat, F.; Smith, P.; Caseri, W., *Adv. Mater.* **2008**, *20*, 2225-2229.
50. Harrypersad, S.; Foucher, D., *Chem. Commun.* **2015**, *51*, 7120-7123.
51. Pau, J.; Lough, A. J.; Wyllie, R. S.; Gossage, R. A.; Foucher, D. A., *Chem. Eur. J.* **2017**, *23*, 14367-14374.
52. D'Amaral, G. Synthesis of Macromolecular Intermediates and Intermolecularly Coordinated Stannanes (Unpublished results). Ryerson University, **2018**.
53. Sedelmeier, J.; Hammerer, T.; Bolm, C., *Org. Lett.* **2008**, *10*, 917-920.
54. Kurti, L.; Czako, B., *Strategic Applications of Named Reactions in Organic Synthesis*. Elsevier Inc.: **2005**; p 758.
55. Scholer, S.; Wahl, M. H.; Wurster, N. I. C.; Puls, A.; Hattig, C.; Dyker, G., *Chem. Commun.* **2014**, *50*, 5909-5911.
56. Gschwend, H. W.; Hamdan, A., *J. Org. Chem.* **1975**, *40*, 2008-2009.
57. Addison, A. W.; Rao, T. N.; Reedijk, J.; van Rijn, J.; Verschoor, G. C., *J. Chem. Soc., Dalton Trans.* **1984**, 1349-1356.
58. Baukov, Y. I.; Tandura, S. N., *The Chemistry of Organic Germanium, Tin and Lead Compounds*. John Wiley & Sons: **2003**; Vol. 2.
59. Loungxay, J., κ₂-C,O- and C,N – chelated polystannanes. Ryerson University: **2018**.
60. Novák, P.; Padělková, Z.; Kolářová, L.; Císařová, I.; Růžička, A.; Holeček, J., *Appl. Organometal. Chem.* **2005**, *19*, 1101-1108.
61. Švec, P.; Růžičková, Z.; Vlasák, P.; Turek, J.; De Proft, F.; Růžička, A., *J. Organomet. Chem.* **2016**, *801*, 14-23.

62. Khan, A.; Komejan, S.; Patel, A.; Lombardi, C.; Lough, A. J.; Foucher, D. A., *J. Organomet. Chem.* **2015**, 776, 180-191.
63. Dhindsa, J. Synthesis and Characterization of Push-Pull Polystannanes. Ryerson University, Toronto, **2017**.

Appendix

List of Appendix Tables

Table A1: Crystal data and structure refinement for 10	77
Table A2: Crystal data and structure refinement for 11	90
Table A3: Crystal data and structure refinement for 13	109
Table A4: Crystal data and structure refinement for 18	119
Table A5: Crystal data and structure refinement for 23	141
Table A6: Crystal data and structure refinement for 24	152

List of Appendix Figures

Figure A1: ^1H NMR spectrum of 8 in CDCl_3^*	166
Figure A2: ^{13}C NMR spectrum of 8 in CDCl_3^*	167
Figure A3: HSQC spectrum of 8 in CDCl_3	168
Figure A4: COSY spectrum of 8 in CDCl_3	169
Figure A5: HMBC spectrum of 8 in CDCl_3	170
Figure A6: ^1H NMR spectrum of 10 in CDCl_3^*	171
Figure A7: ^{13}C NMR spectrum of 10 in CDCl_3^*	172
Figure A8: ^{119}Sn NMR spectrum of 10 in CDCl_3	173
Figure A9: HSQC spectrum of 10 in CDCl_3	174
Figure A10: COSY spectrum 10 in CDCl_3	175
Figure A11: HMBC spectrum of 10 in CDCl_3	176
Figure A12: ^1H NMR spectrum of 11 in CDCl_3	177
Figure A13: ^{13}C NMR spectrum of 11 in CDCl_3^*	178
Figure A14: ^{119}Sn NMR spectrum of 11 in CDCl_3	179
Figure A15: HSQC spectrum of 11 in CDCl_3^*	180
Figure A16: COSY spectrum of 11 in CDCl_3^*	181
Figure A17: HMBC spectrum of 11 in CDCl_3^*	182
Figure A18: ^1H NMR spectrum of 13 in CDCl_3^*	183
Figure A19: ^{13}C NMR spectrum of 13 in CDCl_3^*	184
Figure A20: ^{119}Sn NMR spectrum of 13 in CDCl_3^*	185
Figure A21: HSQC spectrum of 13 in CDCl_3^*	186
Figure A22: COSY spectrum of 13 in CDCl_3^*	187
Figure A23: HMBC spectrum of 13 in CDCl_3^*	188
Figure A24: ^1H NMR spectrum of 14 in CDCl_3^*	189
Figure A25: ^{13}C NMR spectrum of 14 in CDCl_3^*	190
Figure A26: ^{119}Sn NMR spectrum of 14 in CDCl_3^*	191
Figure A27: HSQC spectrum of 14 in C_6D_6	192
Figure A28: COSY spectrum of 14 in C_6D_6	193
Figure A29: HMBC spectrum of 14 in C_6D_6	194
Figure A30: ^1H NMR spectrum of 16 in C_6D_6^*	195
Figure A31: ^{119}Sn NMR spectrum of 16 in C_6D_6^*	196
Figure A32: ^1H NMR spectrum of 17 in CDCl_3^*	197

Figure A33: ^{13}C NMR spectrum of 17 in CDCl_3^*	198
Figure A34: HSQC spectrum of 17 in CDCl_3^*	199
Figure A35: COSY spectrum of 17 in CDCl_3^*	200
Figure A36: HMBC spectrum of 17 in CDCl_3^*	201
Figure A37: ^1H NMR spectrum of 18 in CDCl_3^*	202
Figure A38: ^{13}C NMR spectrum of 18 in CDCl_3^*	203
Figure A39: ^{119}Sn NMR spectrum of 18 in CDCl_3^*	204
Figure A40: HSQC spectrum of 18 in CDCl_3^*	205
Figure A41: COSY spectrum of 18 in CDCl_3^*	206
Figure A42: HMBC spectrum of 18 in CDCl_3^*	207
Figure A43: ^1H NMR spectrum of 20 in CDCl_3^*	208
Figure A44: ^{13}C NMR spectrum of 20 in CDCl_3^*	209
Figure A45: ^{119}Sn NMR spectrum of 20 in CDCl_3^*	210
Figure A46: HSQC spectrum of 20 in CDCl_3^*	211
Figure A47: COSY spectrum of 20 in CDCl_3^*	212
Figure A48: HMBC spectrum of 20 in CDCl_3^*	213
Figure A49: ^1H NMR spectrum of 19 in CDCl_3^*	214
Figure A50: ^{13}C NMR spectrum of 19 in CDCl_3^*	215
Figure A51: ^{119}Sn NMR spectrum of 19 in CDCl_3^*	216
Figure A52: HSQC spectrum of 19 in CDCl_3^*	217
Figure A53: COSY spectrum of 19 in CDCl_3^*	218
Figure A54: HMBC spectrum of 19 in CDCl_3^*	219
Figure A55: ^1H NMR spectrum of 21 in C_6D_6^*	220
Figure A56: ^{13}C NMR spectrum of 21 in C_6D_6^*	221
Figure A57: ^{119}Sn NMR spectrum of 21 in C_6D_6^*	222
Figure A58: HSQC spectrum of 21 in C_6D_6^*	223
Figure A59: COSY spectrum of 21 in C_6D_6^*	224
Figure A60: HMBC spectrum of 21 in C_6D_6^*	225
Figure A61: ^1H NMR spectrum of 23 in CDCl_3^*	226
Figure A62: ^{13}C NMR spectrum of 23 in CDCl_3^*	227
Figure A63: ^{119}Sn NMR spectrum of 23 in CDCl_3^*	228
Figure A64: HSQC spectrum of 23 in CDCl_3^*	229
Figure A65: COSY spectrum of 23 in CDCl_3^*	230
Figure A66: HMBC spectrum of 23 in CDCl_3^*	231
Figure A67: ^1H NMR spectrum of 24 in CDCl_3^*	232
Figure A68: ^{13}C NMR spectrum of 24 in CDCl_3^*	233
Figure A69: ^{119}Sn NMR spectrum of 24 in CDCl_3^*	234
Figure A70: HSQC spectrum of 24 in CDCl_3^*	235
Figure A71: COSY spectrum of 24 in CDCl_3^*	236
Figure A72: HMBC spectrum of 24 in CDCl_3^*	237

Table A1: Crystal data and structure refinement for **10**.

Identification code	d17146_a
Empirical formula	C ₂₉ H ₂₇ N O Sn
Formula weight	524.20
Temperature	150(2) K
Wavelength	0.71073 Å
Crystal system	Monoclinic
Space group	P2 ₁ /n
Unit cell dimensions	a = 9.3351(5) Å b = 18.4709(9) Å c = 14.3598(7) Å
Volume	2470.5(2) Å ³
Z	4
Density (calculated)	1.409 Mg/m ³
Absorption coefficient	1.054 mm ⁻¹
F(000)	1064
Crystal size	0.290 x 0.190 x 0.080 mm ³
Theta range for data collection	1.799 to 27.517°.
Index ranges	-12<=h<=12, -24<=k<=24, -18<=l<=17
Reflections collected	39843
Independent reflections	5684 [R(int) = 0.0229]
Completeness to theta = 25.242°	100.0 %
Absorption correction	Semi-empirical from equivalents
Max. and min. transmission	0.7456 and 0.7028
Refinement method	Full-matrix least-squares on F ²
Data / restraints / parameters	5684 / 0 / 291
Goodness-of-fit on F ²	1.105
Final R indices [I>2sigma(I)]	R1 = 0.0212, wR2 = 0.0423
R indices (all data)	R1 = 0.0281, wR2 = 0.0452
Extinction coefficient	n/a
Largest diff. peak and hole	0.542 and -0.459 e.Å ⁻³

Atomic coordinates ($\times 10^4$) and equivalent isotropic displacement parameters ($\text{\AA}^2 \times 10^3$)
for **10**. U(eq) is defined as one third of the trace of the orthogonalized U^{ij} tensor.

	x	y	z	U(eq)
Sn(1)	5949(1)	7199(1)	4864(1)	20(1)
O(1)	10287(1)	5978(1)	5339(1)	30(1)
N(1)	8330(2)	6389(1)	4490(1)	22(1)
C(1)	8941(2)	6266(1)	5289(1)	21(1)
C(2)	10663(2)	5905(1)	4377(1)	30(1)
C(3)	9313(2)	6155(1)	3777(1)	24(1)
C(4)	9620(2)	6789(1)	3147(2)	38(1)
C(5)	8613(2)	5535(1)	3216(1)	34(1)
C(6)	8271(2)	6396(1)	6171(1)	20(1)
C(7)	8923(2)	6148(1)	7012(1)	25(1)
C(8)	8249(2)	6242(1)	7835(1)	28(1)
C(9)	6927(2)	6582(1)	7817(1)	27(1)
C(10)	6287(2)	6839(1)	6977(1)	23(1)
C(11)	6942(2)	6756(1)	6142(1)	20(1)
C(12)	4144(2)	7800(1)	5358(1)	24(1)
C(13)	4172(2)	8556(1)	5440(1)	29(1)
C(14)	3009(2)	8935(1)	5752(1)	39(1)
C(15)	1799(2)	8569(1)	5990(2)	43(1)
C(16)	1740(2)	7825(1)	5916(2)	42(1)
C(17)	2899(2)	7446(1)	5601(1)	32(1)
C(18)	4904(2)	6454(1)	3904(1)	21(1)
C(19)	5032(2)	5705(1)	3997(1)	31(1)
C(20)	4296(2)	5243(1)	3367(2)	42(1)
C(21)	3449(2)	5518(1)	2631(2)	40(1)
C(22)	3303(2)	6256(1)	2526(1)	34(1)
C(23)	4014(2)	6720(1)	3164(1)	26(1)
C(24)	7154(2)	8036(1)	4240(1)	22(1)
C(25)	8074(2)	8482(1)	4778(1)	35(1)
C(26)	8773(2)	9058(1)	4381(2)	45(1)

C(27)	8578(2)	9191(1)	3440(2)	38(1)
C(28)	7694(2)	8749(1)	2892(2)	36(1)
C(29)	6981(2)	8176(1)	3288(1)	29(1)

—

Bond lengths [Å] and angles [°] for **10**.

Sn(1)-C(18)	2.1378(16)
Sn(1)-C(24)	2.1425(17)
Sn(1)-C(11)	2.1602(16)
Sn(1)-C(12)	2.1752(17)
O(1)-C(1)	1.361(2)
O(1)-C(2)	1.455(2)
N(1)-C(1)	1.268(2)
N(1)-C(3)	1.485(2)
C(1)-C(6)	1.469(2)
C(2)-C(3)	1.549(3)
C(2)-H(2A)	0.9900
C(2)-H(2B)	0.9900
C(3)-C(4)	1.520(2)
C(3)-C(5)	1.522(3)
C(4)-H(4A)	0.9800
C(4)-H(4B)	0.9800
C(4)-H(4C)	0.9800
C(5)-H(5A)	0.9800
C(5)-H(5B)	0.9800
C(5)-H(5C)	0.9800
C(6)-C(7)	1.393(2)
C(6)-C(11)	1.406(2)
C(7)-C(8)	1.387(3)
C(7)-H(7A)	0.9500
C(8)-C(9)	1.383(3)
C(8)-H(8A)	0.9500
C(9)-C(10)	1.393(2)
C(9)-H(9A)	0.9500
C(10)-C(11)	1.391(2)
C(10)-H(10A)	0.9500
C(12)-C(17)	1.398(3)
C(12)-C(13)	1.401(2)
C(13)-C(14)	1.391(3)
C(13)-H(13A)	0.9500

C(14)-C(15)	1.378(3)
C(14)-H(14A)	0.9500
C(15)-C(16)	1.381(3)
C(15)-H(15A)	0.9500
C(16)-C(17)	1.389(3)
C(16)-H(16A)	0.9500
C(17)-H(17A)	0.9500
C(18)-C(19)	1.394(2)
C(18)-C(23)	1.394(2)
C(19)-C(20)	1.391(3)
C(19)-H(19A)	0.9500
C(20)-C(21)	1.374(3)
C(20)-H(20A)	0.9500
C(21)-C(22)	1.377(3)
C(21)-H(21A)	0.9500
C(22)-C(23)	1.389(3)
C(22)-H(22A)	0.9500
C(23)-H(23A)	0.9500
C(24)-C(25)	1.388(3)
C(24)-C(29)	1.390(2)
C(25)-C(26)	1.389(3)
C(25)-H(25A)	0.9500
C(26)-C(27)	1.374(3)
C(26)-H(26A)	0.9500
C(27)-C(28)	1.370(3)
C(27)-H(27A)	0.9500
C(28)-C(29)	1.392(3)
C(28)-H(28A)	0.9500
C(29)-H(29A)	0.9500
C(18)-Sn(1)-C(24)	115.10(6)
C(18)-Sn(1)-C(11)	117.09(6)
C(24)-Sn(1)-C(11)	114.92(6)
C(18)-Sn(1)-C(12)	102.03(6)
C(24)-Sn(1)-C(12)	102.00(7)
C(11)-Sn(1)-C(12)	102.36(6)

C(1)-O(1)-C(2)	105.48(13)
C(1)-N(1)-C(3)	108.09(14)
N(1)-C(1)-O(1)	118.41(15)
N(1)-C(1)-C(6)	123.97(16)
O(1)-C(1)-C(6)	117.60(15)
O(1)-C(2)-C(3)	105.17(14)
O(1)-C(2)-H(2A)	110.7
C(3)-C(2)-H(2A)	110.7
O(1)-C(2)-H(2B)	110.7
C(3)-C(2)-H(2B)	110.7
H(2A)-C(2)-H(2B)	108.8
N(1)-C(3)-C(4)	109.58(14)
N(1)-C(3)-C(5)	108.74(15)
C(4)-C(3)-C(5)	110.91(16)
N(1)-C(3)-C(2)	102.73(14)
C(4)-C(3)-C(2)	112.51(16)
C(5)-C(3)-C(2)	111.99(15)
C(3)-C(4)-H(4A)	109.5
C(3)-C(4)-H(4B)	109.5
H(4A)-C(4)-H(4B)	109.5
C(3)-C(4)-H(4C)	109.5
H(4A)-C(4)-H(4C)	109.5
H(4B)-C(4)-H(4C)	109.5
C(3)-C(5)-H(5A)	109.5
C(3)-C(5)-H(5B)	109.5
H(5A)-C(5)-H(5B)	109.5
C(3)-C(5)-H(5C)	109.5
H(5A)-C(5)-H(5C)	109.5
H(5B)-C(5)-H(5C)	109.5
C(7)-C(6)-C(11)	121.02(16)
C(7)-C(6)-C(1)	120.39(16)
C(11)-C(6)-C(1)	118.56(15)
C(8)-C(7)-C(6)	119.99(17)
C(8)-C(7)-H(7A)	120.0
C(6)-C(7)-H(7A)	120.0
C(9)-C(8)-C(7)	119.80(17)

C(9)-C(8)-H(8A)	120.1
C(7)-C(8)-H(8A)	120.1
C(8)-C(9)-C(10)	120.06(17)
C(8)-C(9)-H(9A)	120.0
C(10)-C(9)-H(9A)	120.0
C(11)-C(10)-C(9)	121.43(17)
C(11)-C(10)-H(10A)	119.3
C(9)-C(10)-H(10A)	119.3
C(10)-C(11)-C(6)	117.67(16)
C(10)-C(11)-Sn(1)	120.17(13)
C(6)-C(11)-Sn(1)	122.14(12)
C(17)-C(12)-C(13)	117.09(17)
C(17)-C(12)-Sn(1)	121.20(13)
C(13)-C(12)-Sn(1)	121.71(14)
C(14)-C(13)-C(12)	121.24(19)
C(14)-C(13)-H(13A)	119.4
C(12)-C(13)-H(13A)	119.4
C(15)-C(14)-C(13)	120.2(2)
C(15)-C(14)-H(14A)	119.9
C(13)-C(14)-H(14A)	119.9
C(14)-C(15)-C(16)	119.86(19)
C(14)-C(15)-H(15A)	120.1
C(16)-C(15)-H(15A)	120.1
C(15)-C(16)-C(17)	119.9(2)
C(15)-C(16)-H(16A)	120.0
C(17)-C(16)-H(16A)	120.0
C(16)-C(17)-C(12)	121.7(2)
C(16)-C(17)-H(17A)	119.2
C(12)-C(17)-H(17A)	119.2
C(19)-C(18)-C(23)	117.78(16)
C(19)-C(18)-Sn(1)	122.99(14)
C(23)-C(18)-Sn(1)	119.21(12)
C(20)-C(19)-C(18)	120.72(19)
C(20)-C(19)-H(19A)	119.6
C(18)-C(19)-H(19A)	119.6
C(21)-C(20)-C(19)	120.43(19)

C(21)-C(20)-H(20A)	119.8
C(19)-C(20)-H(20A)	119.8
C(20)-C(21)-C(22)	119.86(19)
C(20)-C(21)-H(21A)	120.1
C(22)-C(21)-H(21A)	120.1
C(21)-C(22)-C(23)	119.9(2)
C(21)-C(22)-H(22A)	120.0
C(23)-C(22)-H(22A)	120.0
C(22)-C(23)-C(18)	121.26(18)
C(22)-C(23)-H(23A)	119.4
C(18)-C(23)-H(23A)	119.4
C(25)-C(24)-C(29)	117.59(17)
C(25)-C(24)-Sn(1)	121.23(13)
C(29)-C(24)-Sn(1)	121.09(13)
C(24)-C(25)-C(26)	121.09(19)
C(24)-C(25)-H(25A)	119.5
C(26)-C(25)-H(25A)	119.5
C(27)-C(26)-C(25)	120.4(2)
C(27)-C(26)-H(26A)	119.8
C(25)-C(26)-H(26A)	119.8
C(28)-C(27)-C(26)	119.56(19)
C(28)-C(27)-H(27A)	120.2
C(26)-C(27)-H(27A)	120.2
C(27)-C(28)-C(29)	120.23(19)
C(27)-C(28)-H(28A)	119.9
C(29)-C(28)-H(28A)	119.9
C(24)-C(29)-C(28)	121.11(18)
C(24)-C(29)-H(29A)	119.4
C(28)-C(29)-H(29A)	119.4

Symmetry transformations used to generate equivalent atoms:

Anisotropic displacement parameters ($\text{\AA}^2 \times 10^3$) for **10**. The anisotropic displacement factor exponent takes the form: $-2\Box^2 [h^2 a^*{}^2 U^{11} + \dots + 2 h k a^* b^* U^{12}]$

	U ¹¹	U ²²	U ³³	U ²³	U ¹³	U ¹²
Sn(1)	23(1)	18(1)	19(1)	0(1)	1(1)	-1(1)
O(1)	25(1)	38(1)	27(1)	6(1)	5(1)	9(1)
N(1)	23(1)	22(1)	22(1)	0(1)	5(1)	0(1)
C(1)	21(1)	16(1)	26(1)	1(1)	5(1)	0(1)
C(2)	27(1)	35(1)	29(1)	0(1)	9(1)	5(1)
C(3)	26(1)	24(1)	23(1)	3(1)	8(1)	4(1)
C(4)	42(1)	33(1)	40(1)	13(1)	19(1)	7(1)
C(5)	43(1)	32(1)	26(1)	-4(1)	3(1)	7(1)
C(6)	24(1)	16(1)	22(1)	-1(1)	2(1)	-3(1)
C(7)	28(1)	22(1)	24(1)	0(1)	-2(1)	0(1)
C(8)	39(1)	24(1)	20(1)	1(1)	-5(1)	-2(1)
C(9)	38(1)	24(1)	19(1)	-3(1)	6(1)	-5(1)
C(10)	28(1)	20(1)	23(1)	-4(1)	4(1)	-3(1)
C(11)	24(1)	16(1)	19(1)	-1(1)	0(1)	-3(1)
C(12)	26(1)	27(1)	18(1)	-2(1)	-1(1)	3(1)
C(13)	34(1)	27(1)	27(1)	-2(1)	1(1)	4(1)
C(14)	46(1)	35(1)	34(1)	-7(1)	-1(1)	16(1)
C(15)	32(1)	61(2)	38(1)	-9(1)	2(1)	18(1)
C(16)	24(1)	63(2)	39(1)	-6(1)	4(1)	0(1)
C(17)	28(1)	37(1)	31(1)	-4(1)	0(1)	-1(1)
C(18)	20(1)	21(1)	22(1)	-4(1)	6(1)	-2(1)
C(19)	33(1)	23(1)	38(1)	3(1)	4(1)	-2(1)
C(20)	47(1)	21(1)	58(2)	-12(1)	18(1)	-10(1)
C(21)	37(1)	45(1)	39(1)	-21(1)	11(1)	-18(1)
C(22)	27(1)	51(1)	24(1)	-6(1)	2(1)	-9(1)
C(23)	25(1)	27(1)	27(1)	-1(1)	3(1)	-1(1)
C(24)	22(1)	18(1)	25(1)	2(1)	3(1)	3(1)
C(25)	41(1)	35(1)	29(1)	-1(1)	1(1)	-12(1)
C(26)	44(1)	36(1)	53(1)	-1(1)	0(1)	-19(1)
C(27)	31(1)	29(1)	56(1)	16(1)	12(1)	-1(1)
C(28)	35(1)	38(1)	34(1)	15(1)	6(1)	6(1)

C(29)	30(1)	30(1)	26(1)	4(1)	-2(1)	1(1)
<hr/>						

Hydrogen coordinates (x 10⁴) and isotropic displacement parameters (Å² x 10³) for **10**.

	x	y	z	U(eq)
H(2A)	10899	5395	4237	36
H(2B)	11499	6213	4258	36
H(4A)	8725	6947	2811	57
H(4B)	10308	6640	2697	57
H(4C)	10024	7191	3526	57
H(5A)	7704	5700	2907	50
H(5B)	8430	5132	3635	50
H(5C)	9255	5374	2745	50
H(7A)	9831	5914	7021	30
H(8A)	8693	6073	8409	34
H(9A)	6456	6640	8379	33
H(10A)	5383	7075	6975	28
H(13A)	5000	8814	5279	35
H(14A)	3049	9447	5801	46
H(15A)	1008	8830	6205	52
H(16A)	908	7571	6079	51
H(17A)	2845	6934	5550	39
H(19A)	5629	5508	4496	37
H(20A)	4381	4734	3446	50
H(21A)	2964	5200	2196	48
H(22A)	2717	6448	2019	41
H(23A)	3892	7228	3093	31
H(25A)	8229	8393	5428	42
H(26A)	9389	9361	4762	53
H(27A)	9053	9586	3170	46
H(28A)	7568	8834	2239	43
H(29A)	6366	7876	2901	35

Table 6. Torsion angles [°] for **10**.

C(3)-N(1)-C(1)-O(1)	1.3(2)
C(3)-N(1)-C(1)-C(6)	-177.08(15)
C(2)-O(1)-C(1)-N(1)	1.0(2)
C(2)-O(1)-C(1)-C(6)	179.51(14)
C(1)-O(1)-C(2)-C(3)	-2.74(18)
C(1)-N(1)-C(3)-C(4)	-122.64(17)
C(1)-N(1)-C(3)-C(5)	115.98(16)
C(1)-N(1)-C(3)-C(2)	-2.84(18)
O(1)-C(2)-C(3)-N(1)	3.34(18)
O(1)-C(2)-C(3)-C(4)	121.09(17)
O(1)-C(2)-C(3)-C(5)	-113.17(17)
N(1)-C(1)-C(6)-C(7)	170.47(16)
O(1)-C(1)-C(6)-C(7)	-7.9(2)
N(1)-C(1)-C(6)-C(11)	-7.7(2)
O(1)-C(1)-C(6)-C(11)	173.89(14)
C(11)-C(6)-C(7)-C(8)	1.3(3)
C(1)-C(6)-C(7)-C(8)	-176.86(16)
C(6)-C(7)-C(8)-C(9)	0.1(3)
C(7)-C(8)-C(9)-C(10)	-1.0(3)
C(8)-C(9)-C(10)-C(11)	0.6(3)
C(9)-C(10)-C(11)-C(6)	0.8(2)
C(9)-C(10)-C(11)-Sn(1)	-177.65(13)
C(7)-C(6)-C(11)-C(10)	-1.7(2)
C(1)-C(6)-C(11)-C(10)	176.50(15)
C(7)-C(6)-C(11)-Sn(1)	176.69(12)
C(1)-C(6)-C(11)-Sn(1)	-5.1(2)
C(17)-C(12)-C(13)-C(14)	0.1(3)
Sn(1)-C(12)-C(13)-C(14)	179.71(14)
C(12)-C(13)-C(14)-C(15)	0.1(3)
C(13)-C(14)-C(15)-C(16)	-0.2(3)
C(14)-C(15)-C(16)-C(17)	0.0(3)
C(15)-C(16)-C(17)-C(12)	0.3(3)
C(13)-C(12)-C(17)-C(16)	-0.3(3)
Sn(1)-C(12)-C(17)-C(16)	-179.90(15)

C(23)-C(18)-C(19)-C(20)	0.2(3)
Sn(1)-C(18)-C(19)-C(20)	178.18(15)
C(18)-C(19)-C(20)-C(21)	1.1(3)
C(19)-C(20)-C(21)-C(22)	-1.3(3)
C(20)-C(21)-C(22)-C(23)	0.0(3)
C(21)-C(22)-C(23)-C(18)	1.3(3)
C(19)-C(18)-C(23)-C(22)	-1.4(3)
Sn(1)-C(18)-C(23)-C(22)	-179.47(14)
C(29)-C(24)-C(25)-C(26)	1.3(3)
Sn(1)-C(24)-C(25)-C(26)	-175.25(17)
C(24)-C(25)-C(26)-C(27)	-0.8(4)
C(25)-C(26)-C(27)-C(28)	-0.4(3)
C(26)-C(27)-C(28)-C(29)	1.0(3)
C(25)-C(24)-C(29)-C(28)	-0.7(3)
Sn(1)-C(24)-C(29)-C(28)	175.86(14)
C(27)-C(28)-C(29)-C(24)	-0.4(3)

Symmetry transformations used to generate equivalent atoms:

Table A2: Crystal data and structure refinement for **11**.

Identification code	d17148_a
Empirical formula	C23 H22 Cl N O Sn
Formula weight	482.55
Temperature	150(2) K
Wavelength	0.71073 Å
Crystal system	Triclinic
Space group	P-1
Unit cell dimensions	$a = 9.1303(4)$ Å $\alpha = 90.942(1)^\circ$. $b = 9.3020(4)$ Å $\beta = 91.775(1)^\circ$. $c = 24.2461(11)$ Å $\gamma = 91.724(1)^\circ$.
Volume	2056.99(16) Å ³
Z	4
Density (calculated)	1.558 Mg/m ³
Absorption coefficient	1.384 mm ⁻¹
F(000)	968
Crystal size	0.250 x 0.150 x 0.030 mm ³
Theta range for data collection	0.840 to 27.599°.
Index ranges	-11≤h≤11, -12≤k≤12, -31≤l≤31
Reflections collected	66519
Independent reflections	9482 [R(int) = 0.0237]
Completeness to theta = 25.242°	100.0 %
Absorption correction	Semi-empirical from equivalents
Max. and min. transmission	0.7456 and 0.6724
Refinement method	Full-matrix least-squares on F ²
Data / restraints / parameters	9482 / 0 / 491
Goodness-of-fit on F ²	1.096
Final R indices [I>2sigma(I)]	R1 = 0.0205, wR2 = 0.0398
R indices (all data)	R1 = 0.0255, wR2 = 0.0413
Extinction coefficient	n/a
Largest diff. peak and hole	0.429 and -0.600 e.Å ⁻³

Atomic coordinates ($\times 10^4$) and equivalent isotropic displacement parameters ($\text{\AA}^2 \times 10^3$) for **11**. U(eq) is defined as one third of the trace of the orthogonalized U^{ij} tensor.

	x	y	z	U(eq)
Sn(1A)	7188(1)	2414(1)	3954(1)	16(1)
Cl(1A)	4808(1)	3539(1)	4124(1)	25(1)
O(1A)	11520(1)	1080(2)	4575(1)	24(1)
N(1A)	9666(2)	1430(2)	3963(1)	16(1)
C(1A)	10233(2)	1673(2)	4447(1)	17(1)
C(2A)	11838(2)	155(2)	4103(1)	23(1)
C(3A)	10746(2)	609(2)	3644(1)	20(1)
C(4A)	11495(2)	1640(2)	3249(1)	30(1)
C(5A)	9997(2)	-665(2)	3340(1)	30(1)
C(6A)	9560(2)	2570(2)	4864(1)	17(1)
C(7A)	10305(2)	2980(2)	5354(1)	22(1)
C(8A)	9639(2)	3890(2)	5723(1)	24(1)
C(9A)	8248(2)	4371(2)	5607(1)	23(1)
C(10A)	7501(2)	3957(2)	5117(1)	20(1)
C(11A)	8151(2)	3059(2)	4738(1)	16(1)
C(12A)	7611(2)	3616(2)	3231(1)	17(1)
C(13A)	7960(2)	2955(2)	2736(1)	24(1)
C(14A)	8217(2)	3756(2)	2268(1)	30(1)
C(15A)	8151(2)	5240(2)	2291(1)	33(1)
C(16A)	7795(2)	5921(2)	2780(1)	31(1)
C(17A)	7510(2)	5118(2)	3244(1)	23(1)
C(18A)	6248(2)	306(2)	3848(1)	18(1)
C(19A)	6237(2)	-619(2)	4292(1)	27(1)
C(20A)	5548(2)	-1971(2)	4245(1)	34(1)
C(21A)	4871(2)	-2411(2)	3751(1)	32(1)
C(22A)	4866(2)	-1505(2)	3305(1)	31(1)
C(23A)	5553(2)	-146(2)	3354(1)	24(1)
Sn(1B)	2362(1)	7896(1)	1101(1)	16(1)
Cl(1B)	-182(1)	6888(1)	938(1)	26(1)

O(1B)	6667(1)	9152(2)	477(1)	25(1)
N(1B)	4906(2)	8811(2)	1096(1)	17(1)
C(1B)	5385(2)	8538(2)	614(1)	17(1)
C(2B)	7088(2)	10139(2)	931(1)	24(1)
C(3B)	6043(2)	9731(2)	1398(1)	21(1)
C(4B)	6815(2)	8821(2)	1829(1)	31(1)
C(5B)	5355(2)	11033(2)	1661(1)	30(1)
C(6B)	4608(2)	7566(2)	212(1)	18(1)
C(7B)	5273(2)	7106(2)	-264(1)	23(1)
C(8B)	4516(2)	6140(2)	-617(1)	27(1)
C(9B)	3115(2)	5655(2)	-498(1)	28(1)
C(10B)	2448(2)	6129(2)	-21(1)	22(1)
C(11B)	3191(2)	7091(2)	343(1)	17(1)
C(12B)	2769(2)	6728(2)	1837(1)	17(1)
C(13B)	1709(2)	6614(2)	2237(1)	25(1)
C(14B)	1923(2)	5755(2)	2695(1)	31(1)
C(15B)	3186(2)	4978(2)	2752(1)	29(1)
C(16B)	4236(2)	5060(2)	2354(1)	26(1)
C(17B)	4035(2)	5942(2)	1903(1)	21(1)
C(18B)	1660(2)	10051(2)	1130(1)	18(1)
C(19B)	1266(2)	10711(2)	638(1)	23(1)
C(20B)	861(2)	12139(2)	635(1)	33(1)
C(21B)	860(2)	12926(2)	1124(1)	40(1)
C(22B)	1242(3)	12279(2)	1615(1)	40(1)
C(23B)	1624(2)	10851(2)	1619(1)	31(1)

—

Bond lengths [\AA] and angles [$^\circ$] for **11**.

Sn(1A)-C(18A)	2.1250(17)
Sn(1A)-C(12A)	2.1322(16)
Sn(1A)-C(11A)	2.1401(16)
Sn(1A)-N(1A)	2.4658(14)
Sn(1A)-Cl(1A)	2.4832(5)
O(1A)-C(1A)	1.343(2)
O(1A)-C(2A)	1.462(2)
N(1A)-C(1A)	1.282(2)
N(1A)-C(3A)	1.493(2)
C(1A)-C(6A)	1.461(2)
C(2A)-C(3A)	1.544(2)
C(2A)-H(2AA)	0.9900
C(2A)-H(2AB)	0.9900
C(3A)-C(5A)	1.519(3)
C(3A)-C(4A)	1.528(3)
C(4A)-H(4AA)	0.9800
C(4A)-H(4AB)	0.9800
C(4A)-H(4AC)	0.9800
C(5A)-H(5AA)	0.9800
C(5A)-H(5AB)	0.9800
C(5A)-H(5AC)	0.9800
C(6A)-C(7A)	1.394(2)
C(6A)-C(11A)	1.403(2)
C(7A)-C(8A)	1.388(3)
C(7A)-H(7AA)	0.9500
C(8A)-C(9A)	1.381(3)
C(8A)-H(8AA)	0.9500
C(9A)-C(10A)	1.394(2)
C(9A)-H(9AA)	0.9500
C(10A)-C(11A)	1.390(2)
C(10A)-H(10A)	0.9500
C(12A)-C(13A)	1.391(3)
C(12A)-C(17A)	1.403(2)
C(13A)-C(14A)	1.389(3)

C(13A)-H(13A)	0.9500
C(14A)-C(15A)	1.383(3)
C(14A)-H(14A)	0.9500
C(15A)-C(16A)	1.386(3)
C(15A)-H(15A)	0.9500
C(16A)-C(17A)	1.389(3)
C(16A)-H(16A)	0.9500
C(17A)-H(17A)	0.9500
C(18A)-C(19A)	1.390(3)
C(18A)-C(23A)	1.391(2)
C(19A)-C(20A)	1.391(3)
C(19A)-H(19A)	0.9500
C(20A)-C(21A)	1.382(3)
C(20A)-H(20A)	0.9500
C(21A)-C(22A)	1.380(3)
C(21A)-H(21A)	0.9500
C(22A)-C(23A)	1.396(3)
C(22A)-H(22A)	0.9500
C(23A)-H(23A)	0.9500
Sn(1B)-C(18B)	2.1232(17)
Sn(1B)-C(12B)	2.1330(17)
Sn(1B)-C(11B)	2.1422(17)
Sn(1B)-N(1B)	2.4502(14)
Sn(1B)-Cl(1B)	2.4955(5)
O(1B)-C(1B)	1.340(2)
O(1B)-C(2B)	1.457(2)
N(1B)-C(1B)	1.285(2)
N(1B)-C(3B)	1.492(2)
C(1B)-C(6B)	1.469(2)
C(2B)-C(3B)	1.547(2)
C(2B)-H(2BA)	0.9900
C(2B)-H(2BB)	0.9900
C(3B)-C(5B)	1.522(3)
C(3B)-C(4B)	1.526(3)
C(4B)-H(4BA)	0.9800
C(4B)-H(4BB)	0.9800

C(4B)-H(4BC)	0.9800
C(5B)-H(5BA)	0.9800
C(5B)-H(5BB)	0.9800
C(5B)-H(5BC)	0.9800
C(6B)-C(7B)	1.389(2)
C(6B)-C(11B)	1.402(2)
C(7B)-C(8B)	1.386(3)
C(7B)-H(7BA)	0.9500
C(8B)-C(9B)	1.385(3)
C(8B)-H(8BA)	0.9500
C(9B)-C(10B)	1.396(3)
C(9B)-H(9BA)	0.9500
C(10B)-C(11B)	1.392(2)
C(10B)-H(10B)	0.9500
C(12B)-C(17B)	1.392(2)
C(12B)-C(13B)	1.395(2)
C(13B)-C(14B)	1.390(3)
C(13B)-H(13B)	0.9500
C(14B)-C(15B)	1.383(3)
C(14B)-H(14B)	0.9500
C(15B)-C(16B)	1.383(3)
C(15B)-H(15B)	0.9500
C(16B)-C(17B)	1.389(3)
C(16B)-H(16B)	0.9500
C(17B)-H(17B)	0.9500
C(18B)-C(23B)	1.391(3)
C(18B)-C(19B)	1.391(2)
C(19B)-C(20B)	1.389(3)
C(19B)-H(19B)	0.9500
C(20B)-C(21B)	1.382(3)
C(20B)-H(20B)	0.9500
C(21B)-C(22B)	1.383(3)
C(21B)-H(21B)	0.9500
C(22B)-C(23B)	1.383(3)
C(22B)-H(22B)	0.9500
C(23B)-H(23B)	0.9500

C(18A)-Sn(1A)-C(12A)	117.90(7)
C(18A)-Sn(1A)-C(11A)	119.38(6)
C(12A)-Sn(1A)-C(11A)	120.96(6)
C(18A)-Sn(1A)-N(1A)	90.31(6)
C(12A)-Sn(1A)-N(1A)	91.72(6)
C(11A)-Sn(1A)-N(1A)	75.01(6)
C(18A)-Sn(1A)-Cl(1A)	94.18(5)
C(12A)-Sn(1A)-Cl(1A)	94.70(5)
C(11A)-Sn(1A)-Cl(1A)	94.36(5)
N(1A)-Sn(1A)-Cl(1A)	169.33(3)
C(1A)-O(1A)-C(2A)	105.68(13)
C(1A)-N(1A)-C(3A)	107.39(14)
C(1A)-N(1A)-Sn(1A)	107.03(11)
C(3A)-N(1A)-Sn(1A)	145.49(11)
N(1A)-C(1A)-O(1A)	118.02(15)
N(1A)-C(1A)-C(6A)	123.48(15)
O(1A)-C(1A)-C(6A)	118.49(15)
O(1A)-C(2A)-C(3A)	104.31(13)
O(1A)-C(2A)-H(2AA)	110.9
C(3A)-C(2A)-H(2AA)	110.9
O(1A)-C(2A)-H(2AB)	110.9
C(3A)-C(2A)-H(2AB)	110.9
H(2AA)-C(2A)-H(2AB)	108.9
N(1A)-C(3A)-C(5A)	110.78(14)
N(1A)-C(3A)-C(4A)	108.26(15)
C(5A)-C(3A)-C(4A)	111.87(16)
N(1A)-C(3A)-C(2A)	101.97(13)
C(5A)-C(3A)-C(2A)	112.94(16)
C(4A)-C(3A)-C(2A)	110.51(15)
C(3A)-C(4A)-H(4AA)	109.5
C(3A)-C(4A)-H(4AB)	109.5
H(4AA)-C(4A)-H(4AB)	109.5
C(3A)-C(4A)-H(4AC)	109.5
H(4AA)-C(4A)-H(4AC)	109.5
H(4AB)-C(4A)-H(4AC)	109.5

C(3A)-C(5A)-H(5AA)	109.5
C(3A)-C(5A)-H(5AB)	109.5
H(5AA)-C(5A)-H(5AB)	109.5
C(3A)-C(5A)-H(5AC)	109.5
H(5AA)-C(5A)-H(5AC)	109.5
H(5AB)-C(5A)-H(5AC)	109.5
C(7A)-C(6A)-C(11A)	121.17(16)
C(7A)-C(6A)-C(1A)	121.66(16)
C(11A)-C(6A)-C(1A)	117.10(15)
C(8A)-C(7A)-C(6A)	119.16(17)
C(8A)-C(7A)-H(7AA)	120.4
C(6A)-C(7A)-H(7AA)	120.4
C(9A)-C(8A)-C(7A)	120.31(17)
C(9A)-C(8A)-H(8AA)	119.8
C(7A)-C(8A)-H(8AA)	119.8
C(8A)-C(9A)-C(10A)	120.49(17)
C(8A)-C(9A)-H(9AA)	119.8
C(10A)-C(9A)-H(9AA)	119.8
C(11A)-C(10A)-C(9A)	120.32(16)
C(11A)-C(10A)-H(10A)	119.8
C(9A)-C(10A)-H(10A)	119.8
C(10A)-C(11A)-C(6A)	118.53(15)
C(10A)-C(11A)-Sn(1A)	124.63(13)
C(6A)-C(11A)-Sn(1A)	116.79(12)
C(13A)-C(12A)-C(17A)	118.05(16)
C(13A)-C(12A)-Sn(1A)	121.99(13)
C(17A)-C(12A)-Sn(1A)	119.94(13)
C(14A)-C(13A)-C(12A)	121.10(18)
C(14A)-C(13A)-H(13A)	119.4
C(12A)-C(13A)-H(13A)	119.4
C(15A)-C(14A)-C(13A)	120.20(19)
C(15A)-C(14A)-H(14A)	119.9
C(13A)-C(14A)-H(14A)	119.9
C(14A)-C(15A)-C(16A)	119.67(18)
C(14A)-C(15A)-H(15A)	120.2
C(16A)-C(15A)-H(15A)	120.2

C(15A)-C(16A)-C(17A) 120.17(19)
C(15A)-C(16A)-H(16A) 119.9
C(17A)-C(16A)-H(16A) 119.9
C(16A)-C(17A)-C(12A) 120.77(18)
C(16A)-C(17A)-H(17A) 119.6
C(12A)-C(17A)-H(17A) 119.6
C(19A)-C(18A)-C(23A) 118.71(17)
C(19A)-C(18A)-Sn(1A) 119.53(13)
C(23A)-C(18A)-Sn(1A) 121.62(13)
C(18A)-C(19A)-C(20A) 120.77(18)
C(18A)-C(19A)-H(19A) 119.6
C(20A)-C(19A)-H(19A) 119.6
C(21A)-C(20A)-C(19A) 119.96(19)
C(21A)-C(20A)-H(20A) 120.0
C(19A)-C(20A)-H(20A) 120.0
C(22A)-C(21A)-C(20A) 120.07(18)
C(22A)-C(21A)-H(21A) 120.0
C(20A)-C(21A)-H(21A) 120.0
C(21A)-C(22A)-C(23A) 119.97(19)
C(21A)-C(22A)-H(22A) 120.0
C(23A)-C(22A)-H(22A) 120.0
C(18A)-C(23A)-C(22A) 120.52(18)
C(18A)-C(23A)-H(23A) 119.7
C(22A)-C(23A)-H(23A) 119.7
C(18B)-Sn(1B)-C(12B) 121.43(7)
C(18B)-Sn(1B)-C(11B) 118.19(6)
C(12B)-Sn(1B)-C(11B) 118.53(6)
C(18B)-Sn(1B)-N(1B) 89.02(6)
C(12B)-Sn(1B)-N(1B) 91.89(6)
C(11B)-Sn(1B)-N(1B) 75.24(6)
C(18B)-Sn(1B)-Cl(1B) 93.10(5)
C(12B)-Sn(1B)-Cl(1B) 94.97(5)
C(11B)-Sn(1B)-Cl(1B) 95.55(5)
N(1B)-Sn(1B)-Cl(1B) 170.40(4)
C(1B)-O(1B)-C(2B) 105.73(13)
C(1B)-N(1B)-C(3B) 107.45(14)

C(1B)-N(1B)-Sn(1B)	107.06(11)
C(3B)-N(1B)-Sn(1B)	144.67(11)
N(1B)-C(1B)-O(1B)	118.17(15)
N(1B)-C(1B)-C(6B)	123.05(15)
O(1B)-C(1B)-C(6B)	118.76(15)
O(1B)-C(2B)-C(3B)	104.63(14)
O(1B)-C(2B)-H(2BA)	110.8
C(3B)-C(2B)-H(2BA)	110.8
O(1B)-C(2B)-H(2BB)	110.8
C(3B)-C(2B)-H(2BB)	110.8
H(2BA)-C(2B)-H(2BB)	108.9
N(1B)-C(3B)-C(5B)	110.63(15)
N(1B)-C(3B)-C(4B)	108.65(15)
C(5B)-C(3B)-C(4B)	111.36(16)
N(1B)-C(3B)-C(2B)	101.91(13)
C(5B)-C(3B)-C(2B)	112.83(16)
C(4B)-C(3B)-C(2B)	111.01(16)
C(3B)-C(4B)-H(4BA)	109.5
C(3B)-C(4B)-H(4BB)	109.5
H(4BA)-C(4B)-H(4BB)	109.5
C(3B)-C(4B)-H(4BC)	109.5
H(4BA)-C(4B)-H(4BC)	109.5
H(4BB)-C(4B)-H(4BC)	109.5
C(3B)-C(5B)-H(5BA)	109.5
C(3B)-C(5B)-H(5BB)	109.5
H(5BA)-C(5B)-H(5BB)	109.5
C(3B)-C(5B)-H(5BC)	109.5
H(5BA)-C(5B)-H(5BC)	109.5
H(5BB)-C(5B)-H(5BC)	109.5
C(7B)-C(6B)-C(11B)	121.93(16)
C(7B)-C(6B)-C(1B)	121.19(16)
C(11B)-C(6B)-C(1B)	116.85(15)
C(8B)-C(7B)-C(6B)	118.92(17)
C(8B)-C(7B)-H(7BA)	120.5
C(6B)-C(7B)-H(7BA)	120.5
C(9B)-C(8B)-C(7B)	120.30(17)

C(9B)-C(8B)-H(8BA)	119.8
C(7B)-C(8B)-H(8BA)	119.8
C(8B)-C(9B)-C(10B)	120.51(17)
C(8B)-C(9B)-H(9BA)	119.7
C(10B)-C(9B)-H(9BA)	119.7
C(11B)-C(10B)-C(9B)	120.24(17)
C(11B)-C(10B)-H(10B)	119.9
C(9B)-C(10B)-H(10B)	119.9
C(10B)-C(11B)-C(6B)	118.10(16)
C(10B)-C(11B)-Sn(1B)	125.37(13)
C(6B)-C(11B)-Sn(1B)	116.52(12)
C(17B)-C(12B)-C(13B)	118.40(16)
C(17B)-C(12B)-Sn(1B)	120.62(13)
C(13B)-C(12B)-Sn(1B)	120.67(13)
C(14B)-C(13B)-C(12B)	120.72(18)
C(14B)-C(13B)-H(13B)	119.6
C(12B)-C(13B)-H(13B)	119.6
C(15B)-C(14B)-C(13B)	120.02(18)
C(15B)-C(14B)-H(14B)	120.0
C(13B)-C(14B)-H(14B)	120.0
C(16B)-C(15B)-C(14B)	119.95(18)
C(16B)-C(15B)-H(15B)	120.0
C(14B)-C(15B)-H(15B)	120.0
C(15B)-C(16B)-C(17B)	119.98(18)
C(15B)-C(16B)-H(16B)	120.0
C(17B)-C(16B)-H(16B)	120.0
C(16B)-C(17B)-C(12B)	120.91(17)
C(16B)-C(17B)-H(17B)	119.5
C(12B)-C(17B)-H(17B)	119.5
C(23B)-C(18B)-C(19B)	118.37(17)
C(23B)-C(18B)-Sn(1B)	122.68(14)
C(19B)-C(18B)-Sn(1B)	118.91(13)
C(20B)-C(19B)-C(18B)	120.86(18)
C(20B)-C(19B)-H(19B)	119.6
C(18B)-C(19B)-H(19B)	119.6
C(21B)-C(20B)-C(19B)	120.0(2)

C(21B)-C(20B)-H(20B) 120.0
C(19B)-C(20B)-H(20B) 120.0
C(20B)-C(21B)-C(22B) 119.7(2)
C(20B)-C(21B)-H(21B) 120.2
C(22B)-C(21B)-H(21B) 120.2
C(23B)-C(22B)-C(21B) 120.3(2)
C(23B)-C(22B)-H(22B) 119.9
C(21B)-C(22B)-H(22B) 119.9
C(22B)-C(23B)-C(18B) 120.8(2)
C(22B)-C(23B)-H(23B) 119.6
C(18B)-C(23B)-H(23B) 119.6

Symmetry transformations used to generate equivalent atoms:

Anisotropic displacement parameters ($\text{\AA}^2 \times 10^3$) for **11**. The anisotropic displacement factor exponent takes the form: $-2\alpha^2 [h^2 a^* U_{11} + \dots + 2 h k a^* b^* U_{12}]$

	U ¹¹	U ²²	U ³³	U ²³	U ¹³	U ¹²
Sn(1A)	16(1)	16(1)	14(1)	1(1)	-2(1)	0(1)
Cl(1A)	20(1)	30(1)	27(1)	-1(1)	-2(1)	8(1)
O(1A)	19(1)	36(1)	19(1)	-2(1)	-2(1)	10(1)
N(1A)	14(1)	17(1)	17(1)	1(1)	1(1)	0(1)
C(1A)	13(1)	20(1)	18(1)	5(1)	1(1)	-1(1)
C(2A)	21(1)	29(1)	20(1)	-1(1)	2(1)	9(1)
C(3A)	18(1)	23(1)	19(1)	0(1)	3(1)	5(1)
C(4A)	25(1)	43(1)	23(1)	9(1)	5(1)	2(1)
C(5A)	34(1)	26(1)	29(1)	-8(1)	-5(1)	8(1)
C(6A)	17(1)	19(1)	15(1)	3(1)	2(1)	-2(1)
C(7A)	18(1)	29(1)	18(1)	2(1)	-2(1)	-1(1)
C(8A)	24(1)	30(1)	18(1)	-3(1)	-3(1)	-6(1)
C(9A)	26(1)	23(1)	21(1)	-5(1)	3(1)	-1(1)
C(10A)	18(1)	21(1)	20(1)	0(1)	1(1)	1(1)
C(11A)	18(1)	16(1)	14(1)	2(1)	0(1)	-3(1)
C(12A)	15(1)	19(1)	15(1)	4(1)	-4(1)	-2(1)
C(13A)	21(1)	27(1)	24(1)	2(1)	-1(1)	2(1)
C(14A)	21(1)	48(1)	22(1)	4(1)	2(1)	2(1)
C(15A)	22(1)	45(1)	31(1)	20(1)	-2(1)	-6(1)
C(16A)	27(1)	25(1)	39(1)	13(1)	-9(1)	-5(1)
C(17A)	20(1)	23(1)	26(1)	2(1)	-6(1)	0(1)
C(18A)	13(1)	17(1)	22(1)	0(1)	1(1)	1(1)
C(19A)	24(1)	28(1)	28(1)	6(1)	-7(1)	-2(1)
C(20A)	31(1)	26(1)	45(1)	16(1)	-1(1)	-2(1)
C(21A)	28(1)	19(1)	50(1)	-4(1)	8(1)	-4(1)
C(22A)	32(1)	31(1)	30(1)	-13(1)	5(1)	-9(1)
C(23A)	26(1)	26(1)	18(1)	-1(1)	4(1)	-4(1)
Sn(1B)	17(1)	16(1)	16(1)	2(1)	2(1)	2(1)
Cl(1B)	17(1)	28(1)	32(1)	4(1)	0(1)	-3(1)
O(1B)	20(1)	32(1)	22(1)	-2(1)	5(1)	-6(1)
N(1B)	17(1)	17(1)	18(1)	1(1)	0(1)	-1(1)

C(1B)	16(1)	17(1)	18(1)	4(1)	0(1)	2(1)
C(2B)	22(1)	26(1)	25(1)	-1(1)	-1(1)	-5(1)
C(3B)	21(1)	23(1)	19(1)	1(1)	-2(1)	-4(1)
C(4B)	32(1)	36(1)	24(1)	6(1)	-7(1)	-3(1)
C(5B)	33(1)	26(1)	30(1)	-5(1)	2(1)	-4(1)
C(6B)	21(1)	17(1)	16(1)	2(1)	1(1)	3(1)
C(7B)	24(1)	24(1)	21(1)	0(1)	4(1)	3(1)
C(8B)	38(1)	24(1)	21(1)	-4(1)	5(1)	6(1)
C(9B)	37(1)	21(1)	24(1)	-6(1)	-5(1)	1(1)
C(10B)	23(1)	18(1)	24(1)	0(1)	-2(1)	2(1)
C(11B)	20(1)	15(1)	16(1)	2(1)	-1(1)	4(1)
C(12B)	18(1)	17(1)	15(1)	2(1)	-1(1)	-2(1)
C(13B)	21(1)	29(1)	25(1)	3(1)	4(1)	2(1)
C(14B)	30(1)	40(1)	23(1)	7(1)	4(1)	-6(1)
C(15B)	35(1)	27(1)	24(1)	9(1)	-8(1)	-9(1)
C(16B)	24(1)	20(1)	33(1)	4(1)	-8(1)	-1(1)
C(17B)	20(1)	19(1)	23(1)	-1(1)	1(1)	0(1)
C(18B)	14(1)	18(1)	22(1)	1(1)	3(1)	2(1)
C(19B)	22(1)	28(1)	21(1)	5(1)	5(1)	3(1)
C(20B)	27(1)	32(1)	42(1)	19(1)	8(1)	8(1)
C(21B)	34(1)	21(1)	66(2)	2(1)	11(1)	10(1)
C(22B)	40(1)	36(1)	46(1)	-18(1)	0(1)	14(1)
C(23B)	34(1)	33(1)	25(1)	-4(1)	-1(1)	13(1)

Hydrogen coordinates (x 10⁴) and isotropic displacement parameters (Å² x 10³) for **11**.

	x	y	z	U(eq)
H(2AA)	11681	-872	4192	28
H(2AB)	12862	313	3990	28
H(4AA)	10759	2031	2995	45
H(4AB)	12217	1121	3038	45
H(4AC)	11990	2429	3461	45
H(5AA)	9319	-316	3054	45
H(5AB)	9451	-1250	3601	45
H(5AC)	10738	-1251	3167	45
H(7AA)	11257	2640	5435	26
H(8AA)	10142	4184	6057	29
H(9AA)	7797	4989	5863	28
H(10A)	6543	4291	5042	23
H(13A)	8025	1938	2717	29
H(14A)	8438	3284	1932	36
H(15A)	8350	5789	1974	39
H(16A)	7746	6939	2796	37
H(17A)	7242	5592	3575	28
H(19A)	6705	-323	4633	32
H(20A)	5544	-2592	4552	41
H(21A)	4408	-3338	3717	39
H(22A)	4395	-1806	2966	37
H(23A)	5546	475	3046	28
H(2BA)	6962	11150	821	29
H(2BB)	8123	10016	1050	29
H(4BA)	6099	8462	2091	46
H(4BB)	7574	9411	2028	46
H(4BC)	7267	8006	1647	46
H(5BA)	4736	10719	1962	45
H(5BB)	4756	11521	1384	45

H(5BC)	6130	11698	1808	45
H(7BA)	6231	7449	-346	27
H(8BA)	4961	5808	-943	33
H(9BA)	2603	4994	-743	33
H(10B)	1483	5795	56	26
H(13B)	830	7129	2197	30
H(14B)	1202	5701	2968	37
H(15B)	3331	4389	3064	35
H(16B)	5095	4513	2389	31
H(17B)	4772	6011	1635	25
H(19B)	1273	10178	301	28
H(20B)	586	12574	297	40
H(21B)	597	13906	1122	48
H(22B)	1244	12818	1951	49
H(23B)	1863	10412	1959	37

—

Torsion angles [°] for **11**.

C(3A)-N(1A)-C(1A)-O(1A)	-5.4(2)
Sn(1A)-N(1A)-C(1A)-O(1A)	172.06(12)
C(3A)-N(1A)-C(1A)-C(6A)	174.04(15)
Sn(1A)-N(1A)-C(1A)-C(6A)	-8.55(19)
C(2A)-O(1A)-C(1A)-N(1A)	-5.6(2)
C(2A)-O(1A)-C(1A)-C(6A)	174.93(15)
C(1A)-O(1A)-C(2A)-C(3A)	13.44(18)
C(1A)-N(1A)-C(3A)-C(5A)	133.53(16)
Sn(1A)-N(1A)-C(3A)-C(5A)	-42.1(3)
C(1A)-N(1A)-C(3A)-C(4A)	-103.46(17)
Sn(1A)-N(1A)-C(3A)-C(4A)	80.9(2)
C(1A)-N(1A)-C(3A)-C(2A)	13.10(18)
Sn(1A)-N(1A)-C(3A)-C(2A)	-162.52(15)
O(1A)-C(2A)-C(3A)-N(1A)	-15.81(17)
O(1A)-C(2A)-C(3A)-C(5A)	-134.72(16)
O(1A)-C(2A)-C(3A)-C(4A)	99.11(17)
N(1A)-C(1A)-C(6A)-C(7A)	-170.49(17)
O(1A)-C(1A)-C(6A)-C(7A)	8.9(2)
N(1A)-C(1A)-C(6A)-C(11A)	6.6(3)
O(1A)-C(1A)-C(6A)-C(11A)	-173.96(15)
C(11A)-C(6A)-C(7A)-C(8A)	-0.1(3)
C(1A)-C(6A)-C(7A)-C(8A)	176.88(16)
C(6A)-C(7A)-C(8A)-C(9A)	0.6(3)
C(7A)-C(8A)-C(9A)-C(10A)	-0.4(3)
C(8A)-C(9A)-C(10A)-C(11A)	-0.3(3)
C(9A)-C(10A)-C(11A)-C(6A)	0.8(3)
C(9A)-C(10A)-C(11A)-Sn(1A)	-176.94(13)
C(7A)-C(6A)-C(11A)-C(10A)	-0.6(3)
C(1A)-C(6A)-C(11A)-C(10A)	-177.72(15)
C(7A)-C(6A)-C(11A)-Sn(1A)	177.33(13)
C(1A)-C(6A)-C(11A)-Sn(1A)	0.2(2)
C(17A)-C(12A)-C(13A)-C(14A)	0.7(3)
Sn(1A)-C(12A)-C(13A)-C(14A)	179.27(14)
C(12A)-C(13A)-C(14A)-C(15A)	1.0(3)

C(13A)-C(14A)-C(15A)-C(16A)	-1.5(3)
C(14A)-C(15A)-C(16A)-C(17A)	0.2(3)
C(15A)-C(16A)-C(17A)-C(12A)	1.6(3)
C(13A)-C(12A)-C(17A)-C(16A)	-2.0(3)
Sn(1A)-C(12A)-C(17A)-C(16A)	179.40(13)
C(23A)-C(18A)-C(19A)-C(20A)	0.2(3)
Sn(1A)-C(18A)-C(19A)-C(20A)	175.94(15)
C(18A)-C(19A)-C(20A)-C(21A)	0.3(3)
C(19A)-C(20A)-C(21A)-C(22A)	-0.5(3)
C(20A)-C(21A)-C(22A)-C(23A)	0.4(3)
C(19A)-C(18A)-C(23A)-C(22A)	-0.3(3)
Sn(1A)-C(18A)-C(23A)-C(22A)	-176.04(14)
C(21A)-C(22A)-C(23A)-C(18A)	0.1(3)
C(3B)-N(1B)-C(1B)-O(1B)	-3.6(2)
Sn(1B)-N(1B)-C(1B)-O(1B)	168.69(12)
C(3B)-N(1B)-C(1B)-C(6B)	175.23(15)
Sn(1B)-N(1B)-C(1B)-C(6B)	-12.48(19)
C(2B)-O(1B)-C(1B)-N(1B)	-6.2(2)
C(2B)-O(1B)-C(1B)-C(6B)	174.90(15)
C(1B)-O(1B)-C(2B)-C(3B)	12.61(18)
C(1B)-N(1B)-C(3B)-C(5B)	131.21(16)
Sn(1B)-N(1B)-C(3B)-C(5B)	-36.0(3)
C(1B)-N(1B)-C(3B)-C(4B)	-106.25(17)
Sn(1B)-N(1B)-C(3B)-C(4B)	86.6(2)
C(1B)-N(1B)-C(3B)-C(2B)	11.00(18)
Sn(1B)-N(1B)-C(3B)-C(2B)	-156.18(15)
O(1B)-C(2B)-C(3B)-N(1B)	-14.11(18)
O(1B)-C(2B)-C(3B)-C(5B)	-132.77(16)
O(1B)-C(2B)-C(3B)-C(4B)	101.43(17)
N(1B)-C(1B)-C(6B)-C(7B)	-168.88(17)
O(1B)-C(1B)-C(6B)-C(7B)	9.9(2)
N(1B)-C(1B)-C(6B)-C(11B)	9.0(3)
O(1B)-C(1B)-C(6B)-C(11B)	-172.22(15)
C(11B)-C(6B)-C(7B)-C(8B)	-0.6(3)
C(1B)-C(6B)-C(7B)-C(8B)	177.15(17)
C(6B)-C(7B)-C(8B)-C(9B)	0.6(3)

C(7B)-C(8B)-C(9B)-C(10B)	-0.2(3)
C(8B)-C(9B)-C(10B)-C(11B)	-0.4(3)
C(9B)-C(10B)-C(11B)-C(6B)	0.4(3)
C(9B)-C(10B)-C(11B)-Sn(1B)	-178.58(13)
C(7B)-C(6B)-C(11B)-C(10B)	0.0(3)
C(1B)-C(6B)-C(11B)-C(10B)	-177.78(15)
C(7B)-C(6B)-C(11B)-Sn(1B)	179.15(13)
C(1B)-C(6B)-C(11B)-Sn(1B)	1.3(2)
C(17B)-C(12B)-C(13B)-C(14B)	1.0(3)
Sn(1B)-C(12B)-C(13B)-C(14B)	174.59(15)
C(12B)-C(13B)-C(14B)-C(15B)	-1.3(3)
C(13B)-C(14B)-C(15B)-C(16B)	0.1(3)
C(14B)-C(15B)-C(16B)-C(17B)	1.2(3)
C(15B)-C(16B)-C(17B)-C(12B)	-1.5(3)
C(13B)-C(12B)-C(17B)-C(16B)	0.4(3)
Sn(1B)-C(12B)-C(17B)-C(16B)	-173.23(13)
C(23B)-C(18B)-C(19B)-C(20B)	0.8(3)
Sn(1B)-C(18B)-C(19B)-C(20B)	-177.19(14)
C(18B)-C(19B)-C(20B)-C(21B)	0.5(3)
C(19B)-C(20B)-C(21B)-C(22B)	-0.9(3)
C(20B)-C(21B)-C(22B)-C(23B)	-0.1(3)
C(21B)-C(22B)-C(23B)-C(18B)	1.4(3)
C(19B)-C(18B)-C(23B)-C(22B)	-1.7(3)
Sn(1B)-C(18B)-C(23B)-C(22B)	176.13(16)

Symmetry transformations used to generate equivalent atoms:

Table A3: Crystal data and structure refinement for **13**.

Identification code	d17164_a	
Empirical formula	C17 H17 Br2 N O Sn	
Formula weight	529.82	
Temperature	150(2) K	
Wavelength	0.71073 Å	
Crystal system	Monoclinic	
Space group	P2 ₁ /n	
Unit cell dimensions	a = 10.5295(7) Å b = 10.0336(5) Å c = 17.1396(11) Å	□ = 90°. □ = 96.677(2)°. □ = 90°.
Volume	1798.50(19) Å ³	
Z	4	
Density (calculated)	1.957 Mg/m ³	
Absorption coefficient	5.865 mm ⁻¹	
F(000)	1016	
Crystal size	0.120 x 0.090 x 0.050 mm ³	
Theta range for data collection	2.164 to 27.535°.	
Index ranges	-13<=h<=13, -12<=k<=13, -22<=l<=22	
Reflections collected	38637	
Independent reflections	4135 [R(int) = 0.0364]	
Completeness to theta = 25.242°	100.0 %	
Absorption correction	Semi-empirical from equivalents	
Max. and min. transmission	0.7456 and 0.5610	
Refinement method	Full-matrix least-squares on F ²	
Data / restraints / parameters	4135 / 54 / 220	
Goodness-of-fit on F ²	1.052	
Final R indices [I>2sigma(I)]	R1 = 0.0219, wR2 = 0.0383	
R indices (all data)	R1 = 0.0358, wR2 = 0.0422	
Extinction coefficient	n/a	
Largest diff. peak and hole	0.553 and -0.467 e.Å ⁻³	

Atomic coordinates ($\times 10^4$) and equivalent isotropic displacement parameters ($\text{\AA}^2 \times 10^3$) for **13**. $U(\text{eq})$ is defined as one third of the trace of the orthogonalized U^{ij} tensor.

	x	y	z	$U(\text{eq})$
Sn(1)	6822(1)	2886(1)	4710(1)	17(1)
Br(1)	8038(1)	944(1)	5321(1)	29(1)
Br(2)	5466(1)	3086(1)	5892(1)	28(1)
O(1)	9820(30)	4220(40)	3340(20)	20(4)
O(1A)	9640(17)	4319(18)	3239(10)	24(3)
N(1)	8278(2)	2927(2)	3744(1)	18(1)
C(1)	7681(2)	4814(2)	4841(1)	16(1)
C(2)	7364(2)	5779(2)	5362(2)	23(1)
C(3)	7910(3)	7042(3)	5350(2)	29(1)
C(4)	8800(3)	7324(3)	4840(2)	27(1)
C(5)	9152(2)	6360(2)	4327(1)	21(1)
C(6)	8577(2)	5112(2)	4325(1)	16(1)
C(7)	8849(2)	4062(2)	3778(1)	19(1)
C(8)	9670(30)	3130(30)	2770(20)	31(5)
C(8A)	9849(16)	3015(15)	2877(11)	39(3)
C(9)	8732(2)	2142(3)	3090(1)	24(1)
C(10)	9242(3)	798(3)	3378(2)	46(1)
C(11)	7644(3)	1994(3)	2431(2)	38(1)
C(12)	5330(2)	2290(2)	3836(1)	18(1)
C(13)	4863(2)	3196(3)	3261(2)	24(1)
C(14)	3912(3)	2824(3)	2668(2)	32(1)
C(15)	3436(3)	1537(3)	2654(2)	33(1)
C(16)	3888(3)	632(3)	3224(2)	30(1)
C(17)	4838(2)	1008(3)	3817(2)	24(1)

Bond lengths [\AA] and angles [$^\circ$] for **13**.

Sn(1)-C(12)	2.127(2)
Sn(1)-C(1)	2.137(2)
Sn(1)-N(1)	2.383(2)
Sn(1)-Br(1)	2.4943(3)
Sn(1)-Br(2)	2.6180(3)
O(1)-C(7)	1.339(8)
O(1)-C(8)	1.475(11)
O(1A)-C(7)	1.339(5)
O(1A)-C(8A)	1.476(9)
N(1)-C(7)	1.286(3)
N(1)-C(9)	1.493(3)
C(1)-C(2)	1.383(3)
C(1)-C(6)	1.399(3)
C(2)-C(3)	1.393(4)
C(2)-H(2A)	0.9500
C(3)-C(4)	1.384(4)
C(3)-H(3A)	0.9500
C(4)-C(5)	1.386(4)
C(4)-H(4A)	0.9500
C(5)-C(6)	1.391(3)
C(5)-H(5A)	0.9500
C(6)-C(7)	1.460(3)
C(8)-C(9)	1.546(8)
C(8)-H(8A)	0.9900
C(8)-H(8B)	0.9900
C(8A)-C(9)	1.544(6)
C(8A)-H(8AA)	0.9900
C(8A)-H(8AB)	0.9900
C(9)-C(10)	1.513(4)
C(9)-C(11)	1.520(4)
C(10)-H(10A)	0.9800
C(10)-H(10B)	0.9800
C(10)-H(10C)	0.9800
C(11)-H(11A)	0.9800

C(11)-H(11B)	0.9800
C(11)-H(11C)	0.9800
C(12)-C(17)	1.385(3)
C(12)-C(13)	1.388(3)
C(13)-C(14)	1.392(4)
C(13)-H(13A)	0.9500
C(14)-C(15)	1.385(4)
C(14)-H(14A)	0.9500
C(15)-C(16)	1.378(4)
C(15)-H(15A)	0.9500
C(16)-C(17)	1.392(4)
C(16)-H(16A)	0.9500
C(17)-H(17A)	0.9500

C(12)-Sn(1)-C(1)	126.73(9)
C(12)-Sn(1)-N(1)	89.86(8)
C(1)-Sn(1)-N(1)	76.06(8)
C(12)-Sn(1)-Br(1)	112.14(7)
C(1)-Sn(1)-Br(1)	118.23(6)
N(1)-Sn(1)-Br(1)	87.98(5)
C(12)-Sn(1)-Br(2)	98.14(6)
C(1)-Sn(1)-Br(2)	96.41(6)
N(1)-Sn(1)-Br(2)	171.36(5)
Br(1)-Sn(1)-Br(2)	91.994(11)
C(7)-O(1)-C(8)	105(2)
C(7)-O(1A)-C(8A)	104.7(11)
C(7)-N(1)-C(9)	108.2(2)
C(7)-N(1)-Sn(1)	108.60(15)
C(9)-N(1)-Sn(1)	143.15(16)
C(2)-C(1)-C(6)	119.4(2)
C(2)-C(1)-Sn(1)	124.76(18)
C(6)-C(1)-Sn(1)	115.79(16)
C(1)-C(2)-C(3)	119.7(2)
C(1)-C(2)-H(2A)	120.1
C(3)-C(2)-H(2A)	120.1
C(4)-C(3)-C(2)	120.4(2)

C(4)-C(3)-H(3A)	119.8
C(2)-C(3)-H(3A)	119.8
C(3)-C(4)-C(5)	120.6(2)
C(3)-C(4)-H(4A)	119.7
C(5)-C(4)-H(4A)	119.7
C(4)-C(5)-C(6)	118.7(2)
C(4)-C(5)-H(5A)	120.6
C(6)-C(5)-H(5A)	120.6
C(5)-C(6)-C(1)	121.1(2)
C(5)-C(6)-C(7)	122.3(2)
C(1)-C(6)-C(7)	116.7(2)
N(1)-C(7)-O(1)	117.7(16)
N(1)-C(7)-O(1A)	117.7(7)
N(1)-C(7)-C(6)	122.9(2)
O(1)-C(7)-C(6)	119.1(16)
O(1A)-C(7)-C(6)	119.1(7)
O(1)-C(8)-C(9)	105(2)
O(1)-C(8)-H(8A)	110.8
C(9)-C(8)-H(8A)	110.8
O(1)-C(8)-H(8B)	110.8
C(9)-C(8)-H(8B)	110.8
H(8A)-C(8)-H(8B)	108.8
O(1A)-C(8A)-C(9)	104.4(10)
O(1A)-C(8A)-H(8AA)	110.9
C(9)-C(8A)-H(8AA)	110.9
O(1A)-C(8A)-H(8AB)	110.9
C(9)-C(8A)-H(8AB)	110.9
H(8AA)-C(8A)-H(8AB)	108.9
N(1)-C(9)-C(10)	111.0(2)
N(1)-C(9)-C(11)	109.3(2)
C(10)-C(9)-C(11)	111.3(2)
N(1)-C(9)-C(8A)	101.4(6)
C(10)-C(9)-C(8A)	109.3(8)
C(11)-C(9)-C(8A)	114.1(8)
N(1)-C(9)-C(8)	101.9(13)
C(10)-C(9)-C(8)	117.8(17)

C(11)-C(9)-C(8)	104.9(17)
C(9)-C(10)-H(10A)	109.5
C(9)-C(10)-H(10B)	109.5
H(10A)-C(10)-H(10B)	109.5
C(9)-C(10)-H(10C)	109.5
H(10A)-C(10)-H(10C)	109.5
H(10B)-C(10)-H(10C)	109.5
C(9)-C(11)-H(11A)	109.5
C(9)-C(11)-H(11B)	109.5
H(11A)-C(11)-H(11B)	109.5
C(9)-C(11)-H(11C)	109.5
H(11A)-C(11)-H(11C)	109.5
H(11B)-C(11)-H(11C)	109.5
C(17)-C(12)-C(13)	119.4(2)
C(17)-C(12)-Sn(1)	121.44(18)
C(13)-C(12)-Sn(1)	119.16(18)
C(12)-C(13)-C(14)	120.5(2)
C(12)-C(13)-H(13A)	119.7
C(14)-C(13)-H(13A)	119.7
C(15)-C(14)-C(13)	119.5(3)
C(15)-C(14)-H(14A)	120.3
C(13)-C(14)-H(14A)	120.3
C(16)-C(15)-C(14)	120.5(3)
C(16)-C(15)-H(15A)	119.8
C(14)-C(15)-H(15A)	119.8
C(15)-C(16)-C(17)	119.9(3)
C(15)-C(16)-H(16A)	120.0
C(17)-C(16)-H(16A)	120.0
C(12)-C(17)-C(16)	120.3(2)
C(12)-C(17)-H(17A)	119.9
C(16)-C(17)-H(17A)	119.9

Symmetry transformations used to generate equivalent atoms:

Anisotropic displacement parameters ($\text{\AA}^2 \times 10^3$) for **13**. The anisotropic displacement factor exponent takes the form: $-2\alpha^2 [h^2 a^* U_{11} + \dots + 2 h k a^* b^* U_{12}]$

	U ₁₁	U ₂₂	U ₃₃	U ₂₃	U ₁₃	U ₁₂
Sn(1)	17(1)	17(1)	15(1)	1(1)	1(1)	-1(1)
Br(1)	30(1)	25(1)	33(1)	11(1)	4(1)	5(1)
Br(2)	27(1)	38(1)	19(1)	3(1)	8(1)	-1(1)
O(1)	14(6)	34(7)	11(6)	1(5)	-1(5)	-2(5)
O(1A)	25(5)	31(3)	19(5)	-3(3)	8(4)	-2(3)
N(1)	17(1)	20(1)	18(1)	-3(1)	3(1)	2(1)
C(1)	15(1)	17(1)	15(1)	0(1)	-1(1)	1(1)
C(2)	19(1)	26(1)	25(1)	-6(1)	3(1)	1(1)
C(3)	26(2)	24(1)	36(2)	-14(1)	2(1)	2(1)
C(4)	27(2)	17(1)	33(2)	-2(1)	-6(1)	-2(1)
C(5)	16(1)	25(1)	21(1)	3(1)	0(1)	-1(1)
C(6)	16(1)	19(1)	13(1)	1(1)	-3(1)	2(1)
C(7)	17(1)	25(1)	14(1)	1(1)	1(1)	1(1)
C(8)	34(10)	35(7)	28(8)	-11(5)	17(7)	2(6)
C(8A)	32(4)	53(5)	34(6)	-24(4)	14(4)	-6(4)
C(9)	24(1)	29(1)	19(1)	-9(1)	4(1)	4(1)
C(10)	64(2)	39(2)	34(2)	-14(1)	3(2)	24(2)
C(11)	32(2)	59(2)	23(2)	-14(1)	-1(1)	1(2)
C(12)	14(1)	23(1)	16(1)	-4(1)	2(1)	-1(1)
C(13)	24(1)	25(1)	23(1)	1(1)	2(1)	1(1)
C(14)	27(2)	44(2)	24(1)	2(1)	-2(1)	8(1)
C(15)	21(1)	52(2)	26(2)	-14(1)	-1(1)	-2(1)
C(16)	26(2)	32(2)	31(2)	-11(1)	5(1)	-9(1)
C(17)	25(1)	26(1)	21(1)	0(1)	5(1)	-3(1)

Hydrogen coordinates (x 10⁴) and isotropic displacement parameters (Å² x 10³) for **13**.

	x	y	z	U(eq)
H(2A)	6775	5580	5726	28
H(3A)	7670	7714	5695	35
H(4A)	9172	8186	4840	32
H(5A)	9775	6548	3983	25
H(8A)	10508	2690	2729	38
H(8B)	9326	3458	2243	38
H(8AA)	10682	2630	3094	47
H(8AB)	9828	3100	2300	47
H(10A)	8539	254	3531	69
H(10B)	9887	922	3832	69
H(10C)	9629	348	2956	69
H(11A)	6965	1446	2612	58
H(11B)	7963	1565	1978	58
H(11C)	7302	2876	2277	58
H(13A)	5195	4077	3272	29
H(14A)	3592	3448	2277	38
H(15A)	2793	1275	2247	40
H(16A)	3553	-247	3213	36
H(17A)	5149	384	4210	28

Torsion angles [°] for **13**.

C(6)-C(1)-C(2)-C(3)	1.9(4)
Sn(1)-C(1)-C(2)-C(3)	-174.54(19)
C(1)-C(2)-C(3)-C(4)	-2.2(4)
C(2)-C(3)-C(4)-C(5)	0.6(4)
C(3)-C(4)-C(5)-C(6)	1.2(4)
C(4)-C(5)-C(6)-C(1)	-1.5(3)
C(4)-C(5)-C(6)-C(7)	177.0(2)
C(2)-C(1)-C(6)-C(5)	0.0(3)
Sn(1)-C(1)-C(6)-C(5)	176.70(17)
C(2)-C(1)-C(6)-C(7)	-178.6(2)
Sn(1)-C(1)-C(6)-C(7)	-1.9(3)
C(9)-N(1)-C(7)-O(1)	-10(2)
Sn(1)-N(1)-C(7)-O(1)	172(2)
C(9)-N(1)-C(7)-O(1A)	2.5(12)
Sn(1)-N(1)-C(7)-O(1A)	-175.1(12)
C(9)-N(1)-C(7)-C(6)	176.5(2)
Sn(1)-N(1)-C(7)-C(6)	-1.1(3)
C(8)-O(1)-C(7)-N(1)	16(4)
C(8)-O(1)-C(7)-C(6)	-170(3)
C(8A)-O(1A)-C(7)-N(1)	-14(2)
C(8A)-O(1A)-C(7)-C(6)	171.7(13)
C(5)-C(6)-C(7)-N(1)	-176.5(2)
C(1)-C(6)-C(7)-N(1)	2.1(3)
C(5)-C(6)-C(7)-O(1)	10(2)
C(1)-C(6)-C(7)-O(1)	-171(2)
C(5)-C(6)-C(7)-O(1A)	-2.6(12)
C(1)-C(6)-C(7)-O(1A)	176.0(12)
C(7)-O(1)-C(8)-C(9)	-15(5)
C(7)-O(1A)-C(8A)-C(9)	19(2)
C(7)-N(1)-C(9)-C(10)	125.6(2)
Sn(1)-N(1)-C(9)-C(10)	-58.2(3)
C(7)-N(1)-C(9)-C(11)	-111.2(2)
Sn(1)-N(1)-C(9)-C(11)	65.0(3)
C(7)-N(1)-C(9)-C(8A)	9.6(9)

Sn(1)-N(1)-C(9)-C(8A)	-174.2(9)
C(7)-N(1)-C(9)-C(8)	-0.7(19)
Sn(1)-N(1)-C(9)-C(8)	175.6(19)
O(1A)-C(8A)-C(9)-N(1)	-16.8(18)
O(1A)-C(8A)-C(9)-C(10)	-134.1(15)
O(1A)-C(8A)-C(9)-C(11)	100.5(16)
O(1)-C(8)-C(9)-N(1)	9(4)
O(1)-C(8)-C(9)-C(10)	-112(3)
O(1)-C(8)-C(9)-C(11)	123(3)
C(17)-C(12)-C(13)-C(14)	-0.2(4)
Sn(1)-C(12)-C(13)-C(14)	178.2(2)
C(12)-C(13)-C(14)-C(15)	-0.3(4)
C(13)-C(14)-C(15)-C(16)	0.7(4)
C(14)-C(15)-C(16)-C(17)	-0.5(4)
C(13)-C(12)-C(17)-C(16)	0.4(4)
Sn(1)-C(12)-C(17)-C(16)	-178.03(19)
C(15)-C(16)-C(17)-C(12)	0.0(4)

Symmetry transformations used to generate equivalent atoms:

Table A4: Crystal data and structure refinement for **18**.

Identification code	d1887_a
Empirical formula	C ₃₀ H ₂₉ N O Sn
Formula weight	538.23
Temperature	150(2) K
Wavelength	0.71073 Å
Crystal system	Orthorhombic
Space group	P ₂ 12 ₁ 2 ₁
Unit cell dimensions	a = 8.4502(2) Å b = 18.9557(5) Å c = 31.5231(9) Å
Volume	5049.4(2) Å ³
Z	8
Density (calculated)	1.416 Mg/m ³
Absorption coefficient	1.034 mm ⁻¹
F(000)	2192
Crystal size	0.400 x 0.080 x 0.080 mm ³
Theta range for data collection	1.680 to 27.489°.
Index ranges	-10<=h<=8, -24<=k<=21, -40<=l<=40
Reflections collected	27514
Independent reflections	11499 [R(int) = 0.0346]
Completeness to theta = 25.242°	99.5 %
Absorption correction	Semi-empirical from equivalents
Max. and min. transmission	0.7456 and 0.6836
Refinement method	Full-matrix least-squares on F ²
Data / restraints / parameters	11499 / 0 / 599
Goodness-of-fit on F ²	0.987
Final R indices [I>2sigma(I)]	R1 = 0.0316, wR2 = 0.0485
R indices (all data)	R1 = 0.0449, wR2 = 0.0517
Absolute structure parameter	0.008(11)
Extinction coefficient	n/a
Largest diff. peak and hole	0.473 and -0.414 e.Å ⁻³

Atomic coordinates (x 10⁴) and equivalent isotropic displacement parameters (Å² x 10³) for **18**. U(eq) is defined as one third of the trace of the orthogonalized U^{ij} tensor.

	x	y	z	U(eq)
Sn(1A)	7729(1)	6447(1)	3679(1)	19(1)
O(1A)	9605(3)	3999(2)	3330(1)	29(1)
N(1A)	9128(4)	5142(2)	3171(1)	21(1)
C(1A)	6114(4)	5689(2)	3405(1)	22(1)
C(2A)	6100(4)	5032(2)	3665(2)	20(1)
C(3A)	4897(5)	4933(2)	3963(2)	27(1)
C(4A)	4861(5)	4371(3)	4235(2)	34(1)
C(5A)	6025(5)	3847(3)	4208(2)	33(1)
C(6A)	7217(5)	3922(2)	3911(2)	29(1)
C(7A)	7289(4)	4506(2)	3643(1)	20(1)
C(8A)	8677(4)	4587(2)	3365(1)	21(1)
C(9A)	11042(5)	4238(3)	3130(2)	30(1)
C(10A)	10624(5)	4964(2)	2949(1)	22(1)
C(11A)	10309(5)	4941(3)	2475(2)	32(1)
C(12A)	11864(5)	5519(2)	3056(2)	31(1)
C(13A)	6209(5)	7123(2)	4050(1)	20(1)
C(14A)	6579(5)	7281(3)	4471(2)	28(1)
C(15A)	5609(6)	7704(3)	4715(2)	38(1)
C(16A)	4263(6)	7990(3)	4540(2)	39(1)
C(17A)	3869(5)	7841(3)	4130(2)	35(1)
C(18A)	4827(5)	7408(2)	3881(2)	29(1)
C(19A)	8923(4)	7085(2)	3215(1)	20(1)
C(20A)	8750(5)	6976(2)	2784(1)	23(1)
C(21A)	9505(5)	7407(2)	2493(2)	30(1)
C(22A)	10484(5)	7943(2)	2628(2)	31(1)
C(23A)	10700(5)	8055(2)	3057(2)	29(1)
C(24A)	9908(5)	7632(2)	3349(2)	26(1)
C(25A)	9395(5)	6027(2)	4126(1)	20(1)
C(26A)	10918(5)	6308(2)	4148(1)	22(1)

C(27A)	12009(5)	6063(2)	4442(1)	26(1)
C(28A)	11609(5)	5522(2)	4715(1)	28(1)
C(29A)	10108(5)	5234(3)	4697(2)	28(1)
C(30A)	9003(5)	5495(2)	4410(1)	21(1)
Sn(1B)	2962(1)	374(1)	3700(1)	21(1)
O(1B)	4814(3)	2834(2)	3327(1)	33(1)
N(1B)	4352(4)	1690(2)	3164(1)	23(1)
C(1B)	1372(5)	1115(2)	3406(1)	22(1)
C(2B)	1310(4)	1793(2)	3650(2)	20(1)
C(3B)	69(5)	1904(2)	3935(2)	25(1)
C(4B)	-34(5)	2506(3)	4180(2)	29(1)
C(5B)	1097(5)	3026(3)	4149(2)	29(1)
C(6B)	2341(5)	2934(2)	3870(1)	24(1)
C(7B)	2481(4)	2329(2)	3624(1)	21(1)
C(8B)	3883(5)	2241(2)	3354(1)	20(1)
C(9B)	6241(5)	2610(2)	3113(2)	31(1)
C(10B)	5854(5)	1866(2)	2944(2)	23(1)
C(11B)	5574(5)	1868(3)	2466(2)	31(1)
C(12B)	7105(5)	1326(3)	3063(2)	34(1)
C(13B)	1408(5)	-284(2)	4069(1)	23(1)
C(14B)	1671(5)	-401(3)	4498(2)	32(1)
C(15B)	682(5)	-841(3)	4734(2)	38(1)
C(16B)	-581(6)	-1155(3)	4545(2)	36(1)
C(17B)	-900(5)	-1040(3)	4119(2)	35(1)
C(18B)	84(5)	-605(2)	3884(2)	30(1)
C(19B)	4144(4)	-273(2)	3243(1)	21(1)
C(20B)	3993(5)	-156(2)	2811(1)	25(1)
C(21B)	4727(5)	-594(2)	2516(2)	29(1)
C(22B)	5647(5)	-1145(3)	2652(2)	32(1)
C(23B)	5822(5)	-1270(3)	3080(2)	33(1)
C(24B)	5062(5)	-843(2)	3376(2)	29(1)
C(25B)	4631(5)	808(2)	4141(2)	22(1)
C(26B)	6162(5)	530(3)	4169(1)	26(1)
C(27B)	7244(5)	786(3)	4459(1)	34(1)
C(28B)	6840(6)	1342(3)	4721(2)	40(1)
C(29B)	5337(6)	1629(3)	4698(2)	39(1)

C(30B)	4245(5)	1361(3)	4412(2)	32(1)
—				

Bond lengths [\AA] and angles [$^\circ$] for **18**.

Sn(1A)-C(25A)	2.143(4)
Sn(1A)-C(19A)	2.150(4)
Sn(1A)-C(13A)	2.158(4)
Sn(1A)-C(1A)	2.162(4)
O(1A)-C(8A)	1.367(5)
O(1A)-C(9A)	1.441(5)
N(1A)-C(8A)	1.275(5)
N(1A)-C(10A)	1.484(5)
C(1A)-C(2A)	1.490(6)
C(1A)-H(1AA)	0.9900
C(1A)-H(1AB)	0.9900
C(2A)-C(3A)	1.397(6)
C(2A)-C(7A)	1.418(5)
C(3A)-C(4A)	1.368(7)
C(3A)-H(3AA)	0.9500
C(4A)-C(5A)	1.400(7)
C(4A)-H(4AA)	0.9500
C(5A)-C(6A)	1.383(6)
C(5A)-H(5AA)	0.9500
C(6A)-C(7A)	1.393(6)
C(6A)-H(6AA)	0.9500
C(7A)-C(8A)	1.473(5)
C(9A)-C(10A)	1.532(6)
C(9A)-H(9AA)	0.9900
C(9A)-H(9AB)	0.9900
C(10A)-C(11A)	1.519(6)
C(10A)-C(12A)	1.522(6)
C(11A)-H(11A)	0.9800
C(11A)-H(11B)	0.9800
C(11A)-H(11C)	0.9800
C(12A)-H(12A)	0.9800
C(12A)-H(12B)	0.9800
C(12A)-H(12C)	0.9800
C(13A)-C(18A)	1.392(6)

C(13A)-C(14A)	1.396(6)
C(14A)-C(15A)	1.381(6)
C(14A)-H(14A)	0.9500
C(15A)-C(16A)	1.374(7)
C(15A)-H(15A)	0.9500
C(16A)-C(17A)	1.364(7)
C(16A)-H(16A)	0.9500
C(17A)-C(18A)	1.394(6)
C(17A)-H(17A)	0.9500
C(18A)-H(18A)	0.9500
C(19A)-C(20A)	1.383(6)
C(19A)-C(24A)	1.395(6)
C(20A)-C(21A)	1.383(6)
C(20A)-H(20A)	0.9500
C(21A)-C(22A)	1.377(6)
C(21A)-H(21A)	0.9500
C(22A)-C(23A)	1.382(7)
C(22A)-H(22A)	0.9500
C(23A)-C(24A)	1.393(6)
C(23A)-H(23A)	0.9500
C(24A)-H(24A)	0.9500
C(25A)-C(30A)	1.389(6)
C(25A)-C(26A)	1.395(6)
C(26A)-C(27A)	1.388(6)
C(26A)-H(26A)	0.9500
C(27A)-C(28A)	1.381(6)
C(27A)-H(27A)	0.9500
C(28A)-C(29A)	1.382(6)
C(28A)-H(28A)	0.9500
C(29A)-C(30A)	1.392(6)
C(29A)-H(29A)	0.9500
C(30A)-H(30A)	0.9500
Sn(1B)-C(19B)	2.139(4)
Sn(1B)-C(25B)	2.144(4)
Sn(1B)-C(1B)	2.153(4)
Sn(1B)-C(13B)	2.155(4)

O(1B)-C(8B)	1.375(5)
O(1B)-C(9B)	1.446(5)
N(1B)-C(8B)	1.267(5)
N(1B)-C(10B)	1.483(5)
C(1B)-C(2B)	1.500(6)
C(1B)-H(1BA)	0.9900
C(1B)-H(1BB)	0.9900
C(2B)-C(3B)	1.397(6)
C(2B)-C(7B)	1.421(5)
C(3B)-C(4B)	1.380(6)
C(3B)-H(3BA)	0.9500
C(4B)-C(5B)	1.376(6)
C(4B)-H(4BA)	0.9500
C(5B)-C(6B)	1.381(6)
C(5B)-H(5BA)	0.9500
C(6B)-C(7B)	1.389(5)
C(6B)-H(6BA)	0.9500
C(7B)-C(8B)	1.468(5)
C(9B)-C(10B)	1.543(6)
C(9B)-H(9BA)	0.9900
C(9B)-H(9BB)	0.9900
C(10B)-C(12B)	1.518(6)
C(10B)-C(11B)	1.525(6)
C(11B)-H(11D)	0.9800
C(11B)-H(11E)	0.9800
C(11B)-H(11F)	0.9800
C(12B)-H(12D)	0.9800
C(12B)-H(12E)	0.9800
C(12B)-H(12F)	0.9800
C(13B)-C(14B)	1.388(6)
C(13B)-C(18B)	1.400(6)
C(14B)-C(15B)	1.394(6)
C(14B)-H(14B)	0.9500
C(15B)-C(16B)	1.359(7)
C(15B)-H(15B)	0.9500
C(16B)-C(17B)	1.386(7)

C(16B)-H(16B)	0.9500
C(17B)-C(18B)	1.385(6)
C(17B)-H(17B)	0.9500
C(18B)-H(18B)	0.9500
C(19B)-C(20B)	1.386(6)
C(19B)-C(24B)	1.394(6)
C(20B)-C(21B)	1.394(6)
C(20B)-H(20B)	0.9500
C(21B)-C(22B)	1.370(6)
C(21B)-H(21B)	0.9500
C(22B)-C(23B)	1.379(7)
C(22B)-H(22B)	0.9500
C(23B)-C(24B)	1.391(7)
C(23B)-H(23B)	0.9500
C(24B)-H(24B)	0.9500
C(25B)-C(30B)	1.393(6)
C(25B)-C(26B)	1.400(6)
C(26B)-C(27B)	1.382(6)
C(26B)-H(26B)	0.9500
C(27B)-C(28B)	1.380(7)
C(27B)-H(27B)	0.9500
C(28B)-C(29B)	1.384(6)
C(28B)-H(28B)	0.9500
C(29B)-C(30B)	1.387(6)
C(29B)-H(29B)	0.9500
C(30B)-H(30B)	0.9500

C(25A)-Sn(1A)-C(19A)	110.34(15)
C(25A)-Sn(1A)-C(13A)	104.86(16)
C(19A)-Sn(1A)-C(13A)	108.28(16)
C(25A)-Sn(1A)-C(1A)	115.46(16)
C(19A)-Sn(1A)-C(1A)	113.46(17)
C(13A)-Sn(1A)-C(1A)	103.61(16)
C(8A)-O(1A)-C(9A)	105.2(3)
C(8A)-N(1A)-C(10A)	107.1(3)
C(2A)-C(1A)-Sn(1A)	109.9(3)

C(2A)-C(1A)-H(1AA)	109.7
Sn(1A)-C(1A)-H(1AA)	109.7
C(2A)-C(1A)-H(1AB)	109.7
Sn(1A)-C(1A)-H(1AB)	109.7
H(1AA)-C(1A)-H(1AB)	108.2
C(3A)-C(2A)-C(7A)	117.0(4)
C(3A)-C(2A)-C(1A)	119.2(4)
C(7A)-C(2A)-C(1A)	123.7(4)
C(4A)-C(3A)-C(2A)	122.8(4)
C(4A)-C(3A)-H(3AA)	118.6
C(2A)-C(3A)-H(3AA)	118.6
C(3A)-C(4A)-C(5A)	119.9(4)
C(3A)-C(4A)-H(4AA)	120.1
C(5A)-C(4A)-H(4AA)	120.1
C(6A)-C(5A)-C(4A)	118.7(5)
C(6A)-C(5A)-H(5AA)	120.6
C(4A)-C(5A)-H(5AA)	120.6
C(5A)-C(6A)-C(7A)	121.5(4)
C(5A)-C(6A)-H(6AA)	119.2
C(7A)-C(6A)-H(6AA)	119.2
C(6A)-C(7A)-C(2A)	119.9(4)
C(6A)-C(7A)-C(8A)	118.6(3)
C(2A)-C(7A)-C(8A)	121.3(4)
N(1A)-C(8A)-O(1A)	117.6(4)
N(1A)-C(8A)-C(7A)	127.5(4)
O(1A)-C(8A)-C(7A)	114.8(4)
O(1A)-C(9A)-C(10A)	104.6(3)
O(1A)-C(9A)-H(9AA)	110.8
C(10A)-C(9A)-H(9AA)	110.8
O(1A)-C(9A)-H(9AB)	110.8
C(10A)-C(9A)-H(9AB)	110.8
H(9AA)-C(9A)-H(9AB)	108.9
N(1A)-C(10A)-C(11A)	108.8(3)
N(1A)-C(10A)-C(12A)	109.0(4)
C(11A)-C(10A)-C(12A)	111.0(4)
N(1A)-C(10A)-C(9A)	102.9(3)

C(11A)-C(10A)-C(9A) 112.5(4)
C(12A)-C(10A)-C(9A) 112.3(4)
C(10A)-C(11A)-H(11A) 109.5
C(10A)-C(11A)-H(11B) 109.5
H(11A)-C(11A)-H(11B) 109.5
C(10A)-C(11A)-H(11C) 109.5
H(11A)-C(11A)-H(11C) 109.5
H(11B)-C(11A)-H(11C) 109.5
C(10A)-C(12A)-H(12A) 109.5
C(10A)-C(12A)-H(12B) 109.5
H(12A)-C(12A)-H(12B) 109.5
C(10A)-C(12A)-H(12C) 109.5
H(12A)-C(12A)-H(12C) 109.5
H(12B)-C(12A)-H(12C) 109.5
C(18A)-C(13A)-C(14A) 117.9(4)
C(18A)-C(13A)-Sn(1A) 121.5(3)
C(14A)-C(13A)-Sn(1A) 120.6(3)
C(15A)-C(14A)-C(13A) 121.3(4)
C(15A)-C(14A)-H(14A) 119.3
C(13A)-C(14A)-H(14A) 119.3
C(16A)-C(15A)-C(14A) 119.8(5)
C(16A)-C(15A)-H(15A) 120.1
C(14A)-C(15A)-H(15A) 120.1
C(17A)-C(16A)-C(15A) 120.0(5)
C(17A)-C(16A)-H(16A) 120.0
C(15A)-C(16A)-H(16A) 120.0
C(16A)-C(17A)-C(18A) 120.9(5)
C(16A)-C(17A)-H(17A) 119.6
C(18A)-C(17A)-H(17A) 119.6
C(13A)-C(18A)-C(17A) 120.0(5)
C(13A)-C(18A)-H(18A) 120.0
C(17A)-C(18A)-H(18A) 120.0
C(20A)-C(19A)-C(24A) 118.2(4)
C(20A)-C(19A)-Sn(1A) 122.3(3)
C(24A)-C(19A)-Sn(1A) 119.4(3)
C(21A)-C(20A)-C(19A) 120.9(4)

C(21A)-C(20A)-H(20A) 119.6
C(19A)-C(20A)-H(20A) 119.6
C(22A)-C(21A)-C(20A) 120.6(4)
C(22A)-C(21A)-H(21A) 119.7
C(20A)-C(21A)-H(21A) 119.7
C(21A)-C(22A)-C(23A) 119.6(4)
C(21A)-C(22A)-H(22A) 120.2
C(23A)-C(22A)-H(22A) 120.2
C(22A)-C(23A)-C(24A) 119.7(4)
C(22A)-C(23A)-H(23A) 120.2
C(24A)-C(23A)-H(23A) 120.2
C(23A)-C(24A)-C(19A) 120.9(4)
C(23A)-C(24A)-H(24A) 119.5
C(19A)-C(24A)-H(24A) 119.5
C(30A)-C(25A)-C(26A) 117.8(4)
C(30A)-C(25A)-Sn(1A) 122.4(3)
C(26A)-C(25A)-Sn(1A) 119.8(3)
C(27A)-C(26A)-C(25A) 121.2(4)
C(27A)-C(26A)-H(26A) 119.4
C(25A)-C(26A)-H(26A) 119.4
C(28A)-C(27A)-C(26A) 120.2(4)
C(28A)-C(27A)-H(27A) 119.9
C(26A)-C(27A)-H(27A) 119.9
C(27A)-C(28A)-C(29A) 119.6(4)
C(27A)-C(28A)-H(28A) 120.2
C(29A)-C(28A)-H(28A) 120.2
C(28A)-C(29A)-C(30A) 120.1(4)
C(28A)-C(29A)-H(29A) 120.0
C(30A)-C(29A)-H(29A) 120.0
C(25A)-C(30A)-C(29A) 121.2(4)
C(25A)-C(30A)-H(30A) 119.4
C(29A)-C(30A)-H(30A) 119.4
C(19B)-Sn(1B)-C(25B) 110.45(16)
C(19B)-Sn(1B)-C(1B) 112.07(16)
C(25B)-Sn(1B)-C(1B) 116.09(16)
C(19B)-Sn(1B)-C(13B) 108.41(17)

C(25B)-Sn(1B)-C(13B)	105.81(17)
C(1B)-Sn(1B)-C(13B)	103.30(16)
C(8B)-O(1B)-C(9B)	105.4(3)
C(8B)-N(1B)-C(10B)	107.7(4)
C(2B)-C(1B)-Sn(1B)	111.0(3)
C(2B)-C(1B)-H(1BA)	109.4
Sn(1B)-C(1B)-H(1BA)	109.4
C(2B)-C(1B)-H(1BB)	109.4
Sn(1B)-C(1B)-H(1BB)	109.4
H(1BA)-C(1B)-H(1BB)	108.0
C(3B)-C(2B)-C(7B)	117.0(4)
C(3B)-C(2B)-C(1B)	119.1(4)
C(7B)-C(2B)-C(1B)	123.9(4)
C(4B)-C(3B)-C(2B)	122.0(4)
C(4B)-C(3B)-H(3BA)	119.0
C(2B)-C(3B)-H(3BA)	119.0
C(5B)-C(4B)-C(3B)	120.6(4)
C(5B)-C(4B)-H(4BA)	119.7
C(3B)-C(4B)-H(4BA)	119.7
C(4B)-C(5B)-C(6B)	118.9(4)
C(4B)-C(5B)-H(5BA)	120.6
C(6B)-C(5B)-H(5BA)	120.6
C(5B)-C(6B)-C(7B)	121.6(4)
C(5B)-C(6B)-H(6BA)	119.2
C(7B)-C(6B)-H(6BA)	119.2
C(6B)-C(7B)-C(2B)	119.8(4)
C(6B)-C(7B)-C(8B)	119.1(4)
C(2B)-C(7B)-C(8B)	121.0(4)
N(1B)-C(8B)-O(1B)	117.7(4)
N(1B)-C(8B)-C(7B)	128.3(4)
O(1B)-C(8B)-C(7B)	113.9(4)
O(1B)-C(9B)-C(10B)	104.6(3)
O(1B)-C(9B)-H(9BA)	110.8
C(10B)-C(9B)-H(9BA)	110.8
O(1B)-C(9B)-H(9BB)	110.8
C(10B)-C(9B)-H(9BB)	110.8

H(9BA)-C(9B)-H(9BB)	108.9
N(1B)-C(10B)-C(12B)	109.3(4)
N(1B)-C(10B)-C(11B)	109.2(3)
C(12B)-C(10B)-C(11B)	110.8(4)
N(1B)-C(10B)-C(9B)	103.0(3)
C(12B)-C(10B)-C(9B)	112.5(4)
C(11B)-C(10B)-C(9B)	111.8(4)
C(10B)-C(11B)-H(11D)	109.5
C(10B)-C(11B)-H(11E)	109.5
H(11D)-C(11B)-H(11E)	109.5
C(10B)-C(11B)-H(11F)	109.5
H(11D)-C(11B)-H(11F)	109.5
H(11E)-C(11B)-H(11F)	109.5
C(10B)-C(12B)-H(12D)	109.5
C(10B)-C(12B)-H(12E)	109.5
H(12D)-C(12B)-H(12E)	109.5
C(10B)-C(12B)-H(12F)	109.5
H(12D)-C(12B)-H(12F)	109.5
H(12E)-C(12B)-H(12F)	109.5
C(14B)-C(13B)-C(18B)	117.7(4)
C(14B)-C(13B)-Sn(1B)	121.4(3)
C(18B)-C(13B)-Sn(1B)	120.9(3)
C(13B)-C(14B)-C(15B)	121.2(4)
C(13B)-C(14B)-H(14B)	119.4
C(15B)-C(14B)-H(14B)	119.4
C(16B)-C(15B)-C(14B)	120.0(5)
C(16B)-C(15B)-H(15B)	120.0
C(14B)-C(15B)-H(15B)	120.0
C(15B)-C(16B)-C(17B)	120.5(5)
C(15B)-C(16B)-H(16B)	119.7
C(17B)-C(16B)-H(16B)	119.7
C(18B)-C(17B)-C(16B)	119.6(5)
C(18B)-C(17B)-H(17B)	120.2
C(16B)-C(17B)-H(17B)	120.2
C(17B)-C(18B)-C(13B)	121.0(5)
C(17B)-C(18B)-H(18B)	119.5

C(13B)-C(18B)-H(18B) 119.5
C(20B)-C(19B)-C(24B) 118.1(4)
C(20B)-C(19B)-Sn(1B) 121.7(3)
C(24B)-C(19B)-Sn(1B) 120.2(3)
C(19B)-C(20B)-C(21B) 121.3(4)
C(19B)-C(20B)-H(20B) 119.4
C(21B)-C(20B)-H(20B) 119.4
C(22B)-C(21B)-C(20B) 119.9(5)
C(22B)-C(21B)-H(21B) 120.1
C(20B)-C(21B)-H(21B) 120.1
C(21B)-C(22B)-C(23B) 119.9(5)
C(21B)-C(22B)-H(22B) 120.1
C(23B)-C(22B)-H(22B) 120.1
C(22B)-C(23B)-C(24B) 120.4(4)
C(22B)-C(23B)-H(23B) 119.8
C(24B)-C(23B)-H(23B) 119.8
C(23B)-C(24B)-C(19B) 120.4(5)
C(23B)-C(24B)-H(24B) 119.8
C(19B)-C(24B)-H(24B) 119.8
C(30B)-C(25B)-C(26B) 117.4(4)
C(30B)-C(25B)-Sn(1B) 122.2(3)
C(26B)-C(25B)-Sn(1B) 120.3(3)
C(27B)-C(26B)-C(25B) 121.4(5)
C(27B)-C(26B)-H(26B) 119.3
C(25B)-C(26B)-H(26B) 119.3
C(28B)-C(27B)-C(26B) 120.0(4)
C(28B)-C(27B)-H(27B) 120.0
C(26B)-C(27B)-H(27B) 120.0
C(27B)-C(28B)-C(29B) 119.8(4)
C(27B)-C(28B)-H(28B) 120.1
C(29B)-C(28B)-H(28B) 120.1
C(28B)-C(29B)-C(30B) 120.0(5)
C(28B)-C(29B)-H(29B) 120.0
C(30B)-C(29B)-H(29B) 120.0
C(29B)-C(30B)-C(25B) 121.3(4)
C(29B)-C(30B)-H(30B) 119.3

C(25B)-C(30B)-H(30B) 119.3

Symmetry transformations used to generate equivalent atoms:

Anisotropic displacement parameters ($\text{\AA}^2 \times 10^3$) for **18**. The anisotropic displacement factor exponent takes the form: $-2\alpha^2 [h^2 a^* U_{11} + \dots + 2 h k a^* b^* U_{12}]$

	U ₁₁	U ₂₂	U ₃₃	U ₂₃	U ₁₃	U ₁₂
Sn(1A)	18(1)	20(1)	18(1)	0(1)	-2(1)	0(1)
O(1A)	30(2)	23(2)	36(2)	7(2)	8(2)	8(1)
N(1A)	17(2)	21(2)	26(2)	0(2)	0(2)	0(2)
C(1A)	15(2)	24(3)	27(3)	-4(2)	-4(2)	1(2)
C(2A)	17(2)	21(2)	23(2)	-5(2)	-5(2)	-2(2)
C(3A)	21(2)	29(3)	31(3)	-6(2)	1(2)	-2(2)
C(4A)	27(3)	38(3)	37(3)	-4(3)	12(2)	-9(2)
C(5A)	35(3)	32(3)	33(3)	8(2)	5(2)	-6(2)
C(6A)	29(2)	24(2)	35(3)	-2(2)	-2(2)	1(2)
C(7A)	18(2)	18(2)	25(2)	-5(2)	-2(2)	-4(2)
C(8A)	19(2)	19(2)	23(2)	-4(2)	-4(2)	4(2)
C(9A)	19(2)	36(3)	35(3)	4(2)	4(2)	8(2)
C(10A)	16(2)	25(3)	25(3)	1(2)	-2(2)	1(2)
C(11A)	30(3)	38(3)	27(3)	2(2)	-4(2)	-1(2)
C(12A)	21(2)	36(3)	37(3)	-2(2)	2(2)	-3(2)
C(13A)	22(2)	18(2)	19(2)	1(2)	2(2)	-5(2)
C(14A)	32(3)	29(3)	24(3)	-4(2)	-5(2)	0(2)
C(15A)	57(3)	34(3)	25(3)	-6(2)	6(3)	-3(3)
C(16A)	45(3)	26(3)	45(4)	-1(3)	26(3)	4(2)
C(17A)	29(3)	31(3)	45(3)	6(3)	10(2)	7(2)
C(18A)	27(2)	29(3)	29(3)	4(2)	1(2)	4(2)
C(19A)	17(2)	21(2)	21(2)	2(2)	-1(2)	4(2)
C(20A)	25(2)	25(3)	20(2)	-1(2)	0(2)	3(2)
C(21A)	37(3)	32(3)	20(3)	-2(2)	2(2)	9(2)
C(22A)	28(2)	25(3)	38(3)	10(2)	12(2)	3(2)
C(23A)	32(3)	17(3)	38(3)	3(2)	3(2)	-5(2)
C(24A)	31(2)	21(3)	25(3)	0(2)	-4(2)	3(2)
C(25A)	20(2)	20(3)	21(2)	-5(2)	-4(2)	6(2)
C(26A)	23(2)	20(3)	24(3)	1(2)	-1(2)	2(2)
C(27A)	18(2)	29(3)	31(3)	-5(2)	-5(2)	1(2)
C(28A)	27(2)	31(3)	25(3)	0(2)	-9(2)	7(2)

C(29A)	33(3)	28(3)	23(3)	9(2)	-2(2)	-1(2)
C(30A)	21(2)	24(3)	19(2)	2(2)	0(2)	1(2)
Sn(1B)	21(1)	21(1)	20(1)	1(1)	-1(1)	1(1)
O(1B)	32(2)	27(2)	40(2)	-10(2)	15(2)	-8(1)
N(1B)	17(2)	26(2)	27(2)	-3(2)	2(2)	1(2)
C(1B)	22(2)	21(2)	22(2)	1(2)	-1(2)	-2(2)
C(2B)	18(2)	24(2)	17(2)	3(2)	-2(2)	5(2)
C(3B)	23(2)	27(3)	25(3)	7(2)	-2(2)	2(2)
C(4B)	25(2)	37(3)	25(3)	2(2)	6(2)	6(2)
C(5B)	34(3)	28(3)	26(3)	-5(2)	0(2)	11(2)
C(6B)	26(2)	24(2)	21(2)	2(2)	-1(2)	3(2)
C(7B)	23(2)	23(2)	16(2)	4(2)	-2(2)	5(2)
C(8B)	21(2)	18(2)	21(2)	-1(2)	-1(2)	2(2)
C(9B)	26(2)	32(3)	36(3)	-8(2)	9(2)	-5(2)
C(10B)	16(2)	29(3)	25(3)	-4(2)	5(2)	-1(2)
C(11B)	28(2)	35(3)	30(3)	-1(2)	-3(2)	3(2)
C(12B)	21(2)	44(3)	37(3)	4(2)	3(2)	7(2)
C(13B)	24(2)	21(3)	25(3)	3(2)	4(2)	7(2)
C(14B)	28(2)	37(3)	31(3)	5(2)	-3(2)	-5(2)
C(15B)	35(3)	47(4)	32(3)	14(3)	5(2)	-3(2)
C(16B)	34(3)	29(3)	45(4)	4(3)	17(3)	-1(2)
C(17B)	25(3)	30(3)	50(4)	-8(3)	3(2)	-4(2)
C(18B)	34(3)	28(3)	28(3)	-5(2)	-4(2)	-3(2)
C(19B)	19(2)	17(2)	26(3)	2(2)	-3(2)	-3(2)
C(20B)	21(2)	26(3)	28(3)	1(2)	0(2)	1(2)
C(21B)	34(3)	29(3)	23(3)	0(2)	2(2)	-5(2)
C(22B)	28(2)	30(3)	40(3)	-5(2)	15(2)	-3(2)
C(23B)	30(3)	24(3)	45(3)	2(2)	-1(2)	11(2)
C(24B)	35(3)	26(3)	26(3)	3(2)	-3(2)	3(2)
C(25B)	26(2)	21(3)	20(3)	3(2)	-2(2)	-2(2)
C(26B)	27(2)	30(3)	21(3)	5(2)	0(2)	-1(2)
C(27B)	26(2)	46(3)	30(3)	14(2)	-4(2)	-9(2)
C(28B)	44(3)	48(3)	26(3)	8(2)	-15(2)	-20(3)
C(29B)	59(3)	32(3)	26(3)	-2(2)	-9(3)	-3(2)
C(30B)	34(3)	35(3)	25(3)	5(2)	-3(2)	9(2)

Hydrogen coordinates (x 10⁴) and isotropic displacement parameters (Å² x 10³) for **18**.

	x	y	z	U(eq)
H(1AA)	5036	5892	3394	26
H(1AB)	6447	5577	3112	26
H(3AA)	4068	5271	3977	32
H(4AA)	4047	4336	4442	41
H(5AA)	5998	3449	4391	40
H(6AA)	8004	3566	3888	35
H(9AA)	11370	3911	2902	36
H(9AB)	11910	4276	3340	36
H(11A)	9948	5406	2378	48
H(11B)	9492	4588	2415	48
H(11C)	11285	4814	2325	48
H(12A)	11525	5978	2945	47
H(12B)	12877	5388	2926	47
H(12C)	11990	5548	3364	47
H(14A)	7518	7093	4592	34
H(15A)	5870	7798	5002	46
H(16A)	3609	8292	4704	46
H(17A)	2929	8034	4012	42
H(18A)	4537	7307	3596	34
H(20A)	8103	6599	2686	28
H(21A)	9347	7332	2198	35
H(22A)	11007	8234	2426	37
H(23A)	11386	8419	3152	35
H(24A)	10040	7717	3644	31
H(26A)	11214	6674	3958	27
H(27A)	13033	6269	4456	31
H(28A)	12361	5349	4913	33
H(29A)	9831	4857	4882	34
H(30A)	7961	5306	4408	25

H(1BA)	1729	1211	3112	26
H(1BB)	298	907	3391	26
H(3BA)	-729	1553	3962	30
H(4BA)	-893	2563	4371	35
H(5BA)	1023	3441	4316	35
H(6BA)	3120	3293	3846	29
H(9BA)	7145	2594	3313	37
H(9BB)	6504	2934	2877	37
H(11D)	5197	1403	2376	47
H(11E)	6566	1978	2320	47
H(11F)	4777	2225	2396	47
H(12D)	6789	861	2958	51
H(12E)	7214	1310	3373	51
H(12F)	8119	1460	2936	51
H(14B)	2541	-178	4634	38
H(15B)	892	-922	5026	46
H(16B)	-1251	-1455	4706	43
H(17B)	-1788	-1259	3989	42
H(18B)	-143	-522	3593	36
H(20B)	3376	231	2714	30
H(21B)	4591	-512	2221	35
H(22B)	6164	-1440	2451	39
H(23B)	6466	-1650	3174	39
H(24B)	5169	-941	3670	35
H(26B)	6464	157	3985	31
H(27B)	8266	580	4479	41
H(28B)	7592	1526	4915	47
H(29B)	5053	2009	4879	47
H(30B)	3213	1559	4401	38

Torsion angles [°] for **18**.

Sn(1A)-C(1A)-C(2A)-C(3A)	98.0(4)
Sn(1A)-C(1A)-C(2A)-C(7A)	-79.1(5)
C(7A)-C(2A)-C(3A)-C(4A)	2.1(6)
C(1A)-C(2A)-C(3A)-C(4A)	-175.2(4)
C(2A)-C(3A)-C(4A)-C(5A)	-3.0(7)
C(3A)-C(4A)-C(5A)-C(6A)	1.6(7)
C(4A)-C(5A)-C(6A)-C(7A)	0.7(7)
C(5A)-C(6A)-C(7A)-C(2A)	-1.6(6)
C(5A)-C(6A)-C(7A)-C(8A)	173.8(4)
C(3A)-C(2A)-C(7A)-C(6A)	0.2(6)
C(1A)-C(2A)-C(7A)-C(6A)	177.4(4)
C(3A)-C(2A)-C(7A)-C(8A)	-175.0(4)
C(1A)-C(2A)-C(7A)-C(8A)	2.1(6)
C(10A)-N(1A)-C(8A)-O(1A)	0.4(5)
C(10A)-N(1A)-C(8A)-C(7A)	177.4(4)
C(9A)-O(1A)-C(8A)-N(1A)	10.2(5)
C(9A)-O(1A)-C(8A)-C(7A)	-167.2(4)
C(6A)-C(7A)-C(8A)-N(1A)	-163.5(4)
C(2A)-C(7A)-C(8A)-N(1A)	11.8(6)
C(6A)-C(7A)-C(8A)-O(1A)	13.6(5)
C(2A)-C(7A)-C(8A)-O(1A)	-171.1(4)
C(8A)-O(1A)-C(9A)-C(10A)	-15.4(4)
C(8A)-N(1A)-C(10A)-C(11A)	109.4(4)
C(8A)-N(1A)-C(10A)-C(12A)	-129.4(4)
C(8A)-N(1A)-C(10A)-C(9A)	-10.0(4)
O(1A)-C(9A)-C(10A)-N(1A)	15.5(4)
O(1A)-C(9A)-C(10A)-C(11A)	-101.4(4)
O(1A)-C(9A)-C(10A)-C(12A)	132.6(4)
C(18A)-C(13A)-C(14A)-C(15A)	0.2(7)
Sn(1A)-C(13A)-C(14A)-C(15A)	-179.1(4)
C(13A)-C(14A)-C(15A)-C(16A)	-1.3(8)
C(14A)-C(15A)-C(16A)-C(17A)	1.7(8)
C(15A)-C(16A)-C(17A)-C(18A)	-1.0(8)
C(14A)-C(13A)-C(18A)-C(17A)	0.5(6)

Sn(1A)-C(13A)-C(18A)-C(17A)	179.8(3)
C(16A)-C(17A)-C(18A)-C(13A)	-0.1(7)
C(24A)-C(19A)-C(20A)-C(21A)	-1.4(6)
Sn(1A)-C(19A)-C(20A)-C(21A)	178.4(3)
C(19A)-C(20A)-C(21A)-C(22A)	1.9(7)
C(20A)-C(21A)-C(22A)-C(23A)	-0.7(7)
C(21A)-C(22A)-C(23A)-C(24A)	-1.0(7)
C(22A)-C(23A)-C(24A)-C(19A)	1.4(7)
C(20A)-C(19A)-C(24A)-C(23A)	-0.2(6)
Sn(1A)-C(19A)-C(24A)-C(23A)	179.9(3)
C(30A)-C(25A)-C(26A)-C(27A)	0.3(6)
Sn(1A)-C(25A)-C(26A)-C(27A)	177.9(3)
C(25A)-C(26A)-C(27A)-C(28A)	1.3(7)
C(26A)-C(27A)-C(28A)-C(29A)	-1.0(7)
C(27A)-C(28A)-C(29A)-C(30A)	-0.8(7)
C(26A)-C(25A)-C(30A)-C(29A)	-2.2(7)
Sn(1A)-C(25A)-C(30A)-C(29A)	-179.7(3)
C(28A)-C(29A)-C(30A)-C(25A)	2.5(7)
Sn(1B)-C(1B)-C(2B)-C(3B)	-98.2(4)
Sn(1B)-C(1B)-C(2B)-C(7B)	79.4(5)
C(7B)-C(2B)-C(3B)-C(4B)	0.4(6)
C(1B)-C(2B)-C(3B)-C(4B)	178.1(4)
C(2B)-C(3B)-C(4B)-C(5B)	0.2(7)
C(3B)-C(4B)-C(5B)-C(6B)	-0.2(7)
C(4B)-C(5B)-C(6B)-C(7B)	-0.5(6)
C(5B)-C(6B)-C(7B)-C(2B)	1.2(6)
C(5B)-C(6B)-C(7B)-C(8B)	-176.0(4)
C(3B)-C(2B)-C(7B)-C(6B)	-1.1(6)
C(1B)-C(2B)-C(7B)-C(6B)	-178.6(4)
C(3B)-C(2B)-C(7B)-C(8B)	176.1(4)
C(1B)-C(2B)-C(7B)-C(8B)	-1.5(6)
C(10B)-N(1B)-C(8B)-O(1B)	-1.4(5)
C(10B)-N(1B)-C(8B)-C(7B)	-178.2(4)
C(9B)-O(1B)-C(8B)-N(1B)	-6.8(5)
C(9B)-O(1B)-C(8B)-C(7B)	170.5(4)
C(6B)-C(7B)-C(8B)-N(1B)	167.5(4)

C(2B)-C(7B)-C(8B)-N(1B)	-9.7(7)
C(6B)-C(7B)-C(8B)-O(1B)	-9.5(5)
C(2B)-C(7B)-C(8B)-O(1B)	173.4(4)
C(8B)-O(1B)-C(9B)-C(10B)	11.2(5)
C(8B)-N(1B)-C(10B)-C(12B)	128.1(4)
C(8B)-N(1B)-C(10B)-C(11B)	-110.7(4)
C(8B)-N(1B)-C(10B)-C(9B)	8.3(5)
O(1B)-C(9B)-C(10B)-N(1B)	-11.8(5)
O(1B)-C(9B)-C(10B)-C(12B)	-129.3(4)
O(1B)-C(9B)-C(10B)-C(11B)	105.3(4)
C(18B)-C(13B)-C(14B)-C(15B)	2.1(7)
Sn(1B)-C(13B)-C(14B)-C(15B)	-178.5(4)
C(13B)-C(14B)-C(15B)-C(16B)	-1.1(8)
C(14B)-C(15B)-C(16B)-C(17B)	-0.1(8)
C(15B)-C(16B)-C(17B)-C(18B)	0.3(8)
C(16B)-C(17B)-C(18B)-C(13B)	0.7(7)
C(14B)-C(13B)-C(18B)-C(17B)	-1.9(7)
Sn(1B)-C(13B)-C(18B)-C(17B)	178.7(3)
C(24B)-C(19B)-C(20B)-C(21B)	0.3(6)
Sn(1B)-C(19B)-C(20B)-C(21B)	-178.0(3)
C(19B)-C(20B)-C(21B)-C(22B)	-1.4(7)
C(20B)-C(21B)-C(22B)-C(23B)	1.0(7)
C(21B)-C(22B)-C(23B)-C(24B)	0.4(7)
C(22B)-C(23B)-C(24B)-C(19B)	-1.5(7)
C(20B)-C(19B)-C(24B)-C(23B)	1.1(6)
Sn(1B)-C(19B)-C(24B)-C(23B)	179.4(3)
C(30B)-C(25B)-C(26B)-C(27B)	1.0(7)
Sn(1B)-C(25B)-C(26B)-C(27B)	-178.1(3)
C(25B)-C(26B)-C(27B)-C(28B)	-1.9(7)
C(26B)-C(27B)-C(28B)-C(29B)	1.6(7)
C(27B)-C(28B)-C(29B)-C(30B)	-0.4(8)
C(28B)-C(29B)-C(30B)-C(25B)	-0.6(8)
C(26B)-C(25B)-C(30B)-C(29B)	0.3(7)
Sn(1B)-C(25B)-C(30B)-C(29B)	179.3(4)

Symmetry transformations used to generate equivalent atoms:

Table A5: Crystal data and structure refinement for **23**.

Identification code	d18125_a
Empirical formula	C25 H23 N Sn
Formula weight	456.13
Temperature	150(2) K
Wavelength	0.71073 Å
Crystal system	Monoclinic
Space group	P2 ₁ /n
Unit cell dimensions	a = 15.3986(9) Å a= 90°. b = 7.9119(5) Å b= 97.734(2)°. c = 17.214(11) Å g = 90°.
Volume	2078.1(2) Å ³
Z	4
Density (calculated)	1.458 Mg/m ³
Absorption coefficient	1.238 mm ⁻¹
F(000)	920
Crystal size	0.27 x 0.20 x 0.07 mm ³
Theta range for data collection	1.667 to 27.523°.
Index ranges	-19<=h<=20, -10<=k<=10, -22<=l<=22
Reflections collected	30756
Independent reflections	4785 [R(int) = 0.0463]
Completeness to theta = 25.242°	100.0 %
Absorption correction	Semi-empirical from equivalents
Max. and min. transmission	0.7456 and 0.6806
Refinement method	Full-matrix least-squares on F ²
Data / restraints / parameters	4785 / 0 / 244
Goodness-of-fit on F ²	1.025
Final R indices [I>2sigma(I)]	R1 = 0.0240, wR2 = 0.0407
R indices (all data)	R1 = 0.0456, wR2 = 0.0471
Extinction coefficient	n/a
Largest diff. peak and hole	0.833 and -0.437 e.Å ⁻³

Atomic coordinates ($\times 10^4$) and equivalent isotropic displacement parameters ($\text{\AA}^2 \times 10^3$) for **23**. U(eq) is defined as one third of the trace of the orthogonalized U^{ij} tensor.

	x	y	z	U(eq)
Sn(1)	5621(1)	4202(1)	3355(1)	21(1)
N(1)	4694(1)	5729(2)	1960(1)	25(1)
C(1)	5456(2)	6900(3)	3469(1)	28(1)
C(2)	4596(2)	7599(3)	3050(1)	29(1)
C(3)	4499(1)	7293(3)	2181(1)	23(1)
C(4)	4234(2)	8537(3)	1634(2)	31(1)
C(5)	4185(2)	8174(3)	843(2)	37(1)
C(6)	4390(2)	6570(3)	616(1)	33(1)
C(7)	4638(2)	5394(3)	1192(1)	31(1)
C(8)	4457(1)	2779(3)	3484(1)	22(1)
C(9)	3715(2)	2807(3)	2918(1)	29(1)
C(10)	2971(2)	1903(3)	3024(2)	37(1)
C(11)	2944(2)	960(3)	3690(2)	38(1)
C(12)	3670(2)	896(3)	4256(2)	35(1)
C(13)	4421(2)	1797(3)	4152(1)	28(1)
C(14)	6217(1)	3174(3)	2402(1)	22(1)
C(15)	5999(2)	1551(3)	2143(2)	34(1)
C(16)	6358(2)	837(4)	1523(2)	41(1)
C(17)	6948(2)	1734(3)	1156(1)	33(1)
C(18)	7177(2)	3349(3)	1404(1)	33(1)
C(19)	6816(2)	4061(3)	2025(1)	28(1)
C(20)	6561(1)	3562(3)	4360(1)	22(1)
C(21)	7286(2)	2571(3)	4268(1)	27(1)
C(22)	7956(2)	2276(3)	4883(1)	32(1)
C(23)	7911(2)	3000(3)	5603(1)	33(1)
C(24)	7200(2)	3996(3)	5717(1)	32(1)
C(25)	6534(2)	4263(3)	5104(1)	28(1)

Bond lengths [\AA] and angles [$^\circ$] for **23**.

Sn(1)-C(14)	2.144(2)
Sn(1)-C(8)	2.154(2)
Sn(1)-C(20)	2.162(2)
Sn(1)-C(1)	2.162(2)
N(1)-C(7)	1.340(3)
N(1)-C(3)	1.341(3)
C(1)-C(2)	1.524(3)
C(1)-H(1A)	0.9900
C(1)-H(1B)	0.9900
C(2)-C(3)	1.502(3)
C(2)-H(2A)	0.9900
C(2)-H(2B)	0.9900
C(3)-C(4)	1.386(3)
C(4)-C(5)	1.383(3)
C(4)-H(4A)	0.9500
C(5)-C(6)	1.377(3)
C(5)-H(5A)	0.9500
C(6)-C(7)	1.375(3)
C(6)-H(6A)	0.9500
C(7)-H(7A)	0.9500
C(8)-C(13)	1.396(3)
C(8)-C(9)	1.397(3)
C(9)-C(10)	1.384(3)
C(9)-H(9A)	0.9500
C(10)-C(11)	1.373(4)
C(10)-H(10A)	0.9500
C(11)-C(12)	1.381(4)
C(11)-H(11A)	0.9500
C(12)-C(13)	1.390(3)
C(12)-H(12A)	0.9500
C(13)-H(13A)	0.9500
C(14)-C(15)	1.386(3)
C(14)-C(19)	1.388(3)
C(15)-C(16)	1.387(3)

C(15)-H(15A)	0.9500
C(16)-C(17)	1.371(4)
C(16)-H(16A)	0.9500
C(17)-C(18)	1.378(4)
C(17)-H(17A)	0.9500
C(18)-C(19)	1.388(3)
C(18)-H(18A)	0.9500
C(19)-H(19A)	0.9500
C(20)-C(21)	1.391(3)
C(20)-C(25)	1.401(3)
C(21)-C(22)	1.395(3)
C(21)-H(21A)	0.9500
C(22)-C(23)	1.376(3)
C(22)-H(22A)	0.9500
C(23)-C(24)	1.384(3)
C(23)-H(23A)	0.9500
C(24)-C(25)	1.385(3)
C(24)-H(24A)	0.9500
C(25)-H(25A)	0.9500

C(14)-Sn(1)-C(8)	109.18(8)
C(14)-Sn(1)-C(20)	102.38(8)
C(8)-Sn(1)-C(20)	105.77(8)
C(14)-Sn(1)-C(1)	120.81(9)
C(8)-Sn(1)-C(1)	113.38(9)
C(20)-Sn(1)-C(1)	103.44(8)
C(7)-N(1)-C(3)	118.4(2)
C(2)-C(1)-Sn(1)	114.87(16)
C(2)-C(1)-H(1A)	108.6
Sn(1)-C(1)-H(1A)	108.6
C(2)-C(1)-H(1B)	108.6
Sn(1)-C(1)-H(1B)	108.6
H(1A)-C(1)-H(1B)	107.5
C(3)-C(2)-C(1)	112.15(19)
C(3)-C(2)-H(2A)	109.2
C(1)-C(2)-H(2A)	109.2

C(3)-C(2)-H(2B)	109.2
C(1)-C(2)-H(2B)	109.2
H(2A)-C(2)-H(2B)	107.9
N(1)-C(3)-C(4)	121.3(2)
N(1)-C(3)-C(2)	115.8(2)
C(4)-C(3)-C(2)	122.9(2)
C(5)-C(4)-C(3)	119.6(2)
C(5)-C(4)-H(4A)	120.2
C(3)-C(4)-H(4A)	120.2
C(6)-C(5)-C(4)	119.1(2)
C(6)-C(5)-H(5A)	120.4
C(4)-C(5)-H(5A)	120.4
C(7)-C(6)-C(5)	118.1(2)
C(7)-C(6)-H(6A)	121.0
C(5)-C(6)-H(6A)	121.0
N(1)-C(7)-C(6)	123.5(2)
N(1)-C(7)-H(7A)	118.2
C(6)-C(7)-H(7A)	118.2
C(13)-C(8)-C(9)	117.7(2)
C(13)-C(8)-Sn(1)	120.10(16)
C(9)-C(8)-Sn(1)	122.22(17)
C(10)-C(9)-C(8)	120.9(2)
C(10)-C(9)-H(9A)	119.5
C(8)-C(9)-H(9A)	119.5
C(11)-C(10)-C(9)	120.6(2)
C(11)-C(10)-H(10A)	119.7
C(9)-C(10)-H(10A)	119.7
C(10)-C(11)-C(12)	119.8(2)
C(10)-C(11)-H(11A)	120.1
C(12)-C(11)-H(11A)	120.1
C(11)-C(12)-C(13)	120.0(2)
C(11)-C(12)-H(12A)	120.0
C(13)-C(12)-H(12A)	120.0
C(12)-C(13)-C(8)	121.1(2)
C(12)-C(13)-H(13A)	119.5
C(8)-C(13)-H(13A)	119.5

C(15)-C(14)-C(19)	117.8(2)
C(15)-C(14)-Sn(1)	119.17(17)
C(19)-C(14)-Sn(1)	123.08(17)
C(14)-C(15)-C(16)	121.3(2)
C(14)-C(15)-H(15A)	119.3
C(16)-C(15)-H(15A)	119.3
C(17)-C(16)-C(15)	120.1(3)
C(17)-C(16)-H(16A)	119.9
C(15)-C(16)-H(16A)	119.9
C(16)-C(17)-C(18)	119.6(2)
C(16)-C(17)-H(17A)	120.2
C(18)-C(17)-H(17A)	120.2
C(17)-C(18)-C(19)	120.2(2)
C(17)-C(18)-H(18A)	119.9
C(19)-C(18)-H(18A)	119.9
C(14)-C(19)-C(18)	121.0(2)
C(14)-C(19)-H(19A)	119.5
C(18)-C(19)-H(19A)	119.5
C(21)-C(20)-C(25)	116.8(2)
C(21)-C(20)-Sn(1)	120.12(16)
C(25)-C(20)-Sn(1)	122.70(17)
C(20)-C(21)-C(22)	122.1(2)
C(20)-C(21)-H(21A)	119.0
C(22)-C(21)-H(21A)	119.0
C(23)-C(22)-C(21)	119.5(2)
C(23)-C(22)-H(22A)	120.2
C(21)-C(22)-H(22A)	120.2
C(22)-C(23)-C(24)	120.0(2)
C(22)-C(23)-H(23A)	120.0
C(24)-C(23)-H(23A)	120.0
C(23)-C(24)-C(25)	119.9(2)
C(23)-C(24)-H(24A)	120.0
C(25)-C(24)-H(24A)	120.0
C(24)-C(25)-C(20)	121.7(2)
C(24)-C(25)-H(25A)	119.2
C(20)-C(25)-H(25A)	119.2

Symmetry transformations used to generate equivalent atoms:

Anisotropic displacement parameters ($\text{\AA}^2 \times 10^3$) for **13**. The anisotropic displacement factor exponent takes the form: $-2p^2[h^2 a^*{}^2 U^{11} + \dots + 2 h k a^* b^* U^{12}]$

	U ¹¹	U ²²	U ³³	U ²³	U ¹³	U ¹²
Sn(1)	22(1)	22(1)	20(1)	-3(1)	5(1)	-1(1)
N(1)	26(1)	25(1)	26(1)	-2(1)	6(1)	2(1)
C(1)	32(1)	25(1)	25(1)	-7(1)	1(1)	4(1)
C(2)	32(1)	27(1)	29(1)	-2(1)	9(1)	5(1)
C(3)	16(1)	24(1)	28(1)	-2(1)	5(1)	-1(1)
C(4)	30(1)	24(1)	38(1)	-2(1)	-1(1)	4(1)
C(5)	40(2)	35(2)	33(2)	6(1)	-3(1)	3(1)
C(6)	33(1)	41(2)	23(1)	-4(1)	1(1)	1(1)
C(7)	32(1)	30(1)	31(1)	-8(1)	7(1)	2(1)
C(8)	22(1)	21(1)	26(1)	-7(1)	11(1)	0(1)
C(9)	28(1)	31(1)	29(1)	-2(1)	6(1)	-3(1)
C(10)	26(1)	42(2)	44(2)	-6(1)	4(1)	-4(1)
C(11)	29(1)	33(2)	55(2)	-5(1)	19(1)	-6(1)
C(12)	39(1)	29(1)	41(2)	3(1)	20(1)	0(1)
C(13)	29(1)	27(1)	27(1)	-4(1)	8(1)	2(1)
C(14)	21(1)	28(1)	19(1)	-1(1)	1(1)	1(1)
C(15)	34(1)	32(1)	37(2)	-9(1)	14(1)	-7(1)
C(16)	43(2)	37(2)	44(2)	-20(1)	12(1)	-3(1)
C(17)	34(1)	44(2)	23(1)	-4(1)	5(1)	15(1)
C(18)	34(1)	37(2)	32(1)	10(1)	14(1)	9(1)
C(19)	32(1)	24(1)	30(1)	1(1)	9(1)	2(1)
C(20)	25(1)	19(1)	23(1)	1(1)	5(1)	-5(1)
C(21)	34(1)	24(1)	22(1)	-3(1)	5(1)	3(1)
C(22)	32(1)	28(1)	36(1)	1(1)	3(1)	6(1)
C(23)	37(2)	30(1)	28(1)	4(1)	-6(1)	-6(1)
C(24)	43(2)	32(1)	21(1)	-4(1)	4(1)	-8(1)
C(25)	30(1)	27(1)	28(1)	-1(1)	9(1)	-1(1)

Hydrogen coordinates (x 10⁴) and isotropic displacement parameters (Å² x 10³) for **13**.

	x	y	z	U(eq)
H(1A)	5495	7179	4034	33
H(1B)	5946	7478	3262	33
H(2A)	4101	7059	3267	34
H(2B)	4570	8829	3149	34
H(4A)	4086	9632	1800	37
H(5A)	4014	9020	462	44
H(6A)	4361	6283	77	39
H(7A)	4777	4285	1037	37
H(9A)	3722	3456	2455	35
H(10A)	2474	1936	2632	45
H(11A)	2429	352	3761	45
H(12A)	3656	238	4715	42
H(13A)	4919	1742	4543	33
H(15A)	5595	913	2396	40
H(16A)	6196	-274	1352	49
H(17A)	7198	1244	733	40
H(18A)	7583	3978	1150	40
H(19A)	6982	5172	2194	34
H(21A)	7326	2081	3770	32
H(22A)	8440	1580	4805	39
H(23A)	8369	2815	6023	39
H(24A)	7170	4496	6214	38
H(25A)	6046	4939	5191	33

Torsion angles [°] for **13**.

Sn(1)-C(1)-C(2)-C(3)	-60.7(2)
C(7)-N(1)-C(3)-C(4)	1.0(3)
C(7)-N(1)-C(3)-C(2)	-178.5(2)
C(1)-C(2)-C(3)-N(1)	46.2(3)
C(1)-C(2)-C(3)-C(4)	-133.3(2)
N(1)-C(3)-C(4)-C(5)	-1.4(4)
C(2)-C(3)-C(4)-C(5)	178.0(2)
C(3)-C(4)-C(5)-C(6)	1.0(4)
C(4)-C(5)-C(6)-C(7)	-0.2(4)
C(3)-N(1)-C(7)-C(6)	-0.1(3)
C(5)-C(6)-C(7)-N(1)	-0.2(4)
C(13)-C(8)-C(9)-C(10)	0.6(3)
Sn(1)-C(8)-C(9)-C(10)	-178.83(18)
C(8)-C(9)-C(10)-C(11)	0.2(4)
C(9)-C(10)-C(11)-C(12)	-0.7(4)
C(10)-C(11)-C(12)-C(13)	0.5(4)
C(11)-C(12)-C(13)-C(8)	0.3(4)
C(9)-C(8)-C(13)-C(12)	-0.8(3)
Sn(1)-C(8)-C(13)-C(12)	178.62(17)
C(19)-C(14)-C(15)-C(16)	-0.7(4)
Sn(1)-C(14)-C(15)-C(16)	179.2(2)
C(14)-C(15)-C(16)-C(17)	0.6(4)
C(15)-C(16)-C(17)-C(18)	-0.4(4)
C(16)-C(17)-C(18)-C(19)	0.4(4)
C(15)-C(14)-C(19)-C(18)	0.7(3)
Sn(1)-C(14)-C(19)-C(18)	-179.21(18)
C(17)-C(18)-C(19)-C(14)	-0.5(4)
C(25)-C(20)-C(21)-C(22)	0.3(3)
Sn(1)-C(20)-C(21)-C(22)	173.06(18)
C(20)-C(21)-C(22)-C(23)	-0.9(4)
C(21)-C(22)-C(23)-C(24)	0.8(4)
C(22)-C(23)-C(24)-C(25)	0.0(4)
C(23)-C(24)-C(25)-C(20)	-0.7(4)
C(21)-C(20)-C(25)-C(24)	0.5(3)

Sn(1)-C(20)-C(25)-C(24) -172.05(18)

Symmetry transformations used to generate equivalent atoms:

Table A6: Crystal data and structure refinement for **24**.

Identification code	d18128_a
Empirical formula	C13 H13 Br2 N Sn
Formula weight	461.75
Temperature	150(2) K
Wavelength	0.71073 Å
Crystal system	Monoclinic
Space group	P2 ₁ /n
Unit cell dimensions	a = 15.4702(11) Å a= 90°. b = 10.7758(7) Å b= 100.386(2)°. c = 17.9533(12) Å g = 90°.
Volume	2943.8(3) Å ³
Z	8
Density (calculated)	2.084 Mg/m ³
Absorption coefficient	7.144 mm ⁻¹
F(000)	1744
Crystal size	0.350 x 0.200 x 0.020 mm ³
Theta range for data collection	1.601 to 27.562°.
Index ranges	-19<=h<=20, -14<=k<=13, -23<=l<=21
Reflections collected	39833
Independent reflections	6786 [R(int) = 0.0683]
Completeness to theta = 25.242°	100.0 %
Absorption correction	Semi-empirical from equivalents
Max. and min. transmission	0.7456 and 0.4499
Refinement method	Full-matrix least-squares on F ²
Data / restraints / parameters	6786 / 0 / 307
Goodness-of-fit on F ²	1.103
Final R indices [I>2sigma(I)]	R1 = 0.0503, wR2 = 0.0870
R indices (all data)	R1 = 0.0883, wR2 = 0.0995
Extinction coefficient	n/a
Largest diff. peak and hole	1.781 and -1.270 e.Å ⁻³

Atomic coordinates ($\times 10^4$) and equivalent isotropic displacement parameters ($\text{\AA}^2 \times 10^3$) for
24. U(eq) is defined as one third of the trace of the orthogonalized U^{ij} tensor.

	x	y	z	U(eq)
Sn(1A)	2652(1)	4622(1)	8106(1)	20(1)
Br(1A)	1406(1)	3727(1)	7051(1)	27(1)
Br(2A)	3080(1)	2536(1)	8671(1)	45(1)
N(1A)	3872(3)	5529(4)	8923(3)	21(1)
C(1A)	3519(4)	5089(6)	7360(3)	23(1)
C(2A)	4468(4)	5059(6)	7792(3)	28(2)
C(3A)	4557(4)	5675(5)	8558(3)	22(1)
C(4A)	5296(4)	6327(6)	8881(4)	30(2)
C(5A)	5336(5)	6819(6)	9594(4)	34(2)
C(6A)	4646(5)	6668(6)	9969(4)	30(2)
C(7A)	3917(5)	6010(5)	9618(4)	28(2)
C(8A)	1787(4)	5527(6)	8730(4)	29(2)
C(9A)	1325(5)	6545(7)	8442(4)	38(2)
C(10A)	761(6)	7144(8)	8840(5)	52(2)
C(11A)	645(6)	6705(10)	9524(6)	61(3)
C(12A)	1106(6)	5686(9)	9840(5)	58(3)
C(13A)	1688(6)	5077(8)	9439(4)	46(2)
Sn(1B)	7599(1)	7094(1)	7180(1)	23(1)
Br(1B)	7321(1)	7949(1)	8480(1)	36(1)
Br(2B)	8083(1)	9153(1)	6728(1)	36(1)
N(1B)	8046(3)	6291(4)	6084(3)	23(1)
C(1B)	8702(4)	5989(6)	7626(4)	31(2)
C(2B)	9309(4)	5828(7)	7052(4)	32(2)
C(3B)	8822(4)	5713(5)	6244(4)	25(1)
C(4B)	9160(5)	5104(6)	5690(4)	31(2)
C(5B)	8709(5)	5113(6)	4960(4)	38(2)
C(6B)	7921(5)	5737(7)	4793(4)	39(2)
C(7B)	7602(5)	6315(7)	5369(4)	34(2)
C(8B)	6249(4)	6790(5)	6696(3)	16(1)

C(9B)	5624(5)	7655(6)	6725(4)	35(2)
C(10B)	4765(5)	7479(7)	6368(4)	37(2)
C(11B)	4525(5)	6411(7)	5968(4)	36(2)
C(12B)	5141(5)	5494(6)	5938(4)	34(2)
C(13B)	6010(5)	5671(6)	6293(4)	27(2)

—

Bond lengths [\AA] and angles [$^\circ$] for **24**.

Sn(1A)-C(1A)	2.120(6)
Sn(1A)-C(8A)	2.131(7)
Sn(1A)-N(1A)	2.382(5)
Sn(1A)-Br(2A)	2.5058(8)
Sn(1A)-Br(1A)	2.6298(7)
N(1A)-C(7A)	1.340(8)
N(1A)-C(3A)	1.351(8)
C(1A)-C(2A)	1.532(9)
C(1A)-H(1AA)	0.9900
C(1A)-H(1AB)	0.9900
C(2A)-C(3A)	1.509(9)
C(2A)-H(2AA)	0.9900
C(2A)-H(2AB)	0.9900
C(3A)-C(4A)	1.378(9)
C(4A)-C(5A)	1.378(10)
C(4A)-H(4AA)	0.9500
C(5A)-C(6A)	1.370(10)
C(5A)-H(5AA)	0.9500
C(6A)-C(7A)	1.384(9)
C(6A)-H(6AA)	0.9500
C(7A)-H(7AA)	0.9500
C(8A)-C(9A)	1.359(10)
C(8A)-C(13A)	1.397(10)
C(9A)-C(10A)	1.384(11)
C(9A)-H(9AA)	0.9500
C(10A)-C(11A)	1.357(13)
C(10A)-H(10A)	0.9500
C(11A)-C(12A)	1.375(13)
C(11A)-H(11A)	0.9500
C(12A)-C(13A)	1.411(12)
C(12A)-H(12A)	0.9500
C(13A)-H(13A)	0.9500
Sn(1B)-C(1B)	2.115(6)
Sn(1B)-C(8B)	2.138(6)

Sn(1B)-N(1B)	2.363(5)
Sn(1B)-Br(2B)	2.5223(8)
Sn(1B)-Br(1B)	2.6176(8)
N(1B)-C(3B)	1.336(8)
N(1B)-C(7B)	1.342(8)
C(1B)-C(2B)	1.524(9)
C(1B)-H(1BA)	0.9900
C(1B)-H(1BB)	0.9900
C(2B)-C(3B)	1.515(9)
C(2B)-H(2BA)	0.9900
C(2B)-H(2BB)	0.9900
C(3B)-C(4B)	1.371(9)
C(4B)-C(5B)	1.371(10)
C(4B)-H(4BA)	0.9500
C(5B)-C(6B)	1.376(11)
C(5B)-H(5BA)	0.9500
C(6B)-C(7B)	1.373(10)
C(6B)-H(6BA)	0.9500
C(7B)-H(7BA)	0.9500
C(8B)-C(9B)	1.351(9)
C(8B)-C(13B)	1.421(8)
C(9B)-C(10B)	1.381(10)
C(9B)-H(9BA)	0.9500
C(10B)-C(11B)	1.372(10)
C(10B)-H(10B)	0.9500
C(11B)-C(12B)	1.380(10)
C(11B)-H(11B)	0.9500
C(12B)-C(13B)	1.393(10)
C(12B)-H(12B)	0.9500
C(13B)-H(13B)	0.9500

C(1A)-Sn(1A)-C(8A)	138.8(3)
C(1A)-Sn(1A)-N(1A)	76.7(2)
C(8A)-Sn(1A)-N(1A)	89.5(2)
C(1A)-Sn(1A)-Br(2A)	108.53(17)
C(8A)-Sn(1A)-Br(2A)	110.05(19)

N(1A)-Sn(1A)-Br(2A)	89.80(11)
C(1A)-Sn(1A)-Br(1A)	95.55(16)
C(8A)-Sn(1A)-Br(1A)	95.62(16)
N(1A)-Sn(1A)-Br(1A)	172.19(13)
Br(2A)-Sn(1A)-Br(1A)	93.91(3)
C(7A)-N(1A)-C(3A)	119.6(5)
C(7A)-N(1A)-Sn(1A)	129.3(5)
C(3A)-N(1A)-Sn(1A)	110.6(4)
C(2A)-C(1A)-Sn(1A)	109.4(4)
C(2A)-C(1A)-H(1AA)	109.8
Sn(1A)-C(1A)-H(1AA)	109.8
C(2A)-C(1A)-H(1AB)	109.8
Sn(1A)-C(1A)-H(1AB)	109.8
H(1AA)-C(1A)-H(1AB)	108.2
C(3A)-C(2A)-C(1A)	112.0(5)
C(3A)-C(2A)-H(2AA)	109.2
C(1A)-C(2A)-H(2AA)	109.2
C(3A)-C(2A)-H(2AB)	109.2
C(1A)-C(2A)-H(2AB)	109.2
H(2AA)-C(2A)-H(2AB)	107.9
N(1A)-C(3A)-C(4A)	121.2(6)
N(1A)-C(3A)-C(2A)	116.1(5)
C(4A)-C(3A)-C(2A)	122.7(6)
C(3A)-C(4A)-C(5A)	118.9(7)
C(3A)-C(4A)-H(4AA)	120.6
C(5A)-C(4A)-H(4AA)	120.6
C(6A)-C(5A)-C(4A)	120.1(6)
C(6A)-C(5A)-H(5AA)	119.9
C(4A)-C(5A)-H(5AA)	119.9
C(5A)-C(6A)-C(7A)	118.7(6)
C(5A)-C(6A)-H(6AA)	120.6
C(7A)-C(6A)-H(6AA)	120.6
N(1A)-C(7A)-C(6A)	121.5(7)
N(1A)-C(7A)-H(7AA)	119.2
C(6A)-C(7A)-H(7AA)	119.2
C(9A)-C(8A)-C(13A)	119.4(7)

C(9A)-C(8A)-Sn(1A)	120.4(5)
C(13A)-C(8A)-Sn(1A)	120.2(6)
C(8A)-C(9A)-C(10A)	121.2(8)
C(8A)-C(9A)-H(9AA)	119.4
C(10A)-C(9A)-H(9AA)	119.4
C(11A)-C(10A)-C(9A)	120.2(9)
C(11A)-C(10A)-H(10A)	119.9
C(9A)-C(10A)-H(10A)	119.9
C(10A)-C(11A)-C(12A)	120.6(9)
C(10A)-C(11A)-H(11A)	119.7
C(12A)-C(11A)-H(11A)	119.7
C(11A)-C(12A)-C(13A)	119.5(8)
C(11A)-C(12A)-H(12A)	120.3
C(13A)-C(12A)-H(12A)	120.3
C(8A)-C(13A)-C(12A)	119.2(8)
C(8A)-C(13A)-H(13A)	120.4
C(12A)-C(13A)-H(13A)	120.4
C(1B)-Sn(1B)-C(8B)	136.9(2)
C(1B)-Sn(1B)-N(1B)	76.9(2)
C(8B)-Sn(1B)-N(1B)	91.0(2)
C(1B)-Sn(1B)-Br(2B)	110.6(2)
C(8B)-Sn(1B)-Br(2B)	109.21(14)
N(1B)-Sn(1B)-Br(2B)	84.61(12)
C(1B)-Sn(1B)-Br(1B)	96.40(18)
C(8B)-Sn(1B)-Br(1B)	96.33(16)
N(1B)-Sn(1B)-Br(1B)	172.44(13)
Br(2B)-Sn(1B)-Br(1B)	94.74(3)
C(3B)-N(1B)-C(7B)	120.0(6)
C(3B)-N(1B)-Sn(1B)	112.2(4)
C(7B)-N(1B)-Sn(1B)	127.8(4)
C(2B)-C(1B)-Sn(1B)	111.2(4)
C(2B)-C(1B)-H(1BA)	109.4
Sn(1B)-C(1B)-H(1BA)	109.4
C(2B)-C(1B)-H(1BB)	109.4
Sn(1B)-C(1B)-H(1BB)	109.4
H(1BA)-C(1B)-H(1BB)	108.0

C(3B)-C(2B)-C(1B)	113.3(6)
C(3B)-C(2B)-H(2BA)	108.9
C(1B)-C(2B)-H(2BA)	108.9
C(3B)-C(2B)-H(2BB)	108.9
C(1B)-C(2B)-H(2BB)	108.9
H(2BA)-C(2B)-H(2BB)	107.7
N(1B)-C(3B)-C(4B)	120.8(6)
N(1B)-C(3B)-C(2B)	116.1(6)
C(4B)-C(3B)-C(2B)	123.0(6)
C(3B)-C(4B)-C(5B)	119.7(7)
C(3B)-C(4B)-H(4BA)	120.1
C(5B)-C(4B)-H(4BA)	120.1
C(4B)-C(5B)-C(6B)	119.3(7)
C(4B)-C(5B)-H(5BA)	120.4
C(6B)-C(5B)-H(5BA)	120.4
C(7B)-C(6B)-C(5B)	118.9(7)
C(7B)-C(6B)-H(6BA)	120.6
C(5B)-C(6B)-H(6BA)	120.6
N(1B)-C(7B)-C(6B)	121.3(7)
N(1B)-C(7B)-H(7BA)	119.4
C(6B)-C(7B)-H(7BA)	119.4
C(9B)-C(8B)-C(13B)	118.9(6)
C(9B)-C(8B)-Sn(1B)	122.2(5)
C(13B)-C(8B)-Sn(1B)	118.9(4)
C(8B)-C(9B)-C(10B)	121.6(6)
C(8B)-C(9B)-H(9BA)	119.2
C(10B)-C(9B)-H(9BA)	119.2
C(11B)-C(10B)-C(9B)	120.3(7)
C(11B)-C(10B)-H(10B)	119.9
C(9B)-C(10B)-H(10B)	119.9
C(10B)-C(11B)-C(12B)	119.9(7)
C(10B)-C(11B)-H(11B)	120.1
C(12B)-C(11B)-H(11B)	120.1
C(11B)-C(12B)-C(13B)	120.0(6)
C(11B)-C(12B)-H(12B)	120.0
C(13B)-C(12B)-H(12B)	120.0

C(12B)-C(13B)-C(8B) 119.4(6)

C(12B)-C(13B)-H(13B) 120.3

C(8B)-C(13B)-H(13B) 120.3

Symmetry transformations used to generate equivalent atoms:

Anisotropic displacement parameters ($\text{\AA}^2 \times 10^3$) for **24**. The anisotropic displacement factor exponent takes the form: $-2p^2[h^2 a^*{}^2 U^{11} + \dots + 2 h k a^* b^* U^{12}]$

	U ¹¹	U ²²	U ³³	U ²³	U ¹³	U ¹²
Sn(1A)	19(1)	22(1)	19(1)	-1(1)	0(1)	-3(1)
Br(1A)	21(1)	34(1)	24(1)	-3(1)	-3(1)	-5(1)
Br(2A)	55(1)	25(1)	42(1)	9(1)	-23(1)	-10(1)
N(1A)	21(3)	18(2)	21(3)	1(2)	-4(2)	0(2)
C(1A)	19(4)	30(3)	20(3)	2(3)	3(3)	-1(3)
C(2A)	21(4)	38(4)	24(3)	5(3)	4(3)	2(3)
C(3A)	20(4)	18(3)	28(3)	4(2)	0(3)	-1(2)
C(4A)	22(4)	23(3)	42(4)	8(3)	-4(3)	-5(3)
C(5A)	30(4)	19(3)	44(4)	-1(3)	-17(4)	-7(3)
C(6A)	34(5)	20(3)	30(4)	-5(3)	-12(3)	7(3)
C(7A)	33(4)	24(3)	25(3)	-1(3)	1(3)	2(3)
C(8A)	19(4)	44(4)	26(3)	-17(3)	9(3)	-19(3)
C(9A)	33(5)	48(4)	36(4)	-20(3)	11(3)	-7(4)
C(10A)	39(5)	57(5)	61(6)	-24(4)	13(4)	-7(4)
C(11A)	40(6)	79(7)	72(7)	-40(6)	28(5)	-22(5)
C(12A)	60(6)	82(7)	39(5)	-25(5)	30(5)	-40(5)
C(13A)	51(6)	55(5)	37(4)	-13(4)	19(4)	-23(4)
Sn(1B)	20(1)	21(1)	29(1)	-4(1)	7(1)	0(1)
Br(1B)	41(1)	32(1)	39(1)	-14(1)	19(1)	-11(1)
Br(2B)	40(1)	24(1)	47(1)	-2(1)	18(1)	-6(1)
N(1B)	22(3)	21(3)	27(3)	-3(2)	7(2)	-1(2)
C(1B)	24(4)	38(4)	29(4)	0(3)	1(3)	3(3)
C(2B)	17(4)	41(4)	39(4)	4(3)	6(3)	7(3)
C(3B)	21(4)	22(3)	34(4)	3(3)	9(3)	0(3)
C(4B)	31(4)	22(3)	44(4)	-4(3)	17(3)	0(3)
C(5B)	41(5)	36(4)	43(4)	-13(3)	25(4)	-15(3)
C(6B)	38(5)	54(5)	24(4)	-9(3)	8(3)	-12(4)
C(7B)	26(4)	45(4)	33(4)	2(3)	7(3)	-2(3)
C(8B)	10(3)	18(3)	21(3)	7(2)	5(2)	0(2)
C(9B)	37(5)	28(4)	41(4)	-2(3)	10(4)	-6(3)
C(10B)	27(4)	41(4)	45(4)	10(3)	12(4)	5(3)

C(11B)	18(4)	64(5)	25(3)	9(3)	2(3)	-14(4)
C(12B)	43(5)	33(4)	25(3)	-1(3)	8(3)	-14(3)
C(13B)	28(4)	23(3)	31(4)	0(3)	8(3)	1(3)

Hydrogen coordinates (x 10⁴) and isotropic displacement parameters (Å² x 10³) for **25**.

	x	y	z	U(eq)
H(1AA)	3449	4490	6935	28
H(1AB)	3378	5928	7148	28
H(2AA)	4665	4186	7861	33
H(2AB)	4853	5487	7490	33
H(4AA)	5769	6435	8616	36
H(5AA)	5844	7264	9827	41
H(6AA)	4667	7009	10460	36
H(7AA)	3437	5896	9875	33
H(9AA)	1390	6850	7959	46
H(10A)	454	7866	8635	62
H(11A)	241	7104	9786	73
H(12A)	1033	5394	10324	69
H(13A)	2009	4370	9650	55
H(1BA)	9030	6384	8090	37
H(1BB)	8500	5164	7767	37
H(2BA)	9711	6548	7088	38
H(2BB)	9672	5075	7184	38
H(4BA)	9704	4677	5813	38
H(5BA)	8937	4693	4572	45
H(6BA)	7604	5767	4289	46
H(7BA)	7055	6740	5260	41
H(9BA)	5780	8403	6996	42
H(10B)	4337	8100	6401	45
H(11B)	3937	6303	5711	43
H(12B)	4972	4743	5675	40
H(13B)	6438	5049	6266	33

Torsion angles [°] for **24**.

Sn(1A)-C(1A)-C(2A)-C(3A)	-43.8(6)
C(7A)-N(1A)-C(3A)-C(4A)	-1.1(8)
Sn(1A)-N(1A)-C(3A)-C(4A)	171.4(4)
C(7A)-N(1A)-C(3A)-C(2A)	177.5(5)
Sn(1A)-N(1A)-C(3A)-C(2A)	-9.9(6)
C(1A)-C(2A)-C(3A)-N(1A)	35.4(7)
C(1A)-C(2A)-C(3A)-C(4A)	-146.0(6)
N(1A)-C(3A)-C(4A)-C(5A)	1.0(9)
C(2A)-C(3A)-C(4A)-C(5A)	-177.5(6)
C(3A)-C(4A)-C(5A)-C(6A)	-0.6(9)
C(4A)-C(5A)-C(6A)-C(7A)	0.3(9)
C(3A)-N(1A)-C(7A)-C(6A)	0.8(9)
Sn(1A)-N(1A)-C(7A)-C(6A)	-170.1(4)
C(5A)-C(6A)-C(7A)-N(1A)	-0.4(9)
C(13A)-C(8A)-C(9A)-C(10A)	0.2(10)
Sn(1A)-C(8A)-C(9A)-C(10A)	-179.9(5)
C(8A)-C(9A)-C(10A)-C(11A)	-1.4(12)
C(9A)-C(10A)-C(11A)-C(12A)	2.1(13)
C(10A)-C(11A)-C(12A)-C(13A)	-1.5(13)
C(9A)-C(8A)-C(13A)-C(12A)	0.4(10)
Sn(1A)-C(8A)-C(13A)-C(12A)	-179.5(5)
C(11A)-C(12A)-C(13A)-C(8A)	0.3(11)
Sn(1B)-C(1B)-C(2B)-C(3B)	-36.6(7)
C(7B)-N(1B)-C(3B)-C(4B)	-2.1(9)
Sn(1B)-N(1B)-C(3B)-C(4B)	175.0(5)
C(7B)-N(1B)-C(3B)-C(2B)	175.0(6)
Sn(1B)-N(1B)-C(3B)-C(2B)	-7.8(7)
C(1B)-C(2B)-C(3B)-N(1B)	29.1(8)
C(1B)-C(2B)-C(3B)-C(4B)	-153.8(6)
N(1B)-C(3B)-C(4B)-C(5B)	1.6(10)
C(2B)-C(3B)-C(4B)-C(5B)	-175.3(6)
C(3B)-C(4B)-C(5B)-C(6B)	0.1(10)
C(4B)-C(5B)-C(6B)-C(7B)	-1.2(10)
C(3B)-N(1B)-C(7B)-C(6B)	1.0(10)

Sn(1B)-N(1B)-C(7B)-C(6B)	-175.7(5)
C(5B)-C(6B)-C(7B)-N(1B)	0.7(11)
C(13B)-C(8B)-C(9B)-C(10B)	-0.4(10)
Sn(1B)-C(8B)-C(9B)-C(10B)	175.8(5)
C(8B)-C(9B)-C(10B)-C(11B)	-0.5(11)
C(9B)-C(10B)-C(11B)-C(12B)	1.8(11)
C(10B)-C(11B)-C(12B)-C(13B)	-2.1(10)
C(11B)-C(12B)-C(13B)-C(8B)	1.2(10)
C(9B)-C(8B)-C(13B)-C(12B)	0.1(9)
Sn(1B)-C(8B)-C(13B)-C(12B)	-176.3(5)

Symmetry transformations used to generate equivalent atoms:

166

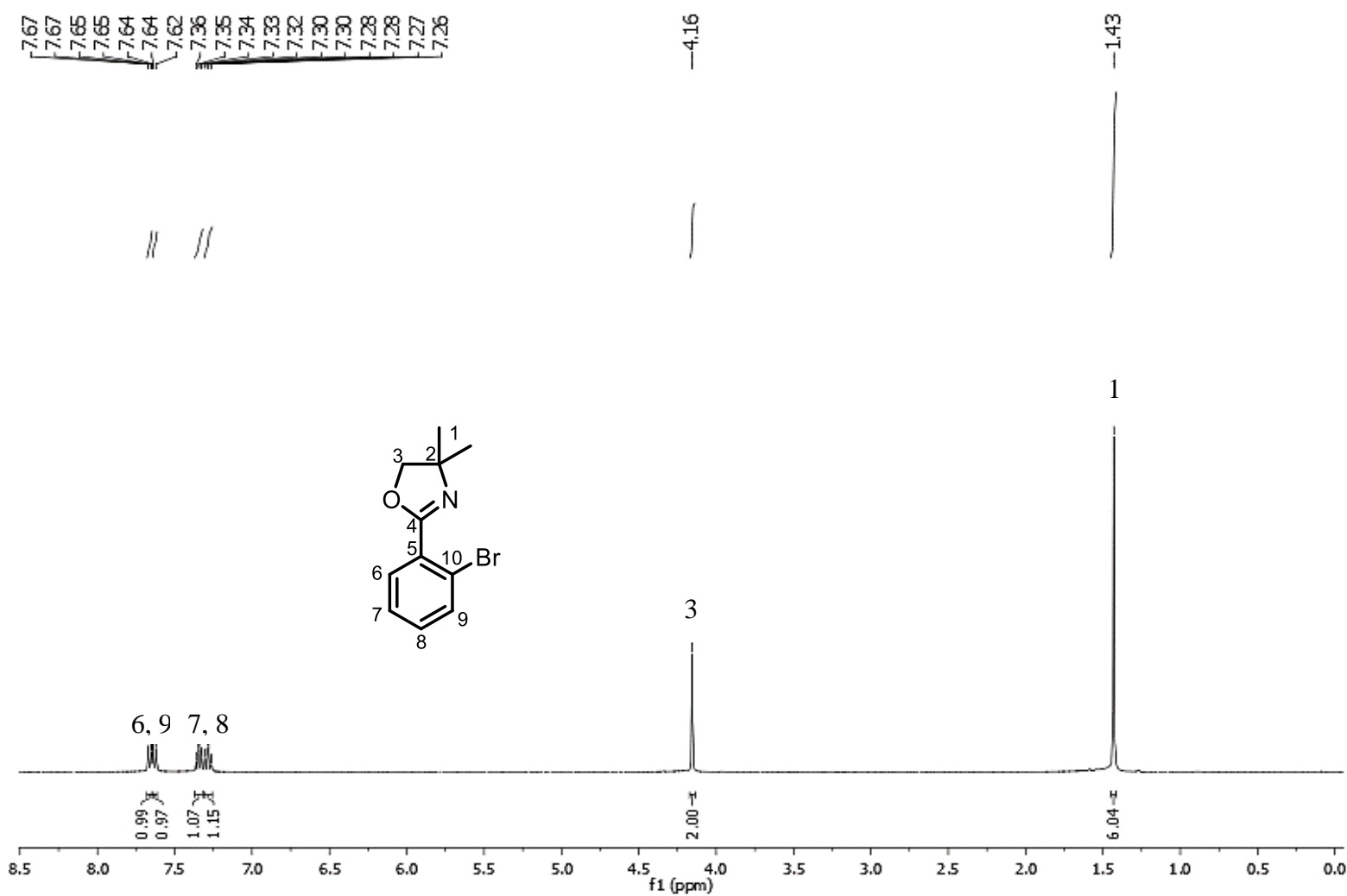


Figure A1: ¹H NMR spectrum of **8** in CDCl_3^* .

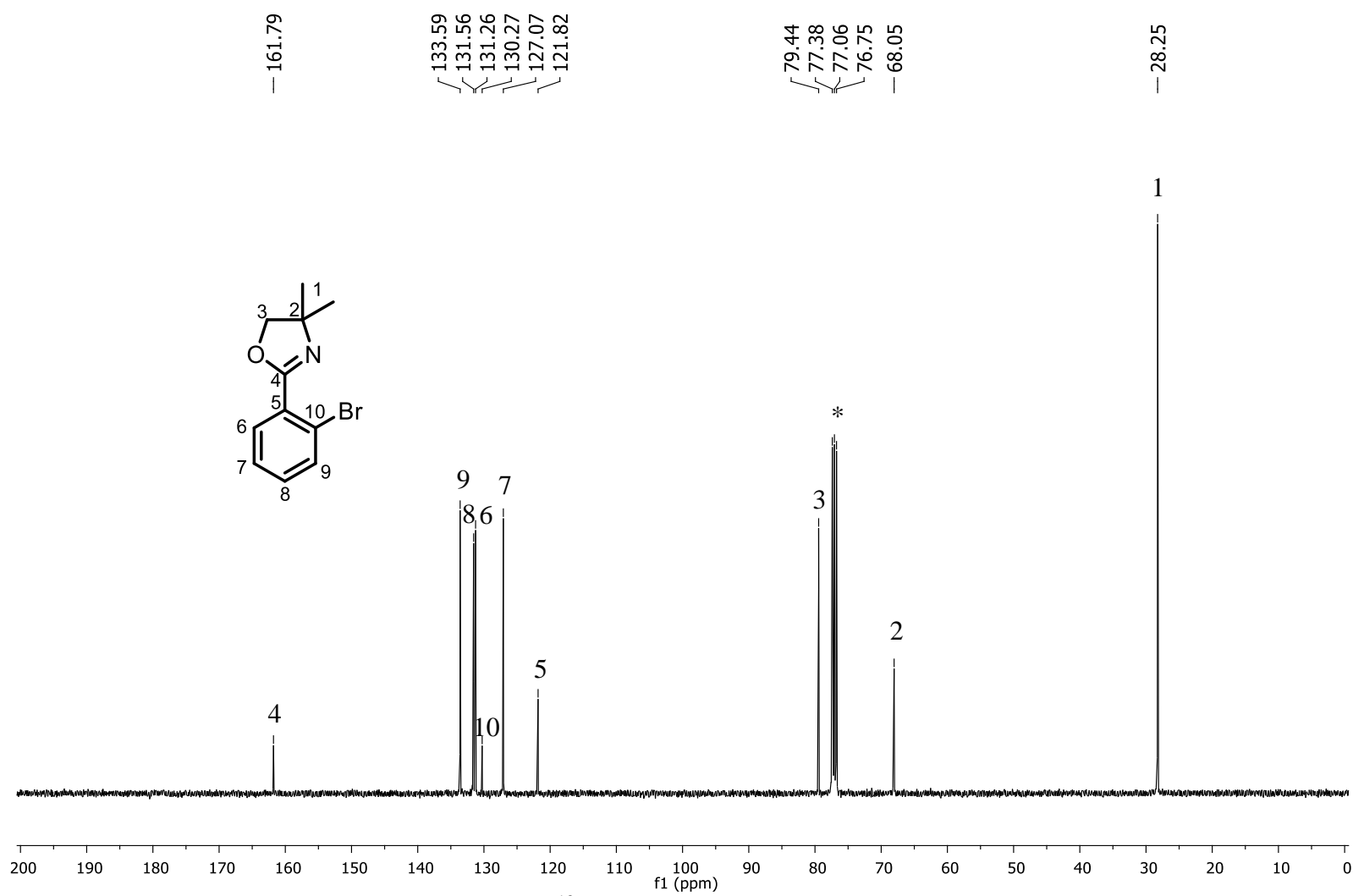


Figure A2: ^{13}C NMR spectrum of **8** in CDCl_3^* .

168

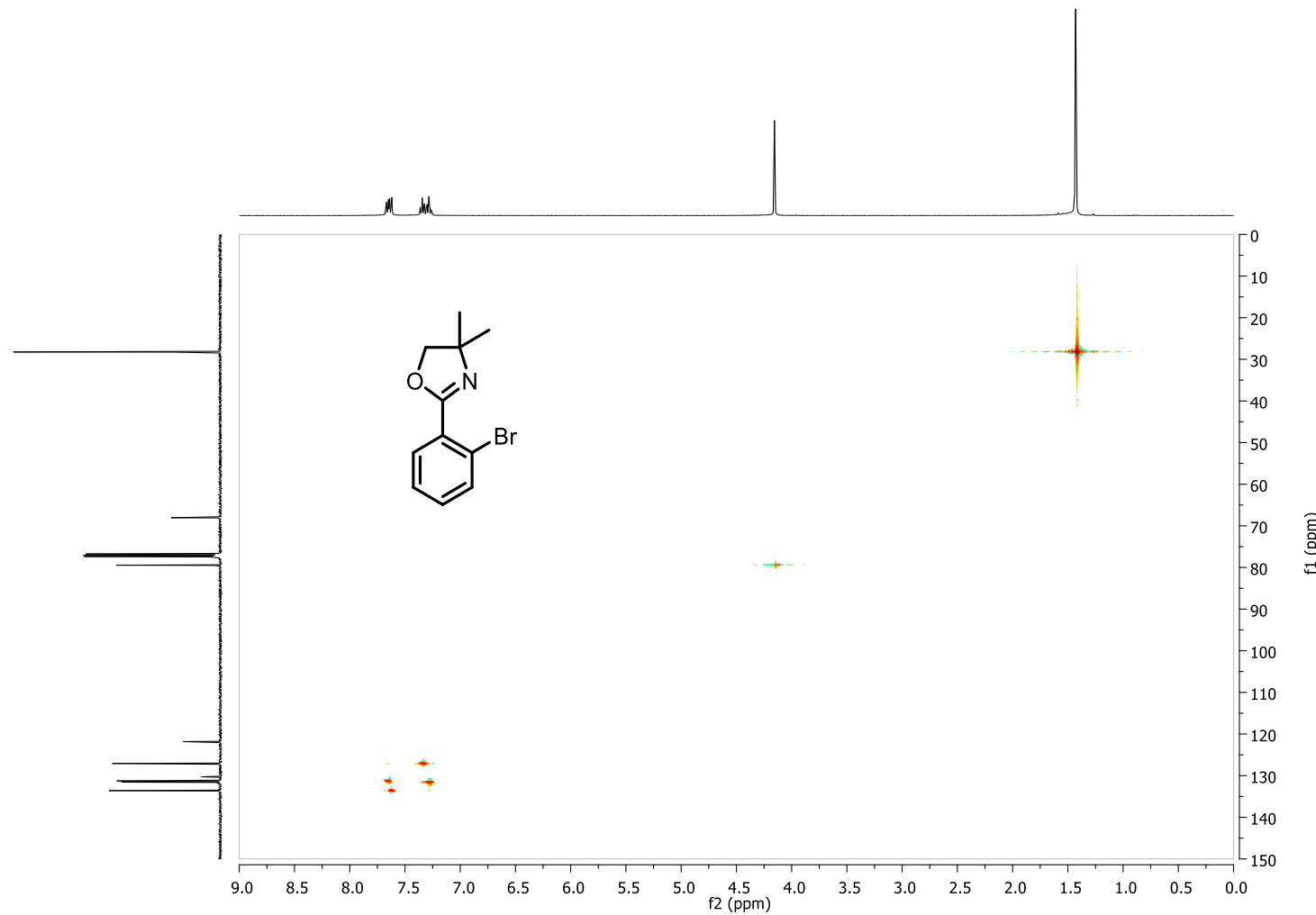


Figure A3: HSQC spectrum of **8** in CDCl_3 .

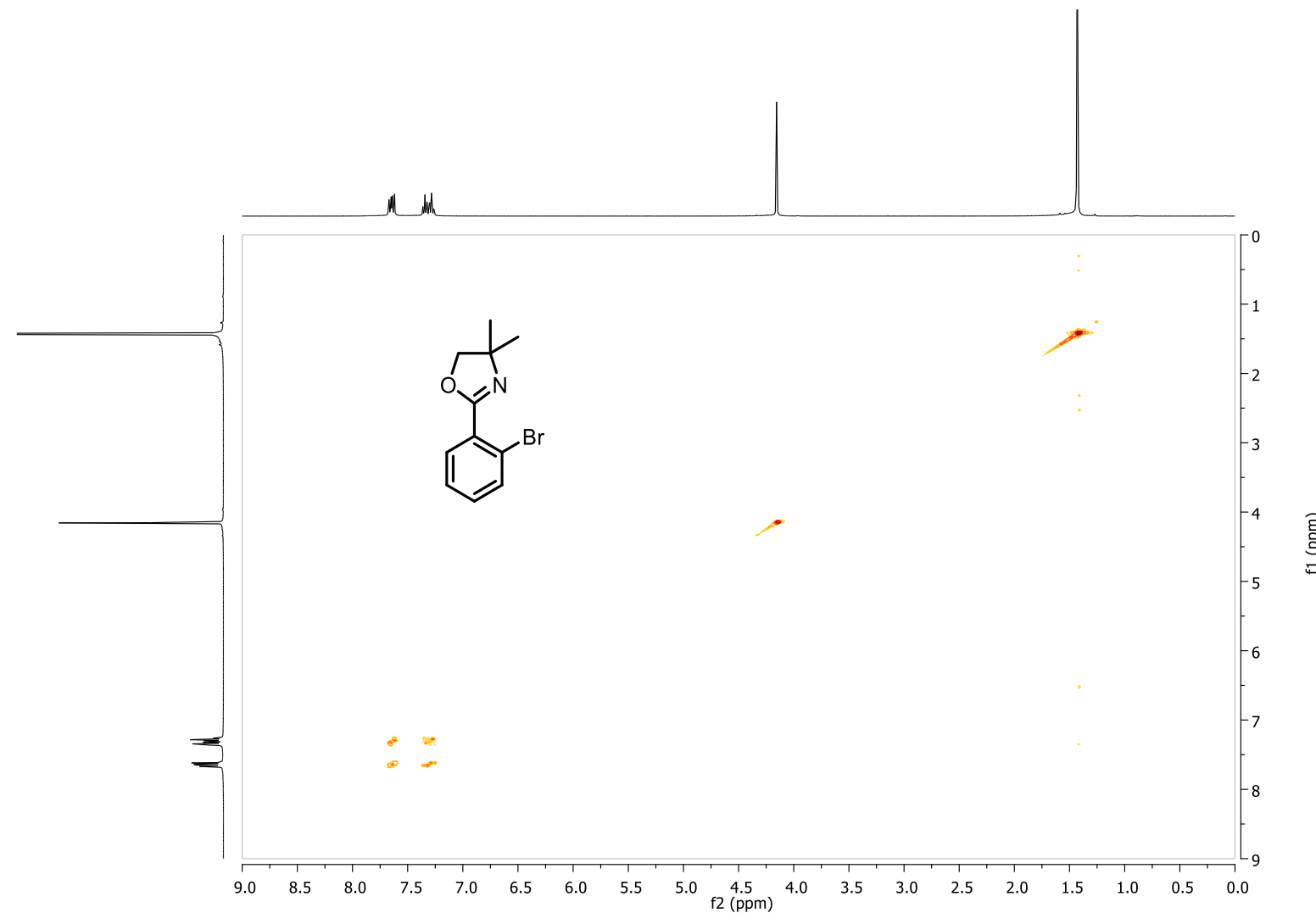


Figure A4: COSY spectrum of **8** in CDCl_3 .

170

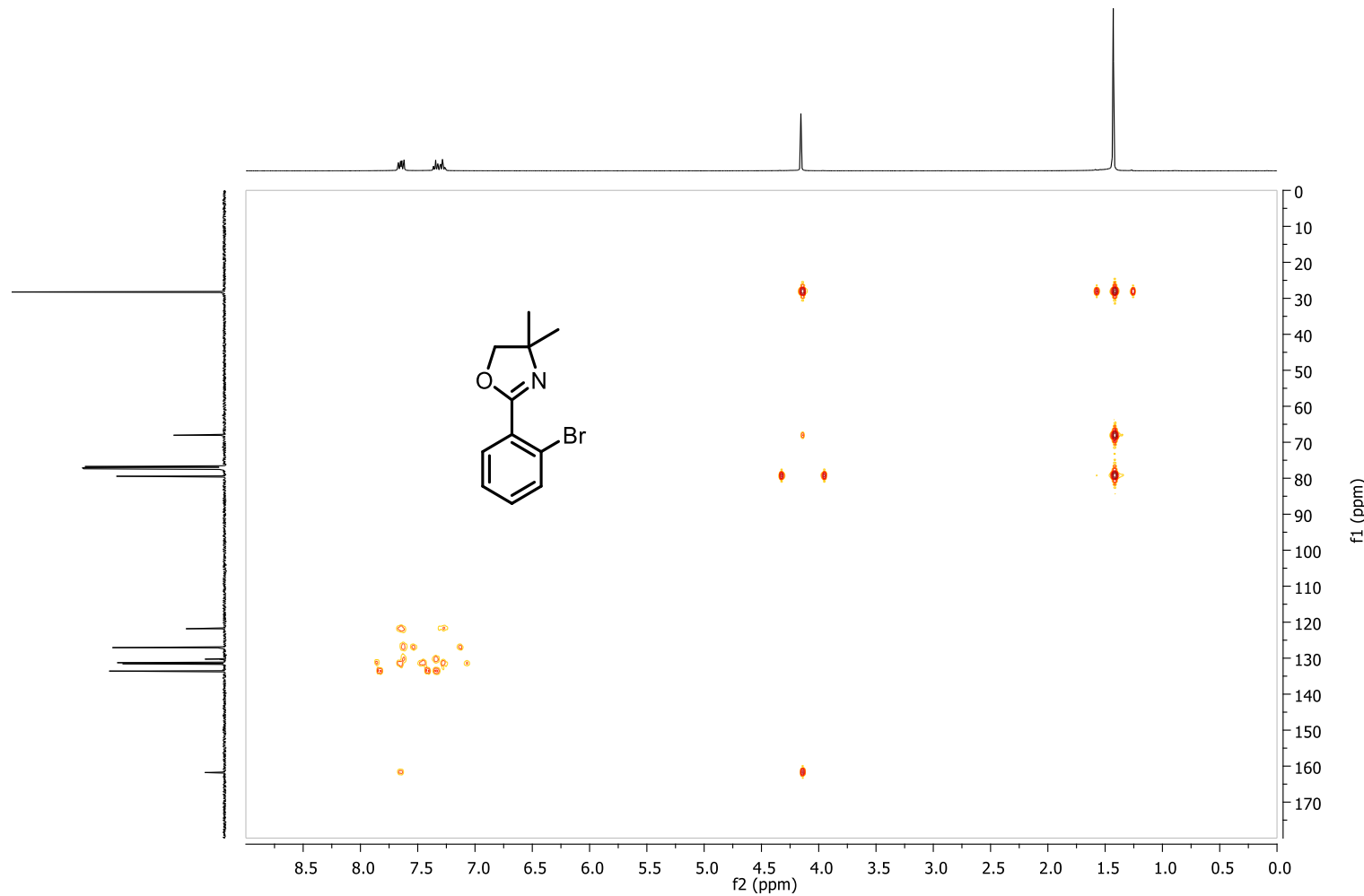


Figure A5: HMBC spectrum of **8** in CDCl_3 .

III

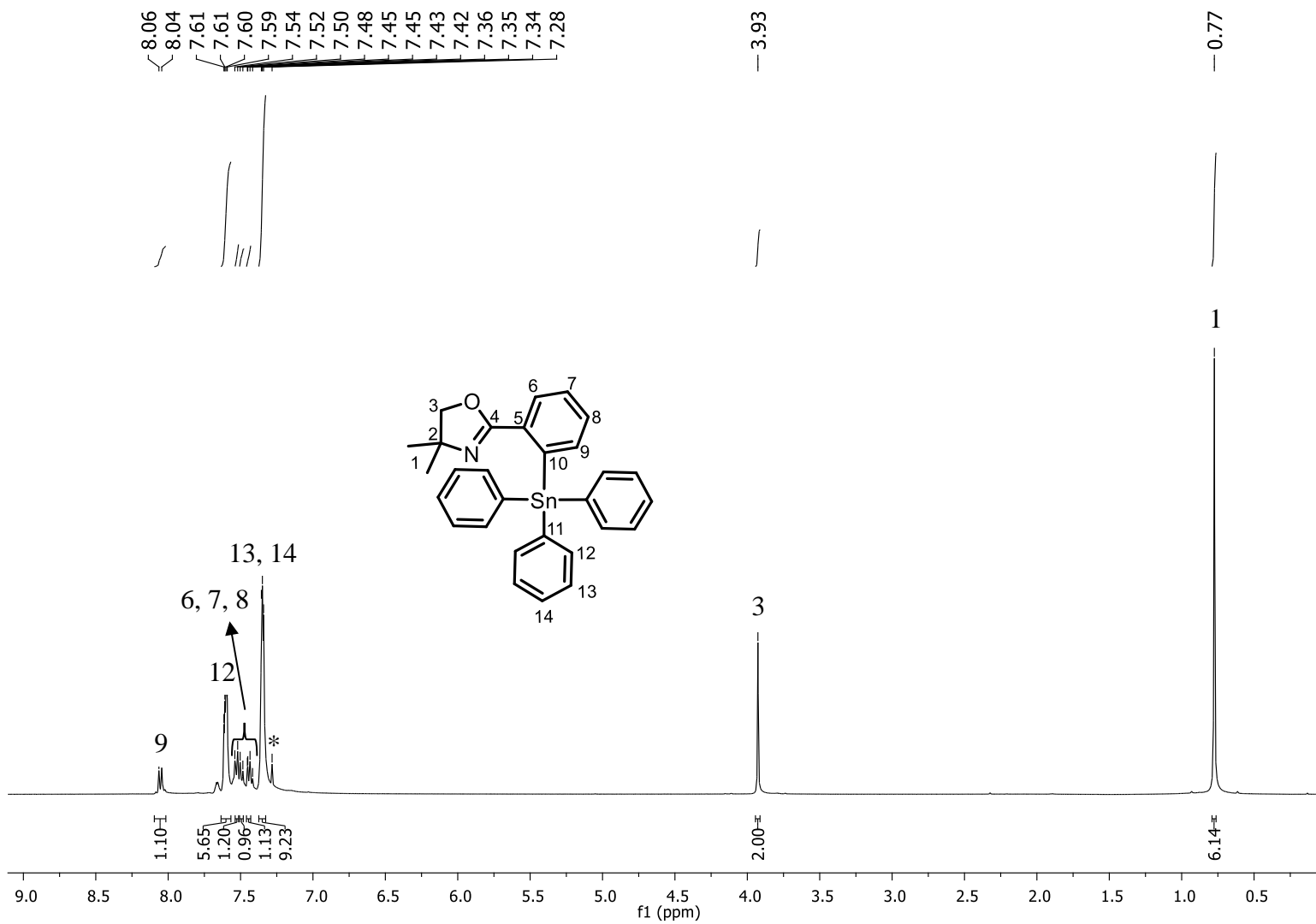


Figure A6: ^1H NMR spectrum of **10** in CDCl_3^* .

172

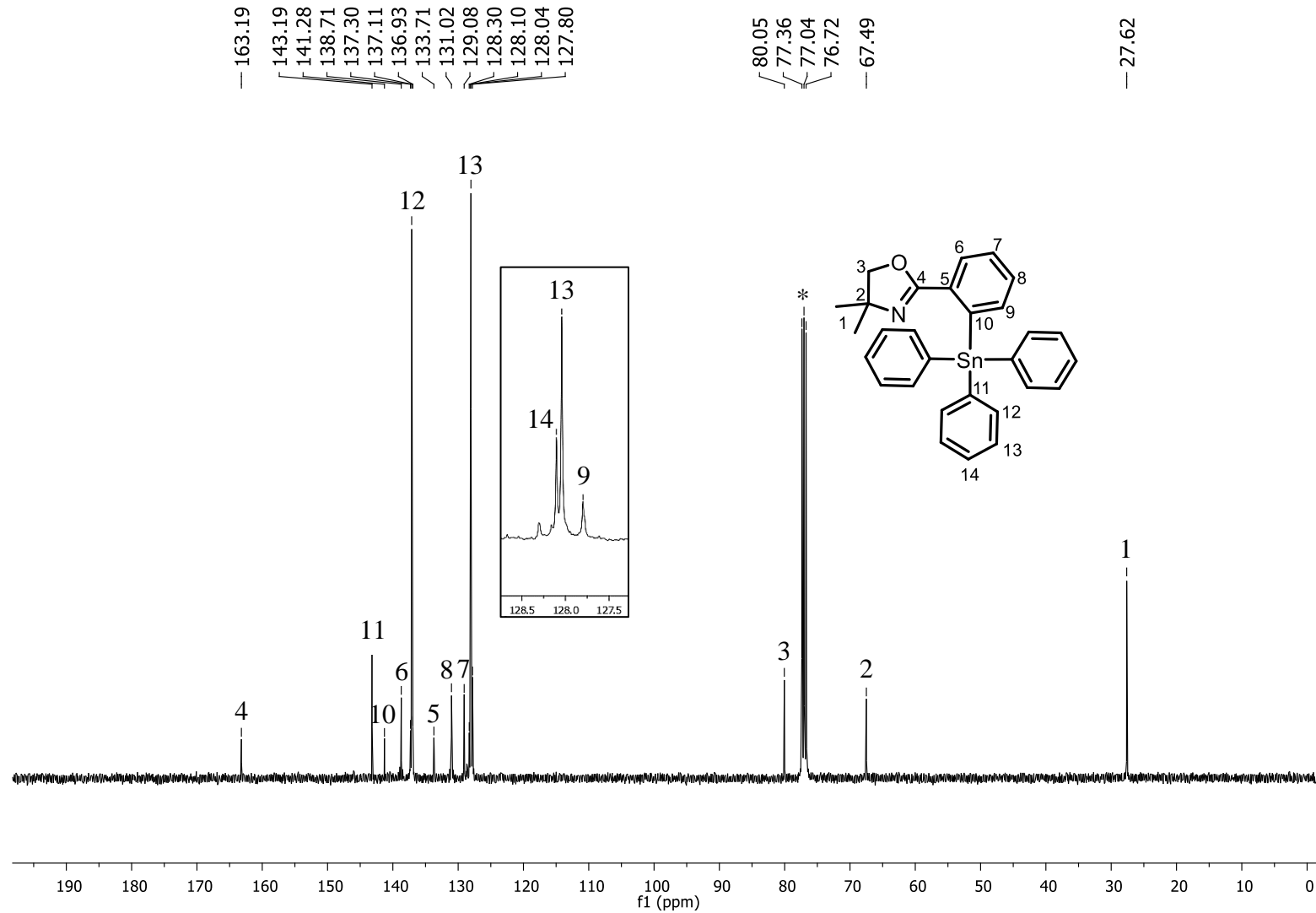


Figure A7: ^{13}C NMR spectrum of **10** in CDCl_3^* .

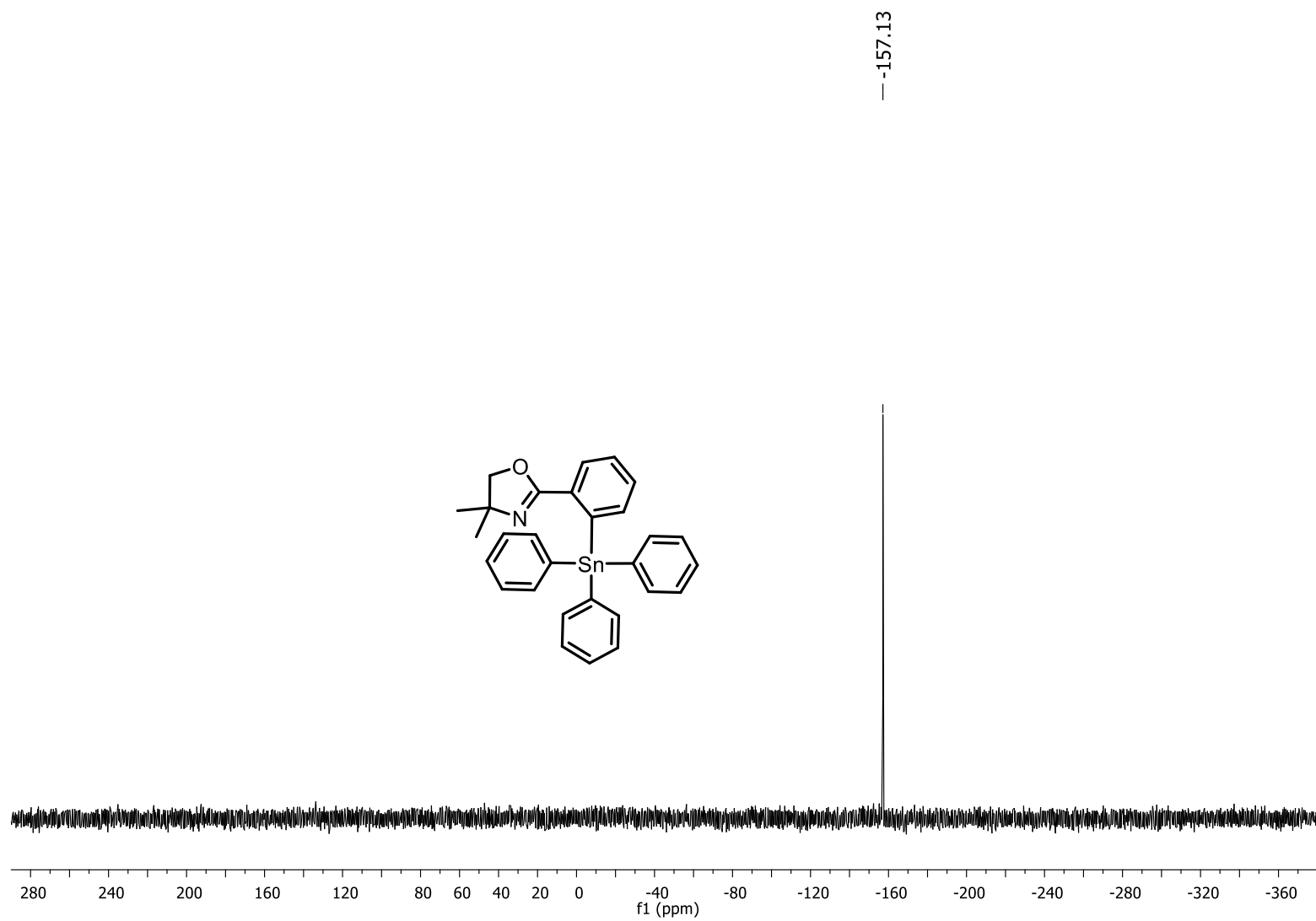


Figure A8: ^{119}Sn NMR spectrum of **10** in CDCl_3 .

174

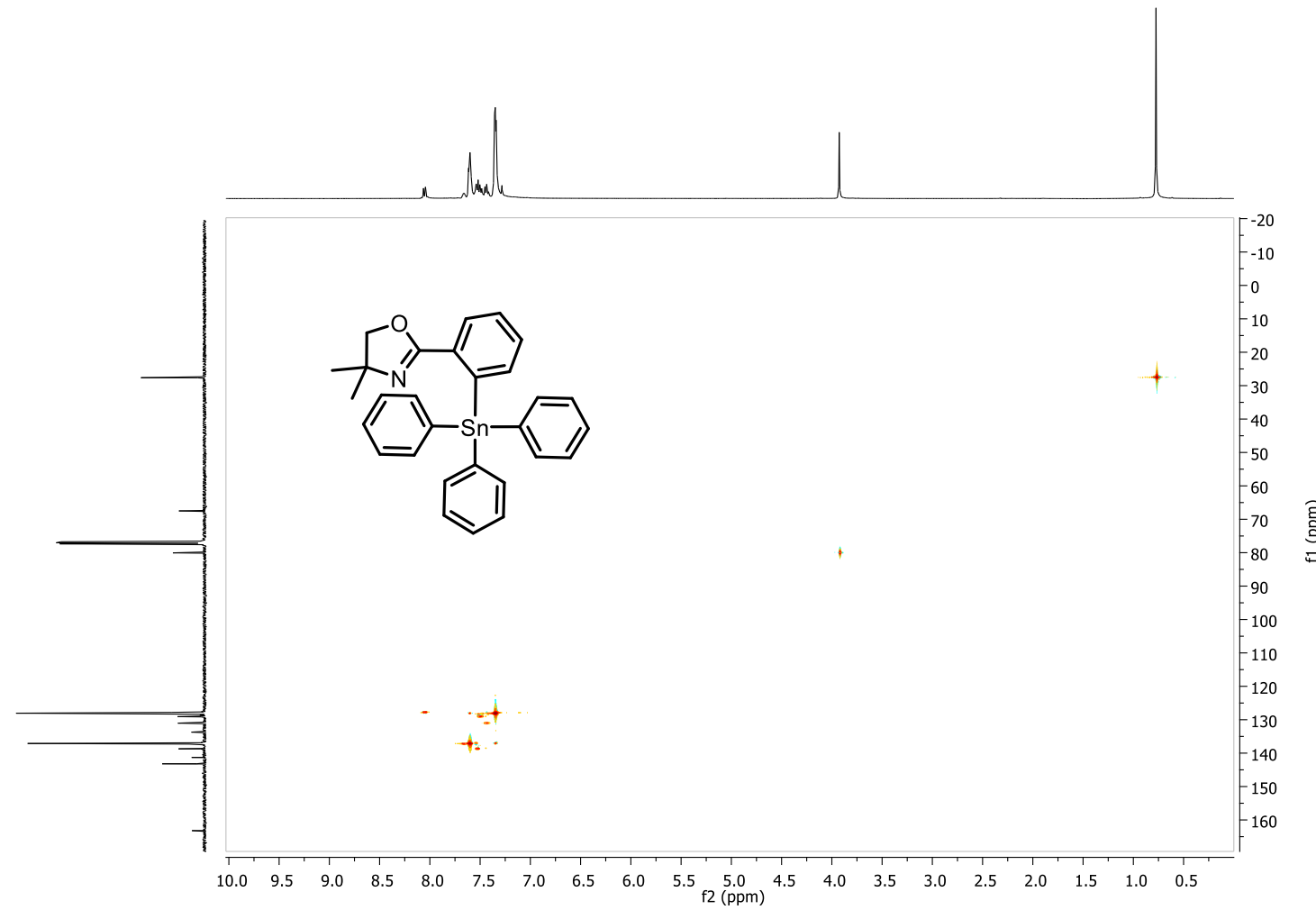


Figure A9: HSQC spectrum of **10** in CDCl_3 .

175

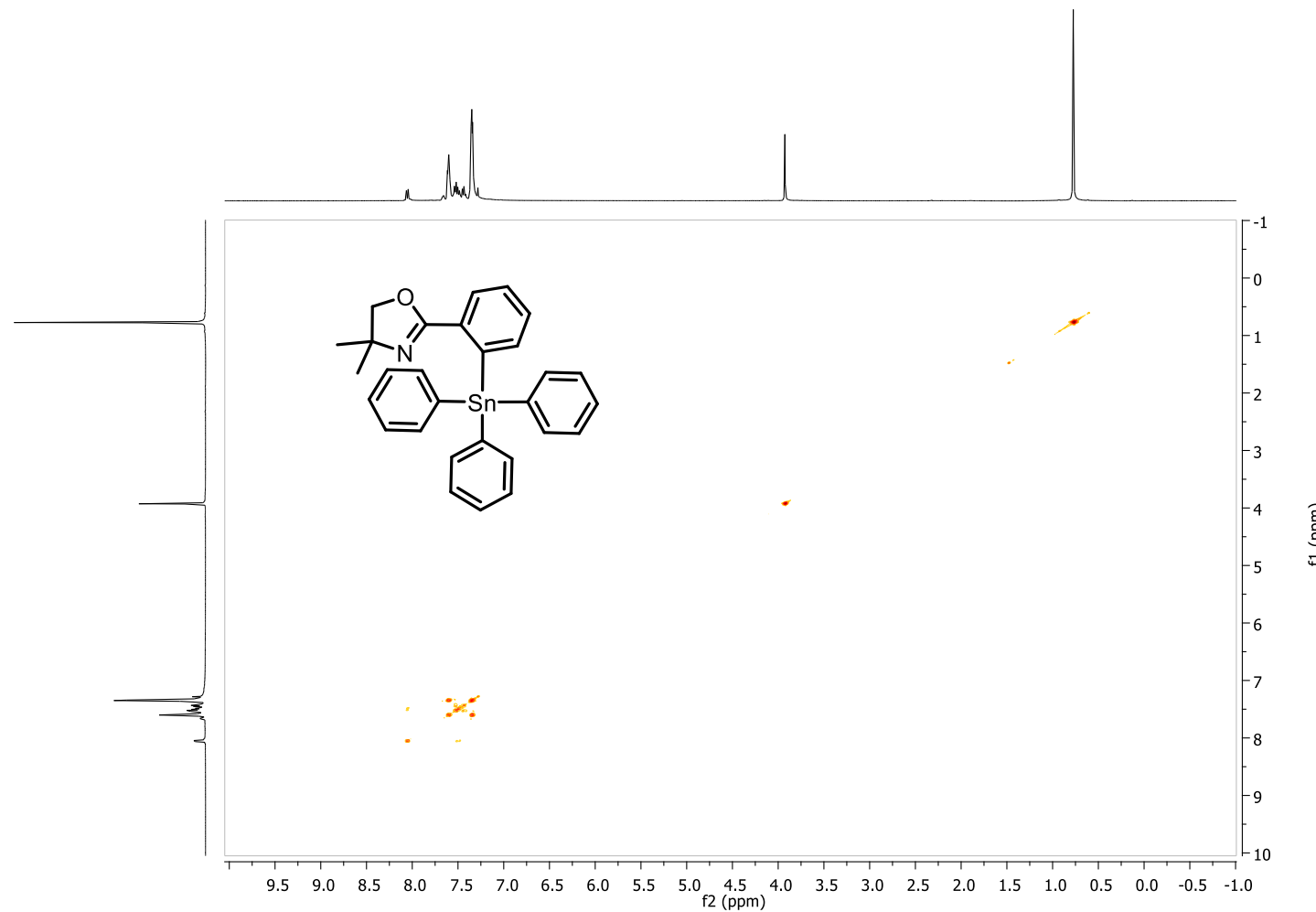


Figure A10: COSY spectrum **10** in CDCl_3 .

176

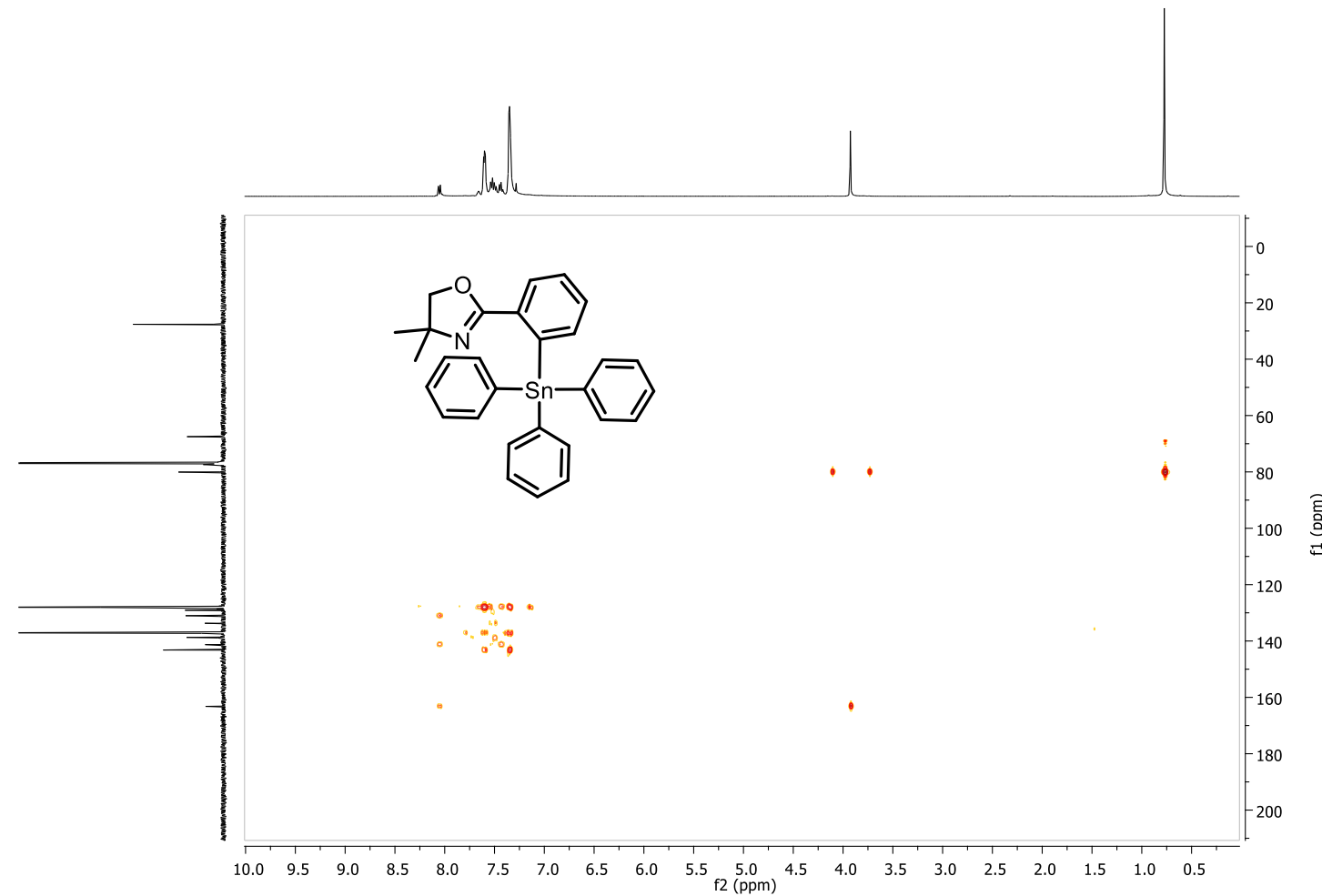


Figure A11: HMBC spectrum of **10** in CDCl_3 .

177

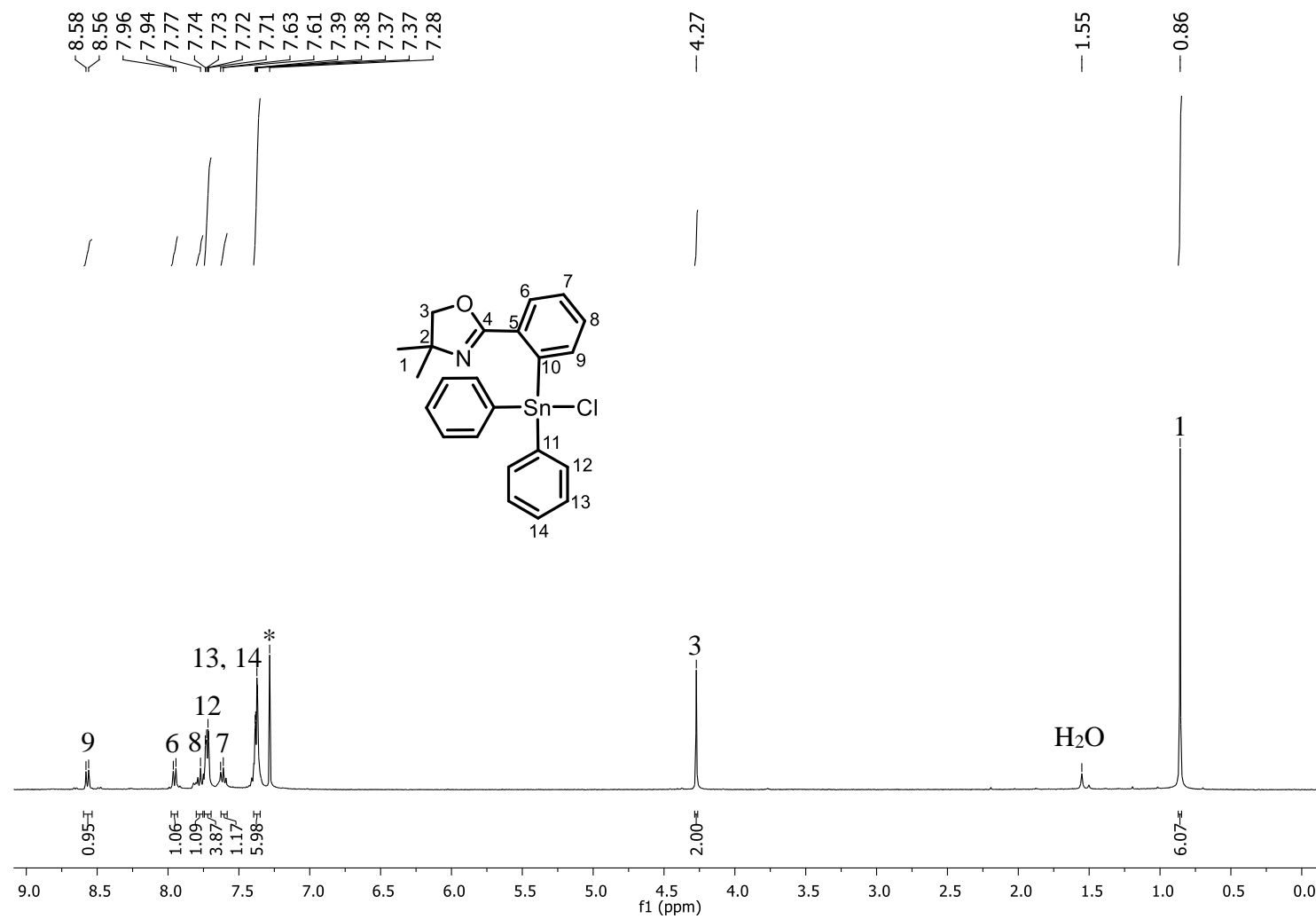


Figure A12: ^1H NMR spectrum of **11** in CDCl_3 .

178

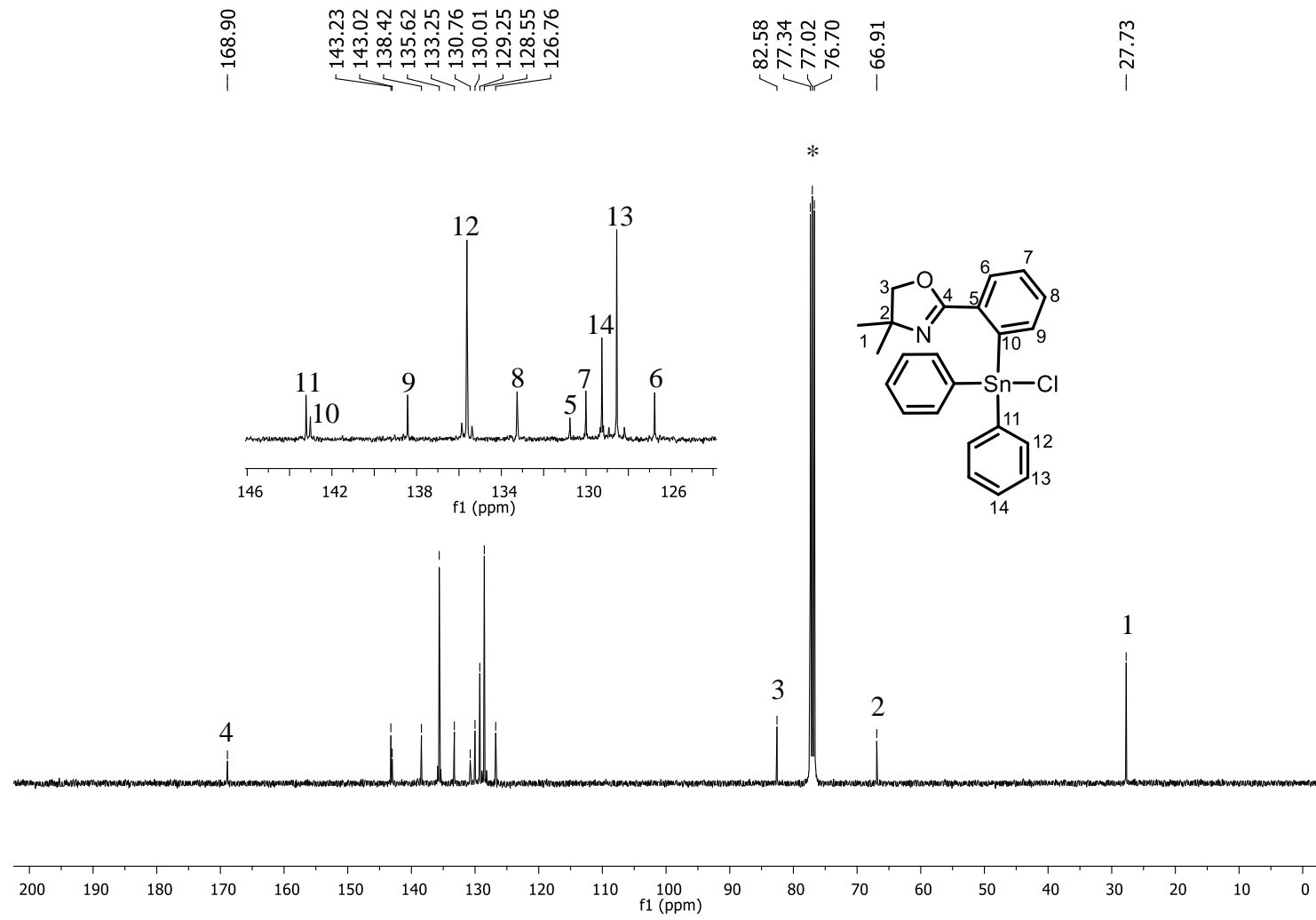


Figure A13: ^{13}C NMR spectrum of **11** in CDCl_3^* .

179

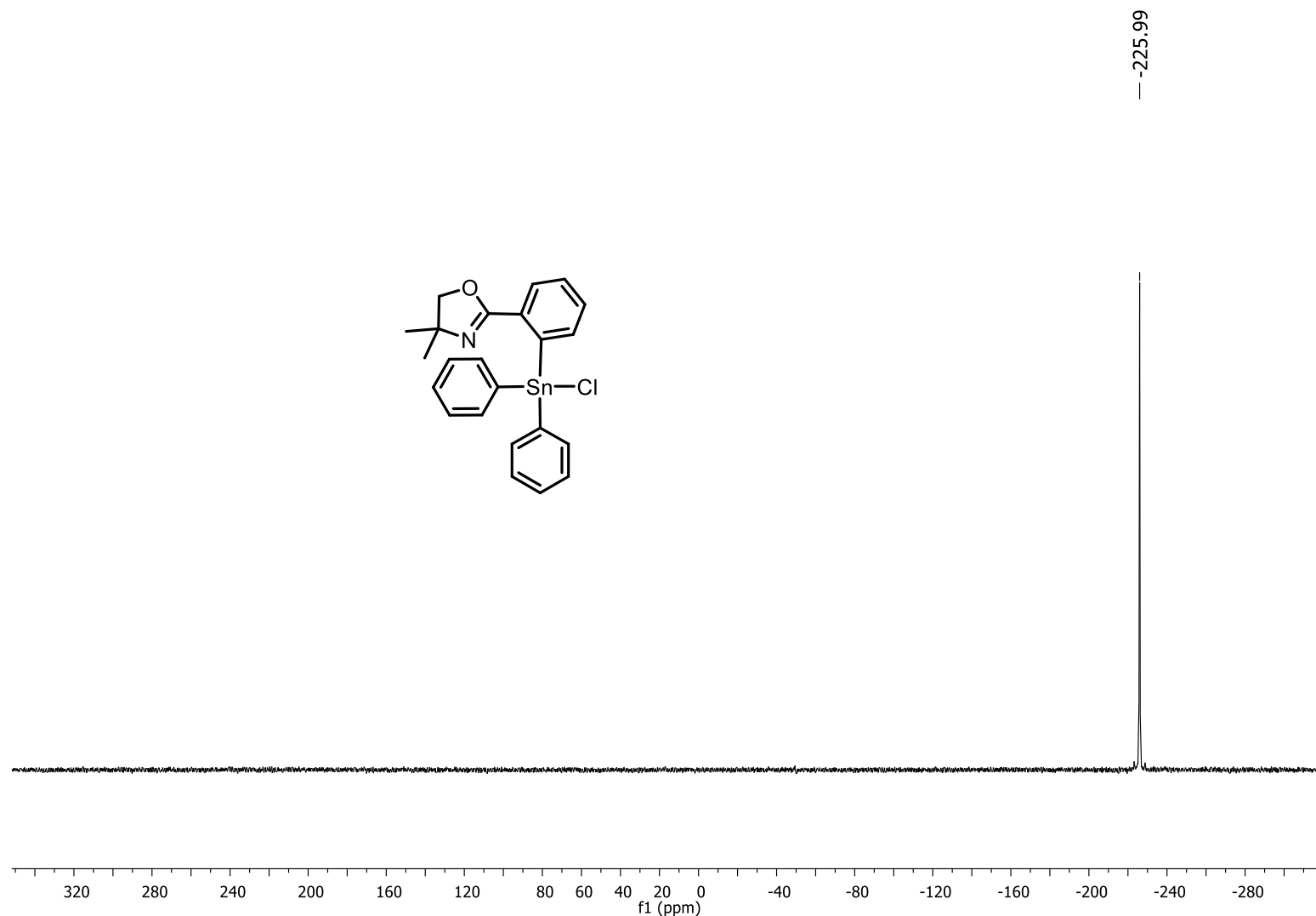


Figure A14: ^{119}Sn NMR spectrum of **11** in CDCl_3 .

180

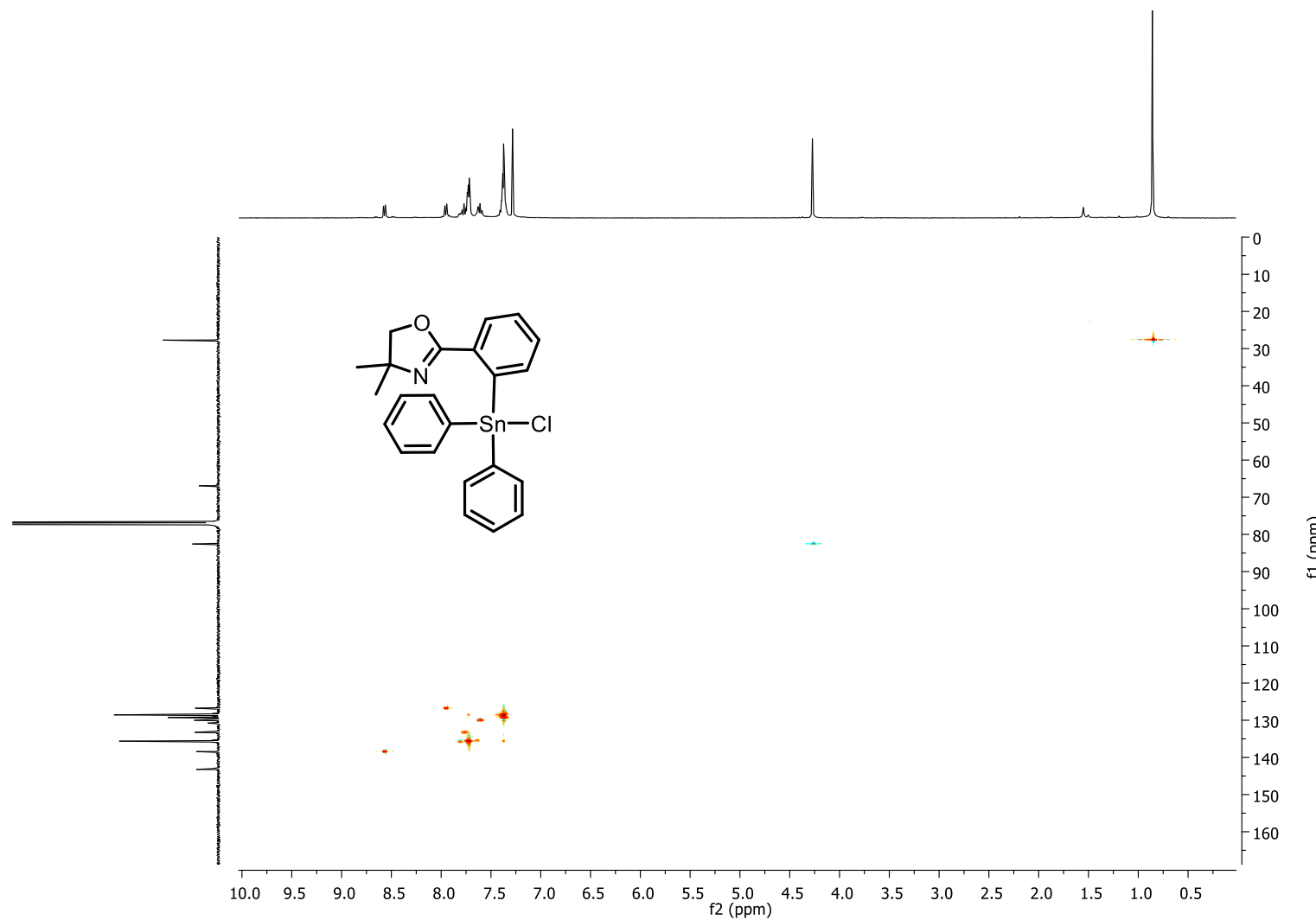


Figure A15: HSQC spectrum of **11** in CDCl_3^* .

181

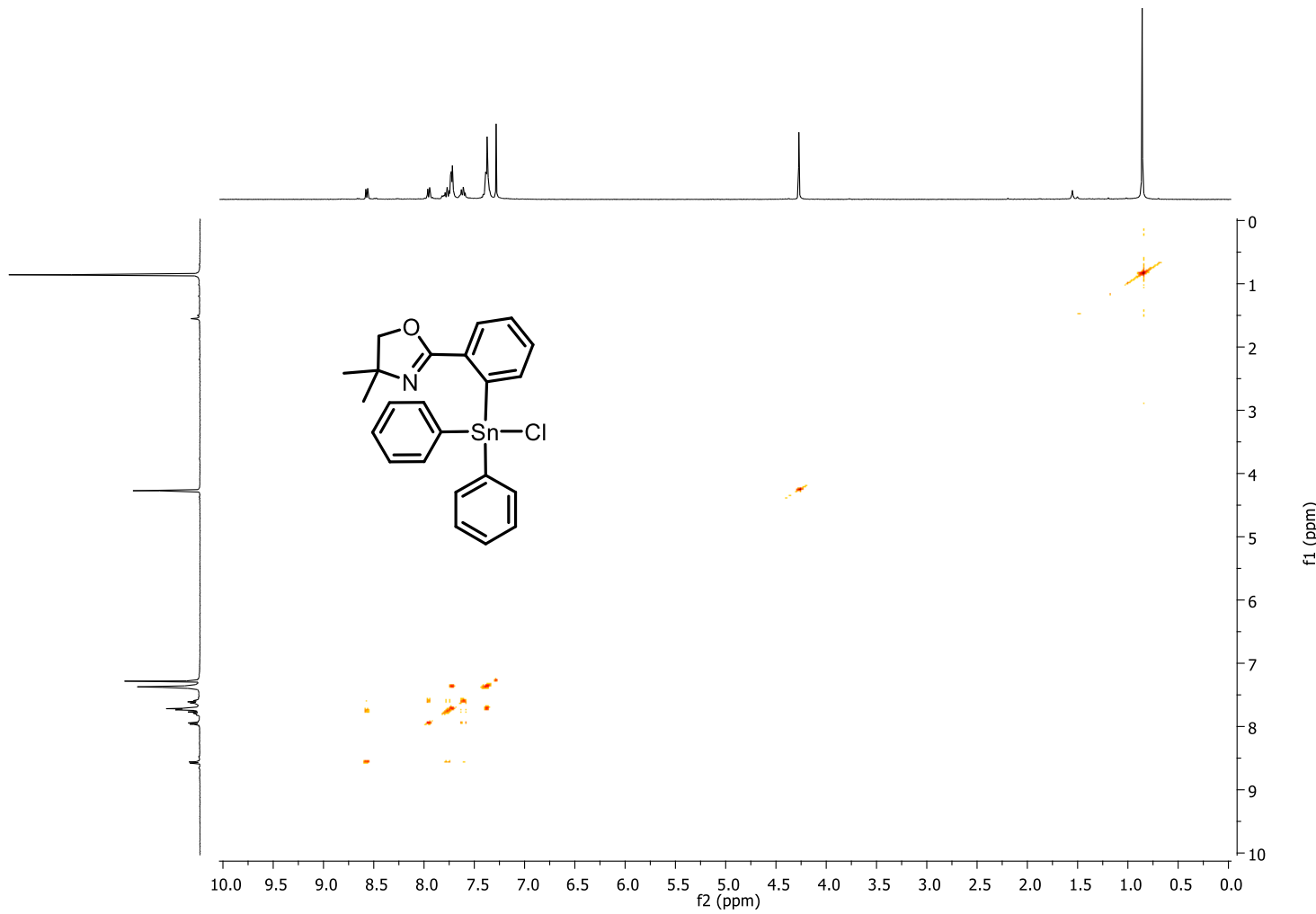


Figure A16: COSY spectrum of **11** in CDCl_3^* .

182

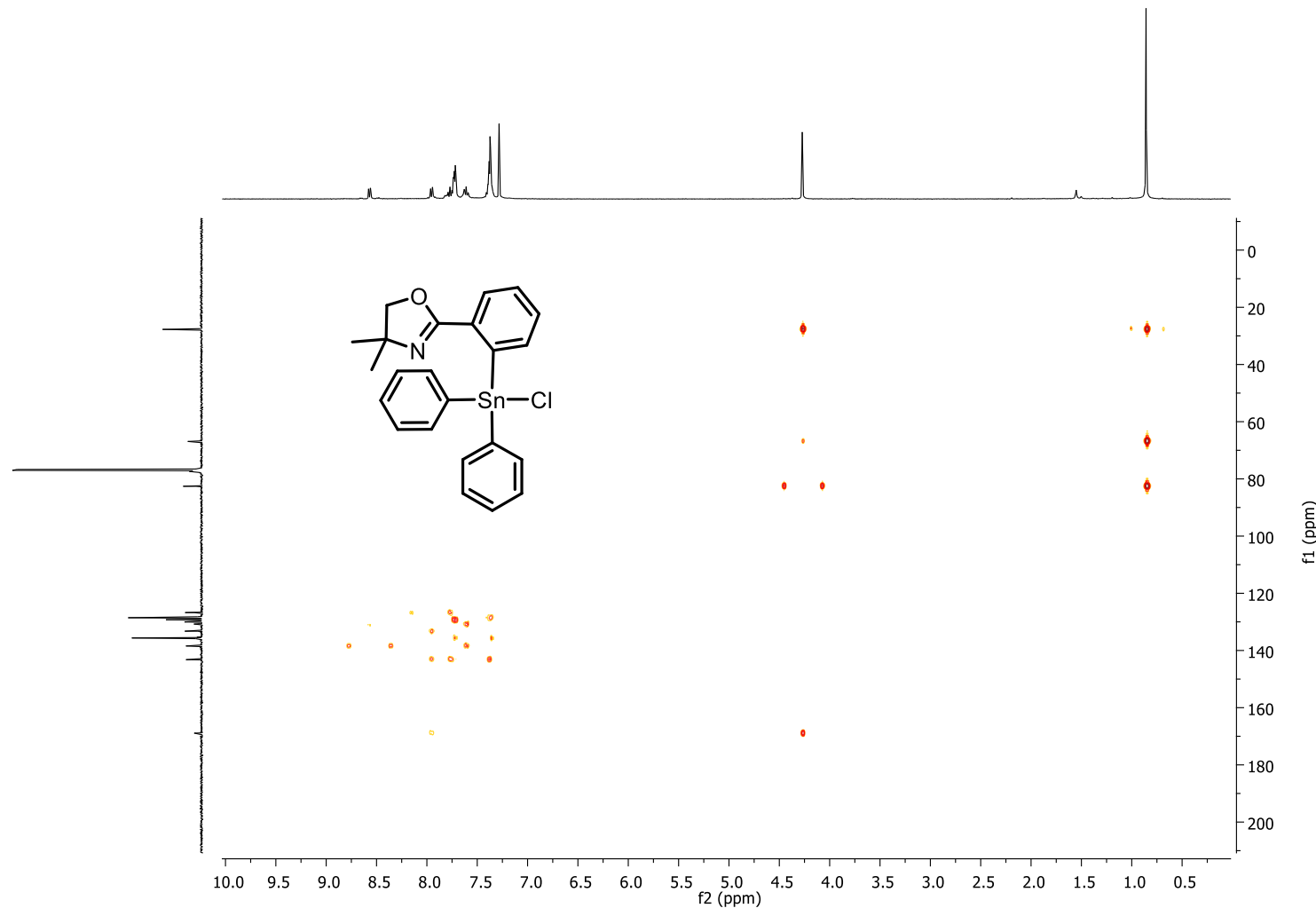


Figure A17: HMBC spectrum of **11** in CDCl_3^* .

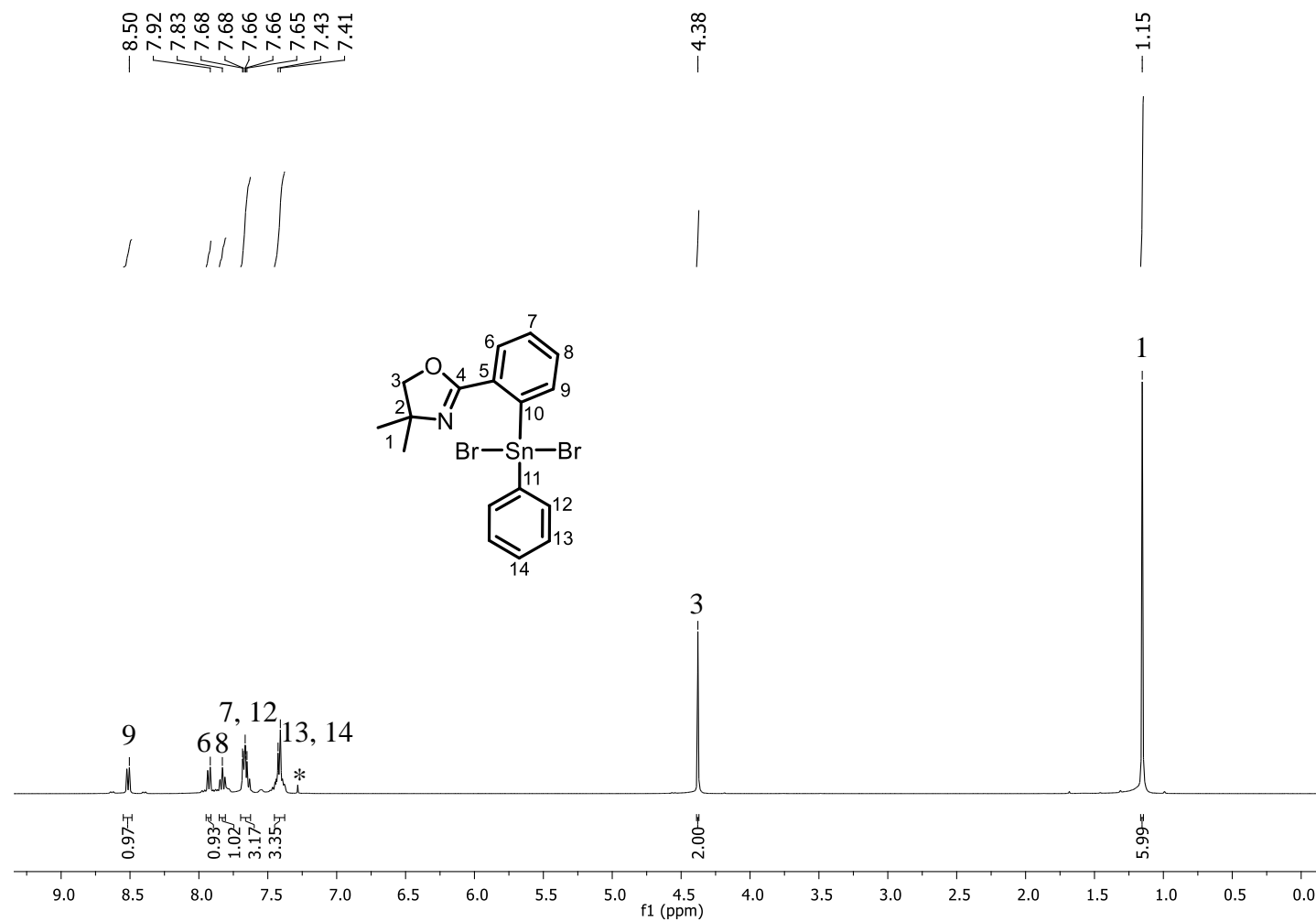


Figure A18: ^1H NMR spectrum of **13** in CDCl_3^* .

184

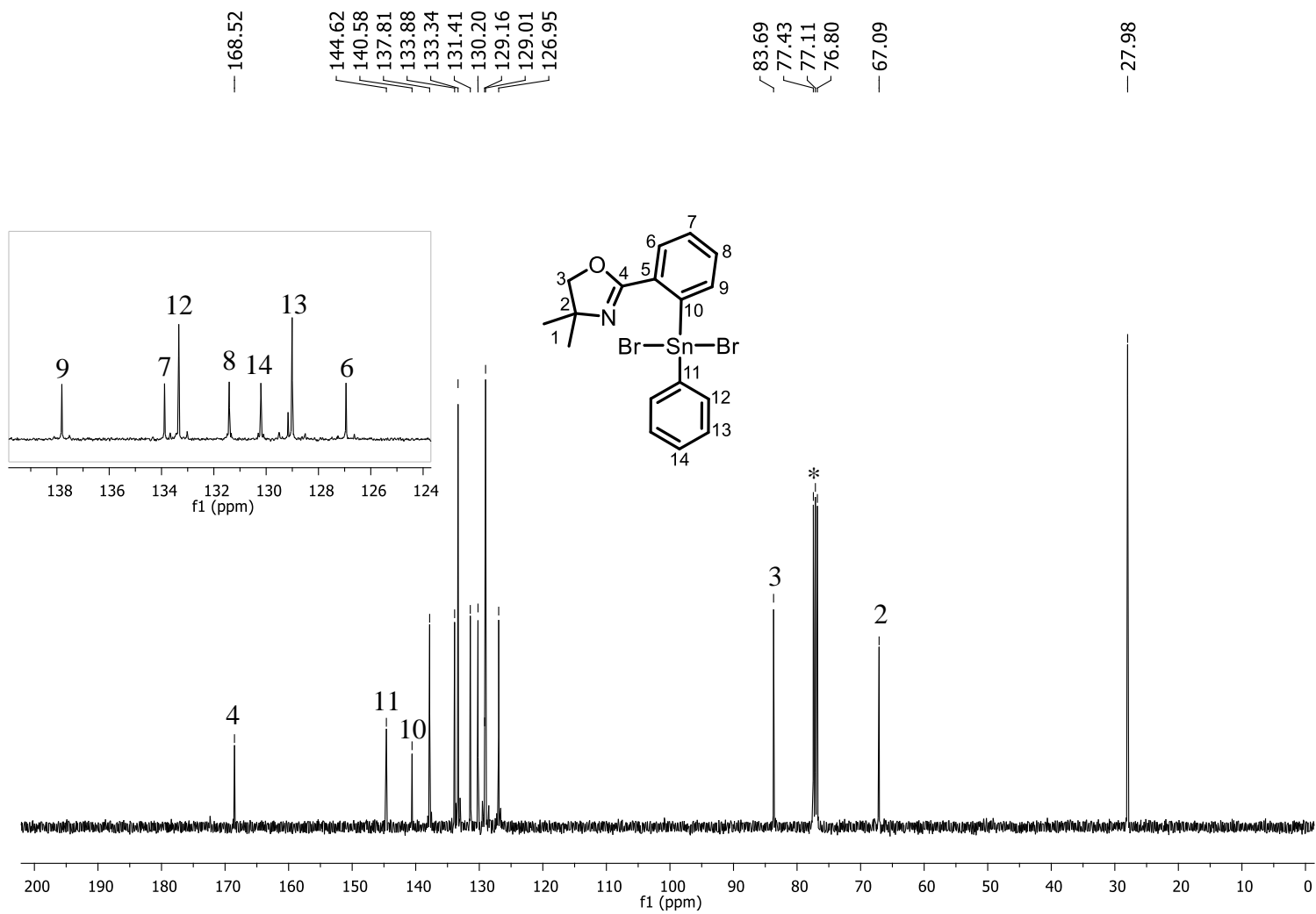


Figure A19: ^{13}C NMR spectrum of **13** in CDCl_3^* .

185

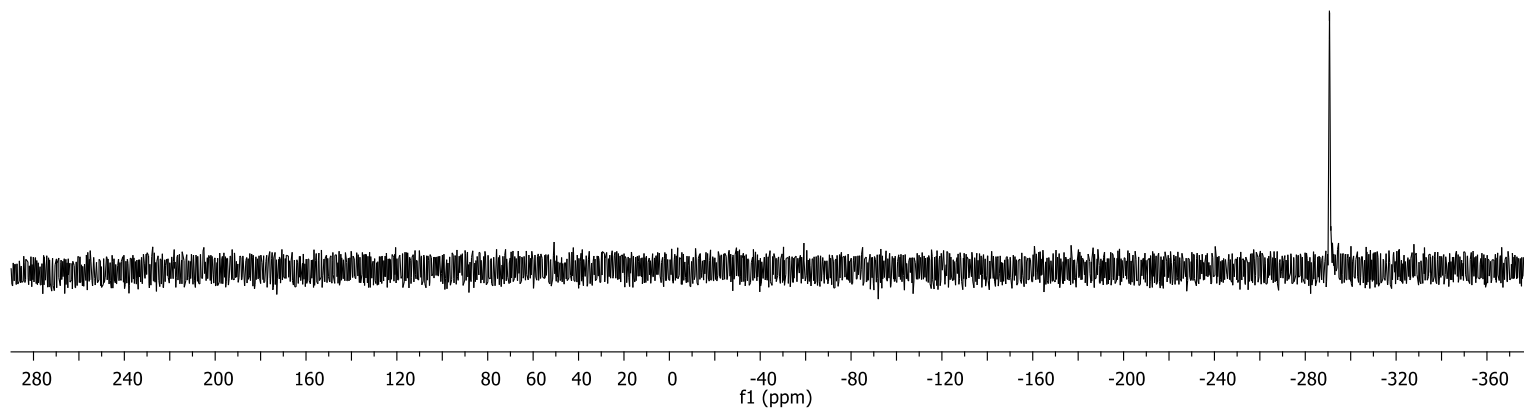
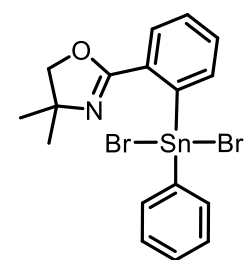


Figure A20: ¹¹⁹Sn NMR spectrum of **13** in CDCl₃*.

186

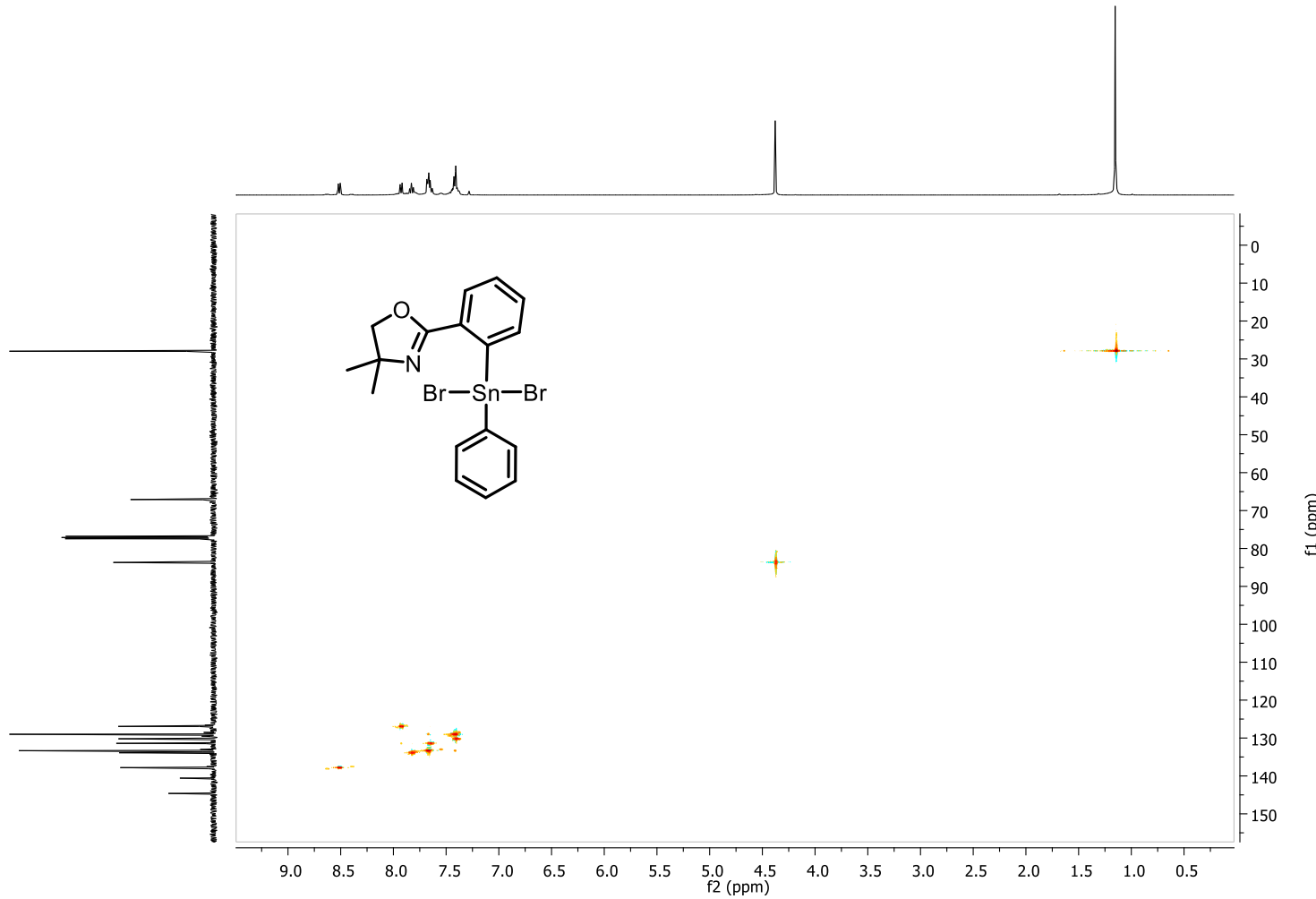


Figure A21: HSQC spectrum of **13** in CDCl_3^* .

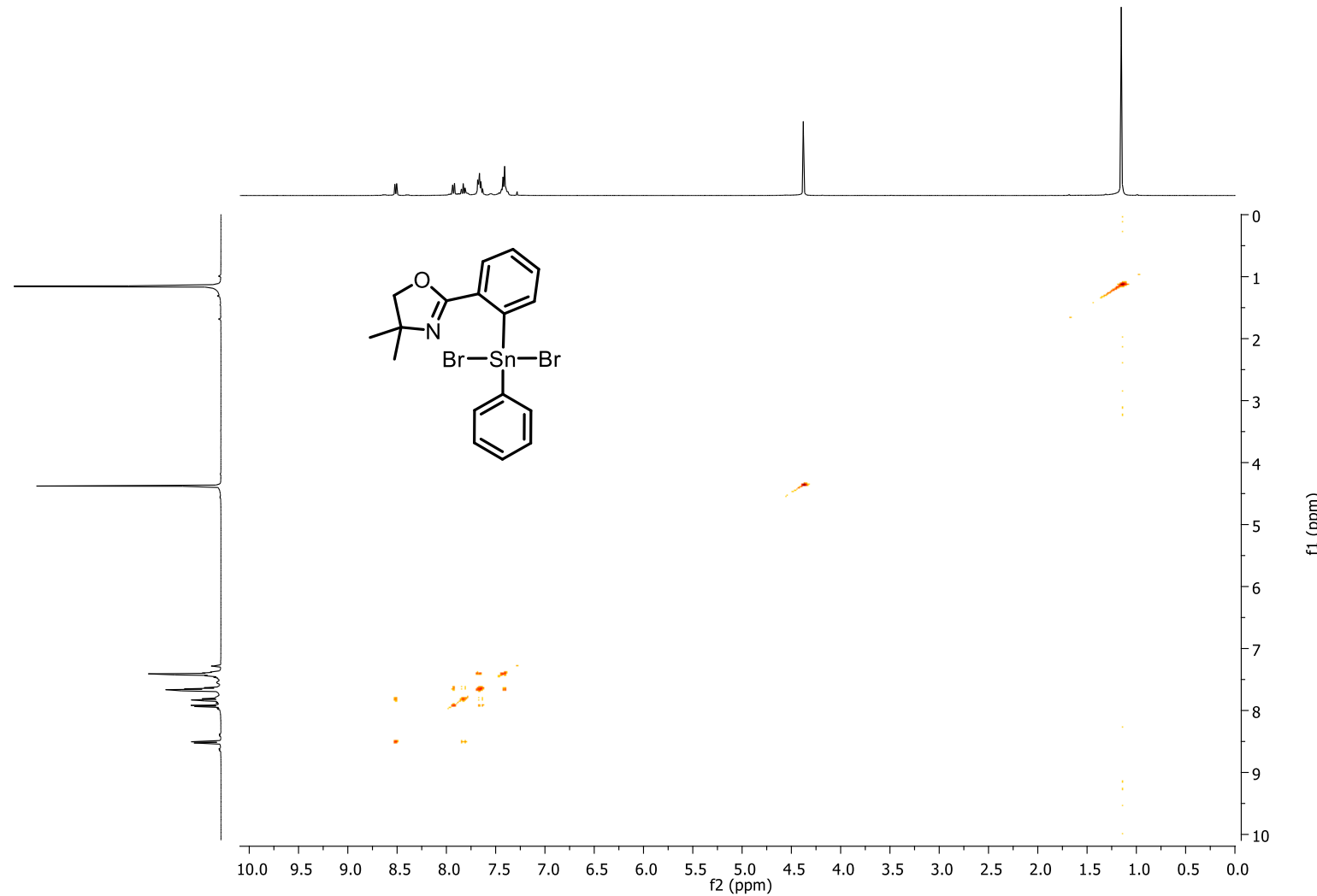


Figure A22: COSY spectrum of **13** in CDCl_3^* .

188



Figure A23: HMBC spectrum of **13** in CDCl_3^* .

189

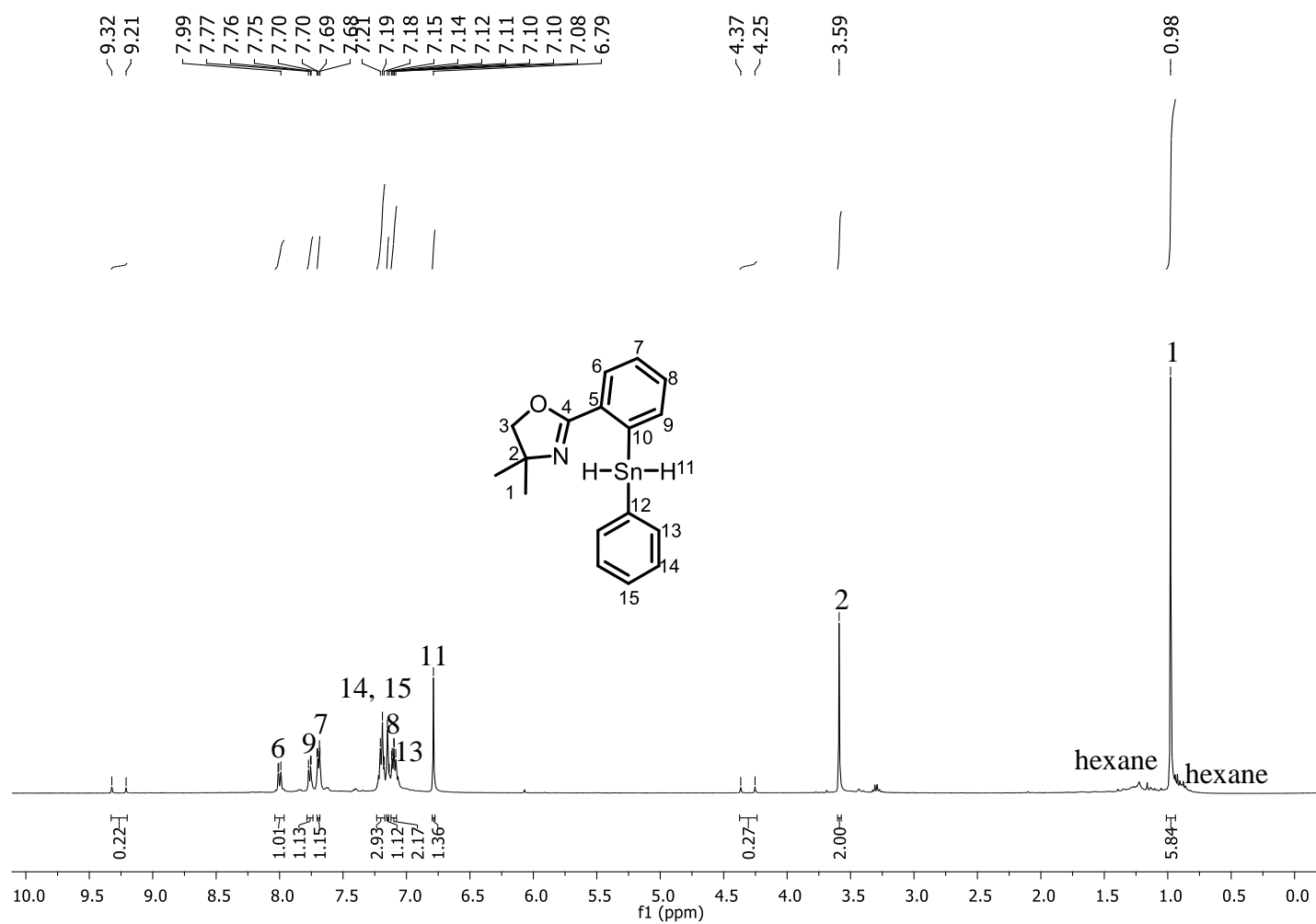


Figure A24: ¹H NMR spectrum of **14** in CDCl_3^* .

190

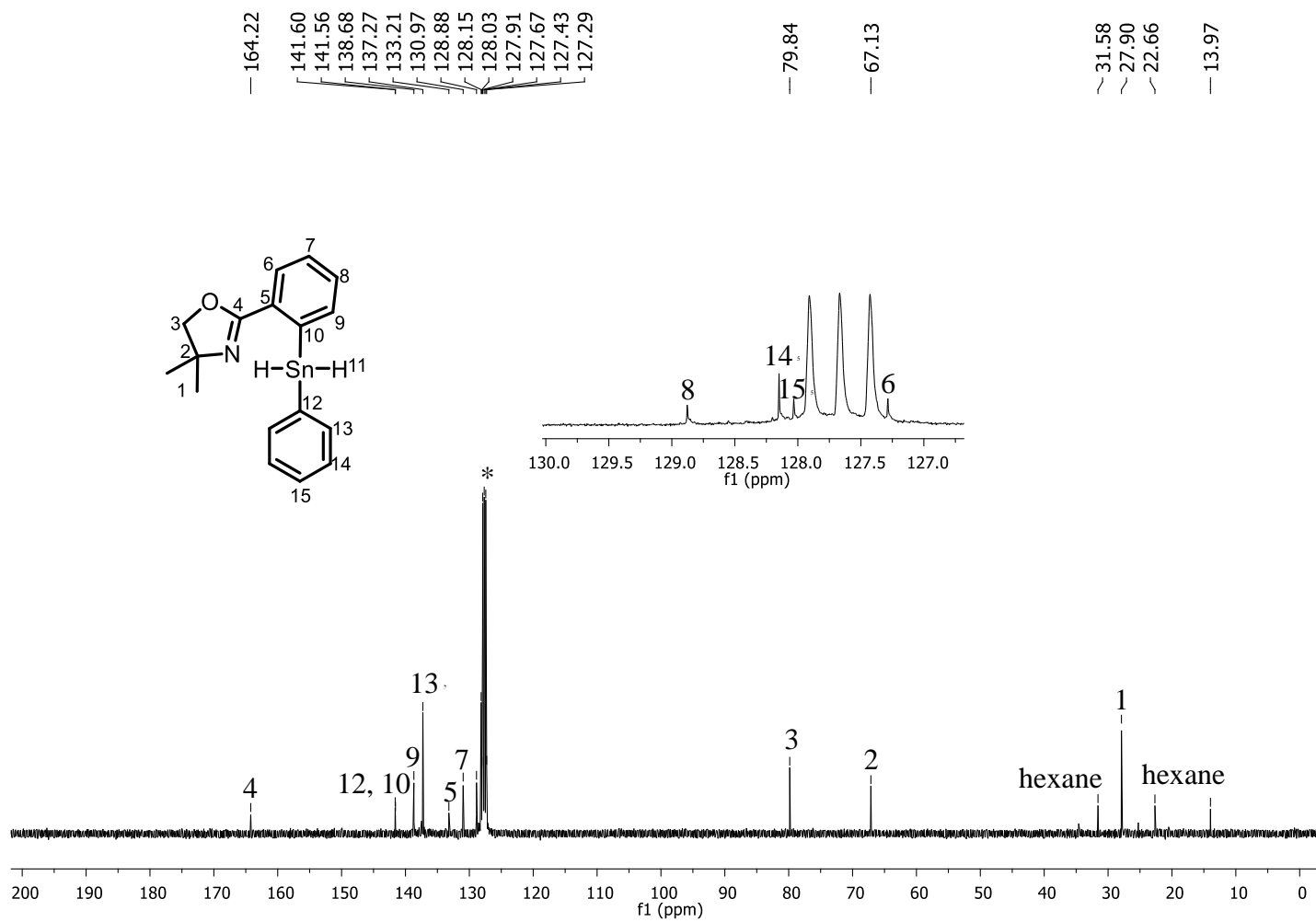


Figure A25: ^{13}C NMR spectrum of **14** in CDCl_3^* .

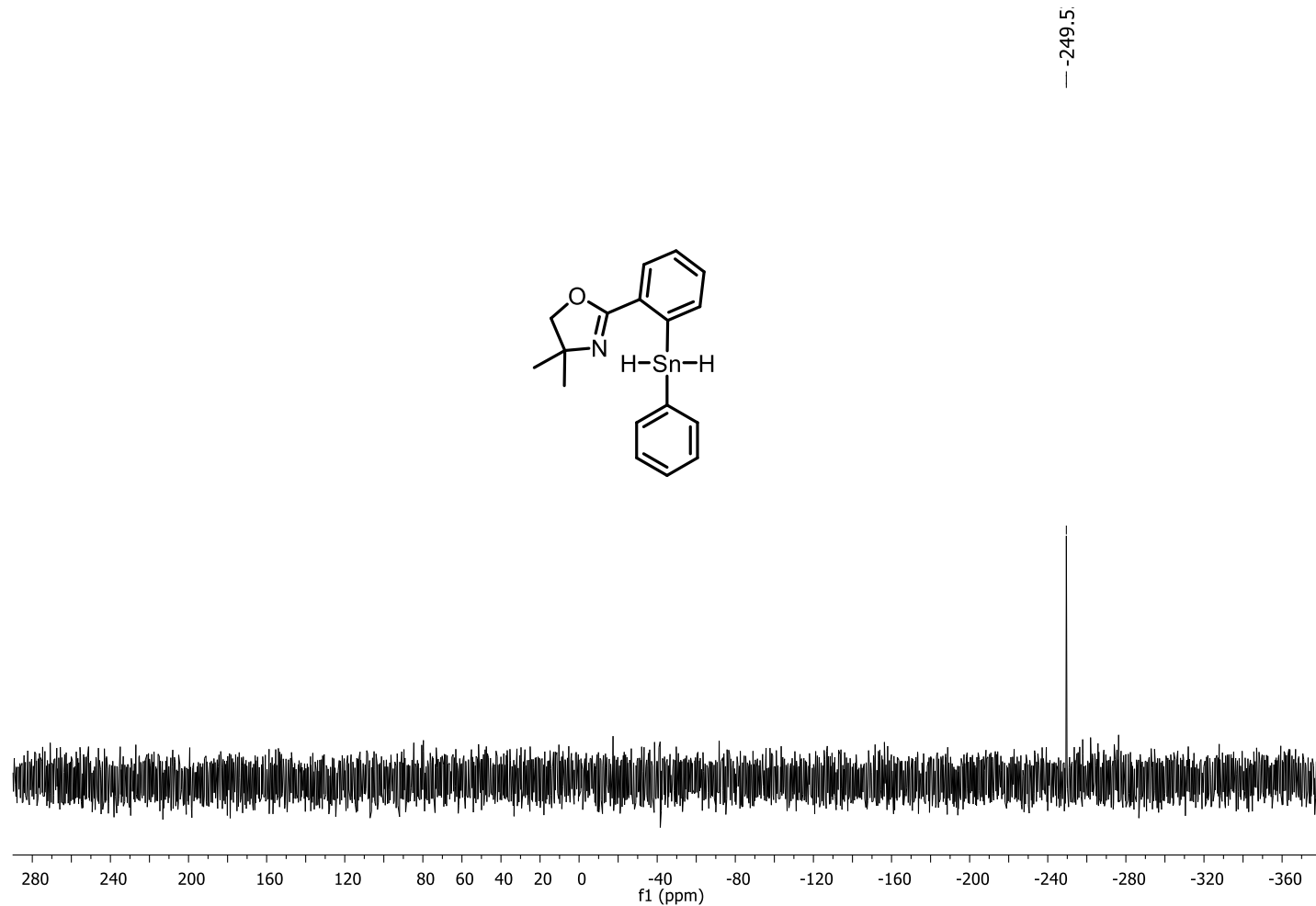


Figure A26: ^{119}Sn NMR spectrum of **14** in CDCl_3^* .

192

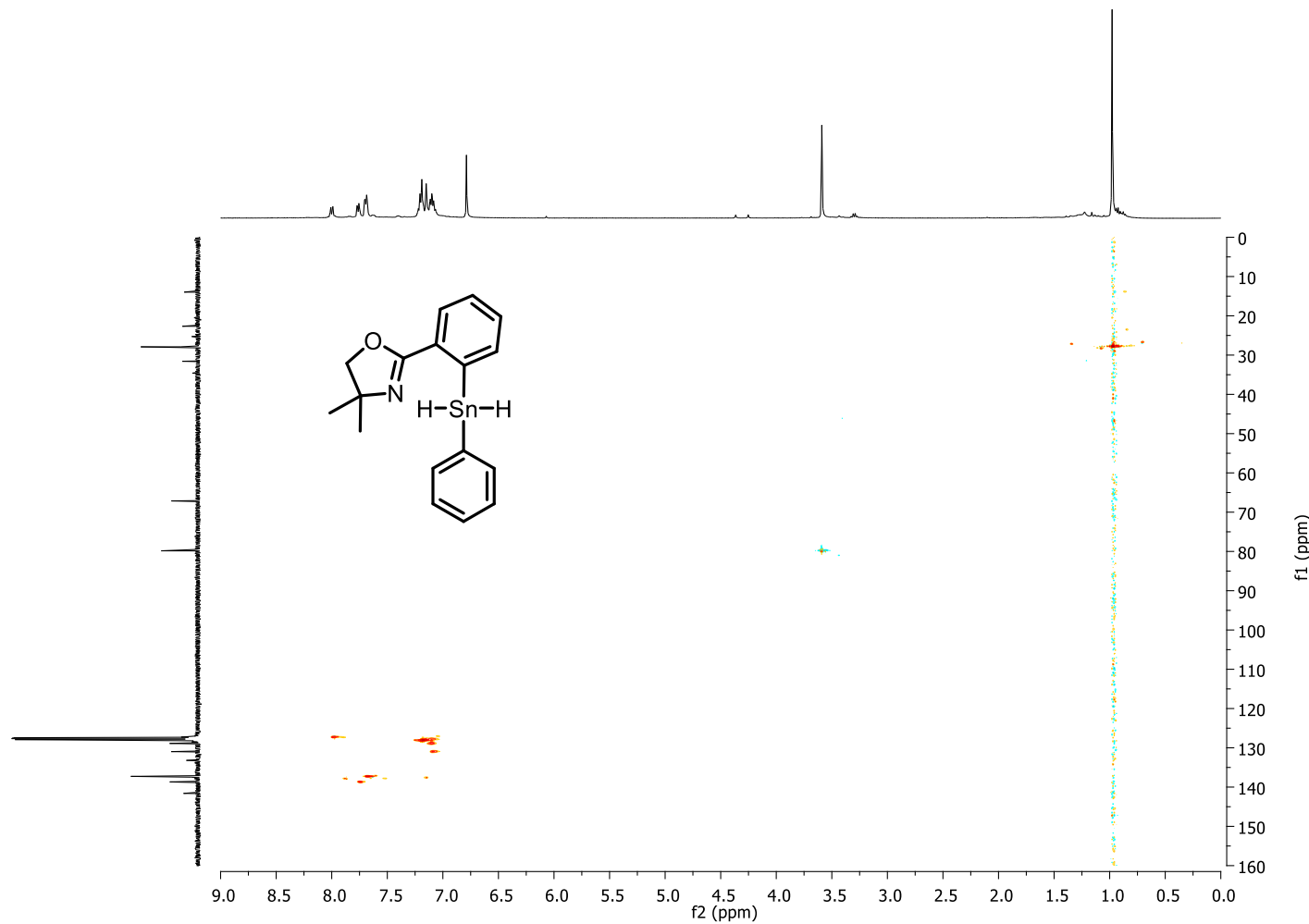


Figure A27: HSQC spectrum of **14** in C_6D_6 .

193

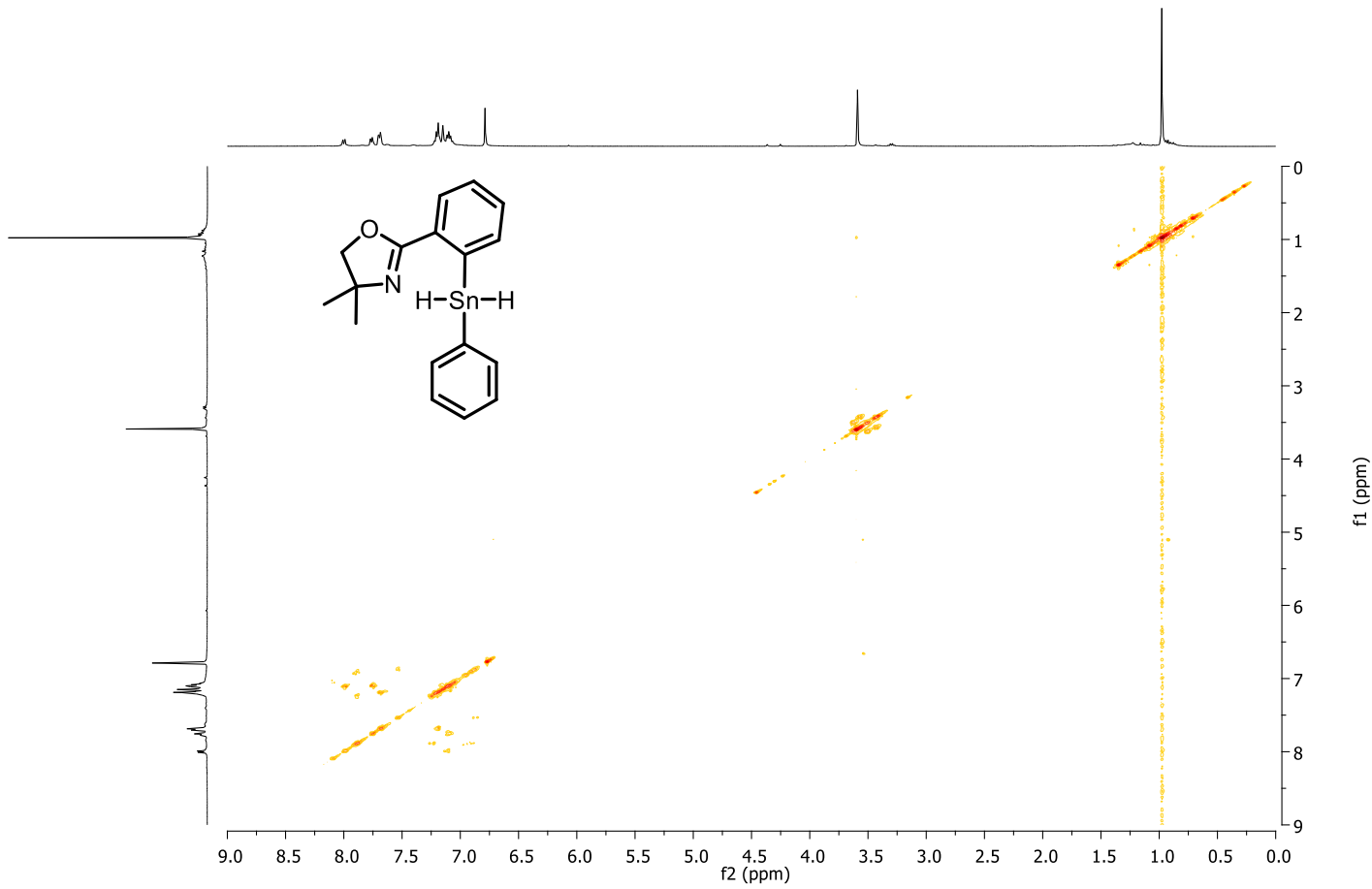


Figure A28: COSY spectrum of **14** in C_6D_6 .

194

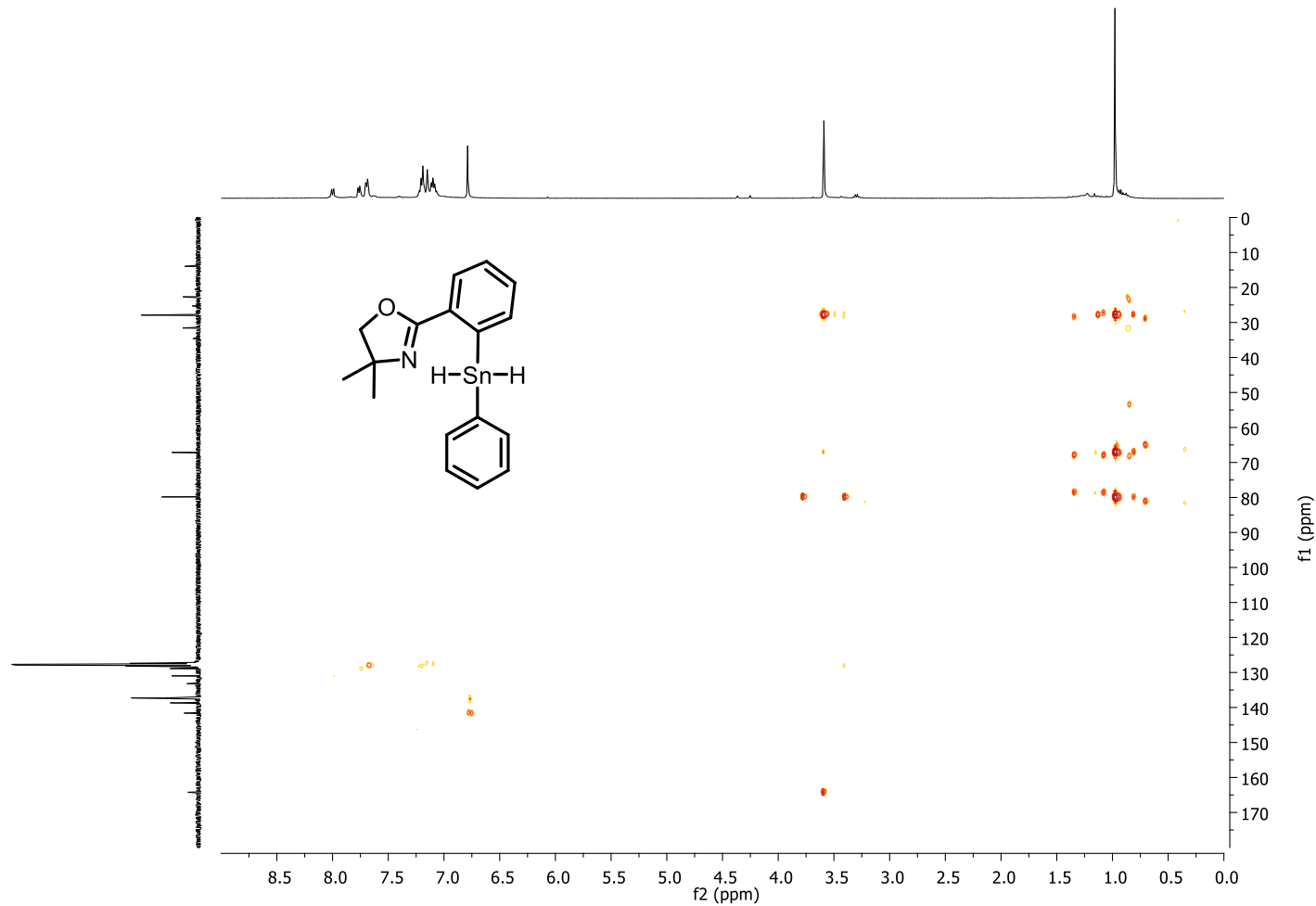


Figure A29: HMBC spectrum of **14** in C_6D_6 .

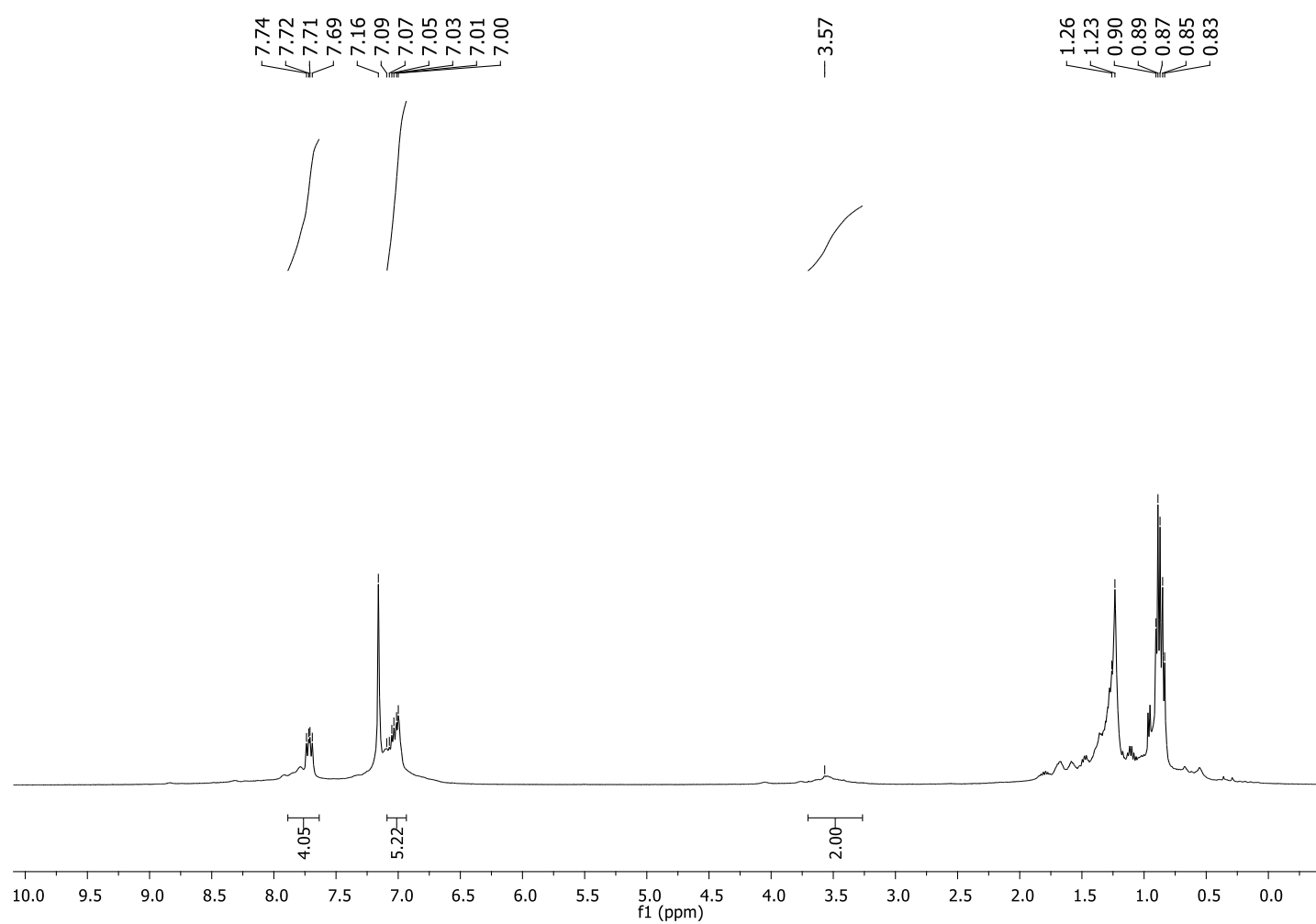


Figure A30: ^1H NMR spectrum of **16** in C_6D_6^* .

196

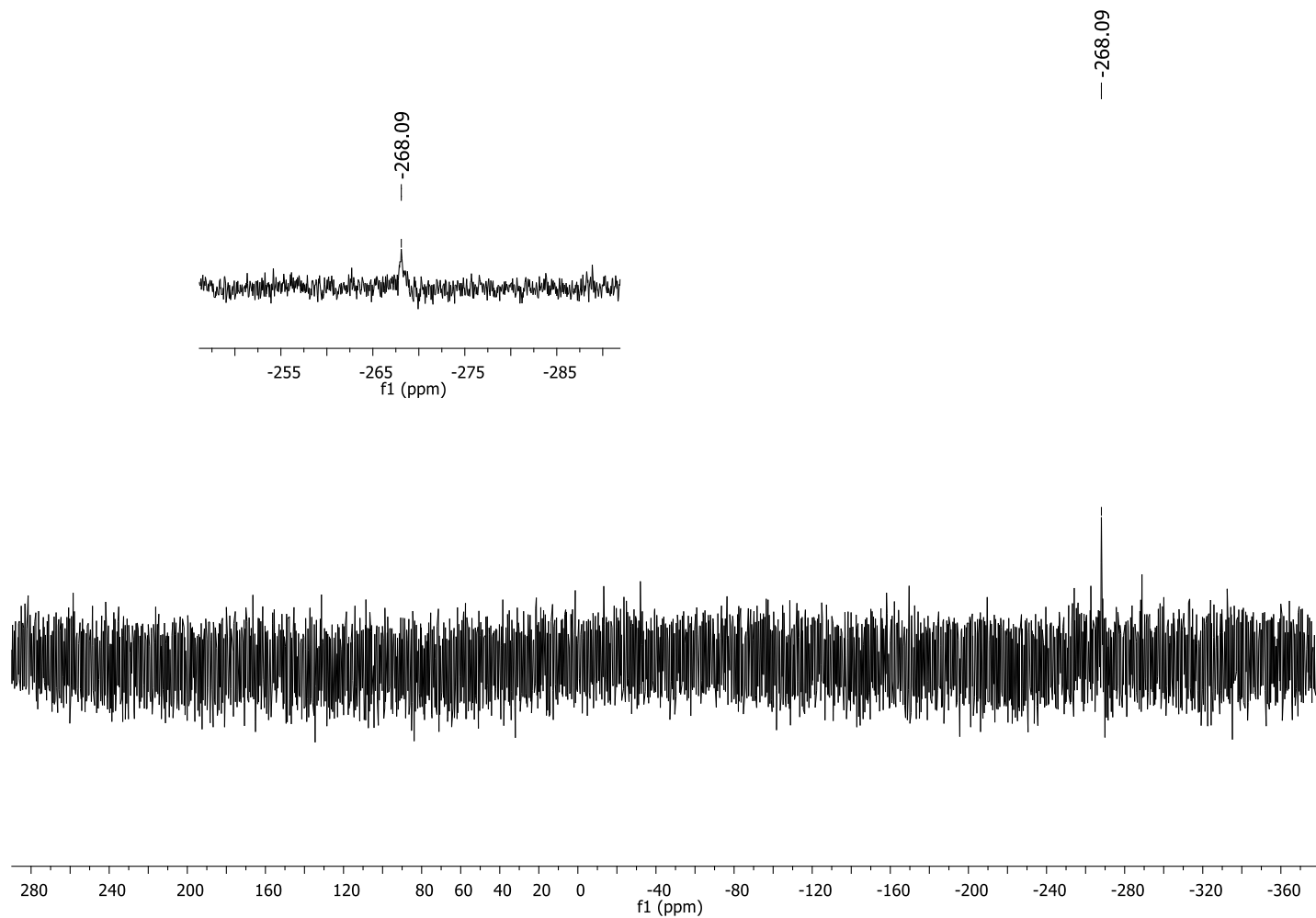


Figure A31: ^{119}Sn NMR spectrum of **16** in C_6D_6^* .

197

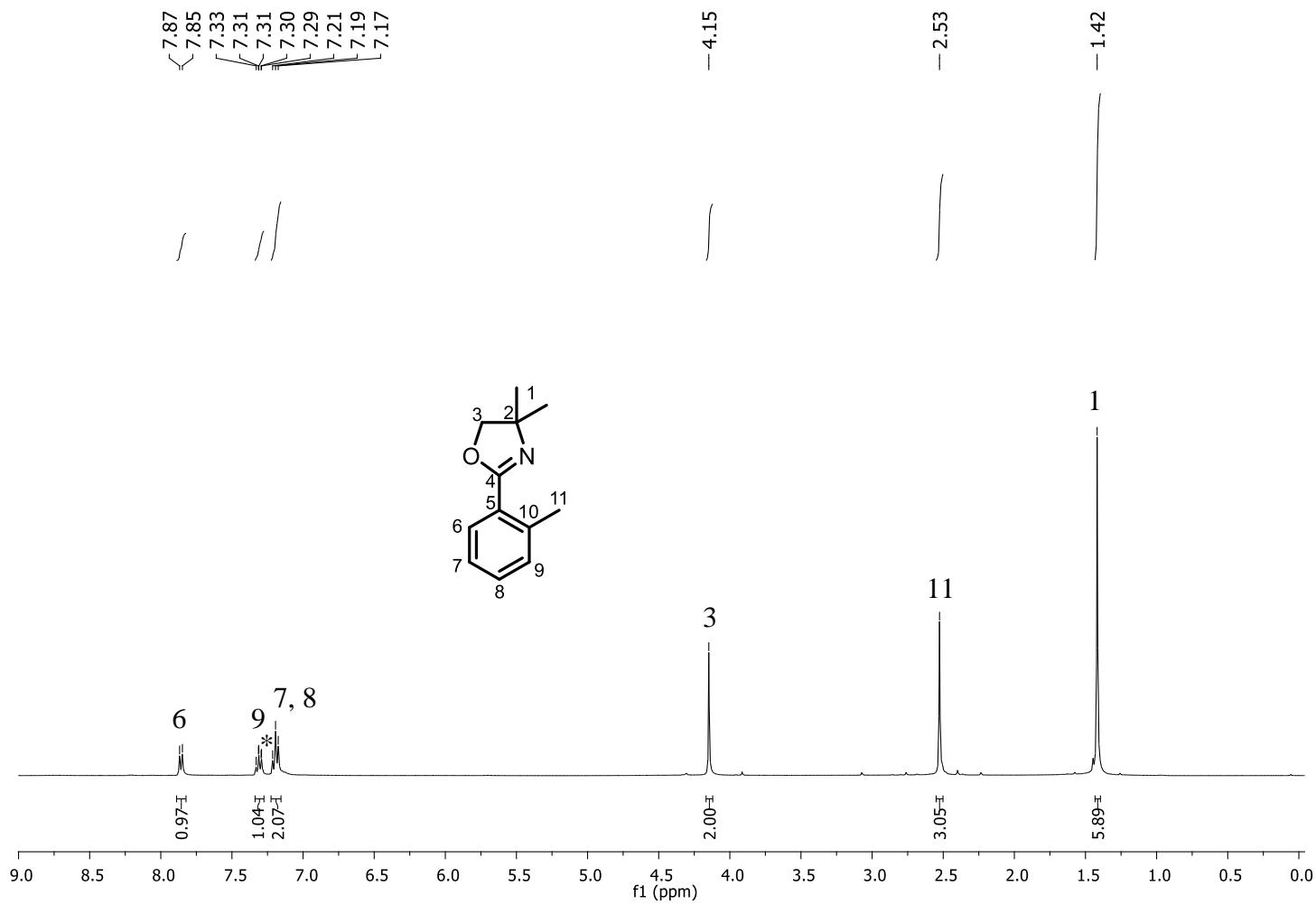


Figure A32: ^1H NMR spectrum of **17** in CDCl_3^* .

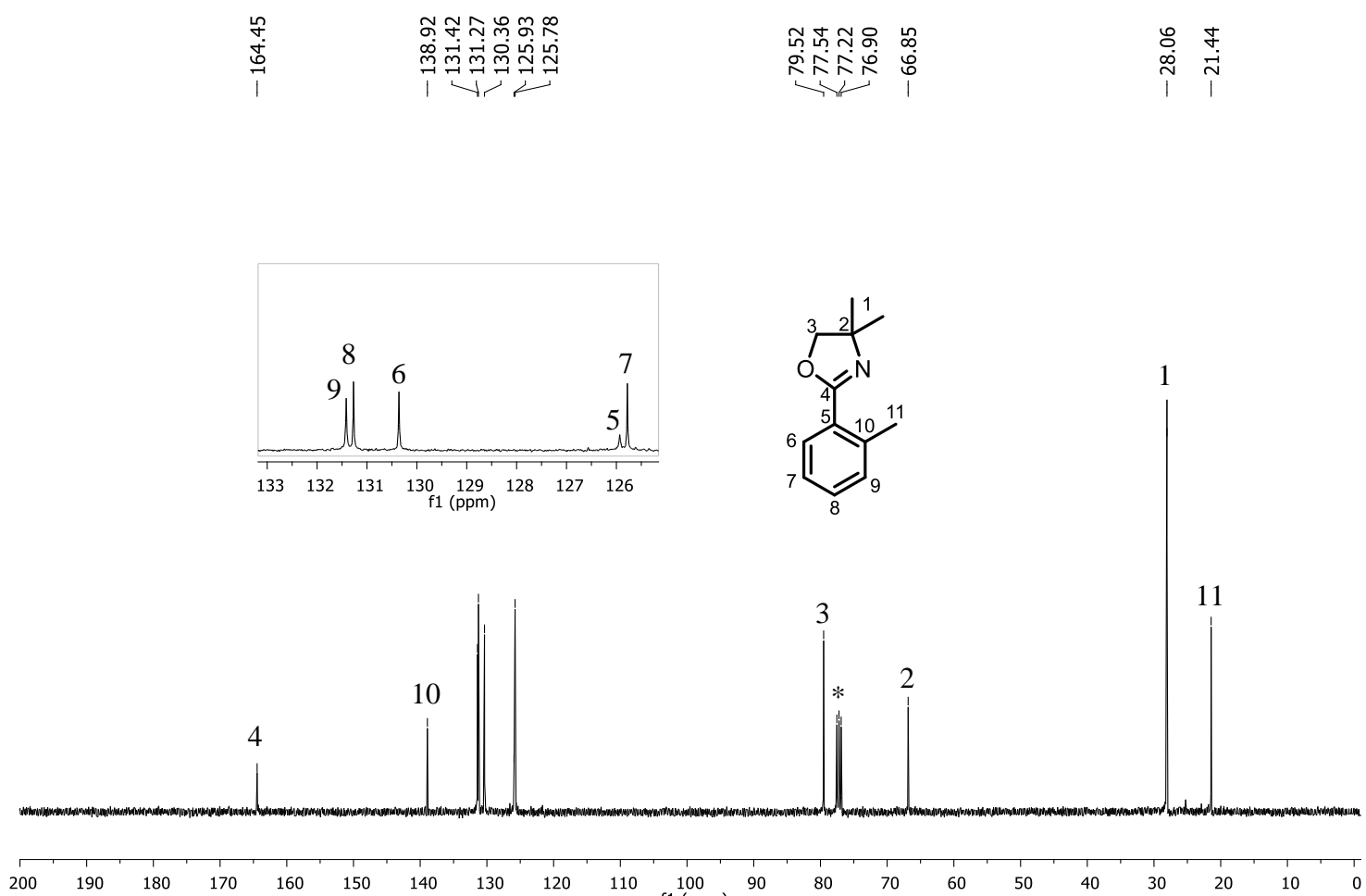


Figure A33: ^{13}C NMR spectrum of **17** in CDCl_3^* .

199

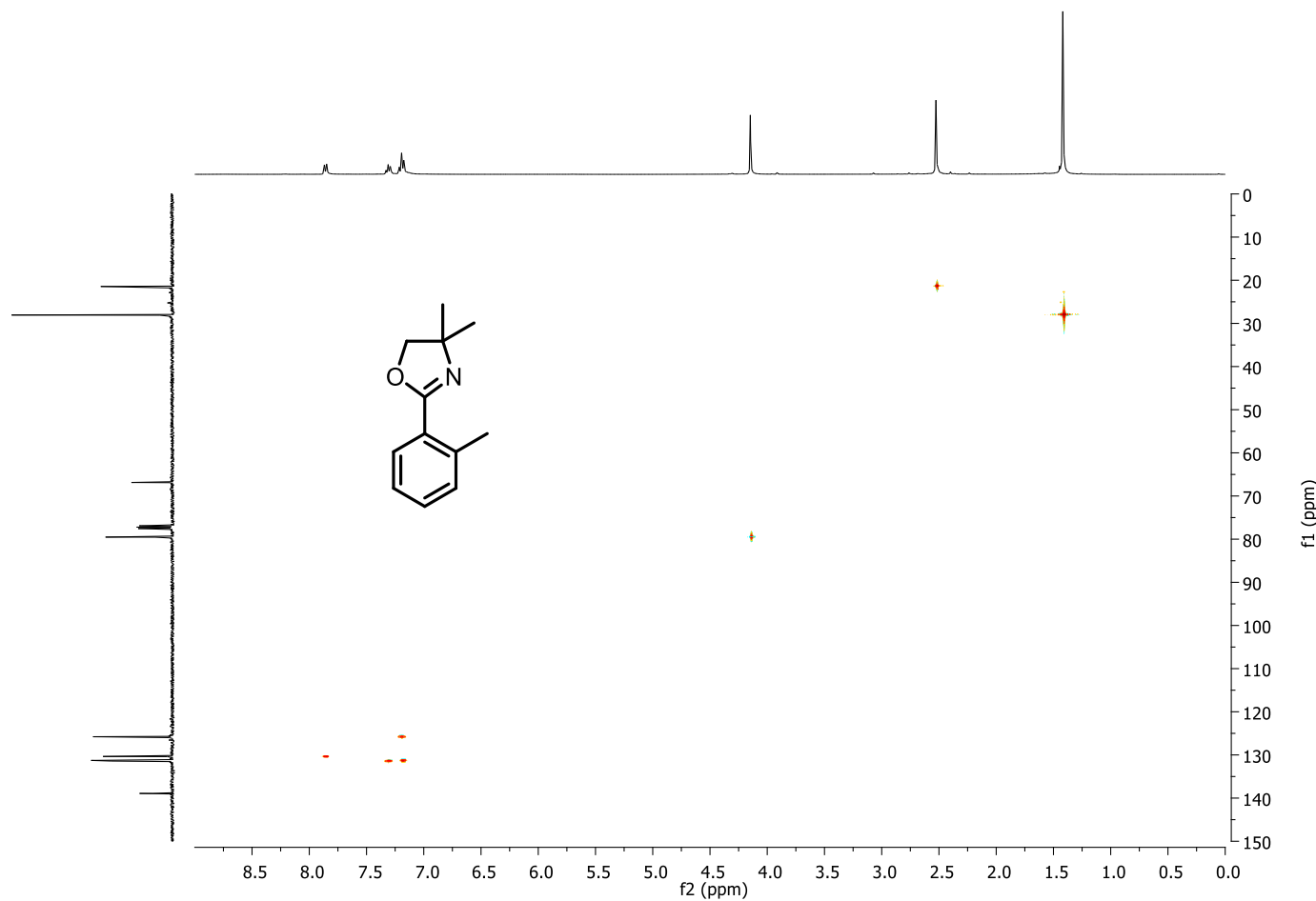


Figure A34: HSQC spectrum of **17** in CDCl_3^* .

200

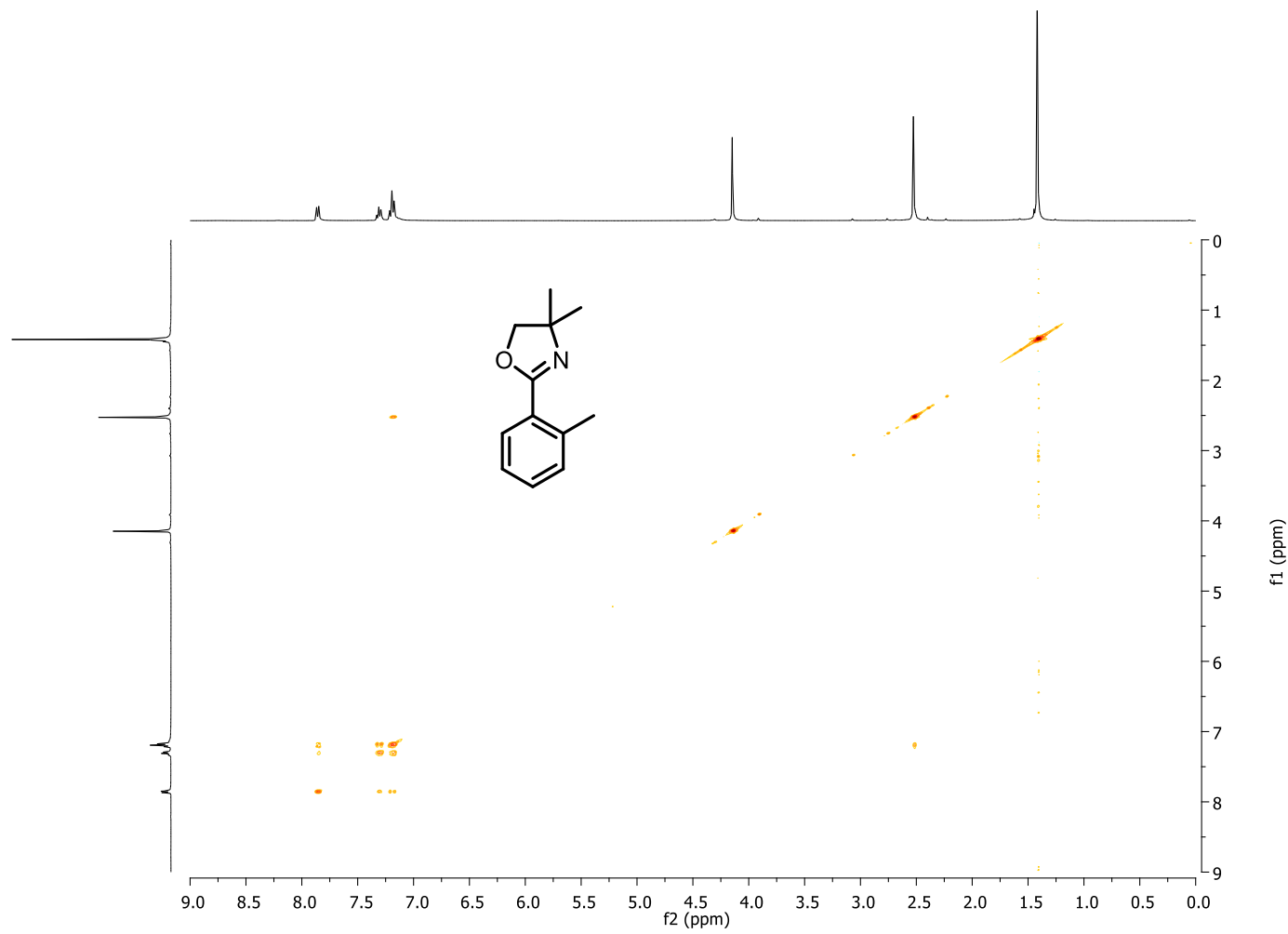


Figure A35: COSY spectrum of **17** in CDCl_3^* .

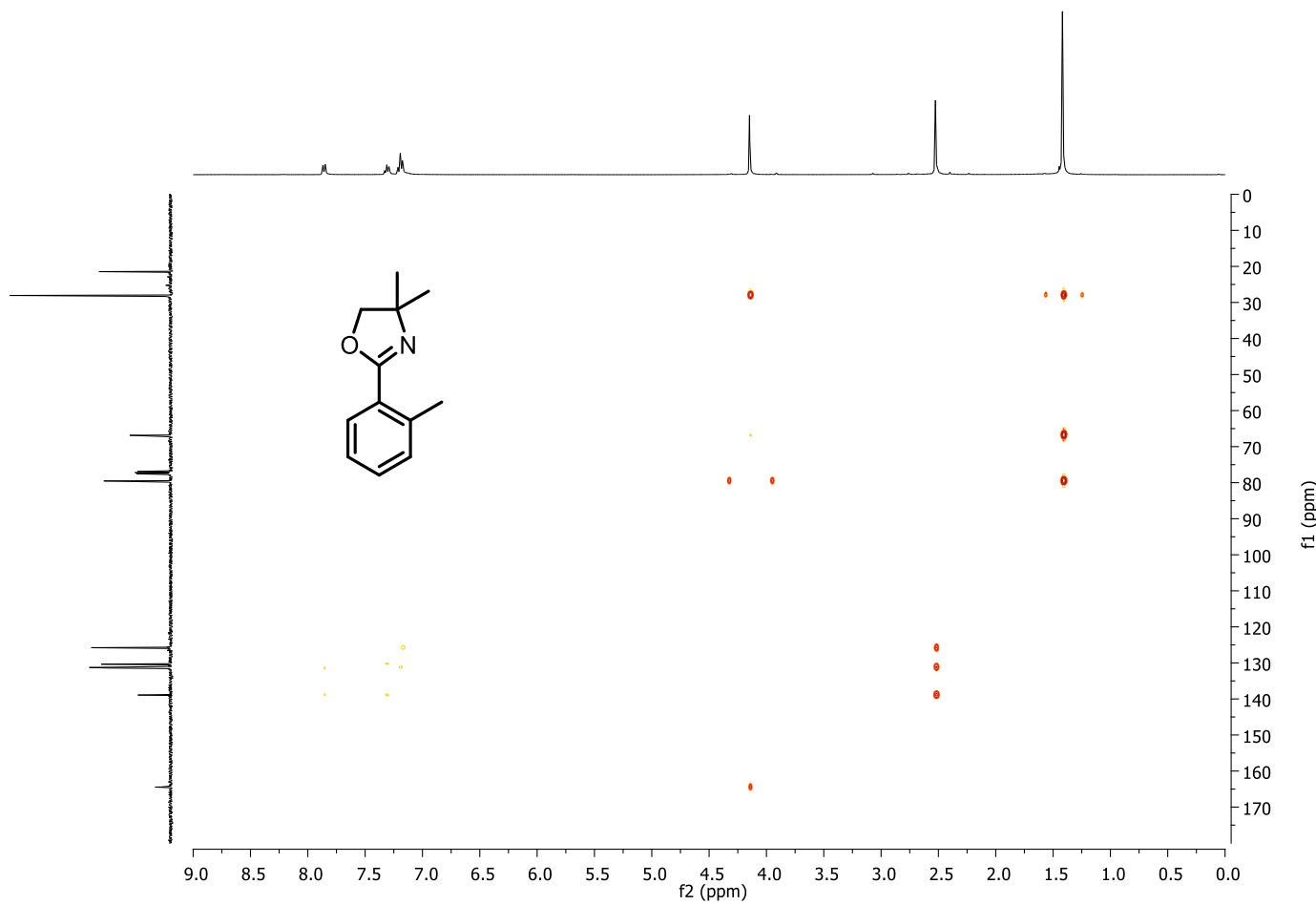


Figure A36: HMBC spectrum of **17** in CDCl_3^* .

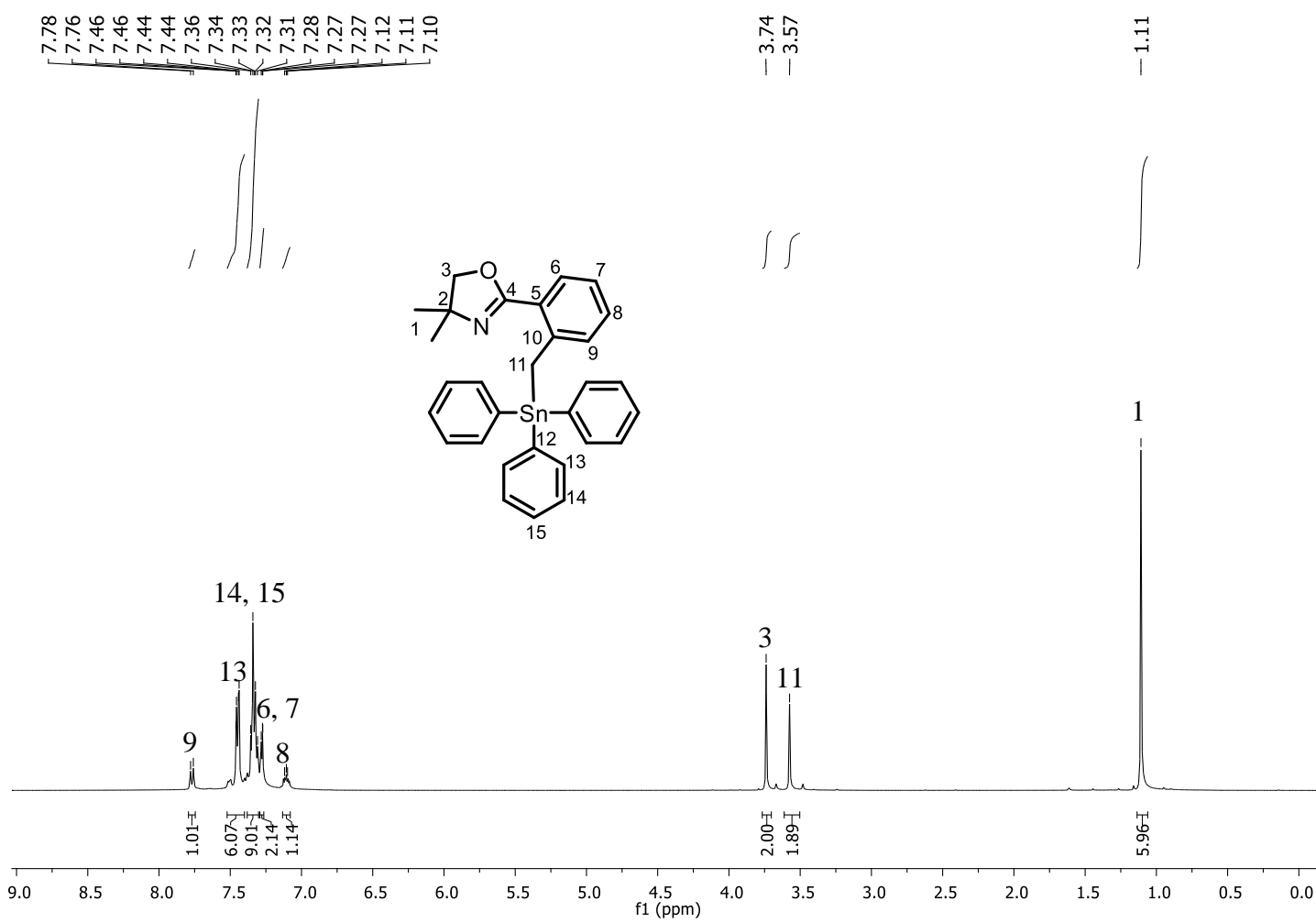


Figure A37: ^1H NMR spectrum of **18** in CDCl_3^* .

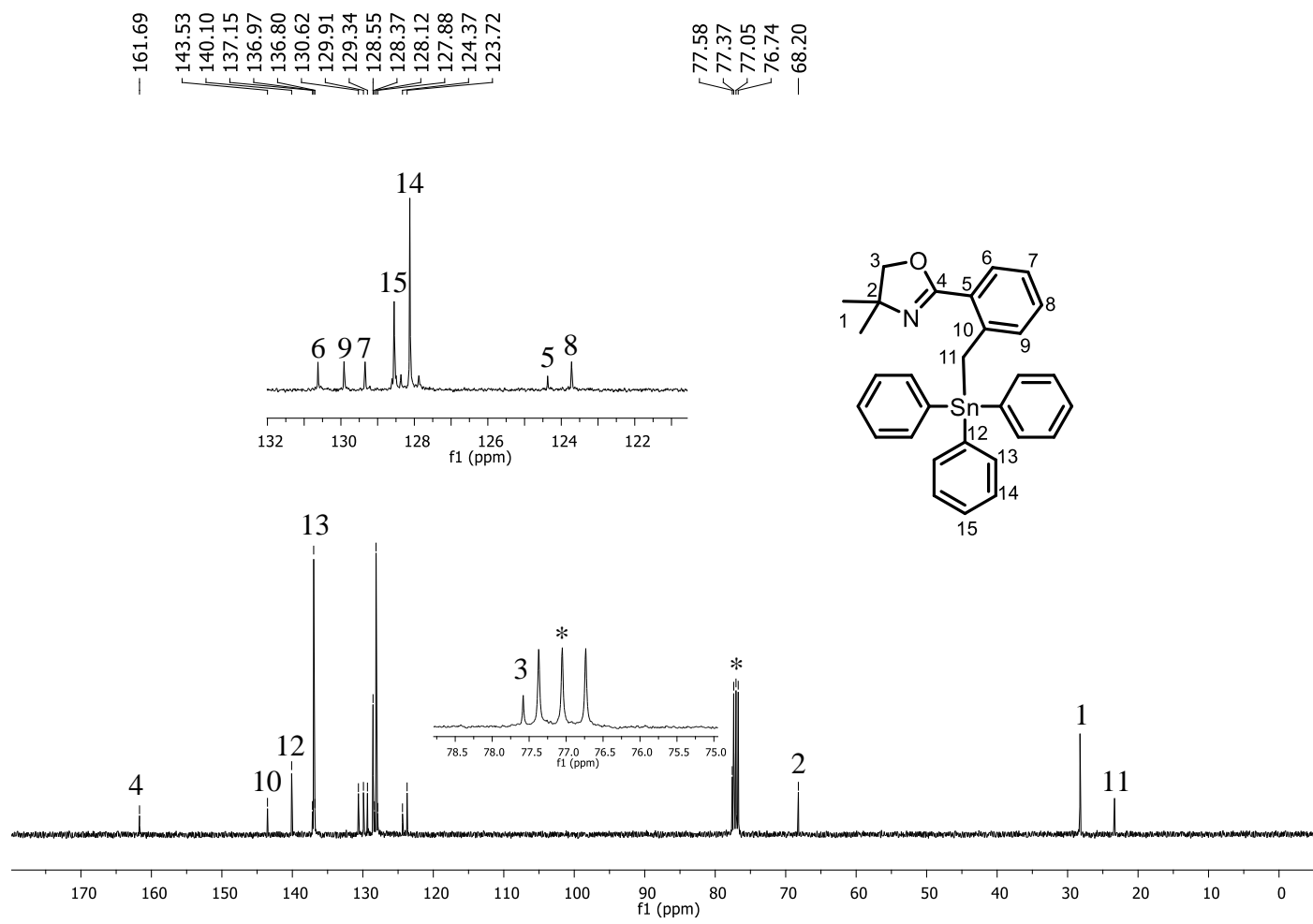


Figure A38: ^{13}C NMR spectrum of **18** in CDCl_3^* .

204

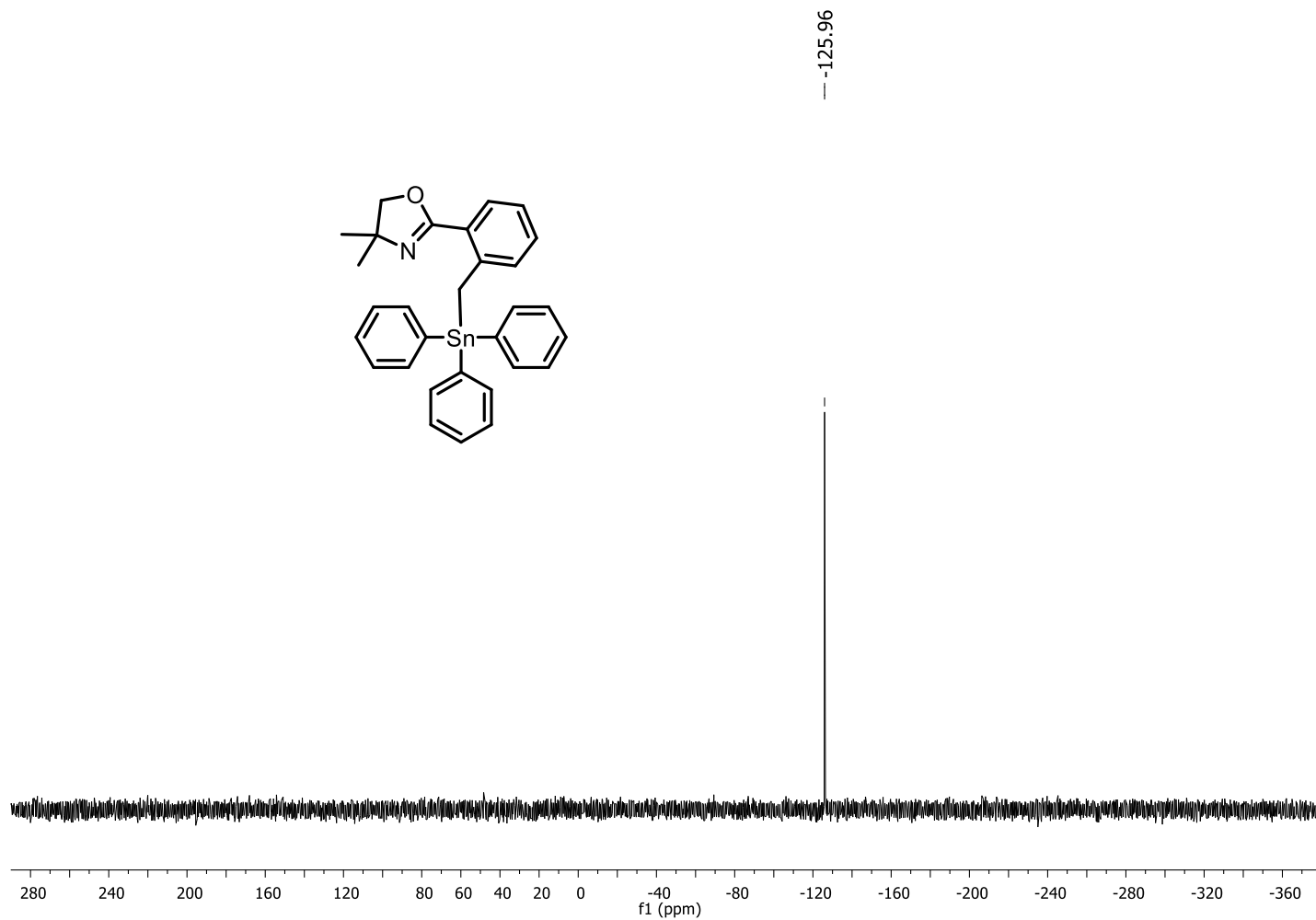


Figure A39: ^{119}Sn NMR spectrum of **18** in CDCl_3^* .

205

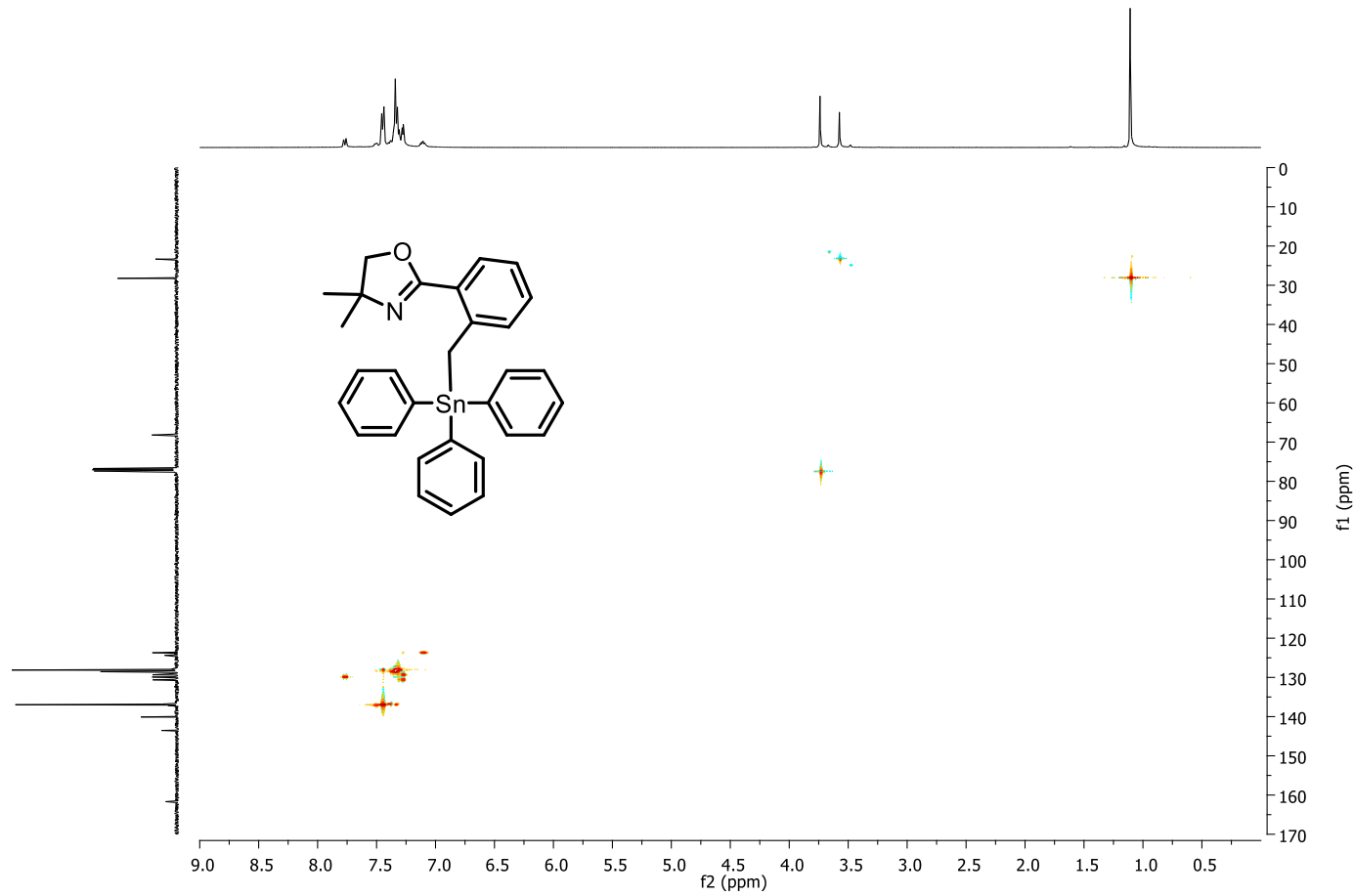


Figure A40: HSQC spectrum of **18** in CDCl_3^* .

206

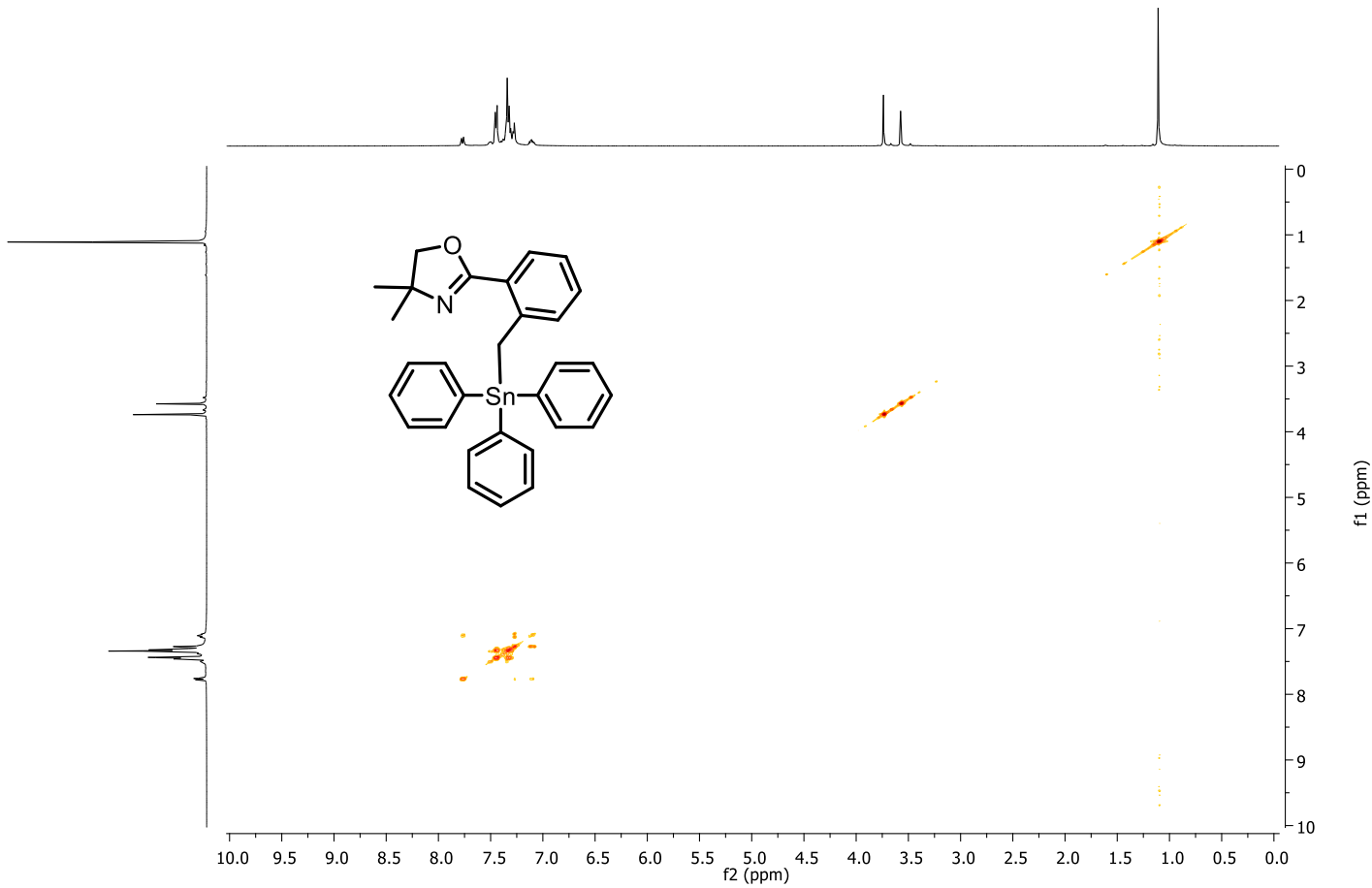


Figure A41: COSY spectrum of **18** in CDCl_3^* .

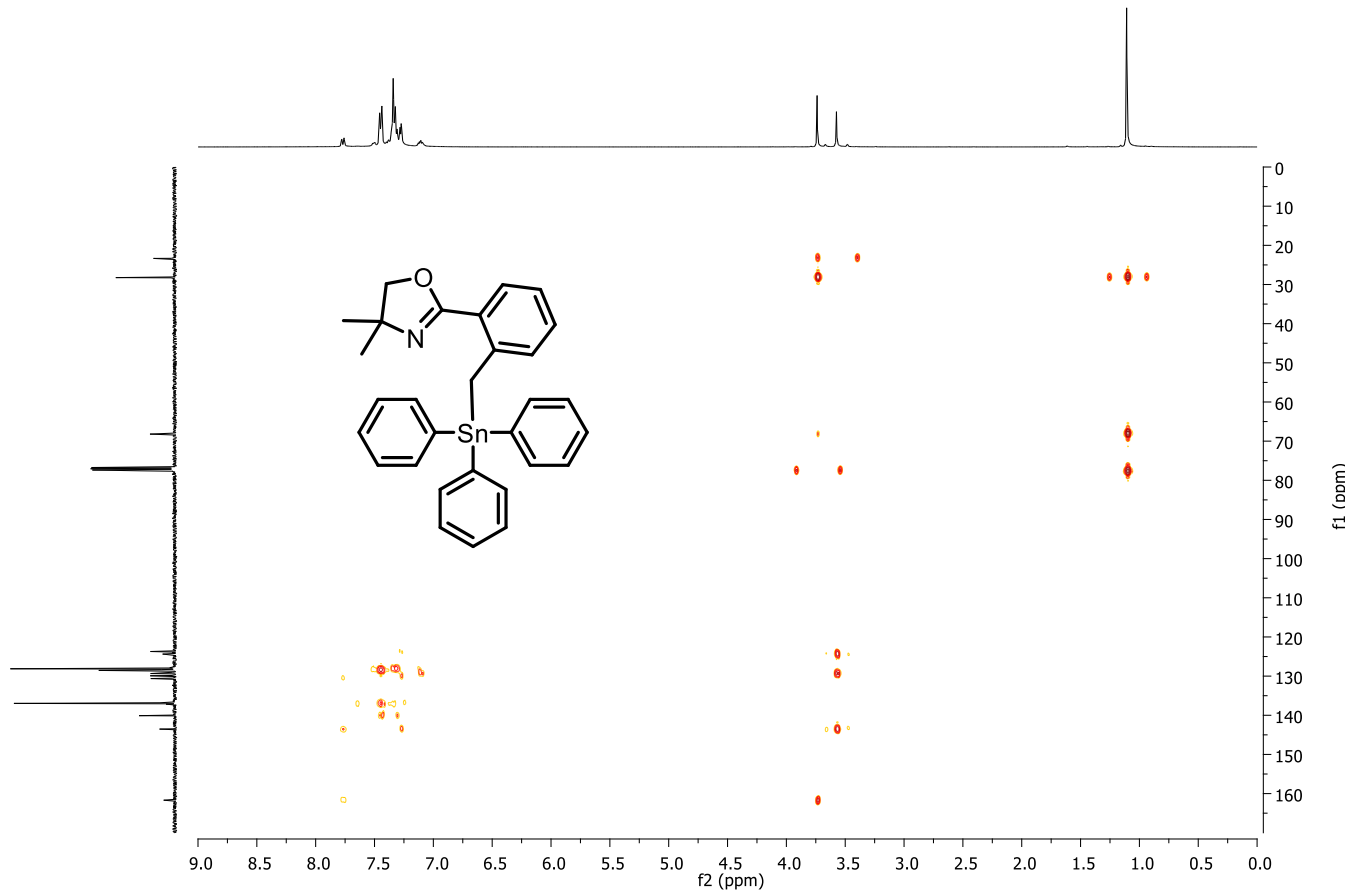


Figure A42: HMBC spectrum of **18** in CDCl_3^* .

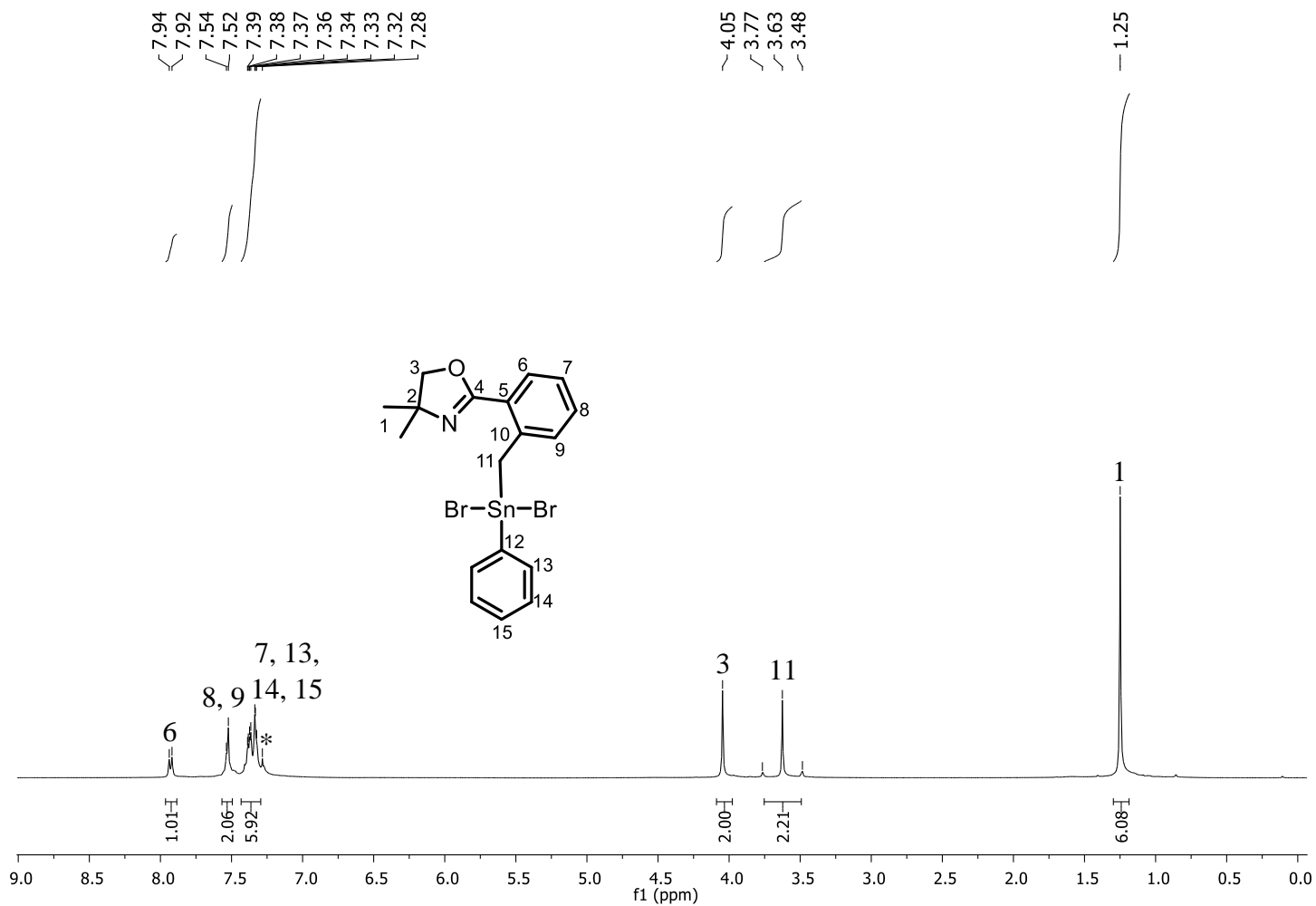


Figure A43: ^1H NMR spectrum of **20** in CDCl_3^* .

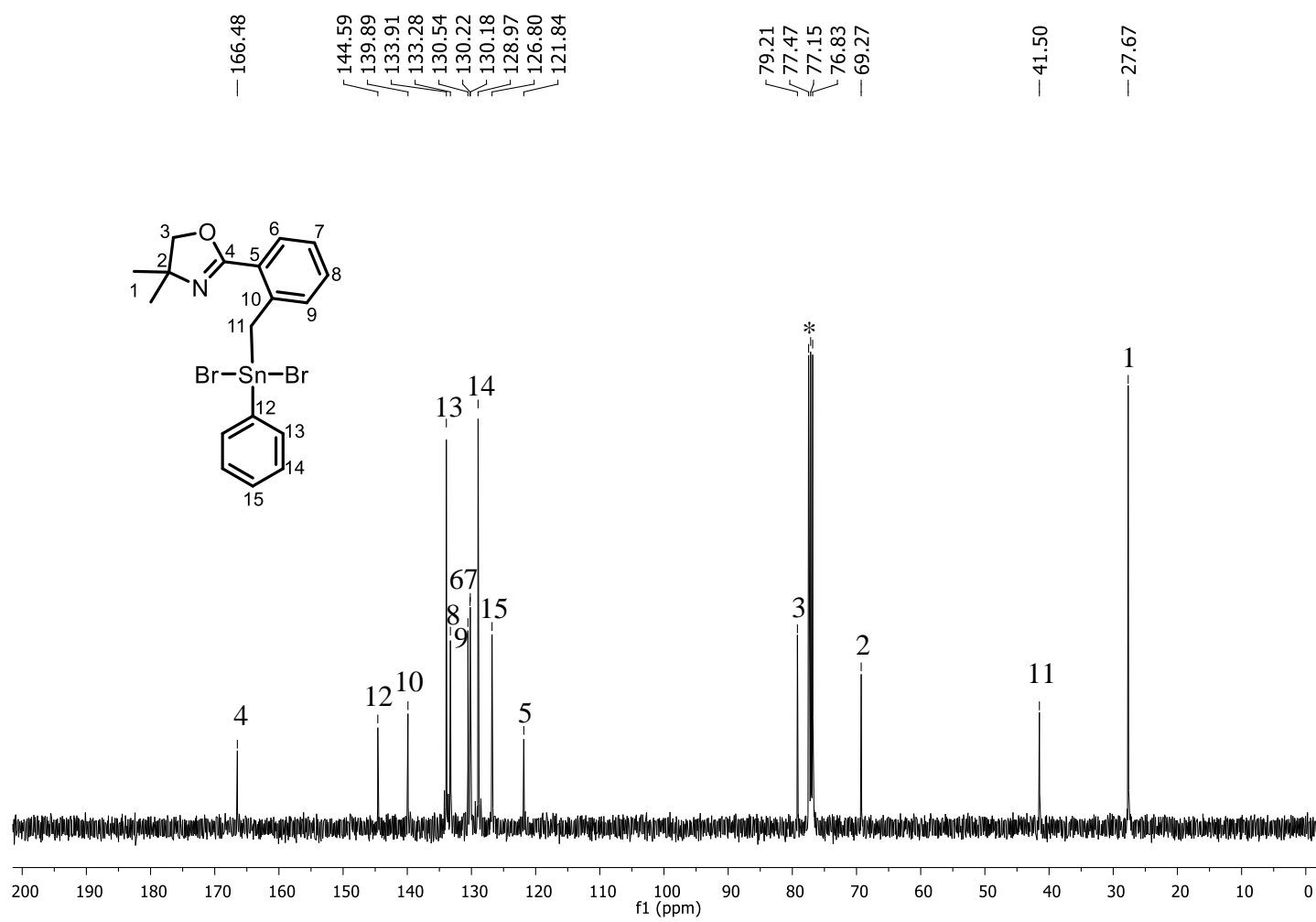


Figure A44: ^{13}C NMR spectrum of **20** in CDCl_3^* .

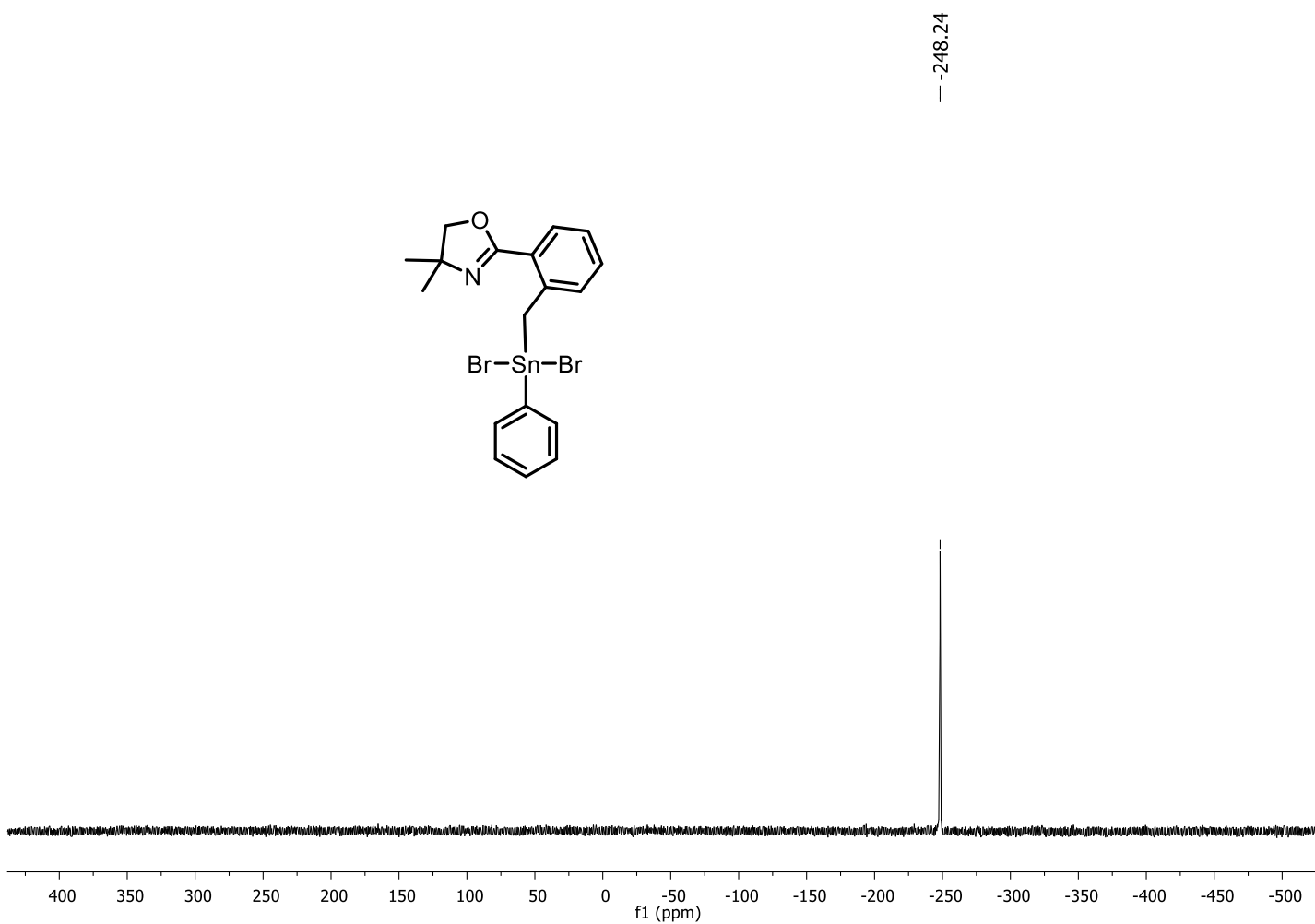


Figure A45: ^{119}Sn NMR spectrum of **20** in CDCl_3^* .

211

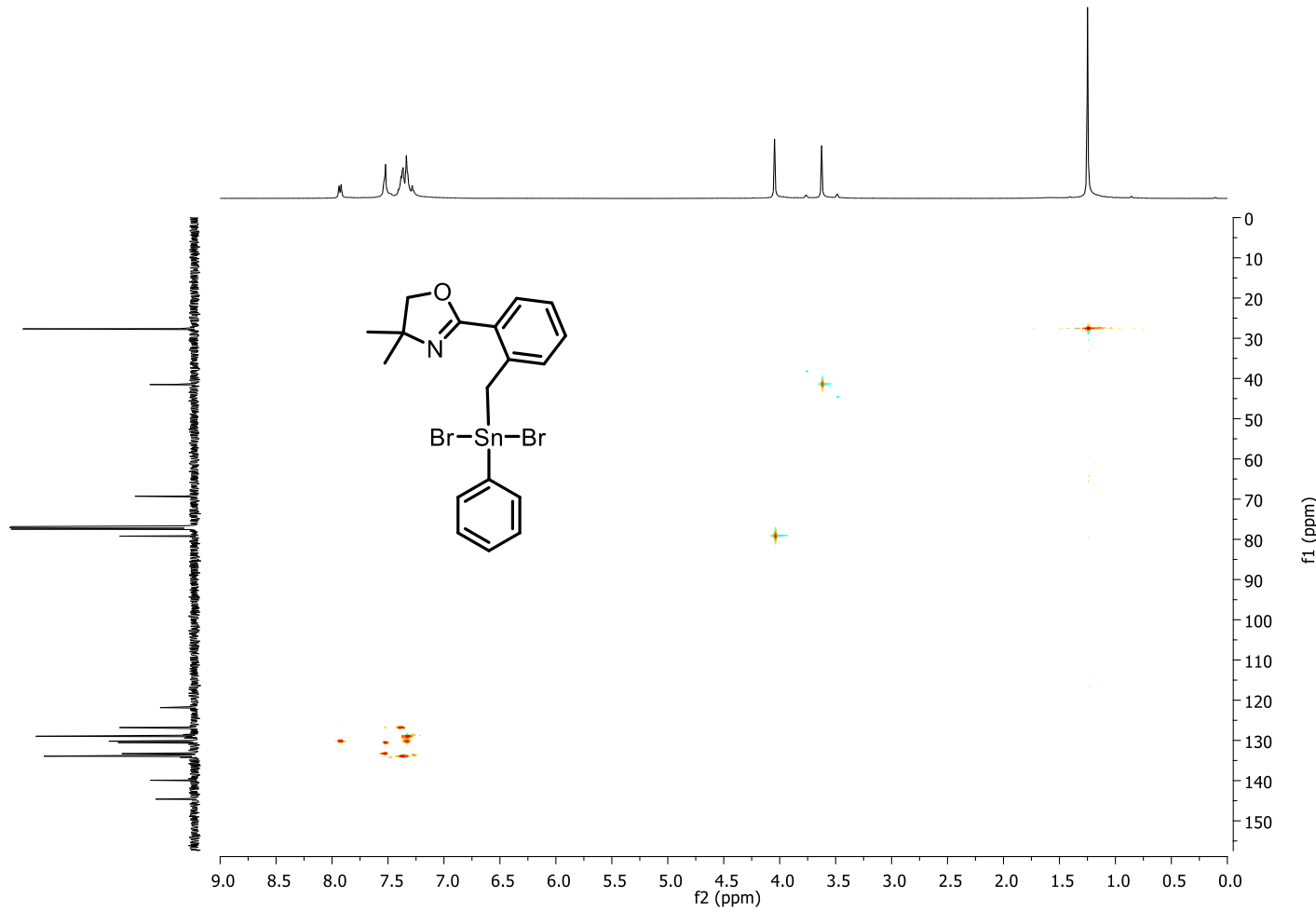


Figure A46: HSQC spectrum of **20** in CDCl_3^* .

212

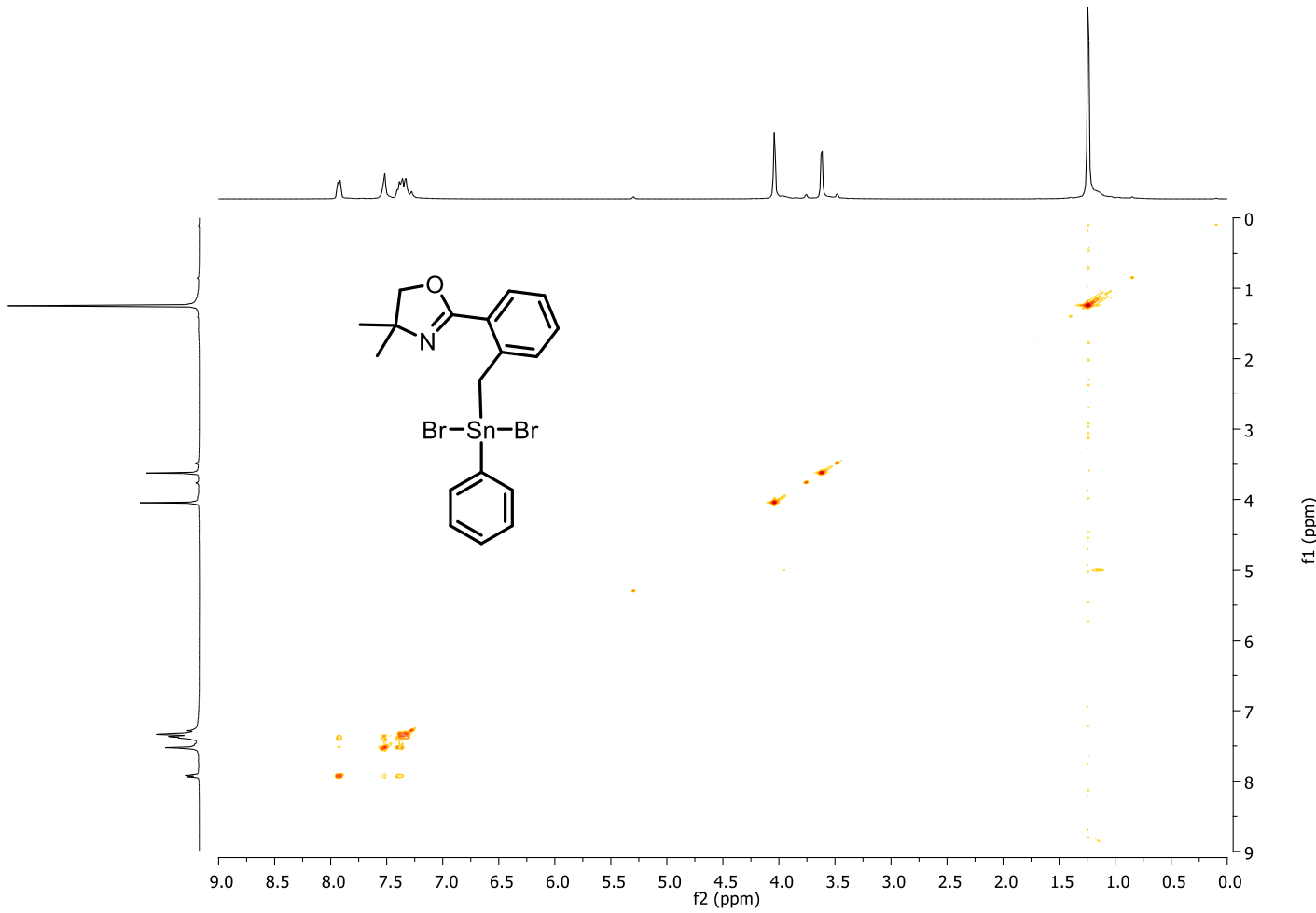


Figure A47: COSY spectrum of **20** in CDCl_3^* .

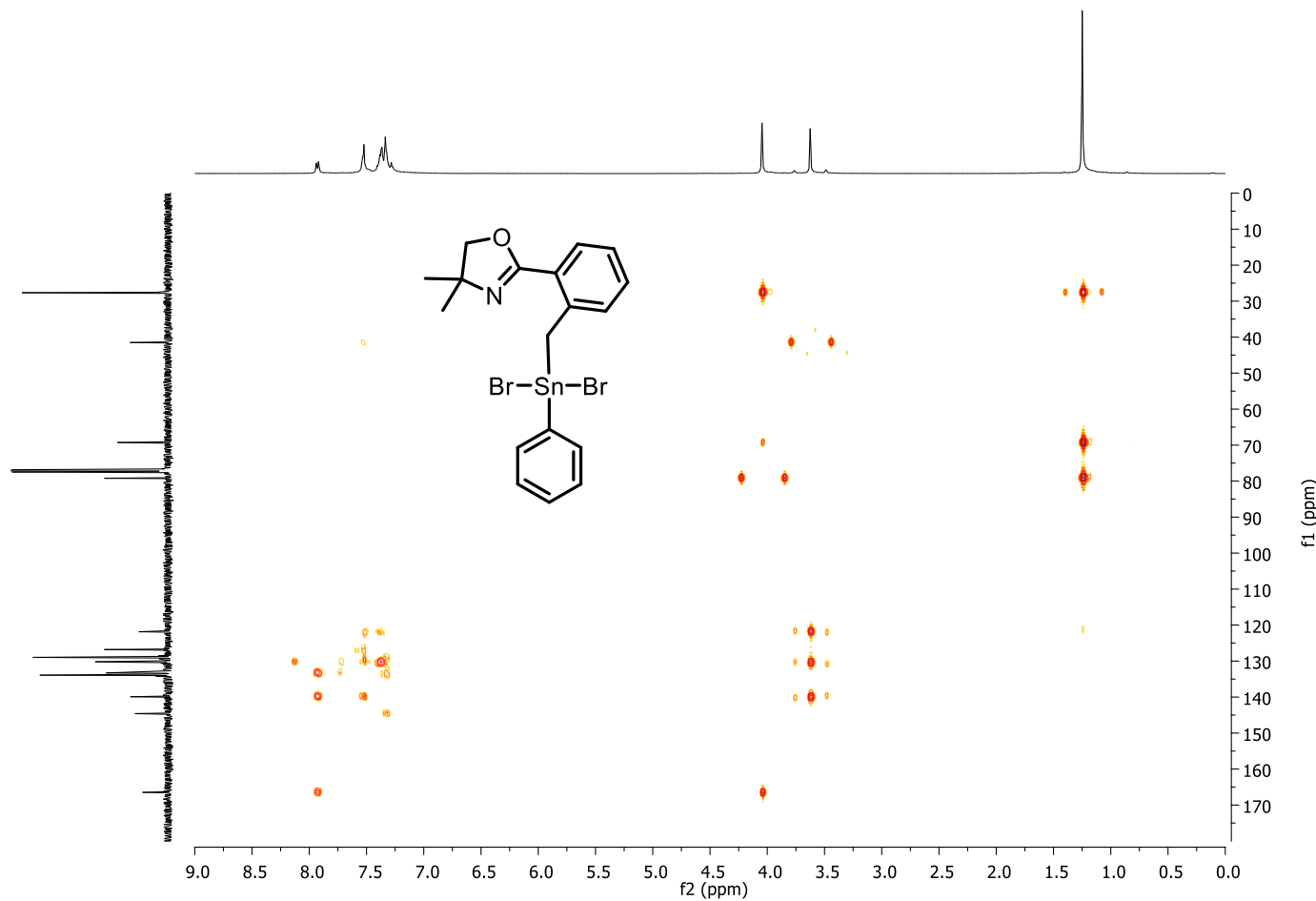


Figure A48: HMBC spectrum of **20** in CDCl_3^* .

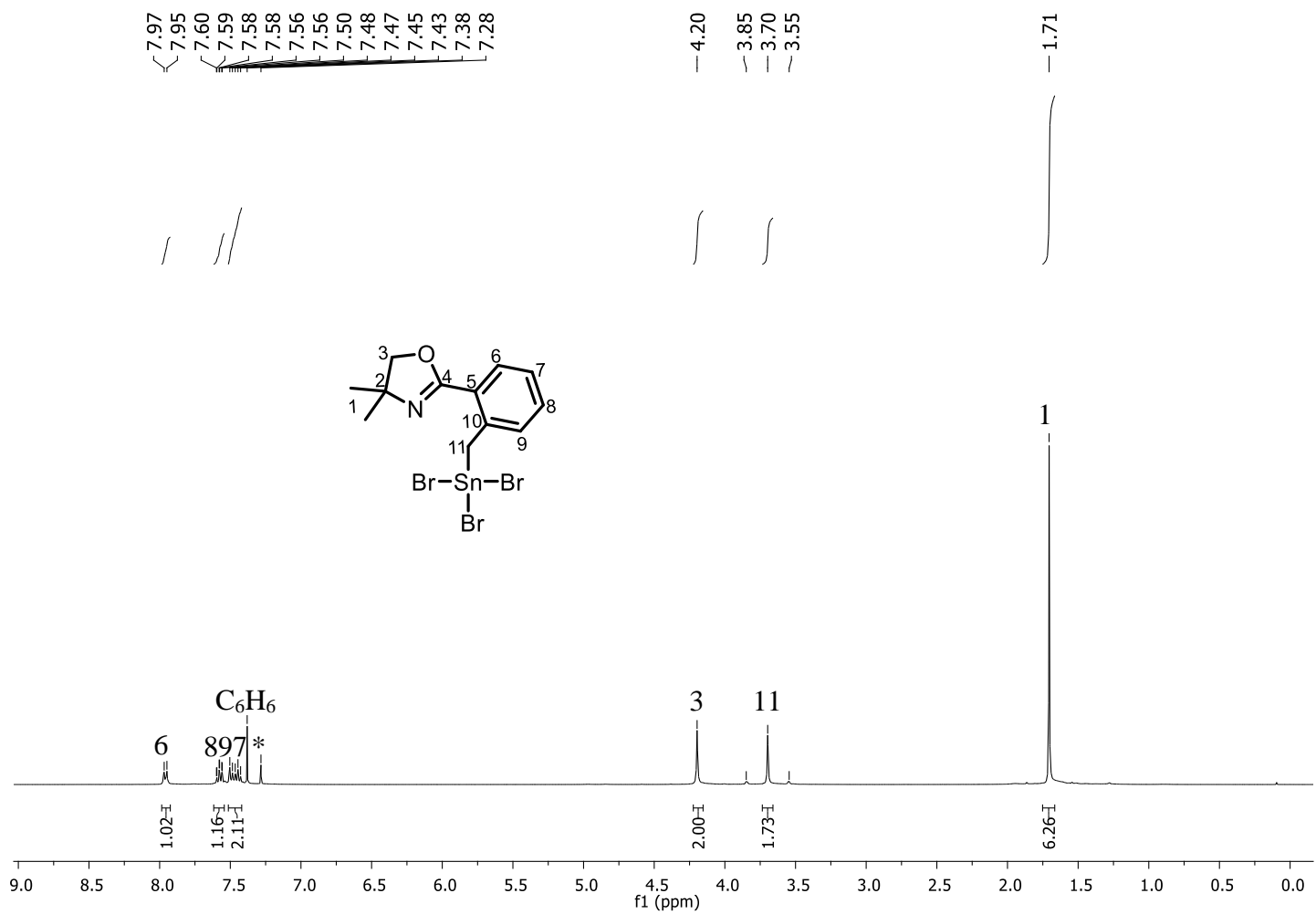


Figure A49: ^1H NMR spectrum of **19** in CDCl_3^* .

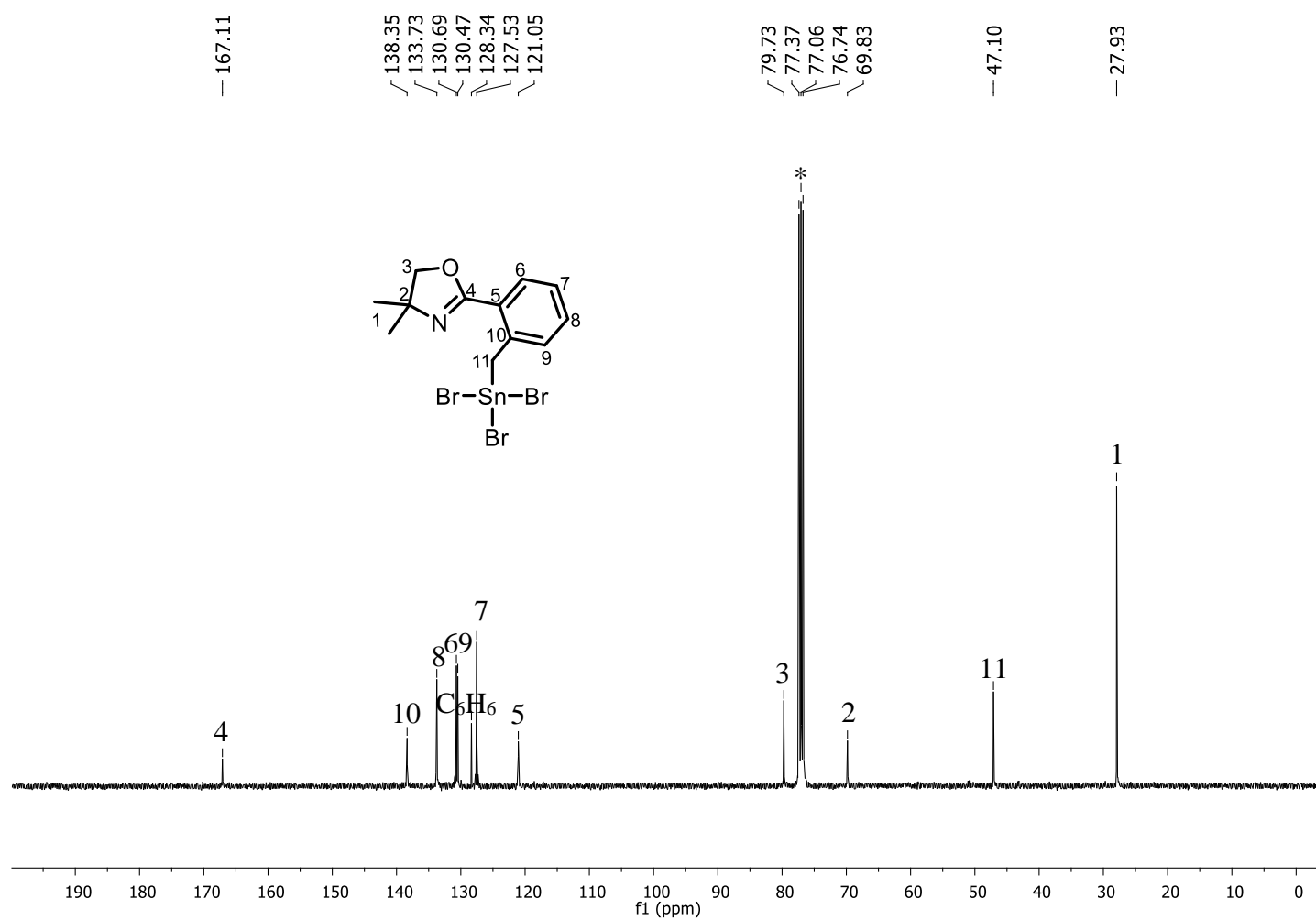


Figure A50: ^{13}C NMR spectrum of **19** in CDCl_3^* .

216

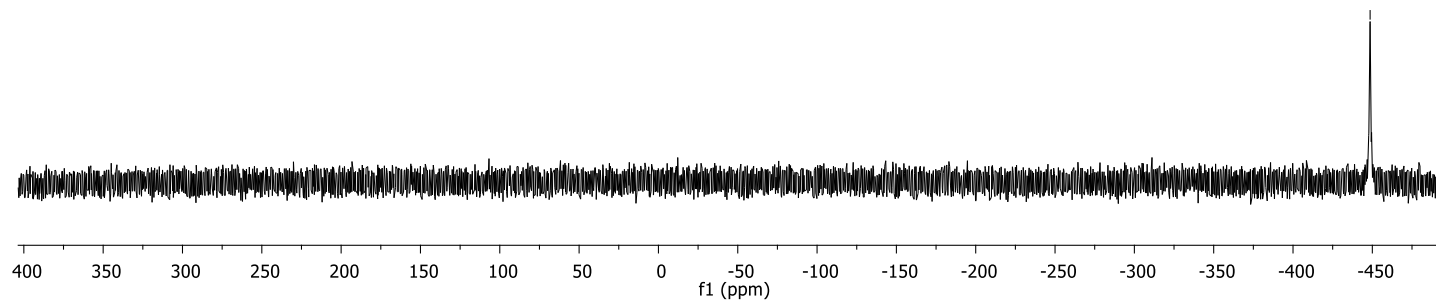
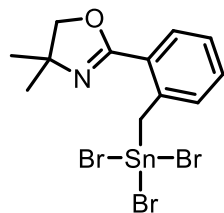


Figure A51: ¹¹⁹Sn NMR spectrum of **19** in CDCl₃*.

-448.60

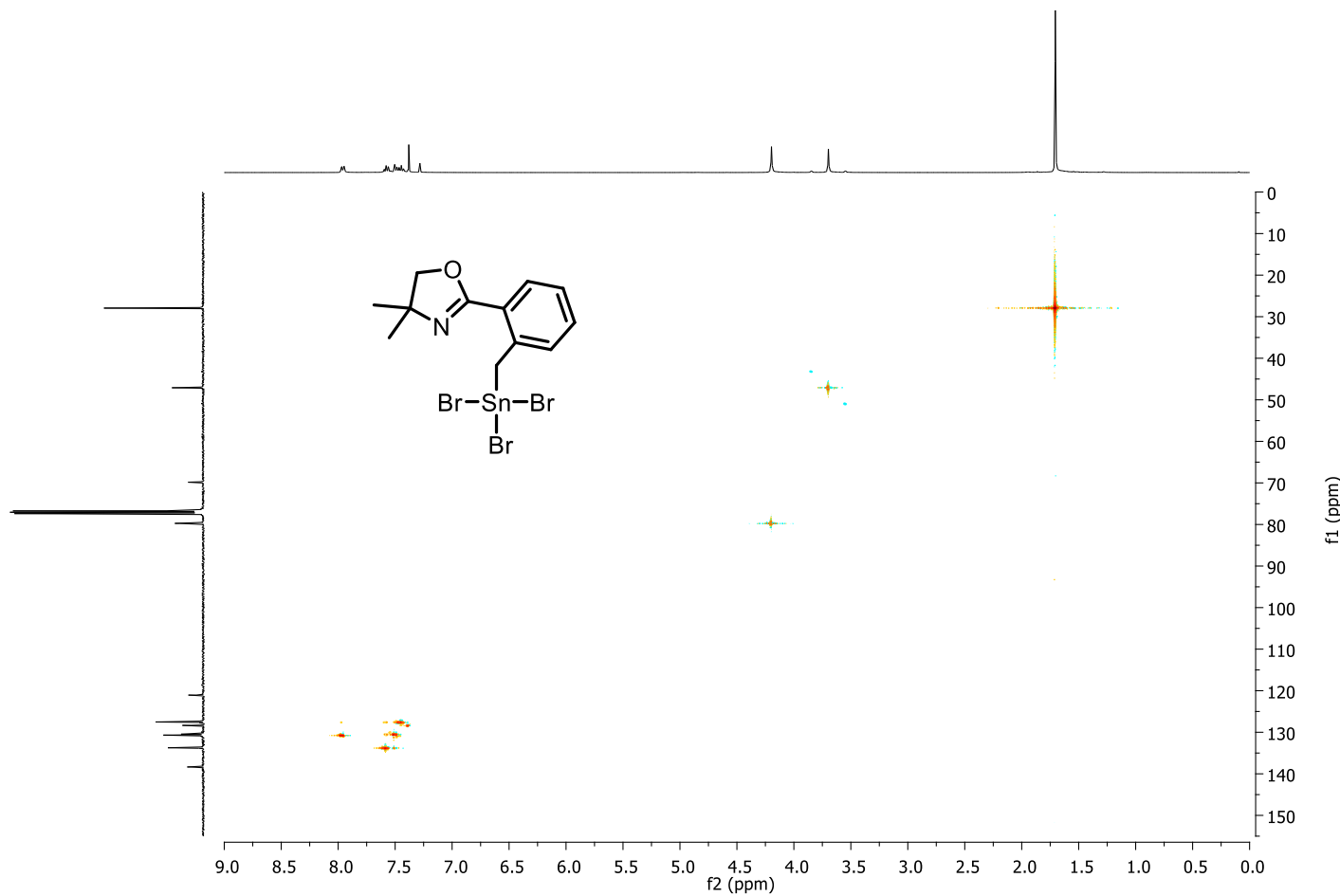


Figure A52: HSQC spectrum of **19** in CDCl_3^* .

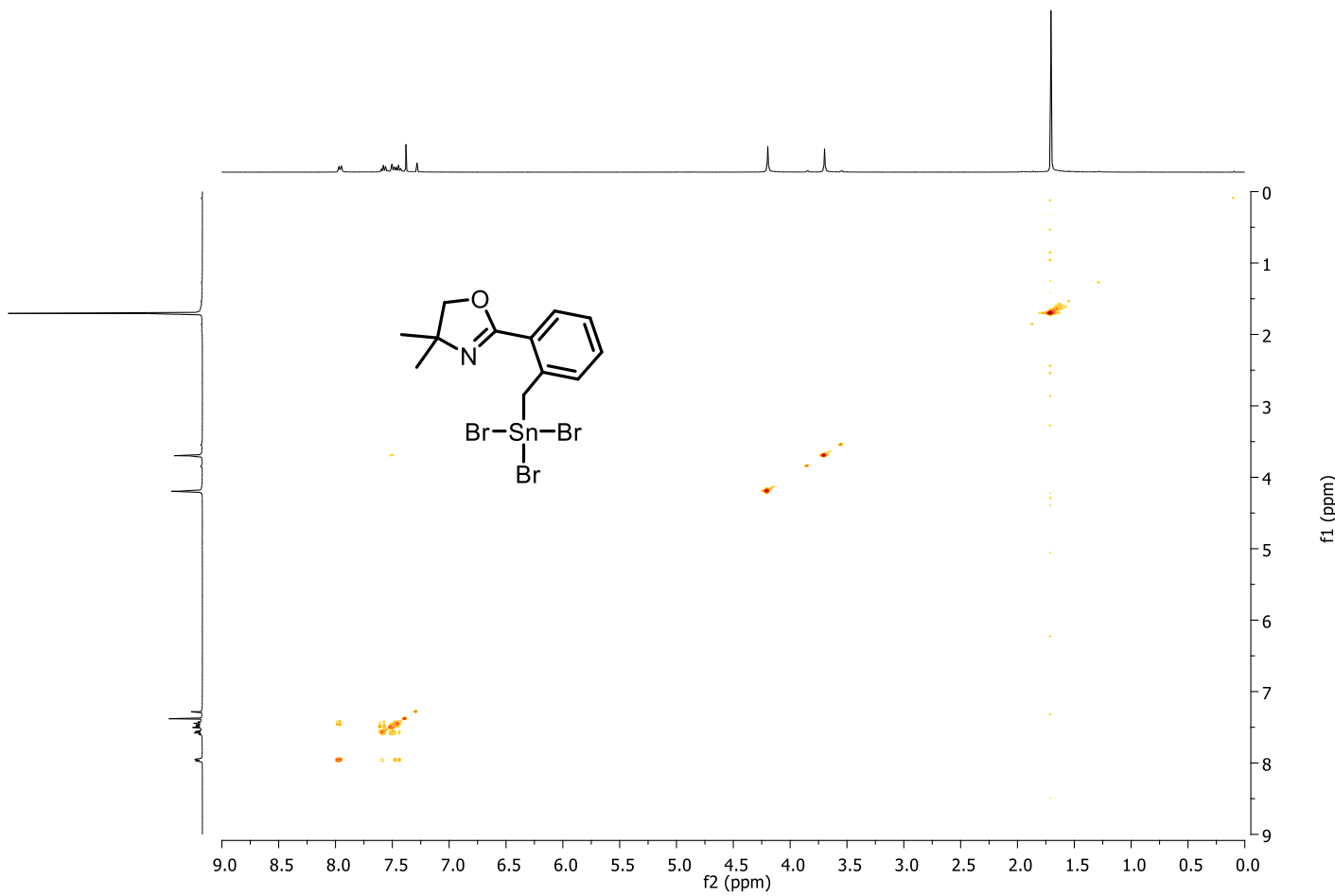


Figure A53: COSY spectrum of **19** in CDCl_3^* .

219

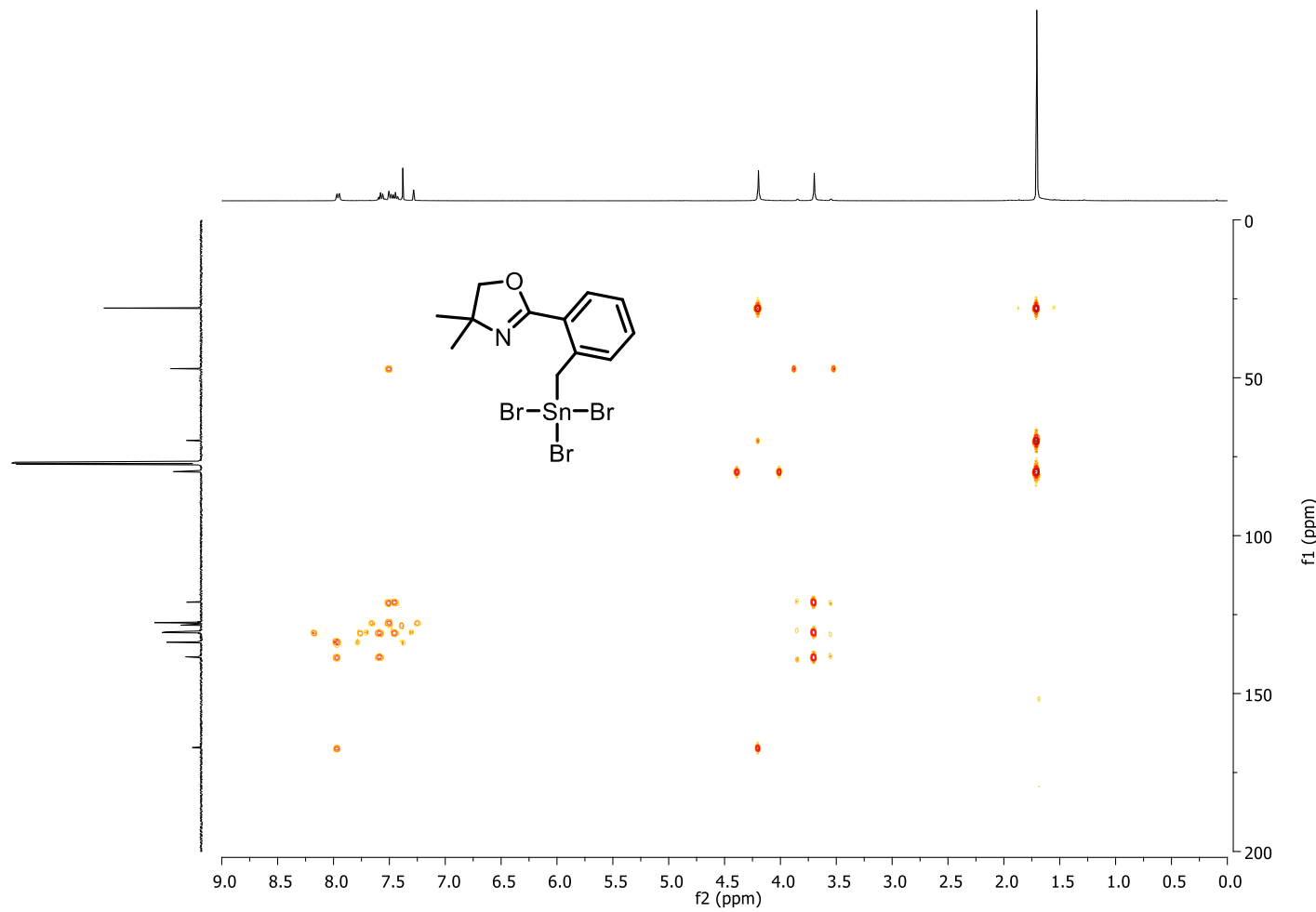


Figure A54: HMBC spectrum of **19** in CDCl_3^* .

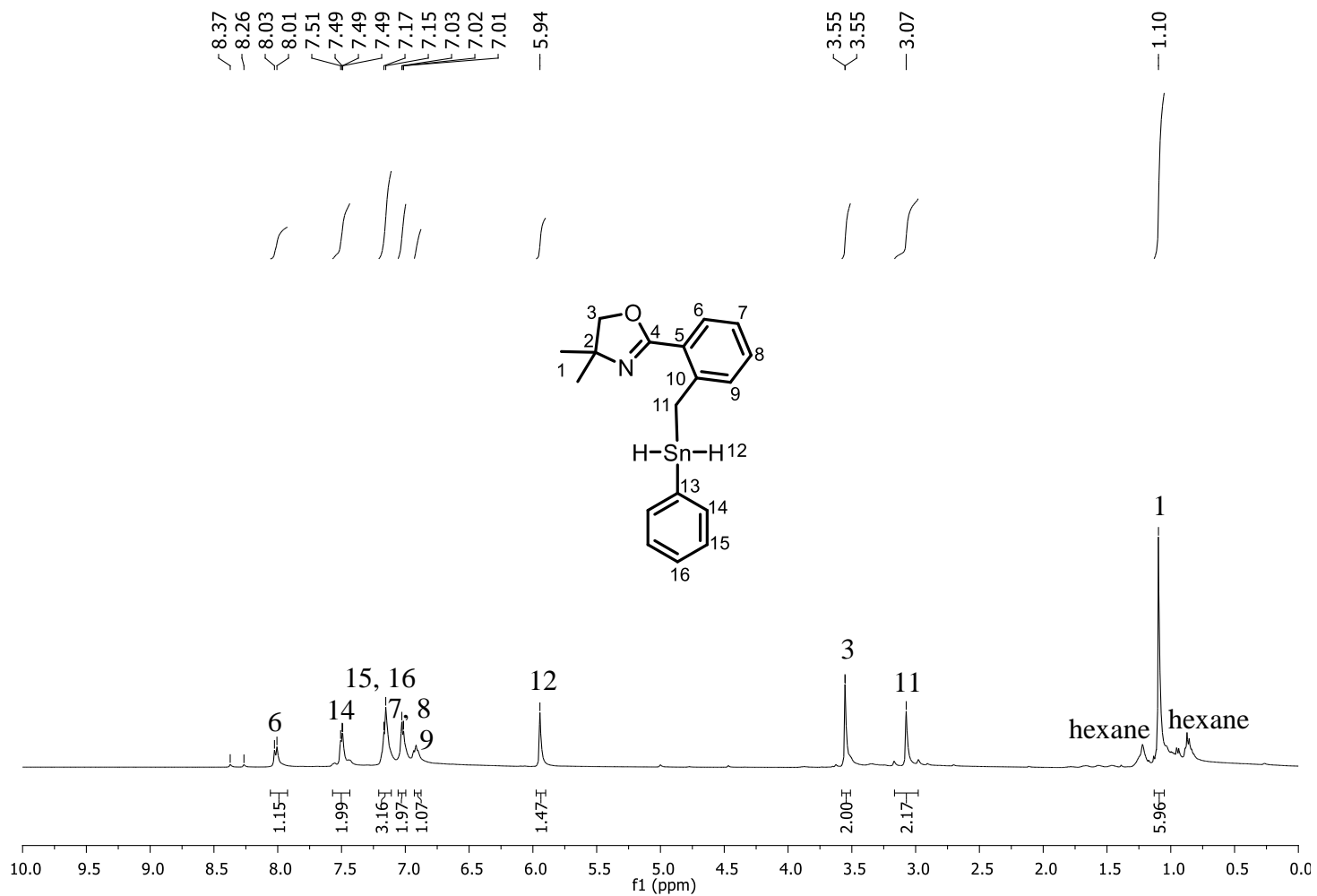


Figure A55: ^1H NMR spectrum of **21** in C_6D_6^* .

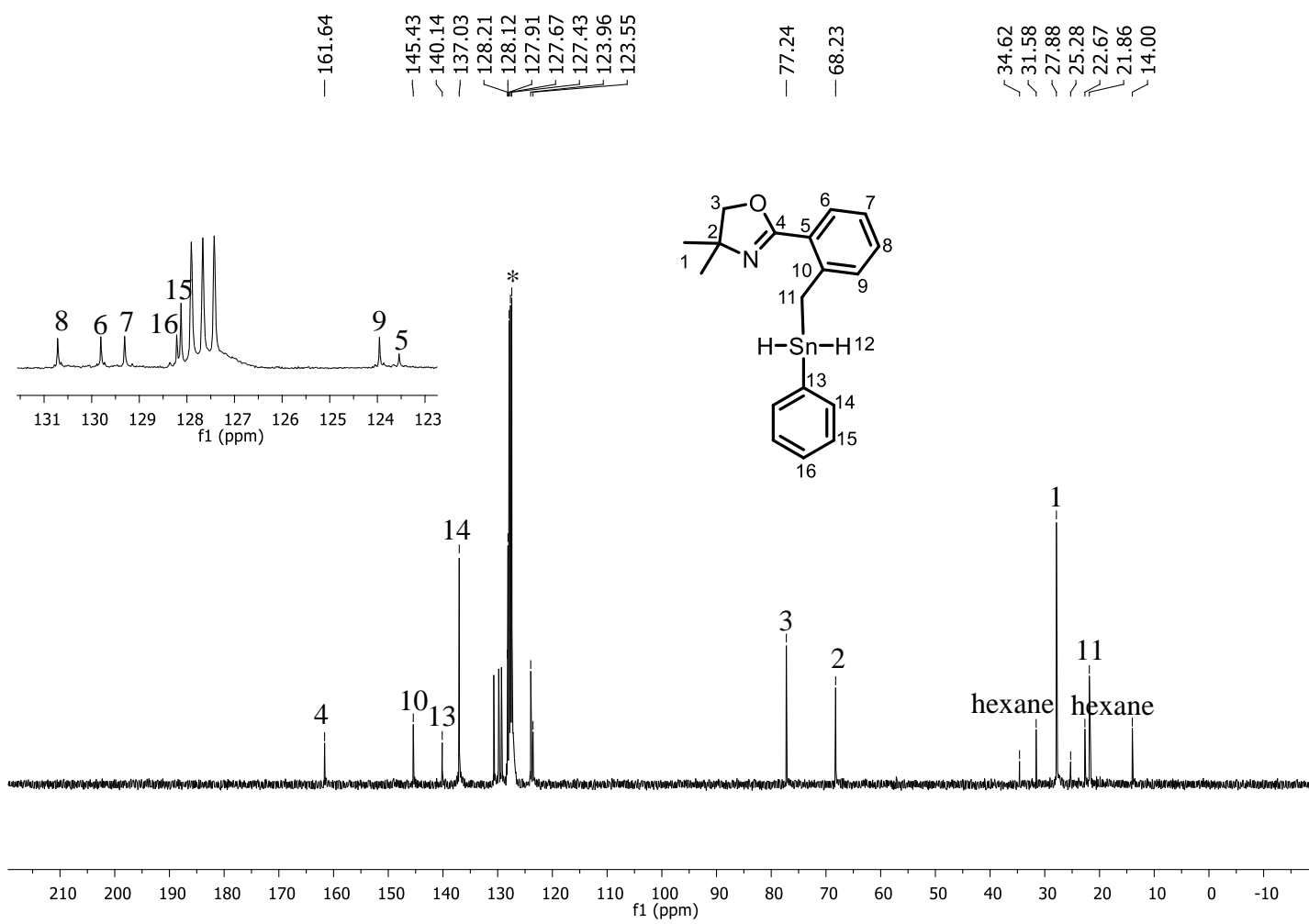


Figure A56: ^{13}C NMR spectrum of **21** in C_6D_6^* .

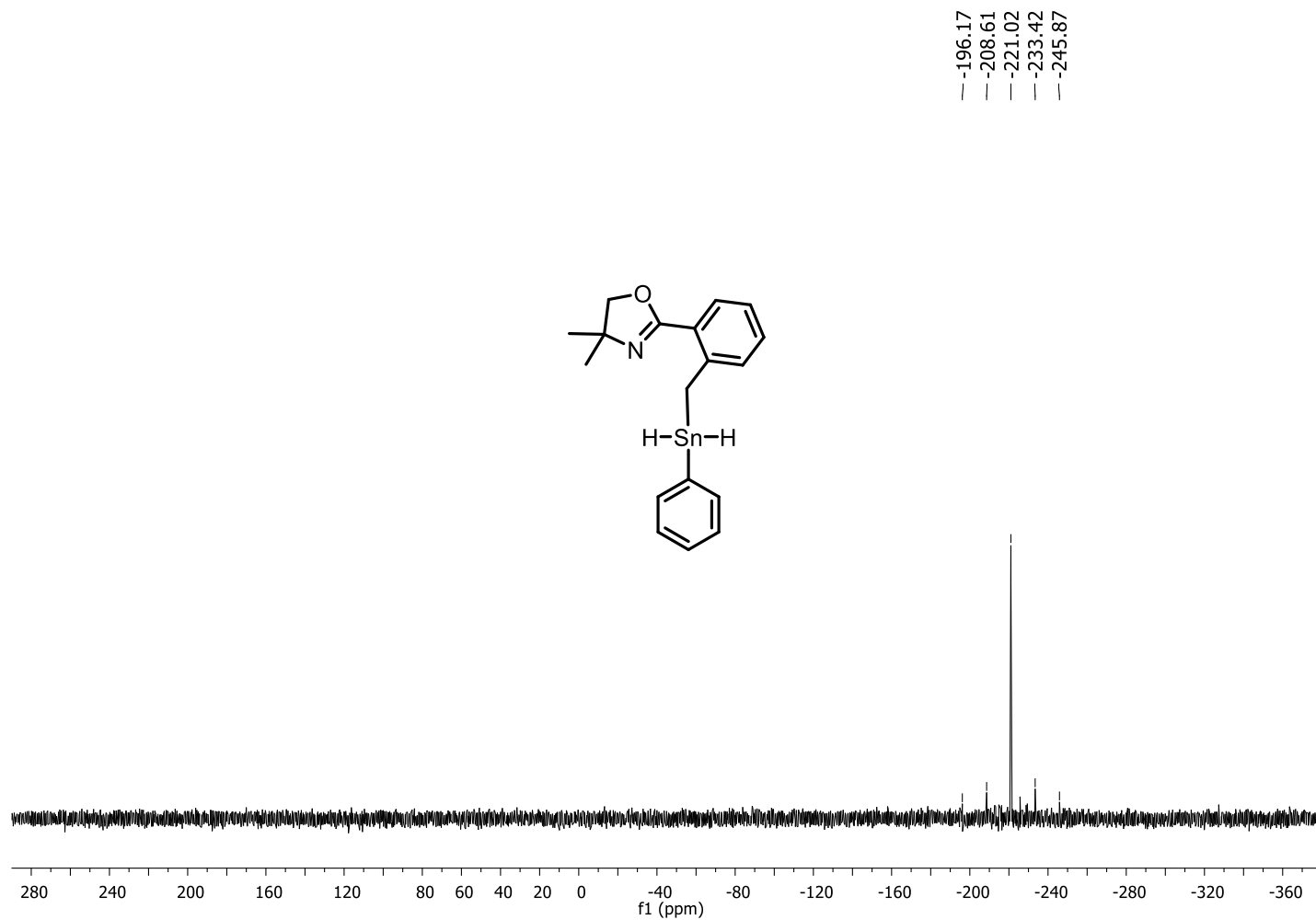


Figure A57: ^{119}Sn NMR spectrum of **21** in C_6D_6^* .

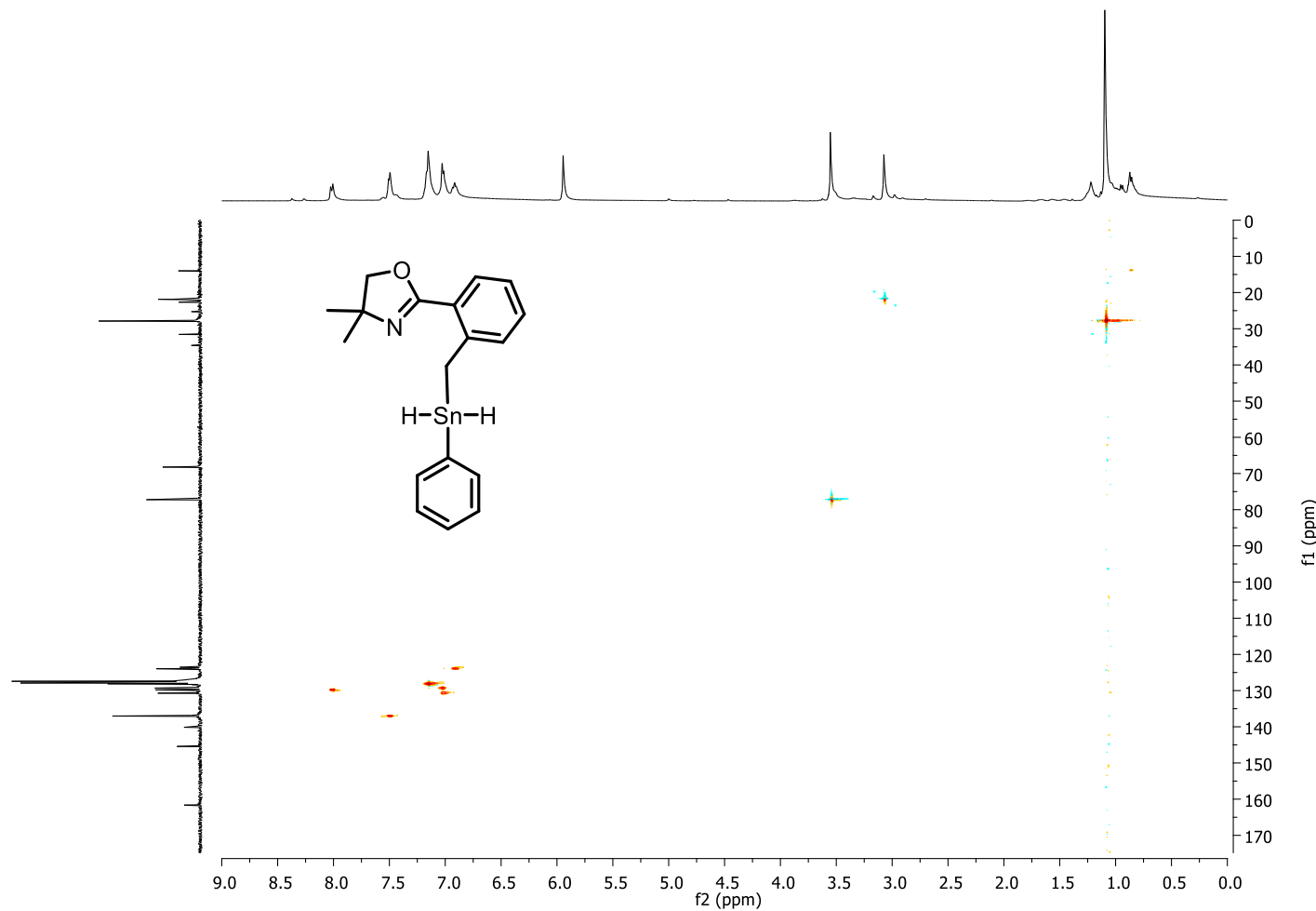


Figure A58: HSQC spectrum of **21** in $C_6D_6^*$.

224

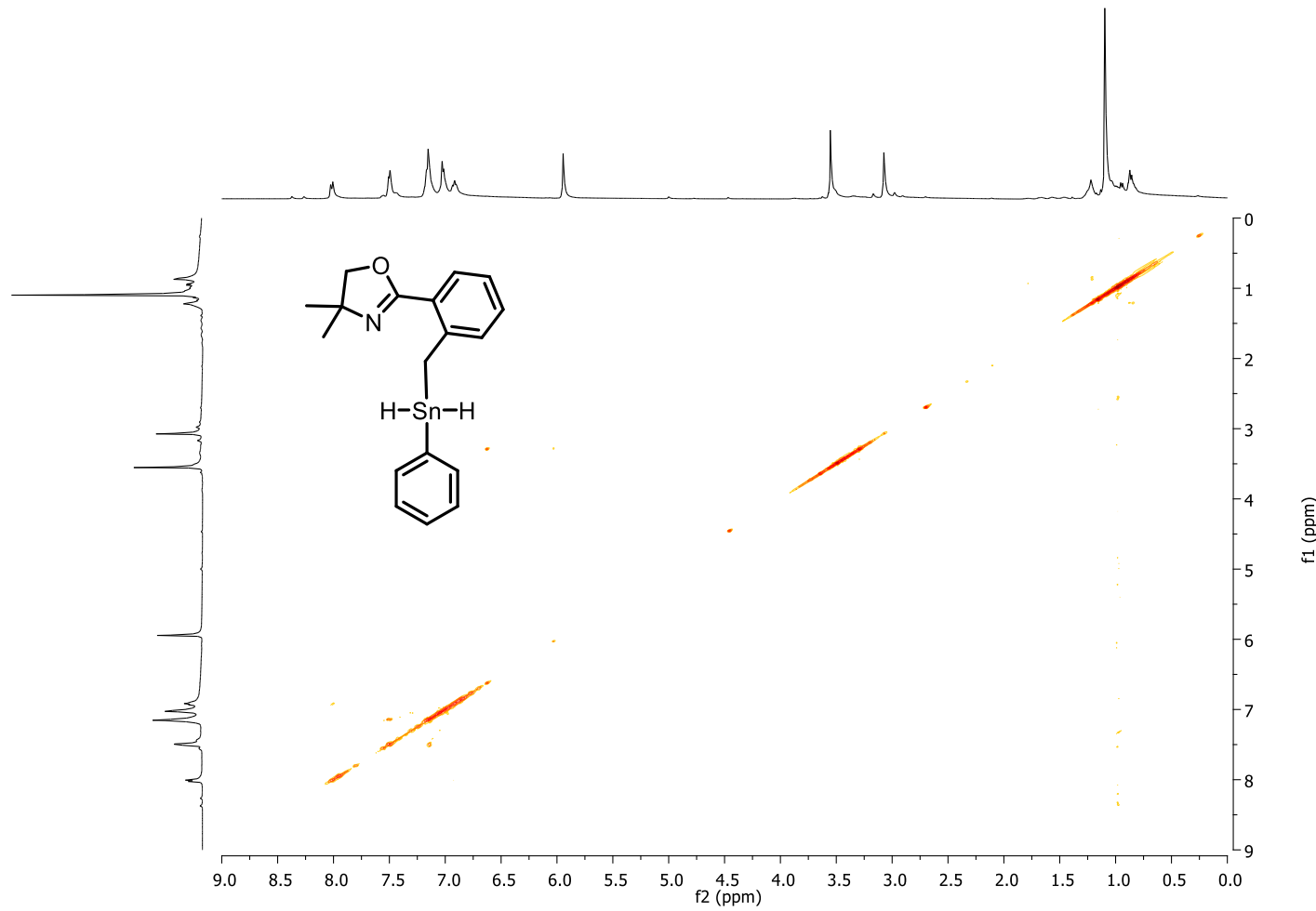


Figure A59: COSY spectrum of **21** in $C_6D_6^*$.

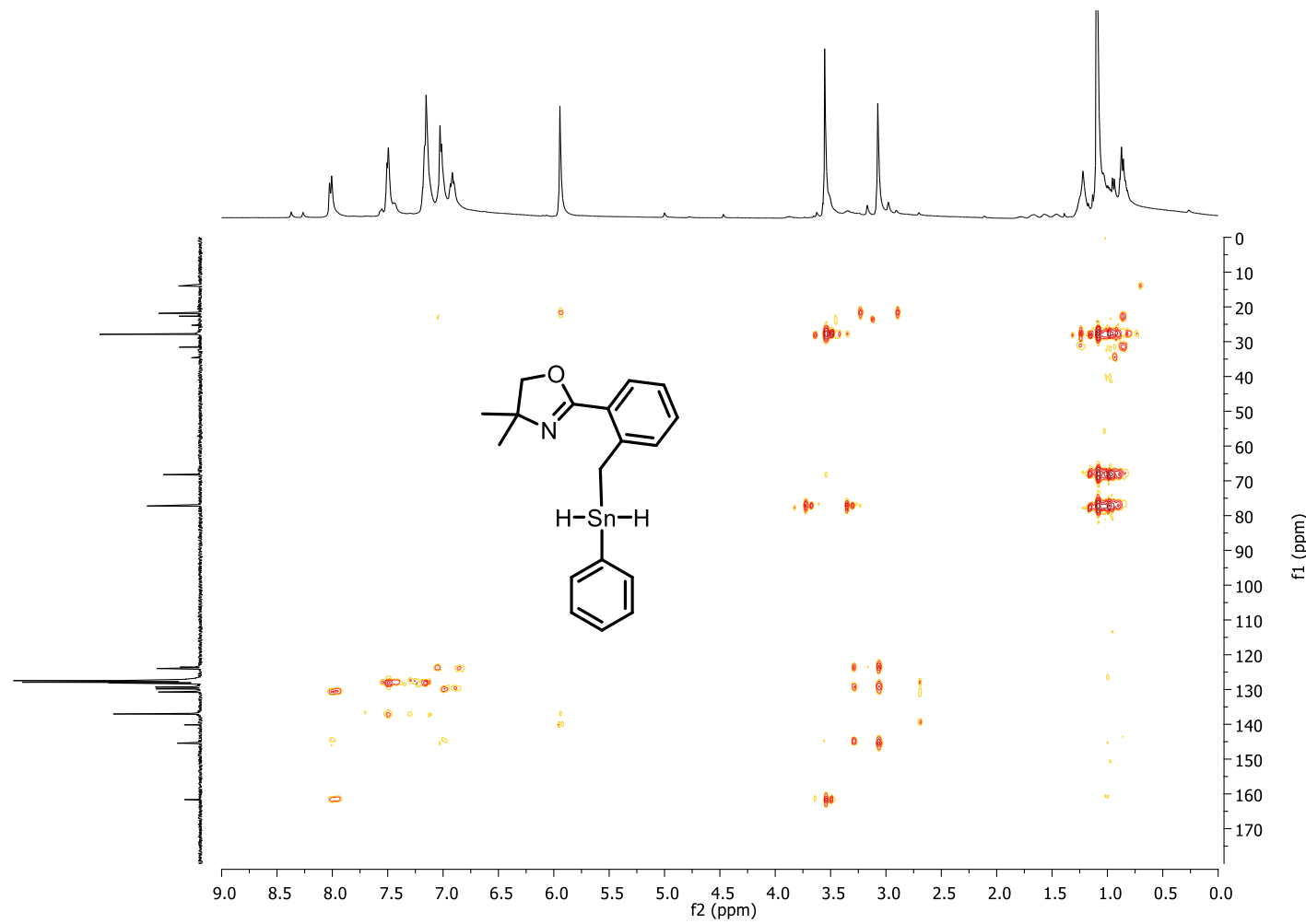


Figure A60: HMBC spectrum of **21** in $C_6D_6^*$.

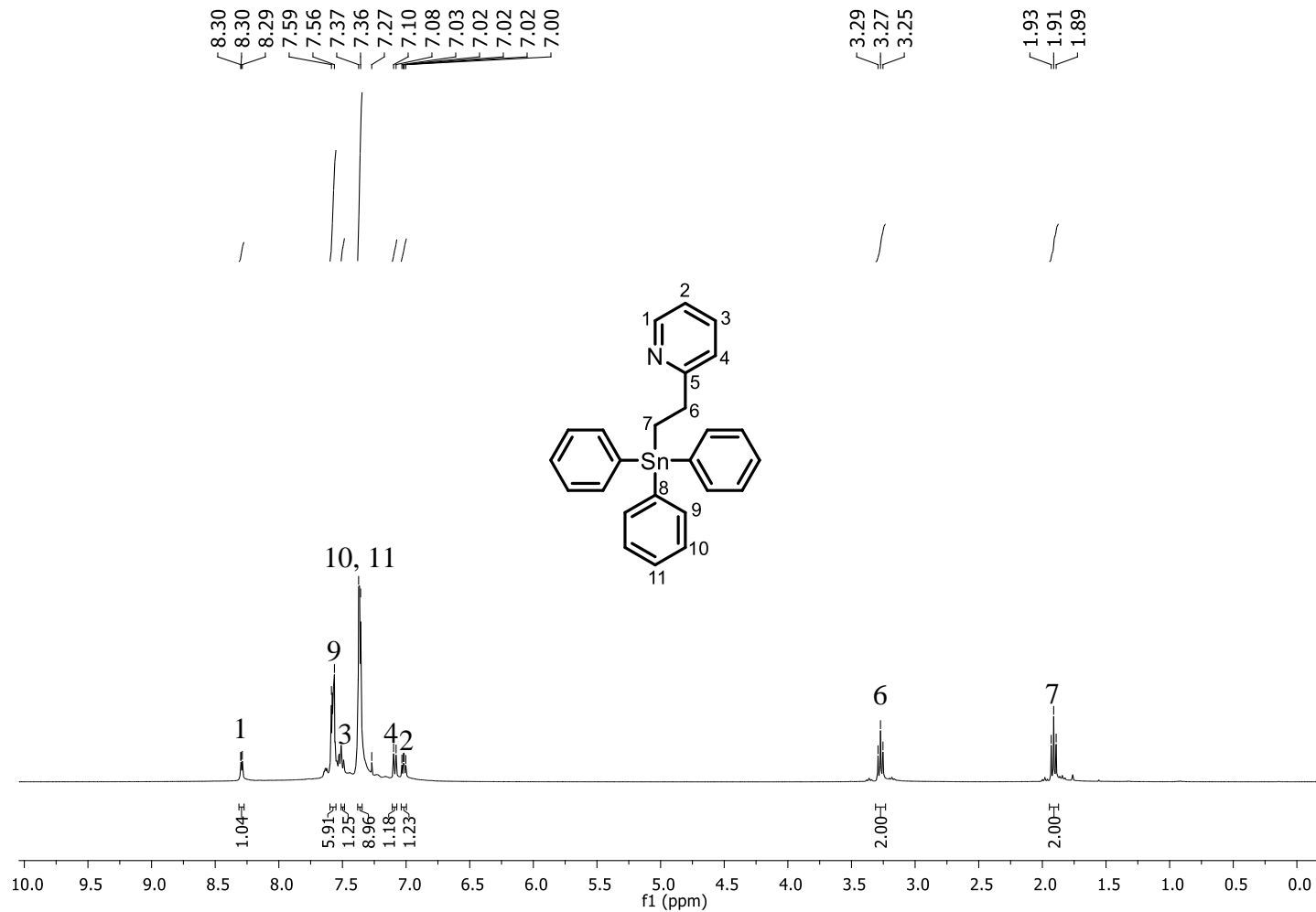


Figure A61: ^1H NMR spectrum of **23** in CDCl_3^* .

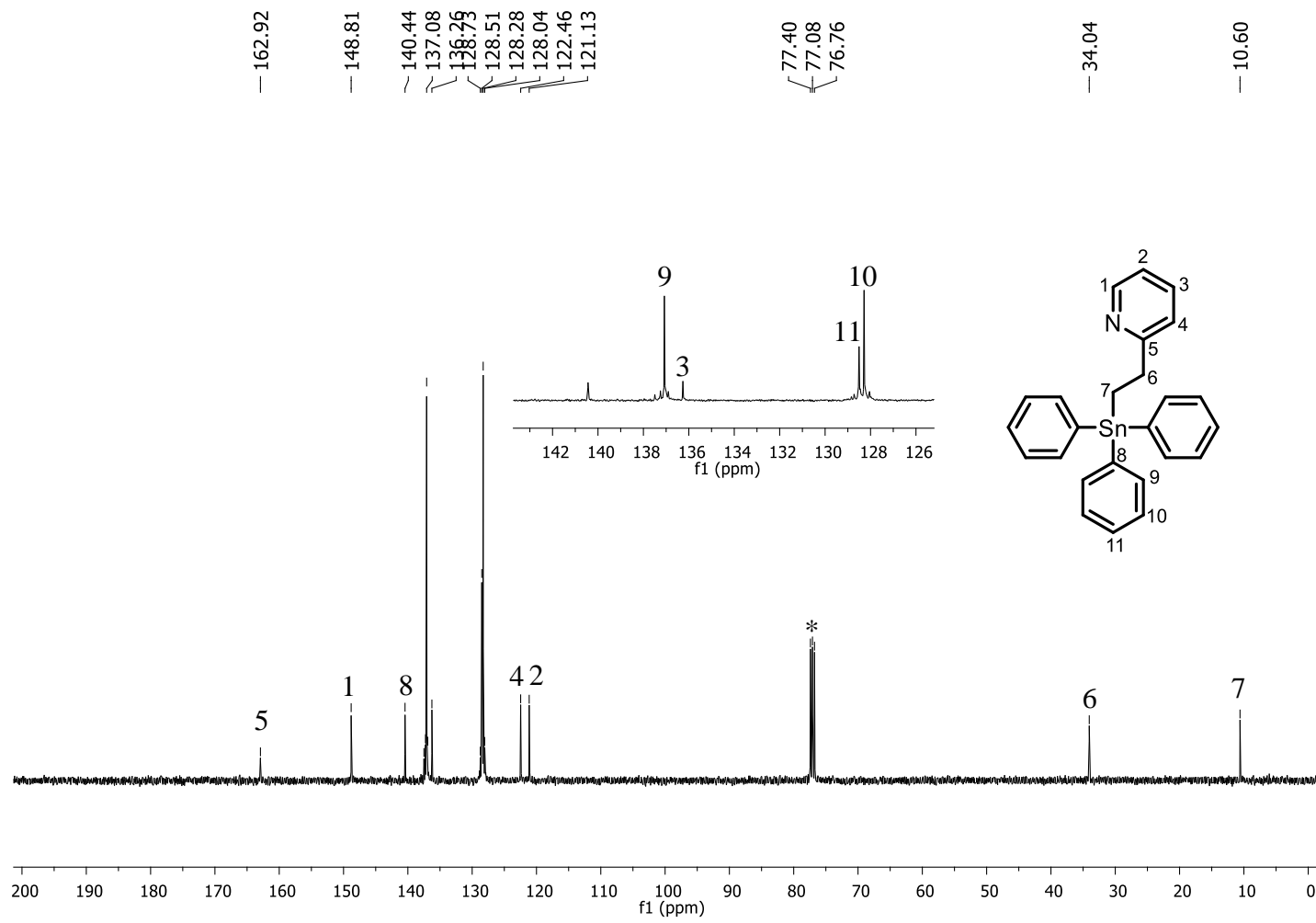


Figure A62: ^{13}C NMR spectrum of **23** in CDCl_3^* .

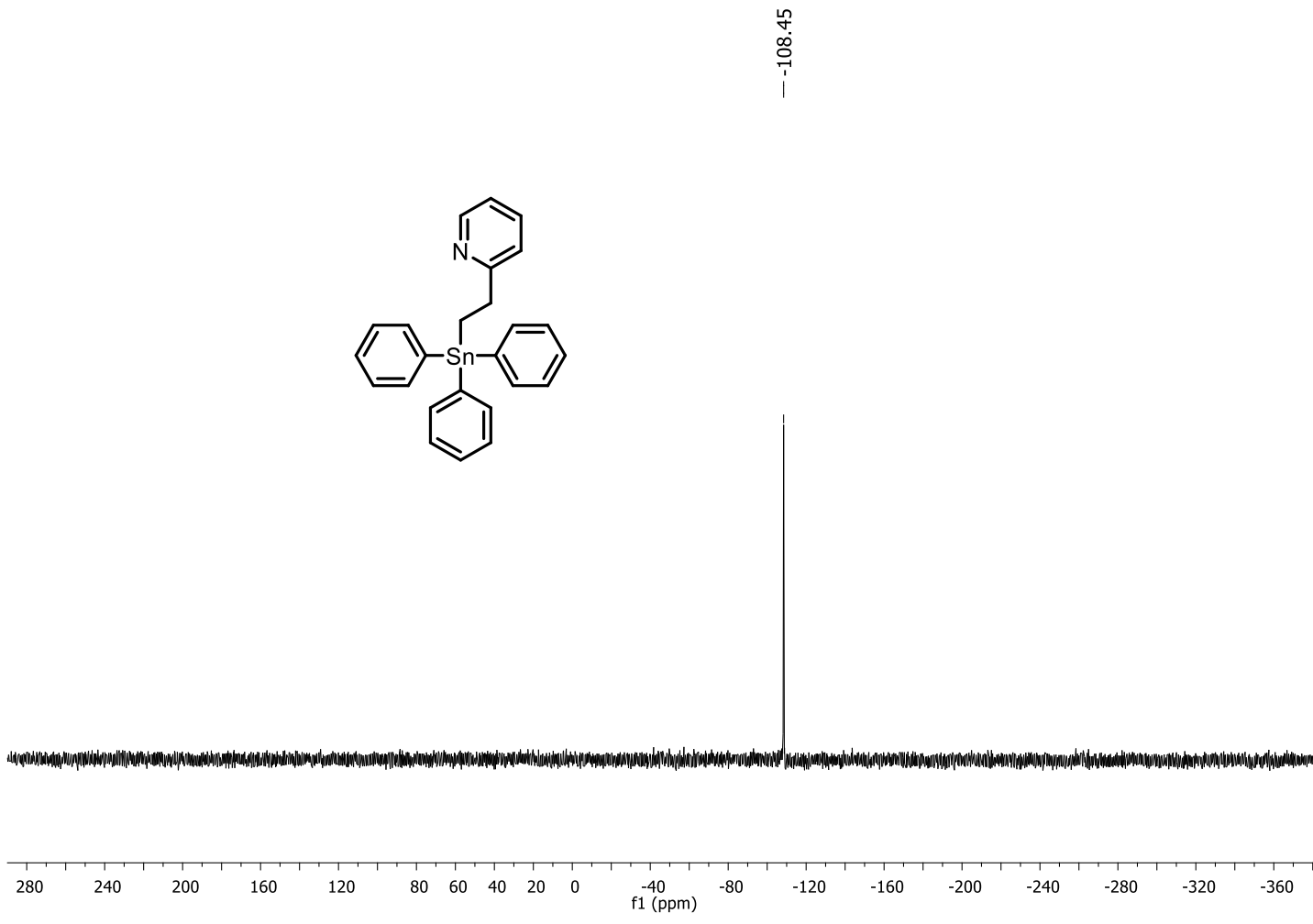


Figure A63: ^{119}Sn NMR spectrum of **23** in CDCl_3^* .

229

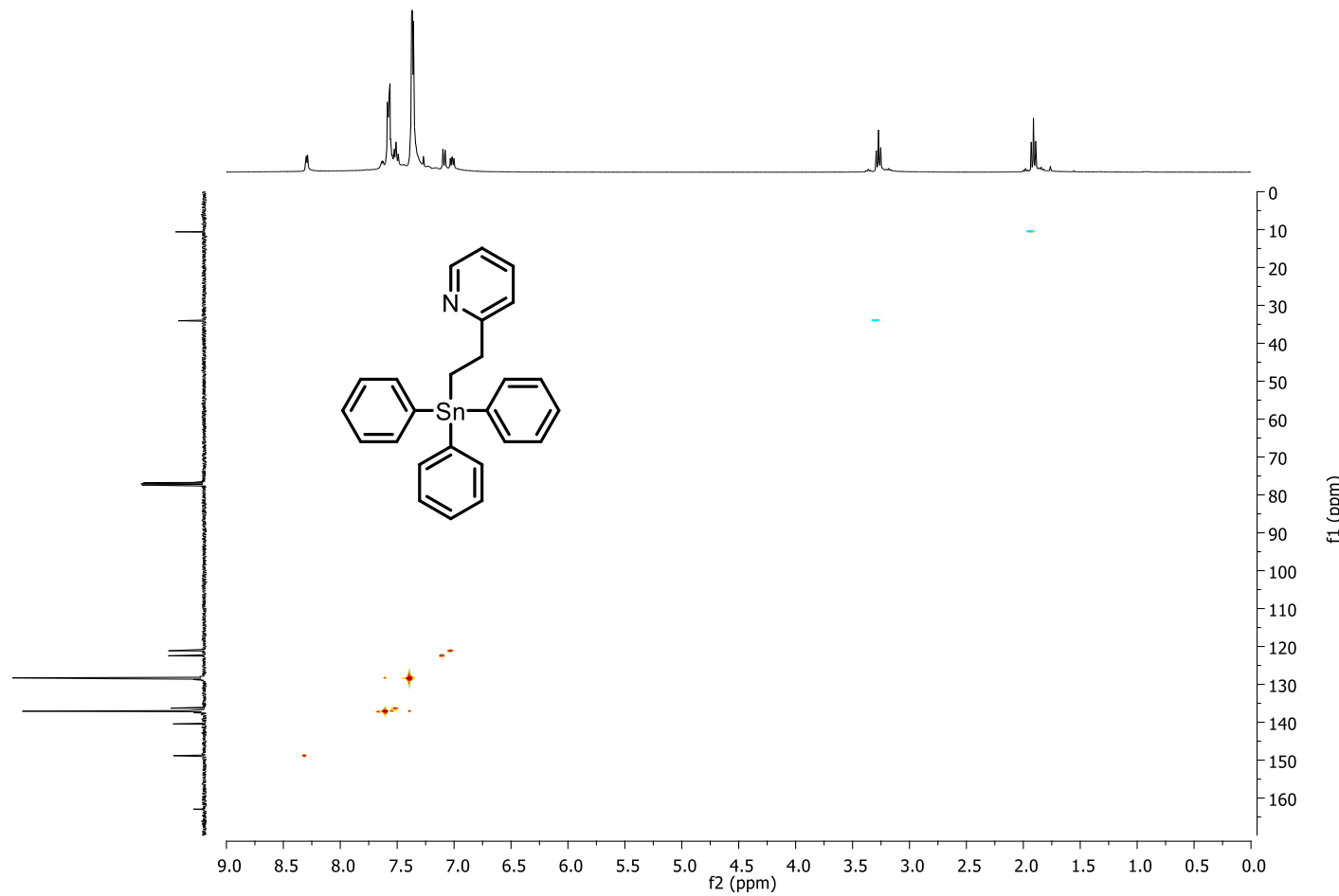


Figure A64: HSQC spectrum of **23** in CDCl_3^* .

230

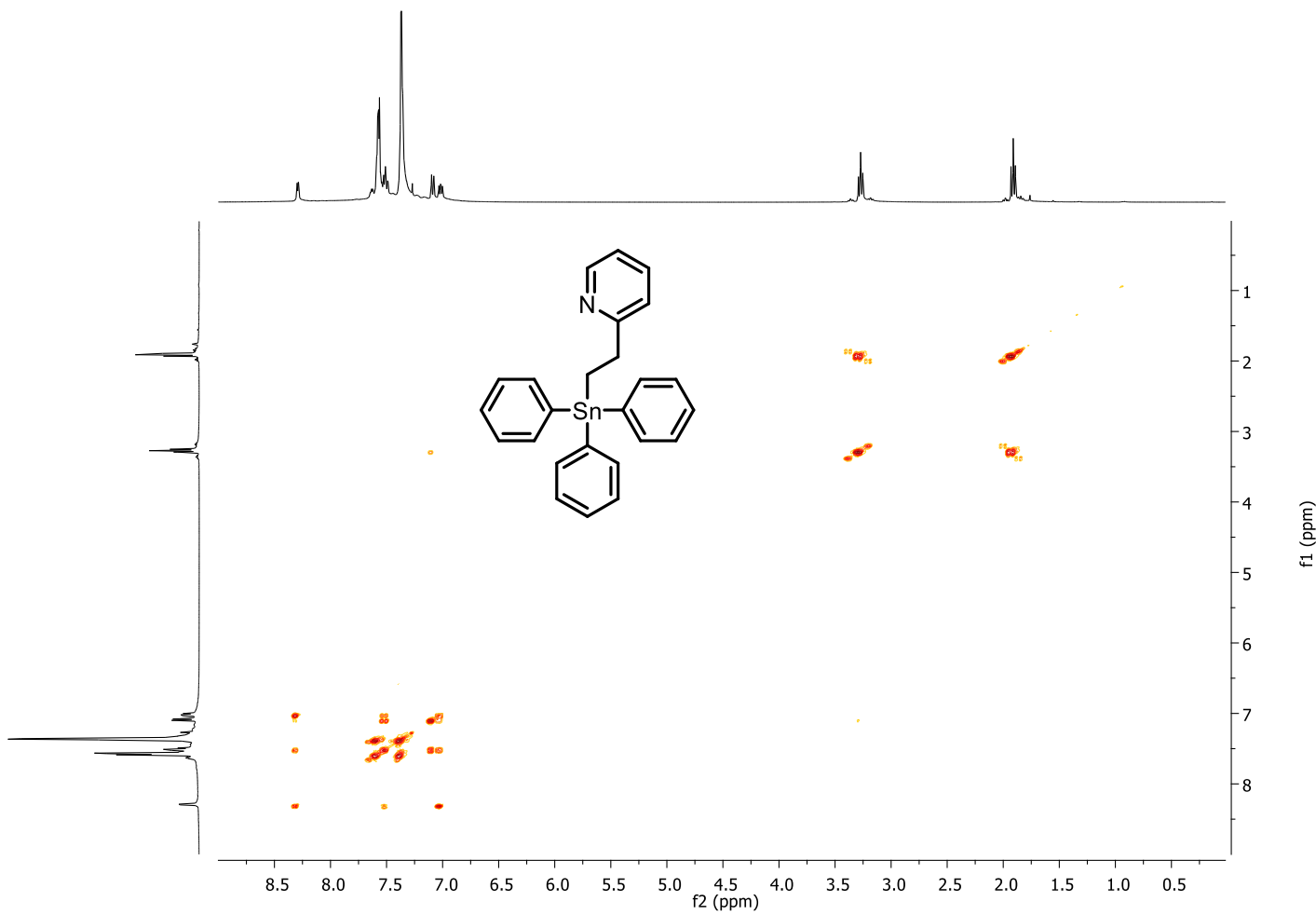


Figure A65: COSY spectrum of **23** in CDCl_3^* .

231

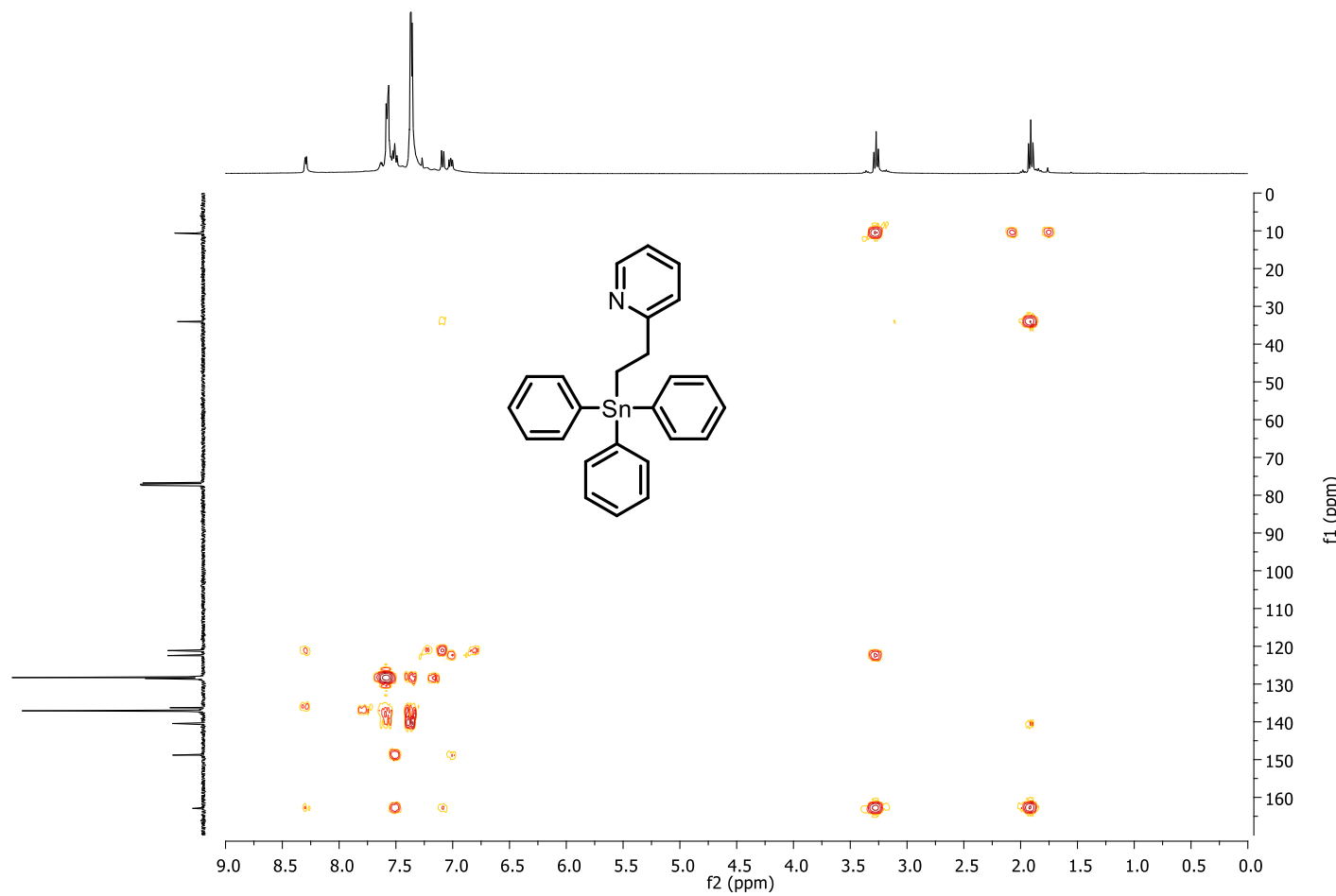


Figure A66: HMBC spectrum of **23** in CDCl_3^* .

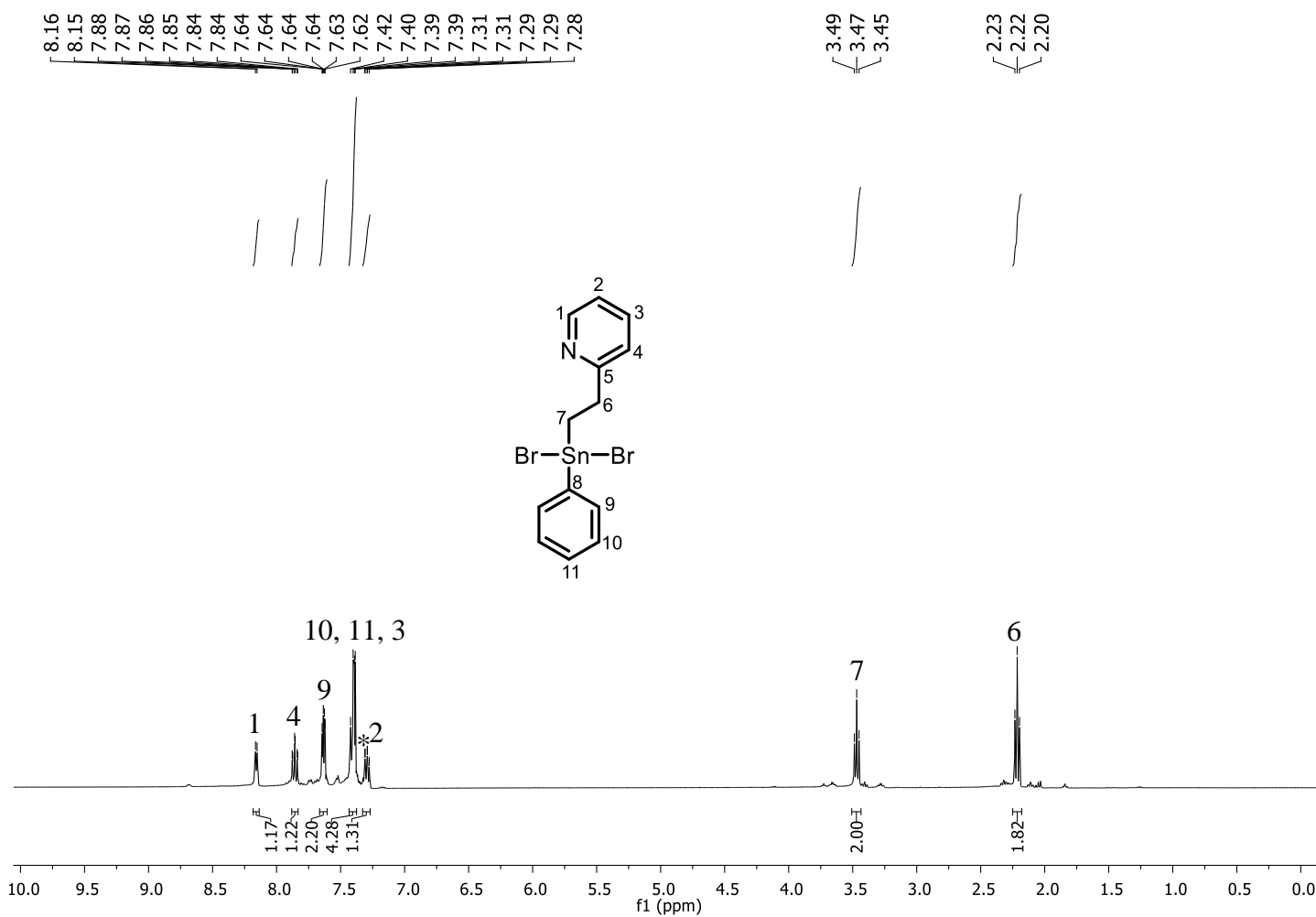


Figure A67: ^1H NMR spectrum of **24** in CDCl_3^* .

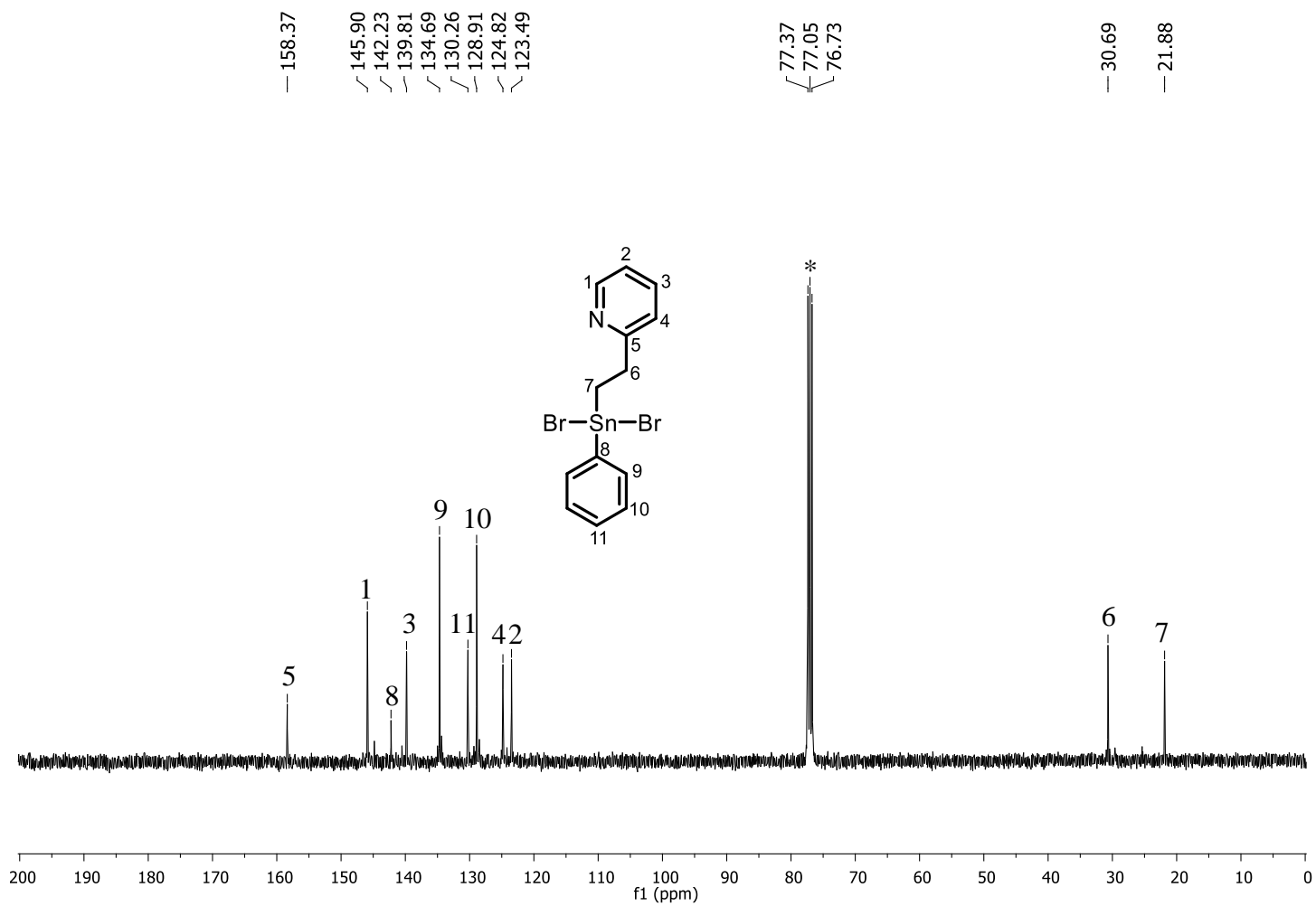


Figure A68: ^{13}C NMR spectrum of **24** in CDCl_3^* .

234

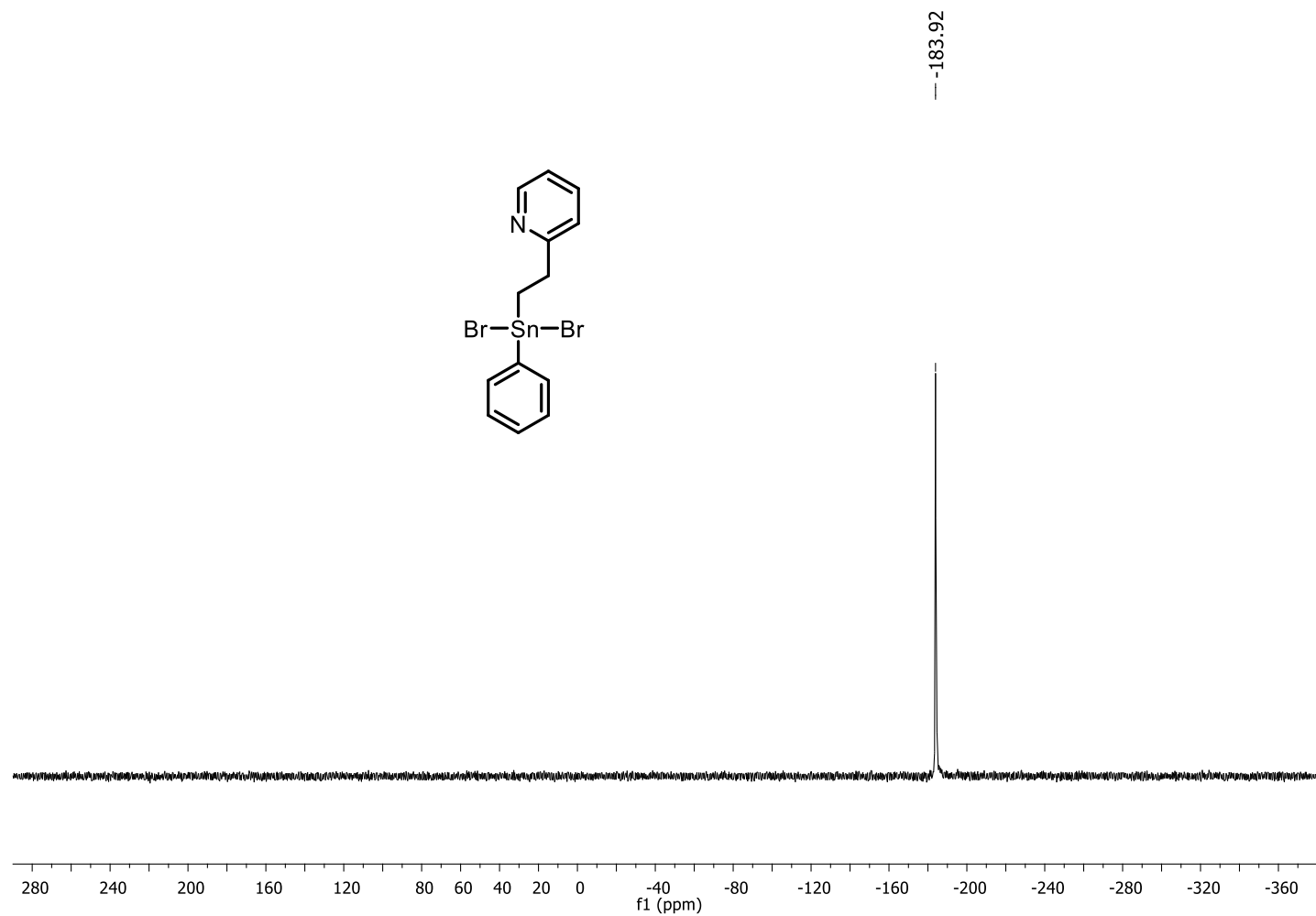


Figure A69: ^{119}Sn NMR spectrum of **24** in CDCl_3^* .

235

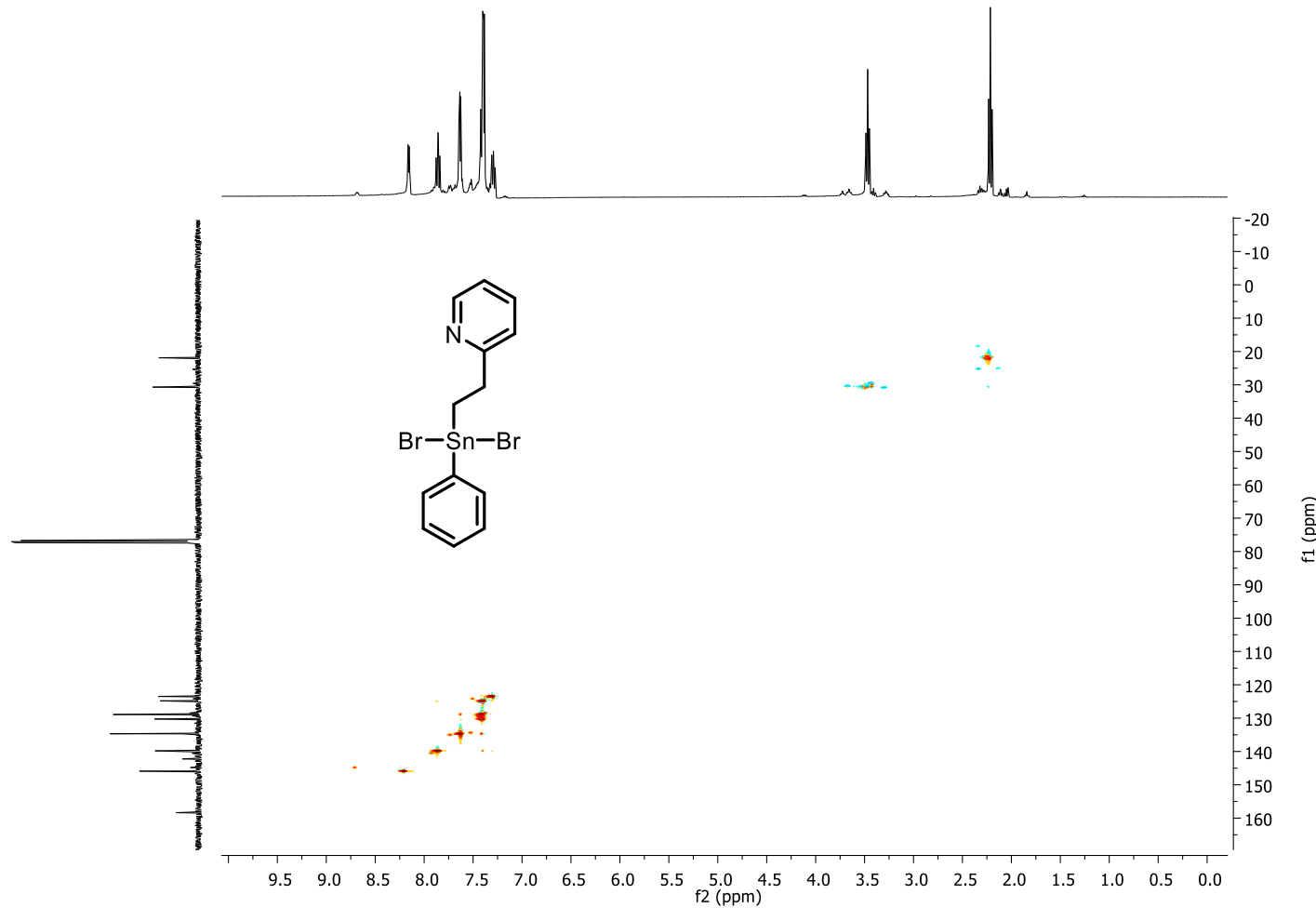


Figure A70: HSQC spectrum of **24** in CDCl_3^* .

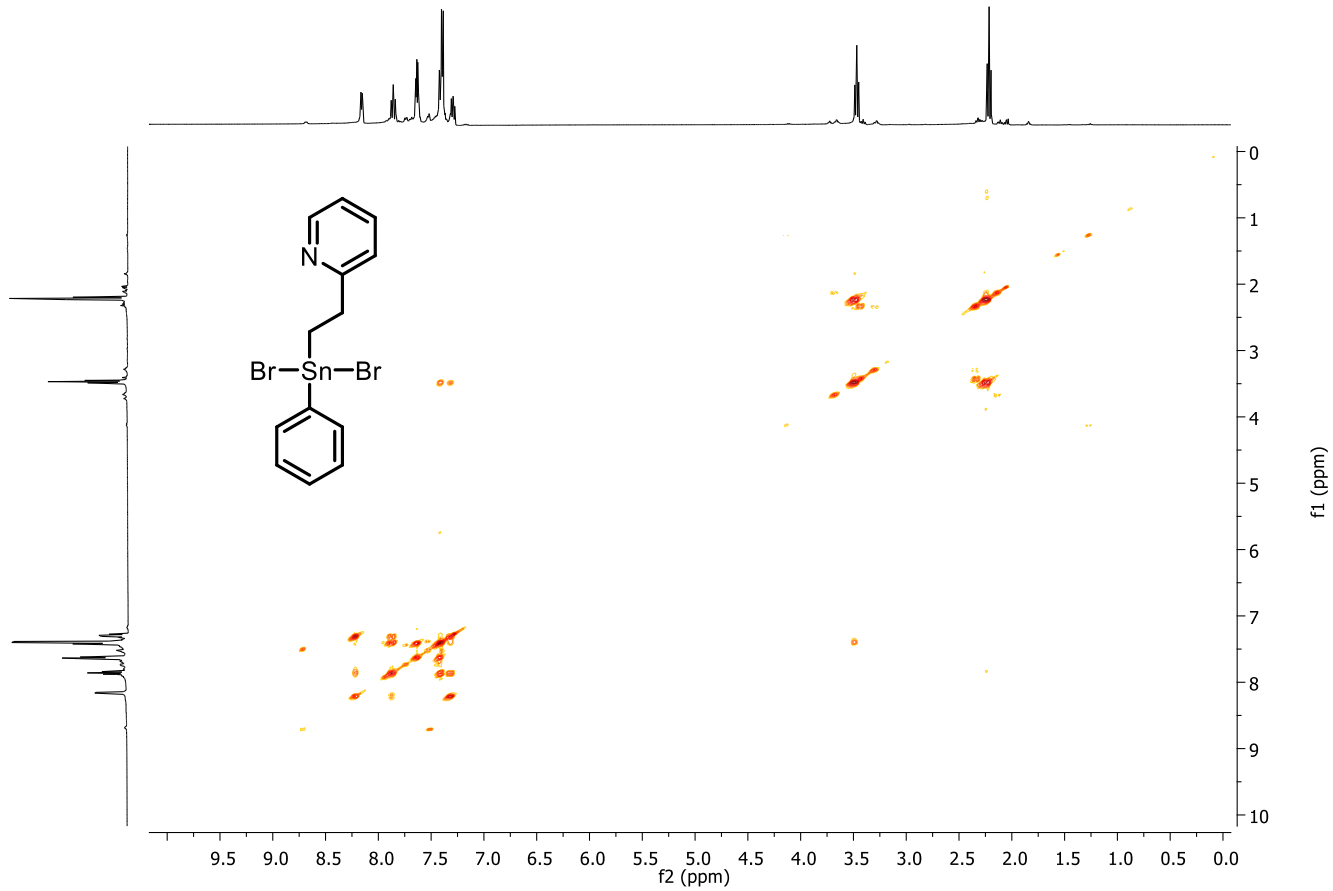


Figure A71: COSY spectrum of **24** in CDCl_3^* .

237

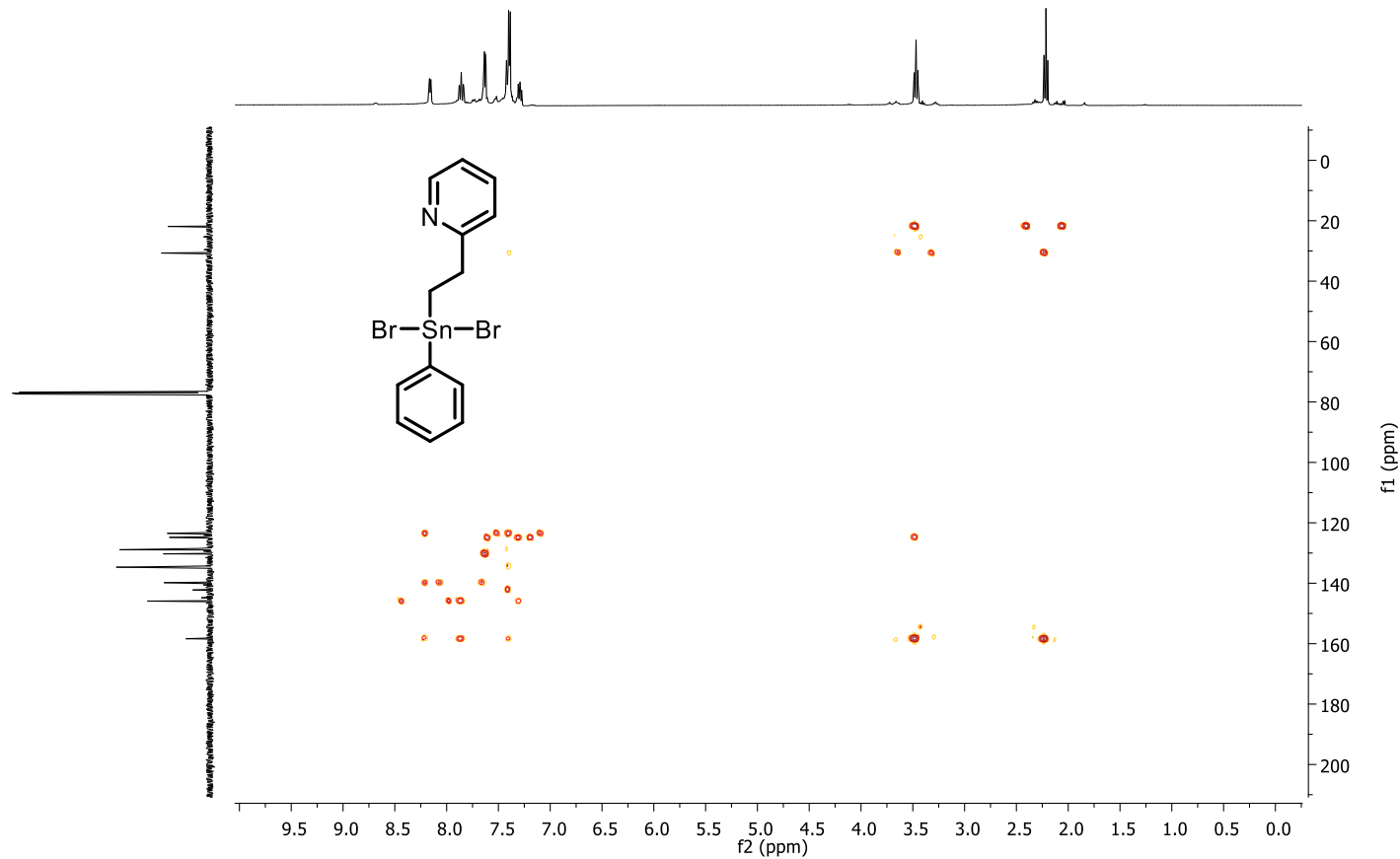


Figure A72: HMBC spectrum of **24** in CDCl_3^* .